STATUS OF THESIS

Title of thesis	**Control Relevant System Identification Using Orthonormal Basis Filter Models**

I, LEMMA DENDENA TUFA, hereby allow my thesis to be placed at the Information Resource Center (IRC) of Universiti Teknologi PETRONAS (UTP) with the following conditions.

1. The thesis becomes the property of UTP
2. The IRC of UTP may make copies of the thesis for academic purpose only
3. The thesis is classified as

    ☐ Confidential

    ☑ Non-Confidential

If the thesis is confidential, please state the reason:

_____
_____
_____

The contents of the thesis will remain confidential for _____years.

Remarks on disclosure:

_____
_____
_____

_____   _____

Signature of Author   Signature of Supervisor

Permanent: Lemma Dendena Tufa
address: Addis Ababa University
Faculty of Technology
Addis Ababa
Ethiopia

Assoc. Prof. Dr. Marappagounder Ramasamy

Date:_____   Date:_____

UNIVERSITI TEKNOLOGI PETRONAS

Approval by Supervisor(s)

The undersigned certify that they have read, and recommended to The Postgraduate Studies Programme for acceptance, a thesis entitled **"Control Relevant System Identification Using Orthonormal Basis Filter Models"** submitted by **Lemma Dendena Tufa** for the fulfilment of the requirements of the degree of Doctor of Philosophy in Chemical Engineering.

_____

Date

Signature : _____

Main Supervisor : Assoc. Prof. Dr. Marappagounder Ramasamy

Date : _____

Co-Supervisor : Dr Shuhaimi Mahadzir.

UNIVERSITI TEKNOLOGI PETRONAS

Control Relevant System Identification Using Orthonormal Basis Filter Models

By

Lemma Dendena Tufa

ATHESIS

SUBMITTED TO THE POSTGRADUATE STUDIES PROGRAMME

AS A REQUIREMENT FOR THE

DEGREE OF DOCTOR OF PHILOSOPHY IN

CHEMICAL ENGINEERING

BANDAR SERI ISKANDAR

PERAK

JULY, 2009

DECLARATION

I hereby declare that the thesis is based on my original work except for quotations and citations which have been duly acknowledged. I also declare that it has not been previously or concurrently submitted for any other degree at UTP or other institutions.

Signature:_____

Name :_____

Date   :_____

DEDICATION

To my beloved mother whom I always admire and miss until I meet her at our eternal

home!

ACKNOWLEDGEMENT

Control Relevant System Identification Using
Orthonormal Basis Filter Models

Abstract

Models are extensively used in advanced process control system design and implementations. Nearly all optimal control design techniques including the widely used model predictive control techniques rely on the use of model of the system to be controlled. There are several linear model structures that are commonly used in control relevant problems in process industries. Some of these model structures are: Auto Regressive with Exogenous Input (ARX), Auto Regressive Moving Average with Exogenous Input (ARMAX), Finite Impulse Response (FIR), Output Error (OE) and Box Jenkins (BJ) models. The selection of the appropriate model structure, among other factors, depend on the consistency of the model parameters, the number of parameters required to describe a system with acceptable accuracy and the computational load in estimating the model parameters.

ARX and ARMAX models suffer from inconsistency problem in most open-loop identification problems. Finite Impulse Response (FIR) models require large number of parameters to describe linear systems with acceptable accuracy. BJ, OE and ARMAX models involve nonlinear optimization in estimating their parameters. In addition, all of the above conventional linear models, except FIR, require the time delay of the system to be separately estimated and included in the estimation of the parameters.

Orthonormal Basis Filter (OBF) models have several advantages over the other conventional linear models. They are consistent in parameters for most open-loop identification problems. They are parsimonious in parameters if the dominant pole(s) of the system are used in their development. The model parameters are easily estimated using the linear least square method. Moreover, the time delay estimation can be easily integrated in the model development. However, there are several problems that are not yet addressed. Some of the outstanding problems are:

(i)   Developing parsimonious OBF models when the dominant poles of the system are not known

(ii)   Obtaining a better estimate of time delay for second or higher order systems

(iii)   Including an explicit noise model in the framework of OBF model structures and determine the parameters and multi-step ahead predictions

(iv)   Closed-loop identification problems in this new OBF plus noise model frame work

This study presents novel schemes that address the above problems. The first problem is addressed by formulating an iterative scheme where one or two of the dominant pole(s) of the system are estimated and used to develop parsimonious OBF models. A unified scheme is formulated where an OBF-deterministic model and an explicit AR or ARMA stochastic (noise) models are developed to address the second problem. The closed-loop identification problem is addressed by developing schemes based on the direct and indirect approaches using OBF based structures. For all the proposed OBF prediction model structures, the method for estimating the model parameters and multi-step ahead prediction are developed. All the proposed schemes are demonstrated with the help of simulation and real plant case studies. The accuracy of the developed OBF-based models is verified using appropriate validation procedures and residual analysis.

Control Relevant System Identification Using

Orthonormal Basis Filter Models

Pengenal-pastian Sistem untuk tujuan Proses Kawalan berasaskan model

'Orthonormal Basis Filter'

Abstrak

Penggunaan model di dalam rekabentuk and perlaksanaan sistem kawalan terkini adalah sesuatu yang sering digunapakai. Hampir keseluruhan teknik rekabentuk kawalan optima termasuklah teknik proses kawalan berasaskan ramalan model ('model predictive control') menggunakan atau memerlukan model sistem terbabit untuk perlaksanaannya. Untuk tujuan proses kawalan, terdapat beberapa jenis struktur model linear yang sering digunapakai untuk pengenal-pastian sistem di industri. Antara struktur-struktur model ini termasuk: 'Auto Regressive with Exogenous Input (ARX)', 'Auto Regressive Moving Average with Exogenous Input (ARMAX)', 'Finite Impulse Response (FIR)', 'Output Error (OE)' dan 'Box Jenkins (BJ)'. Pemilihan struktur model yang tepat bergantung kepada parameter model yang konsisten, bilangan parameter yang diperlukan untuk mengenal-pasti sistem terbabit sepenuhnya dan beban pemprosesan CPU dalam menganggarkan nilai parameter-parameter terbabit.

Model ARX dan ARMAX kerap memberikan model yang tidak konsisten apabila digunakan untuk pengenal-pastian sistem terbuka ('open loop system identification'). Model FIR pula memerlukan bilangan parameter yang banyak untuk mengenal-pasti sesuatu sistem linear sepenuhnya. Model BJ, OE and ARMAX melibatkan 'nonlinear optimization' dalam menganggarkan parameter-parameter berkaitan. Tambahan pula, kesemua model-model yang disebut di atas, kecuali model FIR, mengkehendaki penganggaran 'time delay' sistem dilakukan berasingan dahulu sebelum penganggaran parameter dapat dilakukan.

Model 'Orthonormal Basis Filter (OBF)' mempunyai beberapa kelebihan berbanding model-model linear yang disebut di atas. Parameter-parameter yang diberikan oleh model OBF ini selalunya mempunyai nilai yang konsisten bila digunakan untuk pengenal-pastian sistem terbuka. Bilangan parameter yang diberikan juga adalah terhad pada tahap minimum jika 'pole' dominan untuk sistem berkenaan digunakan semasa pembinaan model OBF tersebut. Parameter-parameter model OBF juga boleh senang didapati dengan menggunakan kaedah 'least square'. Selain itu, penganggaran 'time delay' boleh di

integrasikan dengan mudah secara serentak semasa pembinaan model. Walau bagaimanapun, terdapat beberapa masalah didalam penggunaan model OBF yang masih belum dapat di selesaikan. Antaranya termasuk:

(i) Pembinaan model OBF dengan bilangan parameter terhad pada tahap minimum ('parsimonious OBF model') jika 'pole' dominan sistem berkenaan tidak diketahui

(ii) Mendapatkan anggaran 'time delay' yang lebih tepat untuk sistem tidak linear, i.e. sistem tahap kedua dan ke atas

(iii) Memasukkan model 'noise' yang ekplisit di dalam struktur model OBF dan mendapatkan nilai-nilai parameter dan ramalan unjuran kehadapan ('multi-step ahead predictions')

(iv) Pengenal-pastian sistem tertutup ('closed-loop system identification') dengan menggunakan model OBF yang baru ini bersama dengan model 'noise'

Kajian ini membentangkan kaedah terbaru untuk mengatasi empat perkara yang disebut di atas dan sumbangan utama projek penyelidikan ini adalah terhasilnya model OBF yang baru yang mengambil kira empat perkara tersebut. Perkara pertama diatasi dengan merumuskan 'iterative scheme' dimana satu atau dua daripada 'pole' dominan sistem berkenaan dianggarkan dan digunakan untuk pembinaan model OBF dengan bilangan parameter terhad pada tahap minimum ('parsimonious OBF model'). Rumusan kaedah bersekutu yang melibatkan pembinaan 'OBF-deterministic' model dan eksplisit AR atau ARMA stokastik (noise) model dibentangkan untuk mengatasi perkara kedua di atas. Pengenal-pastian sistem tertutup dibina dengan menggunakan kaedah secara langsung dan tidak langsung berdasarkan struktur OBF. Kaedah untuk menganggarkan parameter model dan ramalan unjuran kehadapan ('multi-step') telah dibina untuk kesemua struktur ramalan model OBF. Semua kaedah/formulasi yang dibentangkan ini di demonstrasikan dengan menggunakan proses simulasi dan kajian semasa loji sebenar. Ketepatan dan keberkesanan model OBF yang diunjurkan di dalam projek penyelidikan ini di uji dan dibuktikan dengan menggunakan prosedur-prosedur keberkesanan yang berkaitan dan analisis residual.

TABLE OF CONTENTS

CHAPTER 3: ORTHONORMAL BASIS FILTER MODELS

CHAPTER 4 : OBF BASED PREDICITON MODELS

CHAPTER 5 : RESULTS AND DISCUSSIONS

CHAPTER 6 : CONCLUSIONS AND RECOMMENDATIONS

LIST OF TABLES

LIST OF FIGURES

xxiii

NOMENCLATURE

$A(q)$ Denominator polynomial of ARX and ARMAX models

AR   Autoregressive

ARMA   Autoregressive Moving Average

ARMAX   Autoregressive Moving Average with Exogenous Input

ARX   Autoregressive with Exogenous Input

$B(q)$ Numerator polynomial of the transfer function of the deterministic model

BJ   Box-Jenkins

$C(q)$ Numerator polynomial of the transfer function of the stochastic model

$D(q)$ Denominator polynomial transfer function of the noise model for BJ, OBF-AR and OBF ARMA structures

$F(q)$ Denominator polynomial of the transfer function of the stochastic model for BJ and OE models

FOPTD   First Order Plus Time Delay

$E_i(q)$ Polynomial for dividing the noise model into current and future parts

F_{st} Flow rate of steam

F_R Reflux flow rate

$F_i(q)$ Polynomial for dividing the noise model into current and future parts

$G(q)$ Transfer function of the deterministic model

GOBF   generalized orthonormal basis filter

H The transfer function of the stochastic (noise) model

L Parameters of a GOBF model

N Number of data points

OBF   Orthonormal basis filter

PRBS	Pseudo Random Binary Signal
SOPTD	Second Order Plus Time Delay
T_1	Temperature at the 1st tray (bottom)
T_{14}	Temperature at the 14th tray (top but one)
X	Regressor matrix
a	Slope
e	white noise with mean 0 and variance σ^2
l	Parameters of Orthonormal Basis Filters Model
m,n	Orders of filters
p	Pole of a system
q	Forward shift operator
$u(k)$	Input sequence
$u_f(k)$	Input sequence filtered by OBF
$v(k)$	Noise sequence
$y(k)$	Output sequence
$\hat{y}(k)$	Predicted output sequence
$\bar{y}(k)$	Mean of the output sequence
$y_{obf}(k)$	The output sequence predicted by the GOBF model
θ	Model parameters
τ	Time constant of a system
τ_D	Time delay

CHAPTER 1
INTRODUCTION

1.7 Background

The stringent environmental and safety requirements and the growing competition in the global market have put a tremendous challenge on process industries. On the other hand, the rapid development in computer and software technology, the advancement of instrumentation and data acquisition facilities and the sustained achievements in the formulation efficient computational algorithms have brought incredible opportunities. The meeting of these strong challenges and resourceful opportunities has led to the birth of several model based technologies, like model based control systems, online process optimizations and fault detection and diagnosis, to mention a few. At the centre of all these technologies is the mathematical model of the system.

Models are extensively used in advanced process control design and implementations. Nearly all optimal control design techniques rely on the use of model of the system to be controlled. In model predictive control (MPC), models are used to predict the future values of the output which is used in calculating the optimal control move.

In control systems, models are used either in simulation or prediction tasks. In simulation, an input $u(k)$ is applied on the process model to compute the undisturbed output sequence $y(k)$, [1, 2]. Simulation models are fully deterministic and they do not include explicit noise models. Simulation is used in optimization, control, fault detection and soft sensors [2]. In prediction, past inputs and outputs are used to predict the current or future outputs. The latter is called multi-step ahead prediction. Prediction models include explicit noise models of the system.

A turning point in the history of process control is the successful introduction of model predictive controllers (MPC) in process industries [3, 4]. MPC has been widely accepted in process industries due to many of their advantages in realizing an efficient control performance especially in multivariable systems. There exist a number of MPC implementations currently each differing from other in terms of how the MPC problem has been formulated, the type of model used for prediction and the techniques used in solving the optimization problem. A complete design of MPC includes the necessary

mechanism for obtaining the best possible model, which captures the dynamics fully and allows the prediction to be calculated [5, 6].

Models can be developed from physical and chemical principles or from experimental data. Models developed from chemical and physical principles are called first-principle or white-box models while models developed from experimental data are called empirical or black-box models. First-principles models are developed using equations derived from theoretical analyses of the physical and chemical processes occurring in the system, *e.g.*, principle of conservation of mass and energy. Black- box models are developed using mathematical and statistical principles. The variables and parameters of first principle models are determined by the physical and chemical principles governing the system. In contrast to black-box models, first-principles models directly incorporate any prior knowledge of the system. Since the parameters of first-principles models are related to system properties, their values can, in principle, be measured directly from the real system, or estimated. However, first principle models are difficult to apply in process industries because of lack of knowledge of the physical and chemical properties of the complex industrial processes. Attempting to fill this gap of knowledge incurs a lot of cost and consumes a lot of time. Therefore, it is the empirical models that are commonly used in process industries.

The process of developing models from experimental data is known as system identification. When the intended use of the model is related to control system design or implementation the process of modeling is known as control-relevant system identification. The development of simple models like first order plus time delay models from simple step test is straightforward and inexpensive in principle. Nevertheless, to develop reliable models from step-test data, either the process should be too simple or the experiment should be carried out in extremely controlled environment. It is difficult to get either of these conditions in industrial processes. Therefore, modern system identification relies on properly designed identification tests with more complex computational facilities. The major steps in system identification are design of experiment, selection of the class of models, selection of the model structures and model validation.

Models may be linear or non-linear. While control technologies using non-linear model are emerging and there are a lot of research in the areas of nonlinear system identification

linear models still dominate the industry. The orthonormal basis filter models which are the focus of this research are linear models.

1.8 Linear Models

There are several linear model structures in use. Some of the most common are Finite Impulse Response (FIR), Auto Regressive with Exogenous input (ARX), Auto Regressive Moving Average with Exogenous Input (ARMAX) and output error (OE) and Box-Jenkins (BJ) models. The structures of the various models are given below:

Auto Regressive with Exogenous Input (ARX):

$$y(k) = \frac{B(q)}{A(q)} u(k) + \frac{1}{A(q)} e(q) \tag{1.1}$$

Auto Regressive Moving Average with Exogenous Input (ARMAX):

$$y(k) = \frac{B(q)}{A(q)} u(k) + \frac{C(q)}{A(q)} e(q) \tag{1.2}$$

Output Error (OE):

$$y(k) = \frac{B(q)}{F(q)} u(k) + e(q) \tag{1.3}$$

Box Jenkins (BJ):

$$y(k) = \frac{B(q)}{F(q)} u(k) + \frac{C(q)}{D(q)} e(q) \tag{1.4}$$

Finite Impulse Response (FIR):

$$y(k) = B(q)u(k) + e(q) \tag{1.5}$$

where $A(q)$, $B(q)$, $C(q)$, $D(q)$ and $F(q)$ are polynomials in the shift operator q and $u(k)$, $y(k)$ and $e(k)$ are the input, output and white noise sequences, respectively.

Some of the most important factors in selecting model structures are:

- The computational load in estimating the model parameters

- The consistency of the model parameters

- The number of parameters required to describe the model with acceptable accuracy.

Auto Regressive with Exogenous Input (ARX) and Finite Impulse Response (FIR) models have been popular because of the computational simplicity with which the model parameters are estimated. In both cases, linear least square method can be used to estimate the parameters. Output error (OE) and Box-Jenkins (BJ) models are very rarely used for complex problems, like MIMO, because of the heavy computational load related to their parameter estimation. Parameter estimations in both OE and BJ involve nonlinear optimization.

Consistency of model parameters is another important factor in model structure selection. Consistency of model parameters refers to the possibility of estimating the model parameters without systematic deviation from their optimal values [1, 2] . The systematic deviation of model parameters from their optimal values is called bias. Model structures suffering from inconsistency in their parameters will result in biased estimates of the parameters and the bias will not be eliminated even if the number of data points is increased to infinity. ARX and ARMAX models suffer from inconsistency in most open-loop identification problems [1, 2, 8]. This is because of the common denominator dynamics of the deterministic and stochastic components, represented by $A(q)$, that the structure requires and which many practical open-loop problems do not satisfy.

The number of parameters required to capture the dynamics of a system with acceptable accuracy is still another factor in selecting the appropriate model for a given identification problem. This will affect both the identification and implementation phases of the model. It is already noted that, no matter what the linear structure is, when the number of parameters increases the variance error in parameter estimation increase[2]. This shows that models which require large number of parameters to capture the dynamics of a system will face the problem of increased variance error in the estimation of their parameters. On the other hand, during implementation like in MPC, an optimization problem is solved using the models to obtain the control output at each move. When the complexity of the model increases, obviously, the computational load of the optimization process at each control move increases. Therefore, it is very advantageous both at identification and implementation stages to get models that are parsimonious in their parameters. FIR models suffer heavily from this problem. They generally require large number of parameters to describe linear systems with acceptable accuracy. BJ models also suffer from this problem due to the large number of parameters, related to the four

polynomials in its structure to be determined. Due to these problems, BJ models are rarely used in MIMO system identification problems[2].

Moreover, it is known that in several control implementations, time delays in the system that is controlled affect the performance of the control system enormously[7]. Therefore, accurate estimation and incorporation of time delays into the model is another critical issue. All conventional linear model structures, except FIR, need the time delay of the system to be separately estimated and included in the model development process. This, in some cases, causes inconvenience in estimation of the model parameters using the conventional linear model structures.

Orthonormal Basis Filter (OBF) models can be considered as a generalization of FIR models in which the trivial filters in FIR models are replaced with more complex and more realistic orthonormal basis filters. OBF models have several characteristics that make them very promising for control relevant system identification compared to most conventional linear models. Their parameters can be easily estimated using linear least square method. They are consistent in their parameters for most practical open-loop identification problems. Parsimonious OBF models can be developed when the dominant pole(s) of the system is (are) known. Time delays can be easily estimated and incorporated into the model. However, there are several problems that are not yet addressed which this research attempts to address. The solution to these outstanding problems will bring significant contribution to linear model development by making OBF models more flexible and comprehensive.

1.9 Research Problems

It is already stated that OBF models have several qualities that make them attractive for control relevant system identification. However, there are still several problems to be addressed to make effective use of OBF models. To develop parsimonious OBF models, estimate of the dominant pole(s) of the system should be known *a priori*. The use of arbitrarily chosen pole(s) leads to a model that needs large number of parameters to describe the system with reasonable accuracy. However, estimation of the dominant pole(s) of a system is not a trivial task and getting estimate from preliminary step tests lead to inaccurate results in complex systems, like multiple-input multiple-output (MIMO) systems, and systems with significant unmeasured disturbances.

Estimation of time delay is another important issue related to OBF model development. Patwardhan *et al.* [8, 9] proposed the tangent method for estimating the time delay(s) of a system from the noise-free step response of its OBF model. The method is effective and accurate for systems that can be described by first order plus time delay (FOPTD) model. However, for second-and higher-order systems with significant time constants the time delay estimate by the tangent method leads to less accurate results.

Another problem of OBF models is the fact that conventional OBF structures do not include explicit noise model. Nevertheless, in several control system design and implementations, including classical and advanced control systems, the noise model plays an essential role [7-9].

Closed-loop identification using OBF models is another issue that did not get sufficient consideration yet. There are several situations where conducting the identification test in closed loop is more preferable than in open loop. Two of the most compelling situations are: when safety and economic considerations make open-loop test not viable and when the system is open-loop unstable and is stabilized by feedback controller. In these situations conducting the identification test in closed-loop becomes the only option. When system identification test is conducted in closed-loop, the input and noise sequences in the resulting identification data set will be correlated. Conventional OBF models fail to give consistent models in such cases. Moreover, the fact that OBF models have non-minimum phase zero in their structure makes them difficult to use in the classical closed-loop identification approaches.

 Therefore the most outstanding problems this research attempt to address are:

(v)   How to develop parsimonious OBF models when the dominant poles of the system are not known?

(vi)   How to obtain a better estimate of time delay for second or higher order systems?

(vii) How to include an explicit noise model in the framework of OBF model structures and determine the parameters and multi-step ahead predictions?

(viii) How to address closed-loop identification problems in this new OBF plus noise model frame work?

1.10   Research Objectives

The objective of this research is to develop control relevant system identification schemes using orthonormal basis filters that address the outstanding problems in the conventional OBF models. This includes

- Developing an identification scheme that enables the development of parsimonious OBF models in the absence of good estimates of the dominant poles of the system

- Developing a method for obtaining a better estimate of the time delay for second- and higher-order systems

- Proposing structures that are based on orthonormal basis filters that include explicit noise models. Deriving the parameter estimation algorithm and the multi-step-ahead prediction formula for both open-loop and closed-loop system identification.

- Developing MATLAB code to conduct system identification using the proposed methods.

- Demonstrating the effectiveness of the proposed schemes using appropriate simulation and real plant case studies.

1.11   Research Methodology

The verification and validation of all proposed structures and schemes will be carried out by rigorous mathematical derivation and relevant case studies.

1.11.1 Rigorous Mathematical Derivation

Methods proposed for developing parsimonious OBF models and time delay estimations will be verified using rigorous mathematical derivations. In addition, the parameter estimation and multi-step-ahead prediction schemes for each proposed model structure will be developed and verified using rigorous mathematical derivations.

1.11.2 Case studies

In addition to rigorous mathematical derivations, the effectiveness of the proposed methods will be demonstrated using relevant simulation and real plant case studies. The simulation case studies will be designed so that they reflect the issues in discussion appropriately and closely match real life problems. In addition, details of the systems, the

inputs, outputs and level and type of noise will be appropriately presented. In both simulation and real plant system identification case studies the appropriate identification procedures will be followed. These include appropriate choice of inputs, choice of excitation signals, model structure selection, appropriate parameters estimation and validation. The choice of inputs in the real plant case studies will be in accordance with the use of the models in control relevant implementations.

Excitation signals

It is known that process behavior that is not represented within the identification data set cannot be described by the model unless prior knowledge is explicitly incorporated[2]. In this research, excitation signals will be designed so as to result in an identification data that adequately represent the system. In addition, in all simulation studies appropriate care will be given to consider limitations in real plant. In real plant system identification the excitation signal is designed so as to give the maximum excitation which results in the maximum possible signal to noise ratio (SNR)[2]. In all simulation case studies in this research, the excitation signals will be designed so as to reflect the limitations in increasing the level of excitation in real plants. Therefore, the SNR in the simulation identification case studies in this research will be limited to less than 10.

The spectrum of the input signal is another design problem that should be properly addressed in all identification case studies since it determines the frequencies where the power is put in. It is known that pseudo random binary signals (PRBS) are well suited for identification since they excite all frequencies equally well[2]. Therefore, in this research in all identification case studies the excitations signal will be PRBS.

Validation

In both, simulation and real plant system identification case studies appropriate validation will be conducted. Validation of the input (deterministic) model will be carried out by comparing the prediction or simulation of the developed model with the output of the system for a separate validation data that is not used in identification. The comparison will be done both graphically by plotting the prediction and the system output and numerically using the percentage prediction error (PPE). The PPE is defined as

$$(\text{PPE})_i = \frac{\sum\limits_{i=1}^{n}(y_i(k) - \hat{y}_i(k))^2}{\sum\limits_{i=1}^{n}\left((y_i(k) - \bar{y}_i(k))\right)^2} \times 100 \tag{1.6}$$

where $\bar{y}_i$ represents the mean value of measurements $\{y_i(k)\}$ and $\hat{y}_i(k)$ predicted value of $y_i(k)$.

Validation of noise models in all simulation identification case studies that involve noise model development are carried out by comparing the spectrum of the estimated noise model with the noise transfer function of the system. The spectrum of a stochastic process described by $v(t) = H(q)e(t)$ where $\{e(t)\}$ is a white noise with mean zero and covariance λ is defined as

$$\Phi(\omega) = \lambda \left| H(e^{iw}) \right|^2 \tag{1.7}$$

where $H(q)$ is the noise transfer function and $v(t)$ is the noise [1]. Numerical values of the comparison are obtained using the PPE.

Residual Analysis

In addition to the above validation procedures, residual analysis is conducted to test the accuracy of the developed overall (deterministic plus stochastic) model of the system. A model is considered to be accurate if the residual of the model, *i.e.*, the system output minus the model prediction, is white noise. If the residual is white noise then the model has extracted all information about the system except a random noise that cannot be predicted. It should be noted that white noise is a random noise with mean zero and variance λ. Three different methods are used to test whether the residual is white noise or not. These methods are: the qq-plot, comparison of the distribution of the residuals and the white noise added to the system and the correlation among the residuals.

The qq-plot is a statistical plot, which is a graphical method of comparing two distributions by plotting their quantiles against each other[10]. Figure 1.1 depicts a typical qq-plot of the residual of a linear model against a white noise added to the system. When two distributions are the same all the points in the qq-plot will lie on a straight line with slope 1 and passing through the origin. If the points lie in a straight line but with different slope and origin the distribution are the same but they have different scales, *i.e.*, mean and

variance for normal distributions. If the points do not lie on a straight line, the two distributions are different.
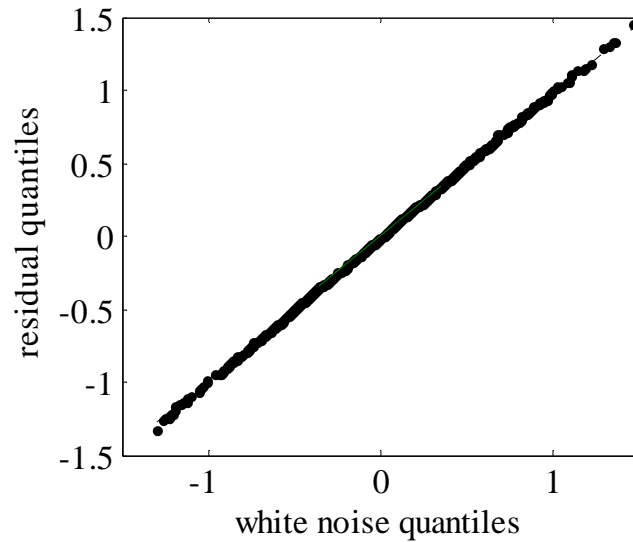
Figure 1.1 Typical qq-plot of the residual of a linear model against a white noise added to the system

Figure 1.2 shows a typical histogram distribution of a white noise signal generated using MATLAB. In this research, the qq-plot will be used in all identification simulation case studies to test if the residuals are white.
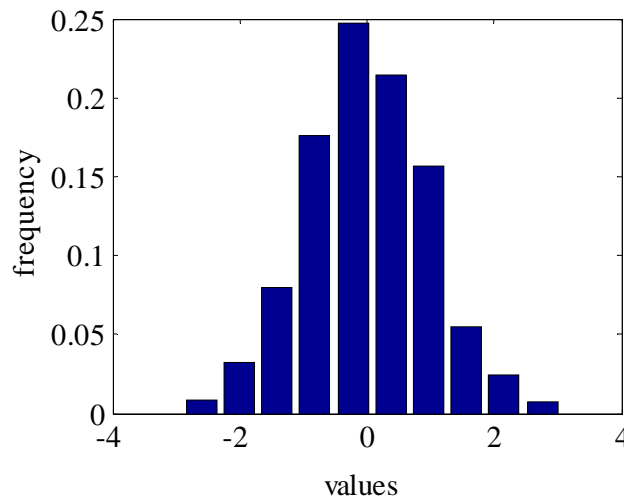
Figure 1.2 Typical histogram distribution of a white noise signal generated using MATLAB

Instead, the whiteness of the residuals is tested by inspection of the histogram distribution of the residuals.

In real plant identification case studies the distribution of the residual can be directly obtained using the MATLAB function '*hist*' which takes the residuals as input. In all distributions, the frequency is normalized. In simulation case studies, the white noise added to the system is available and the distribution of the residuals can be compared to the distribution of the white noise. In such cases the distributions will be shown by plotting the values of the residuals against the frequency which is determined using the MATLAB function '*hist*'. Figure 1.3 shows a typical comparison of the residual of a model and the white noise added to the system.
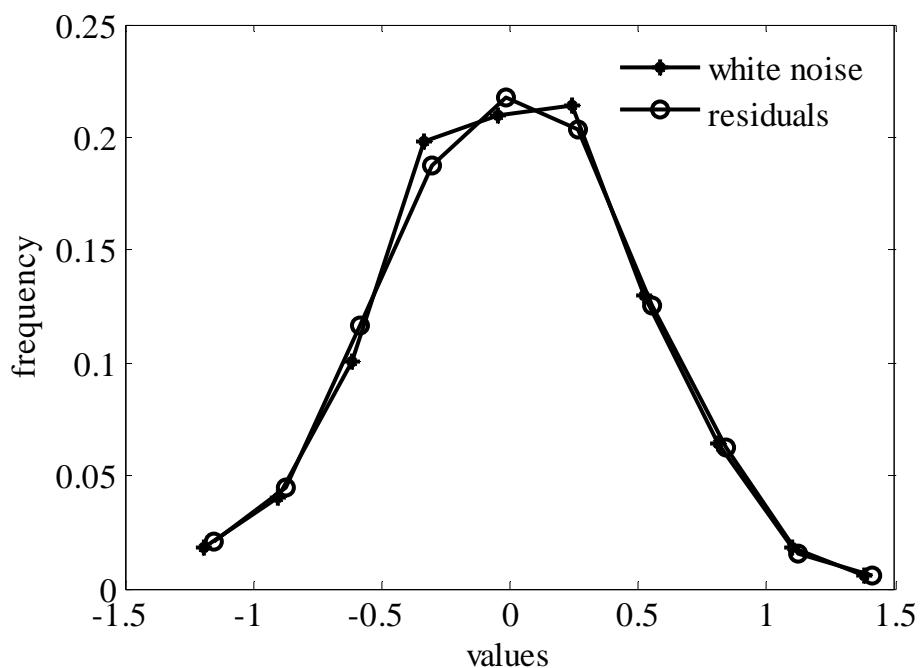
Figure 1.3 Typical distributions of the residuals and the white noise added to the system

1.12 Scope of the Research

The scope of the research will be as stated below.

(i) Development of relevant schemes, methods or structure that address each of the stated problems of the research, the schemes will include:

- An identification scheme (algorithm) to develop parsimonious OBF models in the absence of good estimate of the dominant pole(s) of the system

- A method for estimating the time delay of second order and higher order systems

- A structure that will result in OBF model and a noise model as unified model.

- Methods for estimating the model parameters and multi-step-ahead predictions of the proposed methods

- Closed-loop identification schemes based on OBF model that can handle open-loop stable and open-loop unstable systems.

(ii) Development of MATLAB codes based on the methods and schemes proposed

- All relevant MATLAB codes for conducting system identification based on the proposed schemes and methods.

(iii) Relevant simulation case studies that demonstrate each proposed method

(iv) Open-loop system identification of a pilot scale distillation column using the proposed method and the relevant MATLAB code developed

(v) Real plant, lab-scale, closed-loop identification case study

CHAPTER 2

LITERATURE REVIEW

2.7   Introduction

Models are extensively used in advanced control systems. The performances of such systems heavily rely on the accuracy of the models used in the design and/or implementation of the control system. For example, in model predictive control (MPC), the performance of the control system is directly related to the quality of the prediction model. The complete design of MPC includes the necessary mechanism for obtaining the best possible model which should be accurate enough to fully capture the dynamics and allow the prediction to be calculated.

There are several classical linear model structures that are used in model based control systems. The appropriate choice of a model structure for a particular system depends on factors related to the accuracy of the model, the modeling process and implementations. Some of the most important factors in this respect are: the capacity of the model structures to capture the dynamics of the system satisfactorily, the computational load of estimating the model parameters, the number of parameters required to describe the model with acceptable accuracy.

Most linear models consist of deterministic (plant) and stochastic (noise) models. The plant model describes the relation between the plant input and output while the noise model describes the effect of disturbances on the system output. In many advanced control implementations it is the plant model that is given much emphasis, however, current studies [8, 10] show that the noise model also plays important role in improving the regulatory performance of the control system. Therefore noise (disturbance) model development is becoming an issue in system identification.

System identification tests can be carried out either in open loop or in closed loop. While identification from open-loop test data dominates in industry, there are several instances where closed-loop identification is the only viable option. Two of the most compelling situations are: when safety and economic consideration makes open-loop test not viable and when the system is open-loop unstable. When identification tests are carried out in open loop, in most applications, there is no correlation between the input and the noise

sequences and identification is straightforward. However, when identification tests are undertaken in closed loop the input and noise sequence are correlated and needs more careful treatment.

In this chapter, a review of literature on control relevant system identification and relevant issues are presented. The first section discusses literature related to linear system identification in general, with more emphasis on classical structures. In the second section, the evolution and state of the art of OBF models is discussed. In the third and fourth sections, disturbance modeling and identification from closed-loop data, respectively, are reviewed. The last section gives a brief summary of the chapter.

2.8   System Identification

There exists extensive literature on system identification. One of the most prominent books on system identification is the one written by Ljung [1]. This book provides firm theoretical foundation for users of system identification on the different phases of system identification cycle, from design of experiment to model validation. It covers most of both linear and nonlinear models, identification in closed-loop and subspace methods. There are several works related to the use of linear system identification in modeling industrial processes [11-14].

Ljung [15] presented state of the art of linear system identification in both time and frequency domains. The paper mainly discusses the interplay between methods that use time and frequency domain data. It also discusses direct estimation of continuous-time models.

A very pragmatic approach of system identification is presented by Nelles [2]. Even though, the book is mainly targeted for nonlinear system identification, it also contains a good deal of information on linear models including orthonormal basis filter models. It clearly points out the difference between the various approaches, and their strengths and weaknesses. The book emphasizes on the practical aspects of system identification and it is a very good starting material for practitioners. However, it lacks depth in theoretical aspects of system identification. Another practical oriented system identification book, which includes application to advanced control system, is written by Ikonen and Najim [16]. It includes basic issues in identification, control and prediction. The main system

identification and prediction techniques are given in the form of algorithms. It deals with the most common linear and nonlinear models and also advanced control systems, particularly model predictive control. It treats both linear and nonlinear model predictive control systems. There are several books on both linear and nonlinear system identification with various approaches and emphasis [17-21].   In addition, there is extensive up-to-date literature on the various linear structures used in industrial applications [12, 13, 15, 24-33].

The scope of this research is limited to linear models and particularly orthonormal basis filter (OBF) models. However, to understand the reasons for the OBF model becoming popular, it is necessary to investigate the various linear models and their strengths and weaknesses. A general linear dynamic model consists of a deterministic part and a stochastic part as shown in Figure 2.1. According to this general model, the output is the sum of the input $u(k)$ and noise $e(k)$ filtered by their respective filters [1, 2, 17]. Equation (2.1) represents the general linear model shown in Figure 2.1.
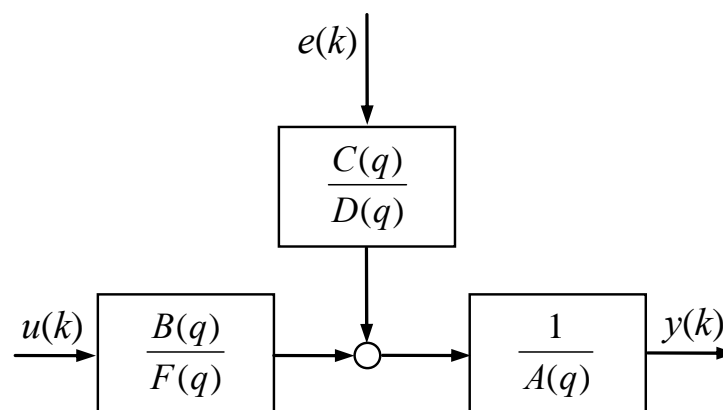
Figure 2.1 Block Diagram for the general linear model

$$y(k) = \frac{B(q)}{F(q)A(q)}u(k) + \frac{C(q)}{A(q)D(q)}e(q)$$
(2.1)

This general model leads to a much complicated model where parameter estimation is very difficult. Therefore, it is most commonly simplified by making assumptions on the polynomials *A, B, C, D* and *F*. The objective of simplifications is either getting a realistic model for a specific problem or making it simple to estimate the model parameters. Some

of the most commonly used linear model structures derived from this general model structure are discussed below.

2.8.1 Auto Regressive with Exogenous Input (ARX) Model

Autoregressive with exogenous input (ARX) model is derived from the general linear model by assuming $C(q) = D(q) = F(q) = 1$. ARX models are very popular in industrial applications because of the simplicity in estimating the model parameters [2]. There are still some works on improved methods for estimating the ARX model parameters [22, 23].

$$y(k) = \frac{B(q)}{A(q)}u(k) + \frac{1}{A(q)}e(q) \qquad (2.2)$$

2.8.2 Auto Regressive Moving Average with Exogenous Input (ARMAX) Model

The ARMAX structure is derived from the general linear model by assuming $D(q) = F(q) = 1$. The parameters of the ARMAX model are calculated by nonlinear optimization or by extended least square method. In the extended least square method, first a high order ARX model is developed, and the prediction error is taken as an approximation for the white noise $e(q)$ in calculating the ARMAX model. Moore *et al.* [13, 28] present various techniques for estimating the parameters of ARMAX model in the presence of unmeasured disturbances.

$$y(k) = \frac{B(q)}{A(q)}u(k) + \frac{C(q)}{A(q)}e(q) \qquad (2.3)$$

2.8.3 Output Error (OE) Model

The output error structure does not include a noise model where $A(q)=C(q)=D(q)= 1$.

$$y(k) = \frac{B(q)}{F(q)}u(k) + e(q) \qquad (2.4)$$

2.8.4 Box Jenkins (BJ) Model

The Box Jenkins structure is the most flexible among the linear model structures. It is derived from the general structure by assuming $A(q) = 1$ [2]. Pintelon *et al.* [24-26]

presented three consecutive papers, on the theoretical and application aspects of BJ models.

$$y(k) = \frac{B(q)}{F(q)}u(k) + \frac{C(q)}{D(q)}e(q)$$ (2.5)

2.8.5   Finite Impulse Response (FIR) Model

The finite impulse response model is the simplest of the linear models. It is a linear combination of delay filters, q^{-1}, q^{-2}, …, q^{-m}. Lo and Kwon [27] developed a technique for estimating the parameters of the FIR model by combining time domain and frequency domain techniques. Theoretically, the presented techniques lead to parameters that are globally optimum.

$$y(k) = B(q)u(k) + e(q)$$ (2.6)

The most widely used linear models are the ARX and FIR models[2]. Their popularity is due to the simplicity in estimating the model parameters using the linear least square method [2].   However, it is known that both ARX and FIR models have serious drawbacks in application [1, 2, 20] . The ARX model structure leads to biased and non-consistent parameter estimation and the FIR model needs very large number of parameters to capture the dynamics of a system with acceptable accuracy. Bias, as described by Nelles [2], is the systematic deviation of the model parameters from their optimal value. Inconsistency refers to the fact that the bias does not approach zero as the number of data points approach infinity. This inconsistency in estimates of the ARX model parameters is caused by the assumption of common denominator dynamics for both the input and noise transfer functions given by $1/A(q)$, which does not describe most practical open-loop processes. As indicated by Nelles [2], all model structures that have an independently parameterized transfer function and noise model allow one to estimate the parameters of the transfer function consistently even if the noise model is not appropriate. However, ARX and ARMAX models do not fulfill this condition and lead to non-consistent parameter estimation in most systems. As it is noted previously, the FIR model, the other very popular model, needs a very large number of parameters to capture the dynamics of a system with reasonable degree of accuracy [2, 8, 20]. To understand this fact, the FIR model can be considered as truncated form of the convolution sum where the model parameters are the impulse responses of the system. For a stable system,

the impulse response, g_i, decays to zero as *i* goes to infinity. If the sampling rate of the process is 1/10 of the slowest time constant and the settling time is taken to be T_{95} (4τ), then the number of parameters required to describe the system will be 30.

The output error (OE) and the Box Jenkins (BJ) model structures assume independent transfer function and noise models, and hence they allow consistent parameter estimation. However, the OE structure do not include explicit noise model and in cases where the noise of the system is colored and noise model is required, it becomes inadequate. The BJ model structure is the most flexible form of the linear models [1, 2, 17]. However, determination of the model parameters in both cases involves nonlinear optimization. In addition, in case of BJ, because of the large number of parameters involved in the equation, it is rarely used in practice, especially, in MIMO systems [2]. Moreover all linear models that are discussed, except FIR, assume *a priori* knowledge of the time delay of the system in estimating their parameters. Therefore to use these linear models effectively, time delays must be known, or estimated separately.

2.9   Orthonormal Basis Filter Models

One of the earliest works on rational orthonormal bases was contributed by Takenaka [36] in the 1920's in relation to approximation via interpolation, with the subsequent implications for generalized quadrature formula. In subsequent works, in the 1960s, Walsh [37] contributed extensively in the applications of orthonormal bases for approximation, both in discrete time and continuous time analysis. In similar periods, Wiener [38] examined applications of continuous time Laguerre networks for the purpose of building optimal predictor. Kautz [39, 40] contributes significantly on the formulation of generalized orthonormal basis filters (GOBF) and their continuous versions for the purpose of network synthesis.

Engineering applications of orthonormal parameterizations emerged in the 1970s in the areas of digital filter structure's implementations [41]; and Laguerre bases were examined for the purposes of system identification in the same period [41]. In the period 1980s-1990s, there was a great deal of interest in engineering literature in control relevant system identification [42-48], signal processing [49-53], and applications to modeling and predicting stochastic stationary processes [54-55]. In the last decade there has been quite a lot of work in the approximation properties of orthonormal bases functions [56-64].

New methods for finding optimal function approximations can be found in [65-72]. Realization theory is another area where there has been major progress since 1999 [73-83]. Fast algorithms for adaptive signal processing have recently been derived in [84-87].

One of the most comprehensive linear model structures, as noted previously, is the box Jenkins (BJ) model structure. However, BJ model structure is nonlinear in its parameters and the parameter estimation involves nonlinear optimization. Reformulating the problem as linear regression may help in estimation of the parameters using linear least squares. However, the estimated parameters affect both the transfer function and the noise model and can cause biased parameter estimation. One possibility to deal with this problem is to develop a linear structure that is *a priori* linear in parameters [88].

$$y(k) = \left(\sum_{i=0}^{n-1} \theta_i f_i(q) \right) u(k) \tag{2.7}$$

where

θ = the model parameters

$y(k)$ = output sequence

$u(k)$ = input sequence

f_i = a set of rational functions in the shift operator q

n = model order

Since the model is linear in its parameter and the parameters are linear in $y(k)$ and if $u(k)$ is not correlated with the noise, finite data variance for θ can be calculated. Furthermore, θ parameterizes only the transfer function and not the noise model, and therefore it is not biased by measurement noise [88].

The next problem is the choice of appropriate rational functions that will result in fast convergence. In the simplest case, when $f_i(q)$ is a set of delays, the resulting model will be a finite impulse response (FIR) model. However, when the dynamics of the true system has a slow pole, FIR needs very large number of parameters to accurately capture the system dynamics [20, 88].

The solution for this problem was found by selecting the function $f_i(q)$ such that it incorporates *a priori* knowledge of the system in the form of the system's poles. This led to the extensive use of Laguerre and Kautz filters which are sets of orthonormal basis

functions [43, 47-49, 62, 68, 69, 71-73, 89-91]. The Laguerre and Kautz filters allow incorporation of one real pole, and a pair of complex conjugate poles, respectively. Then generalized constructions of orthonormal basis functions which allow incorporation of multiple poles into the rational function were introduced [46, 88]. It was also shown by Van den Hof *et al.* [92] that Laguerre and Kautz filters are special cases of the generalized orthonormal basis filter model. Finding an appropriate estimate of the poles for the filters is an important step in estimating the parameters of the OBF models. Arbitrary choice of poles may lead to a non-parsimonious model. Van den Hof *et al.* [92] showed that for a SISO system with poles $\{a_j : |a_j| < 1 \; for \; j = 1, 2, ..., n_0\}$, the rate of convergence of the model parameters is determined by the lowest magnitude of Eigen value.

$$\rho = \max_{j} \prod_{k=1}^{n} \left| \frac{a_j - p_k}{1 - \overline{p}_k a_j} \right| \tag{2.8}$$

where p_k is an arbitrary set of poles.

Therefore, a good approximation by a small number of parameters can be obtained by choosing a basis for which ρ is small. It was shown that the poles determined by Van Den Hof *et al.* [92] method, closely match the dominant poles of the system [48]. If the dominant poles of the system are known then it is possible to develop parsimonious OBF models with an appropriate selection of the type of filter.

Laguerre and Kautz filter models have shortcomings concerning time delays. Time delays in both cases are estimated by non-minimum phase zeros. This shortcoming is alleviated by using the Markov-OBF structure. Time delay in Markov-OBF is included by placing some of the poles at the origin [8]. For a SISO system with dead time equal to d samples, the basis function can be selected as:

$$f_i = q^{-i} \qquad \text{for } i = 1, 2, ..., d \tag{2.9}$$

$$f_{i+d}(q, p) = \frac{\sqrt{1 - |p_i|^2}}{(q - p_i)} \prod_{j=1}^{i-1} \frac{(1 - p_j^* q)}{(q - p_j)} q^{-d} \quad \text{for } i = 1, 2, ..., N \tag{2.10}$$

Patwardhan and Shah [8] presented a two-step method for estimating and incorporating time delays into GOBF models. In the first step, the time delays in all input-output

channels are assumed zero and the model is identified with GOBF. In GOBF models the time delay is approximated by a non-minimum phase zero and the corresponding step response is an inverse response. The time delay is then estimated from a tangent drawn at the point of inflection and incorporated into the GOBF model using (2.10).

OBF model structures have several advantages over the conventional linear model structures. Unlike ARX and ARMAX model structures, OBF models result in consistent parameter estimation. OBF models can capture the dynamics of linear systems, with acceptable accuracy, with much fewer numbers of parameters than FIR models. The parameters of OBF models can be easily estimated using linear least square method. In addition, in OBF model development *a priori* knowledge of time delay is not required, but can be easily estimated and incorporated into the model.

However, there are still some problems to be addressed. First, there are several instances where it is difficult to find the dominant time constant of the process easily. One such situation is where there is significant unmeasured disturbance in the system. In such cases, finding a good estimate of the dominant pole is not a trivial task. If arbitrary poles are used to formulate the orthonormal basis filters, the resulting OBF model will require large number of parameter to capture the dynamics with acceptable accuracy. Second, OBF models are essentially simulation models and do not provide explicit noise models[2]. However, in design of control systems with disturbance rejection the noise model plays an essential role.

2.10   Disturbance Modeling

Disturbance models play a central role in any advanced control system design that includes disturbance rejection [9, 28]. In model predictive control (MPC) application, plant-model mismatch and unmeasured disturbances can lead to offset unless the controller design addresses these problems appropriately [28]. In the early formulation of MPC, the offset problem was handled by designing an *ad-hoc* disturbance estimator which gives the controller an implicit integral action. The simplest method for incorporating integral actions in MPC is to generate the output targets by shifting the set points using disturbance estimates. The disturbance model in this approach assumes that the plant-model mismatch is due to step disturbances in the output and the disturbances remains constant throughout the prediction horizon. Disturbance models are also essential

in feedforward control system design. In fact, the performance of any feedforward control system highly depends on the accuracy of the disturbance model [29] .

In their conventional form, OBF model structures cannot be effectively used in the presence of unmeasured disturbances unless a noise model is developed and included in the control system design. Patwardhan *et al.* [10] showed that the regulatory performance of MPC system improves significantly by including a noise model to the OBF simulation model. In their work [8], the residual of the OBF model is whitened with auto regressive (AR) noise model. The AR noise model is parameterized in terms of OBF parameters and a minimal-order state-space model is realized. In their subsequent paper [9], they used this state-space model in MPC and fault tolerant control systems. However, AR models are not parsimonious and they need a large number of parameters to capture the dynamics of the unmeasured disturbance with acceptable accuracy. In addition, development of the noise model could be integrated with the development of the OBF model so that a unified OBF model and the corresponding disturbance model are developed together as a single model. Combining the noise model to an OBF model and treating it as a single model would also improve the predictive capability of the model.

2.11   System Identification Using Closed loop Data

System identification can be carried out using input-output data either from open-loop or closed-loop tests. When a system identification test is carried out in open loop, in most cases, the noise sequence is not correlated to the input sequence and OBF model identification is carried in a straight forward manner. However, when the system identification test is carried out in closed loop, *i.e.,* the data is collected while the system is controlled using feedback controller, the input sequence is correlated to the noise sequence [30-32] . In such cases, if conventional OBF model development technique is used, the resulting model will not be consistent in parameters[2]. Nevertheless, there are several reasons to conduct the identification tests in closed-loop in many instances, viz., [1, 2, 30-32] :

- Feedback controller is required to stabilize the process
- Safety and cost consideration may not allow the process to run open-loop
- The excited frequencies in closed-loop operation are better suited than the frequency band in open-loop operation

- The linearization of the controller is desired
- The model is to be used for the design of improved controller

Figure 2.2 depicts the configuration of the closed-loop system identification.
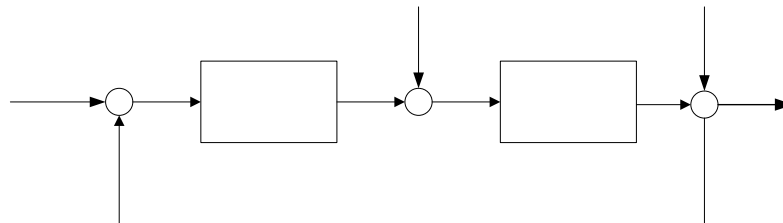
Figure 2.2 Configuration for closed-loop identification test

There are various approaches for handling system identification from closed-loop data. Van den Hof [33] discusses the various issues and approaches in closed-loop system identification of both parametric and non-parametric models. In the parametric identification there are three approaches:

- Direct identification
- Indirect identification
- Joint input/output identification

2.11.1 Direct Identification

In the direct identification, the standard identification approach (prediction error) is directly applied without considering the effect of the feedback controller [2, 33]. Due to the ignored correlation between the input and noise sequences, all methods which are based on correlations such as instrumental variable, spectral analysis and correlation analysis cannot be used[2]. In the direct method, if the system is present in the model set, then a consistent estimate is obtained in each of the following conditions:

- Sufficiently exciting signal r_1 and r_2 are present
- C is a controller of sufficiently higher order
- C is a controller that switches between several settings during the experiment

However, if the system is not in the model set the direct identification method fails [33].

2.11.2 Indirect Identification

The indirect identification method is based on external excitation signals r_1 and/or r_2. The two prominent indirect identification methods are the two-stage method and the coprime factor identification method [2, 33] . In the two-stage method, the process input sequence u is replaced by a simulated input sequence u^r which is uncorrelated to the noise sequence. Then the standard prediction error method is utilized. In the first stage, the transfer function $S(q)$ relating u and r_1 is estimated. The simulated process input u^r is, then, determined by filtering $r_1(k)$ using $S(q)$. In the second stage, the noise-free simulated input sequence u^r and the plant output sequence, $y(k)$, are used to develop the plant model using the standard prediction error method. In the coprime factor identification, the transfer functions $G^y(q)$ and $G^u(q)$, from r_1 to y, and from r_1 to u, respectively, are identified and the ratio of $G^y(q)$ to $G^u(q)$ is taken as an estimate of the plant model.

Although there is a wide-ranging literature on closed-loop identification, only limited material related to OBF model development using closed-loop test data is available. Gáspér *et al*. [94] used the two-stage method to identify a GOBF model from a closed-loop simulation data. While this paper is the only one in this area, it lacks clarity and depth on its presentation and the simulation exercise, which is the main subject of the paper, is less relevant to closed-loop identification. First, in the simulation model, which is used to generate the identification data, only the plant and the controller transfer functions are given. It appears that, no noise or unmeasured disturbance is introduced into the simulation system. This makes the identification case-study less relevant to closed-loop identification; since it is the correlation of the noise sequence to the input sequence that makes closed-loop identification unique and difficult. The soul of the problem is missing or at least not described. Second, the work did not use any standard validation procedure to judge the accuracy of the developed GOBF model. Third, the GOBF model is not explicitly presented in the paper; therefore it is impossible to make any conclusion about it. Fourth, the paper does not give any information about noise model development.

2.12 Summary

There is extensive literature both on system identification, in general, and OBF models in particular. From the literature review, it is observed that there is a lot of significant development in the area of linear system identification for dynamic systems. Compared to

most classical linear models, OBF models have several characteristics that make them very promising for control relevant system identification. They are parsimonious in their parameters, the parameters can be easily calculated using linear least square method, their models are consistent in parameters and time delays can be easily estimated and incorporated into the model. On the other hand, there are several issues that are not yet addressed. First, parsimonious OBF models are developed only if the poles of the system or at least the dominant poles of the system are known *a priori*. However, there are many instances where it is difficult to get good estimate of the time constants from simple preliminary tests. Second, OBF models are simulation models and therefore they do not provide explicit noise model. It is already discussed that in many control applications the noise models play critical role in improving the performance of the control system. In addition, it is observed that there is almost nothing in the open literature on closed loop identification related to OBF models. However, there many instances where closed loop identification is the best or even the only possibility to develop prediction models. These observations show that while there is significant progress in control relevant system identification using OBF models, there is still significant room for improvement.

CHAPTER 3

ORTHONORMAL BASIS FILTER MODELS

3.8   Introduction

One of the major advantages of orthonormal basis filter (OBF) models, as discussed in the earlier chapters, is that they can capture the dynamics of a linear system with acceptable accuracy with relatively fewer number of parameters, i.e., they are parsimonious in parameters. However, this is true only if the poles used in the model development are close to the dominant poles of the system [8, 20, 93]. If the poles used in the OBF model development are far away from the dominant pole of the system, OBF models need larger number of parameters to capture the dynamics with reasonable accuracy. Therefore, when it is difficult to obtain a good estimate of the dominant poles of the system, the conventional OBF model development approach may result in non-parsimonious models.

Another important advantage of OBF model is the fact that time delays can be easily estimated and incorporated into the model. It is pointed out, in the literature review, that Patwardhan and Shah [8] proposed a method to estimate the time delay by drawing a tangent at the inflection point of the step response of the OBF model. While this method is very effective to estimate the time delay of systems that can be accurately modeled by FOPTD models, the accuracy is low for systems with second and higher order dynamics. This is because of the sigmoidal nature of the step response of higher order systems.

In this chapter these two problems are addressed. The problem of parsimonious OBF model development is addressed by first developing an OBF model from arbitrary set of poles. Then a FOPTD or a SOPTD model is developed from the step response of the noise-free OBF model. Estimates of one or two of the dominant poles of the system are then obtained from the FOPTD or SOPTD model, respectively, and used to develop parsimonious OBF models. The process is repeated, iteratively, until a convergence criterion is fulfilled. The second problem is addressed by developing a scheme where the time delay contribution of the sigmoidal step response curve is estimated and subtracted from the time delay estimate by the tangent method, to get a better estimate of the apparent time delay.

In the first section, the theory of OBF model development is presented. In the second and third sections, development of FOPTD and SOPTD models from noisy data using OBF models, respectively, are addressed. In the fourth section, development of parsimonious OBF models from arbitrary set of poles is treated. The methods developed are demonstrated using illustrations and simulation case studies.

3.9   Theory of OBF models

The notations and terminologies differ very much among the published literature and text books. Ljung [1] has been accepted and followed as a standard by many authors in the field of linear system identification. The notations and terminologies in this thesis, whenever possible, follow Ljung. However, the notations in OBF models follow Heuberger *et al.* [20].

Consider a discrete time linear system

$$y(t) = G(q)u(t)$$
(3.1)

where $u(t) =$ the input signal

$\quad y(t) =$ output signal

$\quad G(q) =$ the transfer function of the system

The q in (3.1) is the forward shift operator which defines $q\, u(t) = u(t + 1)$ and q^{-1} is the delay (backward shift) operator, $q^{-1}u(t) = u(t - 1)$.

For stable systems, the impulse response representation is given by

$$y(t) = \sum_{k=0}^{\infty} g_k u(t - k)$$
(3.2)

where g_k are the impulse response coefficients and the corresponding transfer function is defined as

$$G(q) = \sum_{k=0}^{\infty} g_k q^{-k}$$
(3.3)

The transfer function on the complex plane $z \in \mathbb{C}$ is denoted by

$$G(z) = \sum_{k=0}^{\infty} g_k z^{-k}$$
(3.4)

The frequency response of the system is represented by $G(e^{i\omega})$. In most systems, there is at least one delay between the input and the output signals, therefore strictly proper transfer function is assumed.

$$\lim_{|z|\to\infty} G(z) = 0$$
(3.5)

i.e., $g_0 = 0$. This is because the input normally does not instantly affect the output. Let T denote the unit circle $\{z: |z| = 1\}$ and E denote exterior of unit disc $\{z: |z| > 1\}$. The Hardy space $\mathcal{H}_2$, of square integrable functions on T and analytic in E is considered. The inner product of two filters, $(f_1(z)$ and $f_2(z)$ $) \in \mathcal{H}_2$, is denoted by (3.6) [20].

$$\langle f_1(z), f_2(z)\rangle = \frac{T}{2\pi} \int_{-\pi/T}^{\pi/T} f_1(e^{i\omega'T}) f_2(e^{i\omega'T}) * d\omega'$$

$$= \frac{1}{2\pi} \int_{-\pi}^{\pi} f_1(e^{i\omega'T}) f_2(e^{i\omega'T}) * d\omega'$$
(3.6)

where * denotes the complex conjugate. The norm of $f_1(z)$ is defined as

$$\|f_1(z)\| = \sqrt{\langle f_1(z) f_1(z)\rangle}$$

The filters are said to be orthonormal if they satisfy the property

$$\langle f_1(z), f_2(z)\rangle = 0$$

$$\|f_1(z)\| = \|f_2(z)\| = 1$$

A stable system, $G(q)$, can be approximately represented by a finite–length generalized Fourier series expansion as:

$$G(q) = \sum_{i=1}^{n} l_i f_i(q)$$
(3.7)

where $\{l_i\}$, $i =1, 2, \ldots, n$ are the model parameters, n is the number of parameters, and $f_i(q)$ are the orthonormal basis filters for the system $G(q)$.

3.9.1 Types of Orthonormal Basis Filters

There are various types of orthonormal basis filters. The selection of an appropriate type of filter for a given system is one of the most important steps in OBF model development. The different types of filters are discussed in this section.

3.9.1.1 Laguerre Filter

The Laguerre filters are first-order lag filters with one real pole. They are, therefore, more appropriate for well damped processes [2, 20, 44]. The Laguerre filters are given by

$$f_i = \sqrt{(1-p^2)} \frac{(1-pq)^{i-1}}{(q-p)^i}, \quad |p| < 1 \tag{3.8}$$

where p is the estimated pole which is related to the time constant, τ, of the system by

$$p = e^{-(T_s/\tau)} \tag{3.9}$$

3.9.1.2 Kautz Filter

Kautz filters allow the incorporation of a pair of conjugate complex poles. They are, therefore, effective for modeling weakly damped processes [2, 8, 20]. The Kautz filters are defined by

$$f_{2i-1} = \frac{\sqrt{(1-a^2)(1-b^2)}}{q^2 + a(b-1)q - b} g(a,b,q,i) \tag{3.10a}$$

$$f_{2i} = \frac{\sqrt{(1-b^2)}(q-a)}{q^2 + a(b-1)q - b} g(a,b,q,i) \tag{3.10b}$$

where

$$g(a,b,q,i) = \left(\frac{-bq^2 + a(b-1)q + 1}{q^2 + a(b-1) - b} \right)^{i-1} \tag{3.10c}$$

$-1 < a < 1$ and $-1 < b < 1$ $n = 1, 2, \ldots$

3.9.1.3 Generalized Orthonormal Basis Filter

Van den Hof *et al.* [46] introduced the generalized orthonormal basis filters and showed the existence of orthogonal functions that, in a natural way, are generated by stable linear dynamic systems and that form an orthonormal basis for the linear signal space ℓ_2^n. They showed that pulse, Laguerre and Kautz filters are generated from inner functions and their minimal balanced realizations. Ninness and Gustafsson [88] unified the construction of orthonormal basis filters. The GOBF filters are formulated as

$$f_i(q,p) = \frac{\sqrt{1-|p_i|^2}}{(q-p_i)} \prod_{j=1}^{i-1} \frac{(1-p_j^* q)}{(q-p_j)} \qquad (3.11)$$

where $\boldsymbol{p} \equiv \{p_j : j = 1, 2, 3, \dots\}$ is an arbitrary sequence of poles inside the unit circle appearing in complex conjugate pairs.

3.9.1.4 Markov-OBF

When a system involves time delay and an estimate of the time delay is available, Markov-OBF can be used. The time delay in Markov-OBF is included by placing some of the poles at the origin [8]. For a SISO system with time delay equal to d samples, the basis function can be selected as:

$$f_i = z^{-i} \text{ for } i = 1, 2, \dots, d \qquad (3.12a)$$

$$f_{i+d}(q,p) = \frac{\sqrt{1-|p_i|^2}}{(q-p_i)} \prod_{j=1}^{i-1} \frac{(1-p_j^* q)}{(q-p_j)} z^{-d} \text{ for } i = 1, 2, \dots, N \qquad (3.12b)$$

Patwardhan and Shah [8] presented a two-step method for estimating time delays from step response of GOBF models. In the first step, the time delays in all input-output channels are assumed zero and the model is identified with GOBF. In GOBF models, the time delay is approximated by a non-minimum phase zero and the corresponding step response is an inverse response. The time delay is then estimated from a tangent drawn at the point of inflection.

3.9.2 Estimation of GOBF Poles

Finding an appropriate estimate of the poles for the filters is an important step in estimating the parameters of the OBF models. Arbitrary choice of poles may lead to a non-parsimonious model. Van den Hof *et al.* [92] showed that for a SISO system with poles $\{a_j : |a_j| < 1 \text{ for } j = 1, 2, \dots, n\}$, the rate of convergence of the model parameters is determined by the magnitude of the slowest Eigen value.

$$\rho = \max_j \prod_{k=1}^{n} \left| \frac{a_j - p_k}{1 - \overline{p}_k a_j} \right| \qquad (3.13)$$

where p_k = arbitrary poles.

Therefore, a good approximation by a small number of parameters can be obtained by choosing a basis for which ρ is small. It is shown that the poles determined by Van den Hof *et al.* method closely match the dominant poles of the system [8, 20, 48, 92].

3.9.3   Model Parameter Estimation

In using OBF models, the output can be expressed as a linear combination of the input sequence filtered by the respective filters. Expanding (3.7)

$$\hat{y}(k) = l_1 f_1(q)u(k) + l_2 f_2(q)u(k) + \dots + l_n f_n(q)u(k)$$

(3.14)

Equation (3.14) is not linear in its parameters and therefore estimation of parameters is not a simple task. However, (3.14) can be modified such that it is linear in parameters, as

$$\hat{y}(k) = l_1 u_{f1}(k) + l_2 u_{f2}(k) + \dots + l_n u_{fn}(k)$$

(3.15)

where $u_{fi}(k)$ is the filtered input given by

$$u_{fi}(k) = f_i(q)u(k)$$

(3.16)

Once the dominant poles of the system and the types of filters are chosen, the filters $f_1,\ f_2,\ \dots, f_n$ are fixed. The filtered input, u_{fi}, is determined by filtering the input sequence with the corresponding filter.

For an OBF model with n parameters, naturally, the prediction can be started from the nth instant in time. Equation (3.15) can be expanded and written in matrix form as

$$
\begin{bmatrix}
\hat{y}_{n+1} \\
\hat{y}_{n+2} \\
. \\
. \\
. \\
\hat{y}_N
\end{bmatrix}
=
\begin{bmatrix}
u_{f1}(n) & u_{f2}(n-1) & \dots & u_{fn}(1) \\
u_{f1}(n+1) & u_{f2}(n) & \dots & u_{fn}(2) \\
. & . & & . \\
. & . & & . \\
. & . & & . \\
u_{f1}(N-1) & u_{f2}(N-2) & \dots & u_{fn}(N-n)
\end{bmatrix}
\begin{bmatrix}
l_1 \\
l_2 \\
. \\
. \\
. \\
l_n
\end{bmatrix}
$$

(3.17)

where N is the future time instant.

Equation (3.17) in vector-matrix notation is given by

$$\hat{y} = X\theta$$

(3.18)

where $\boldsymbol{\theta} = [l_1,\ l_2,...,l_n]^T$ is the parameter vector, $\hat{\boldsymbol{y}}$ is the output vector $\hat{\boldsymbol{y}} = [y_n\ \hat{y}_{n+1},...,\hat{y}_N]$ and X is the regressor matrix given by

$$X = \begin{bmatrix} u_{f1}(n) & u_{f2}(n-1) & ... & u_{fm}(1) \\ u_{f1}(n+1) & u_{f2}(n) & ... & u_{fm}(2) \\ . & . & & . \\ . & . & & . \\ . & . & & . \\ u_{f1}(N-1) & u_{f2}(N-2) & ... & u_{fm}(N-n) \end{bmatrix} \qquad (3.19)$$

Since (3.18) is linear in parameters, the model parameters can be estimated using linear least square formula (3.20).

$$\hat{\boldsymbol{\theta}} = (\boldsymbol{X}^T \boldsymbol{X})^{-1} \boldsymbol{X}^T \boldsymbol{y} \qquad (3.20)$$

3.10 Development of FOPTD model from OBF model

Parsimonious OBF models can be developed from arbitrary set of poles by first developing an OBF model and estimating the dominant poles of the system from its noise free step response. Then these dominant poles can be used instead of the arbitrary poles to develop parsimonious OBF models. A typical step response of an OBF model for a well damped system is shown in Figure 3.1.
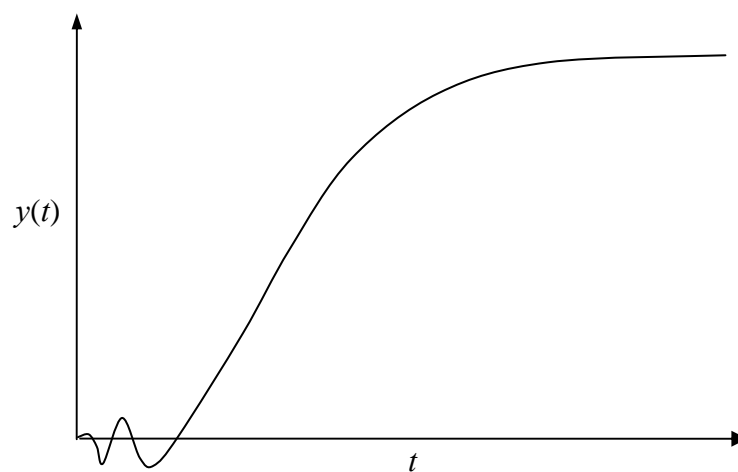
Figure 3.1 Typical step response of an OBF model for a well damped system

This process can be repeated iteratively to get more accurate parsimonious OBF model. For a well damped system, estimate of one dominant pole and time delay of the system can be obtained by developing a FOPTD model from the step response of the OBF model. It is observed from Figure 3.1 that time delay in OBF models are estimated by non-minimum phase zero and the step response appears as an inverse response. Three different approaches are compared to develop FOPTD models from the step or impulse response of OBF models and they are discussed in the following sections.

3.10.1 Estimation of FOPTD parameters

The transfer function of a FOPTD model is given by

$$G(s) = \frac{Ke^{-\tau_d s}}{\tau s + 1}$$

(3.21)

The parameters of the FOPTD models are estimated from the step or impulse response of the OBF model. Three different methods, namely, the moment, the tangent and interpolation methods are compared.

3.10.1.1   Moment method

The moment method for estimation of model parameters from impulse response is discussed in detail in [34]. In this section, estimation of FOPTD model parameters is discussed. The jth moment and normalized moment of the impulse-response function $g(t)$ is defined by (3.22) and (3.23), respectively

$$m_j = \int_0^\infty t^j g(t) dt$$

(3.22)

$$\mu_j = \frac{m_j}{m_0}$$

(3.23)

The parameters of FOPTD model are estimated from the moments of the impulse response $g(t)$ by (3.23)-(3.26).

$$K = m_0$$

(3.24)

$$\tau = \mu_2 - \left(\mu_1\right)^2$$

(3.25)

$$\tau_d = \mu_1 - \tau$$

(3.26)

3.10.1.2   Tangent Method

In the tangent method, the gain of the system is first estimated from the step response of the model using

$$K = \lim_{s \to 0} G(s)$$
(3.27)

The time constant and the time delay can be estimated from the tangent line drawn at the point of inflection on the normalized response curve as shown in Figure 3.2.
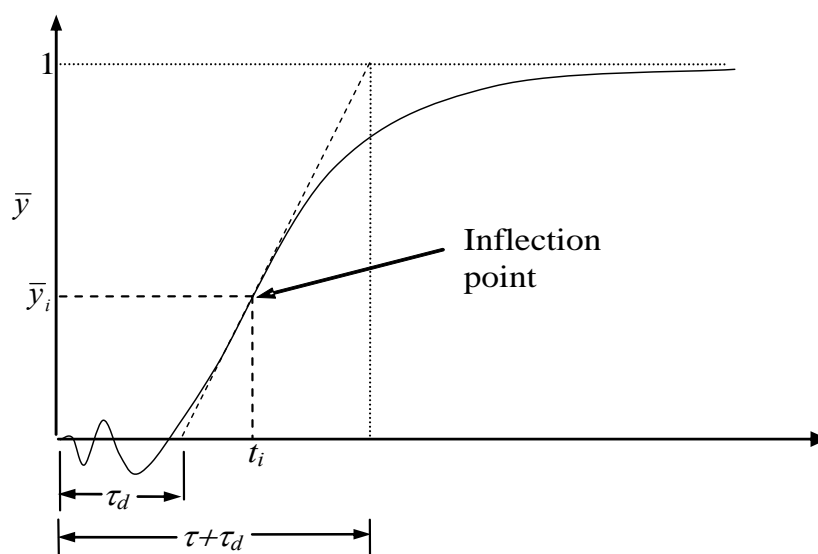
Figure 3.2 Determination of FOPTD parameters using the tangent method

The inflection point is the point at which the tangent to the step response curve attains the maximum slope. It can be easily found by determining the instant of maximum slope, i.e., by filtering the step response $y(k)$ with the filter given in (3.28) and finding the value of k at which Δy is maximum.

$$\Delta y = (1 - q^{-1})y(k)$$
(3.28)

Since the tangent is a translated function of a straight line passing through the origin, its equation for the tangent line is given by

$$\bar{y} = a_i(t - \tau_d)$$
(3.29)

where a_i is the slope at the inflection point and τ_d is the time delay. From the inflection point (t_i, y_i), τ_d is determined as

$$\tau_d = t_i - \frac{\bar{y}_i}{a_i}$$

(3.30)

The time constant is estimated from the inverse of the slope a_i as

$$\tau = \frac{1}{a_i}$$

(3.31)

Equations (3.27), (3.30) and (3.31) define the FOPTD model by the tangent method.

3.10.1.3   The interpolation method

The interpolation method is the simplest of the three methods. First, the time delay is estimated using (3.30) of the tangent method. The time constant is determined from the response time at which $\bar{y} = 0.632$. This method is found effective if the procedure is applied at several points and the average of the estimates of the time constants is taken as the estimate of the time constant. To find the average of the estimated time constants at several points, the following procedure is used.

The step response of FOPTD model is given by

$$\bar{y} = 1 - e^{-(t-\tau_d)/\tau}$$

(3.32)

For $t = \alpha\tau + \tau_d$ (3.32) becomes,

$$\bar{y}_\alpha = 1 - e^{-\alpha}$$

(3.33)

For a given $\bar{y}_\alpha$, the response time t_α is obtained using interpolation from the normalized response curve.

The time constant at $t = t_\alpha$

$$\tau = \frac{t_\alpha - \tau_d}{\alpha}$$

(3.34)

The mean time constant can be estimated by

$$\tau = \frac{\sum_{i=1}^{n}(t_{\alpha i} - \tau_d)}{\sum_{i=1}^{n}\alpha_i}$$

(3.35)

It is observed that values of α between 0.8 and 2 gives good results. From several simulation studies it is also observed that the third method is more reliable and gives more accurate estimate than the other two.

3.10.2 Estimation of the dominant time constant

It is already pointed out that to develop parsimonious OBF models, it is essential to get good estimate of one or more of the dominant poles of the system. For systems that have well damped second order or higher order dynamics with one dominant time constant, the time constant estimated by the proposed interpolation method is close to the dominant time constant. This is based on the fact that in systems that have only one dominant time constant the contribution of the other time constants dies out quickly and the time constant which is estimated by the interpolation method will be close to the dominant time constant. Therefore, once estimate of the dominant time constant is obtained by the proposed method, the discrete dominant pole is easily calculated using (3.9).

3.10.3 Simulation Studies

The purpose of the case study in this section is to show that a well damped higher order system can be effectively approximated by a FOPTD model using the proposed interpolation method from a noisy identification data with an arbitrary initial pole of the OBF model. The dominant pole and the time delay can then be determined from the estimated FOPTD model. The system is represented by a fourth order transfer function plus time delay and unmeasured disturbance, given by

$$Y(s) = \frac{10e^{-12s}}{(16s+1)(1.5s+1)(s+1)(0.5s+1)}U(s) + \frac{1}{2.5s+1}E(s) \qquad (3.36)$$

where $U(s)$ and $E(s)$ is the are the plant input and white noise, respectively.

The four poles of the system are -1/16, -1/1.5, -1 and -1/0.5. The corresponding discrete poles of the input transfer function are 0.9394, 0.5134, 0.3679 and 0.1353. The dominant pole obviously is 0.9394 which corresponds to the dominant time constant of 16. The identification data is shown in Figure 3.3.
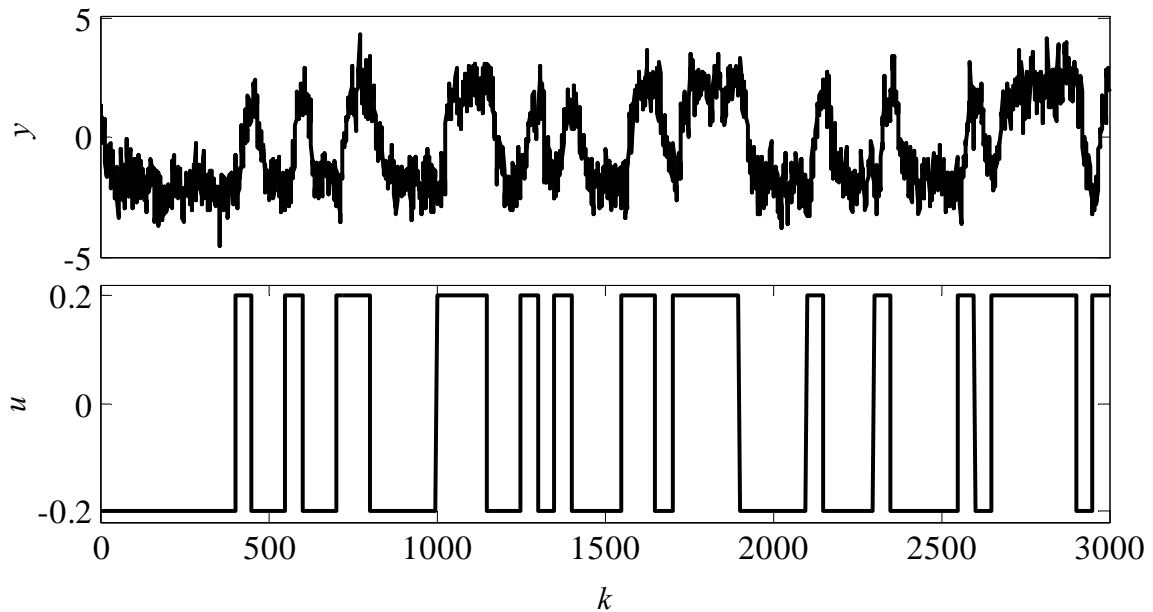
Figure 3.3 Input-output data used for identification of system (3.36)

For the purpose of identification, a PRBS signal generated with the MATLAB function *'idinput'* of band [0 0.02] is introduced into the system. The output of the system is corrupted with unmeasured disturbance whose input is a white noise of mean 0.0126 and standard deviation of 0.5979. The signal to noise ratio (SNR) is 7.7356. Four thousand data points are generated using SIMULINK and 3000 of them are used for modeling and the remaining for validation. An OBF model with 12 Laguerre filters and a crude estimate of the dominant pole of 0.8187 corresponding to a time constant of 5 is developed. The parameters of the OBF model are

l =[0.0051   0.7205   1.1478   0.9917 -0.0253   0.0339   0.3872 -0.1978   0.1545
   -0.0393   0.0221   0.0121];

τ_d =14 (discrete)

The step response of the OBF model and the system are shown in Figure 3.4.
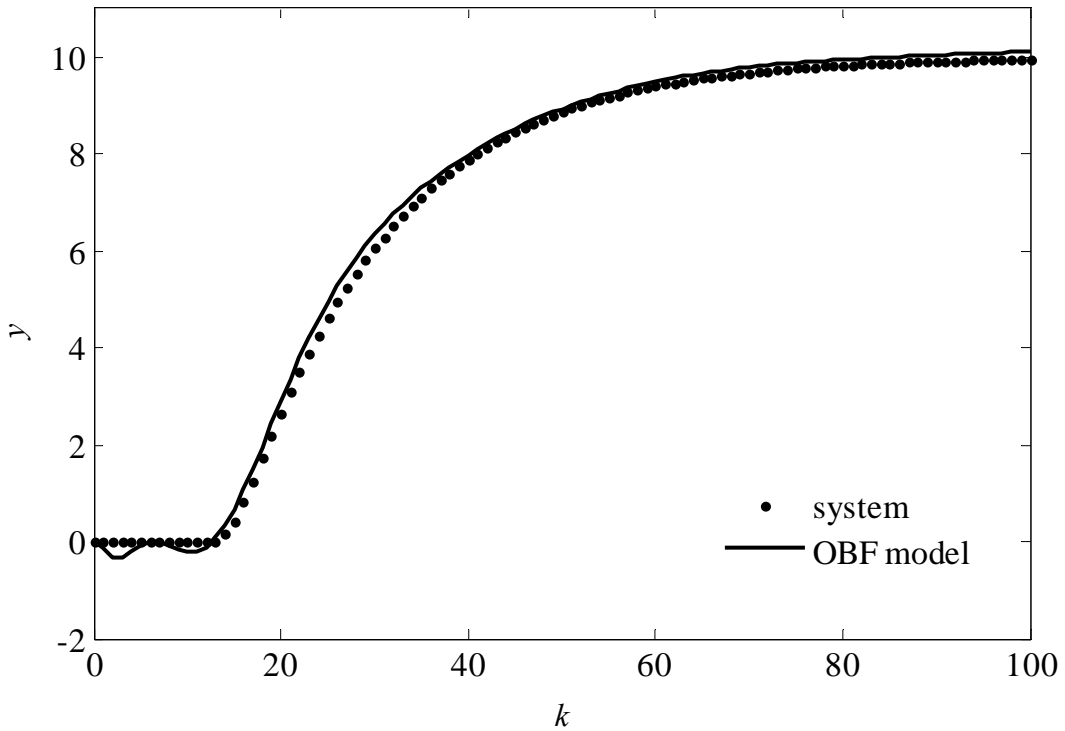
Figure 3.4 Step responses the OBF model compared to the system (3.36)

A FOPTD model is developed from the step response of the OBF model by the proposed interpolation method. The estimated FOPTD model is given by

$$\hat{G}(s) = \frac{10.17e^{-13.9}}{16.8s+1} \qquad (3.37)$$

The step responses of the OBF model and the FOPTD model given by (3.37) are shown in Figure 3.5. It is observed from the figure that the FOPTD model closely matches the OBF model.

It is also observed from (3.37) that the time constant and the time delay estimates are close to the dominant time constant and time delay of the system 16 and 12, respectively. The corresponding dominant discrete pole of the system for sampling interval of 1 time unit is 0.9414. The simulation study shows that a FOPTD model that approximate a well damped higher order system that has one dominant pole can be effectively developed from the noise free OBF model, which itself is developed from the noisy identification data. It also shows that the time constant and time delay estimates of the FOPTD model are close to the dominant time constant and time delay of the system.
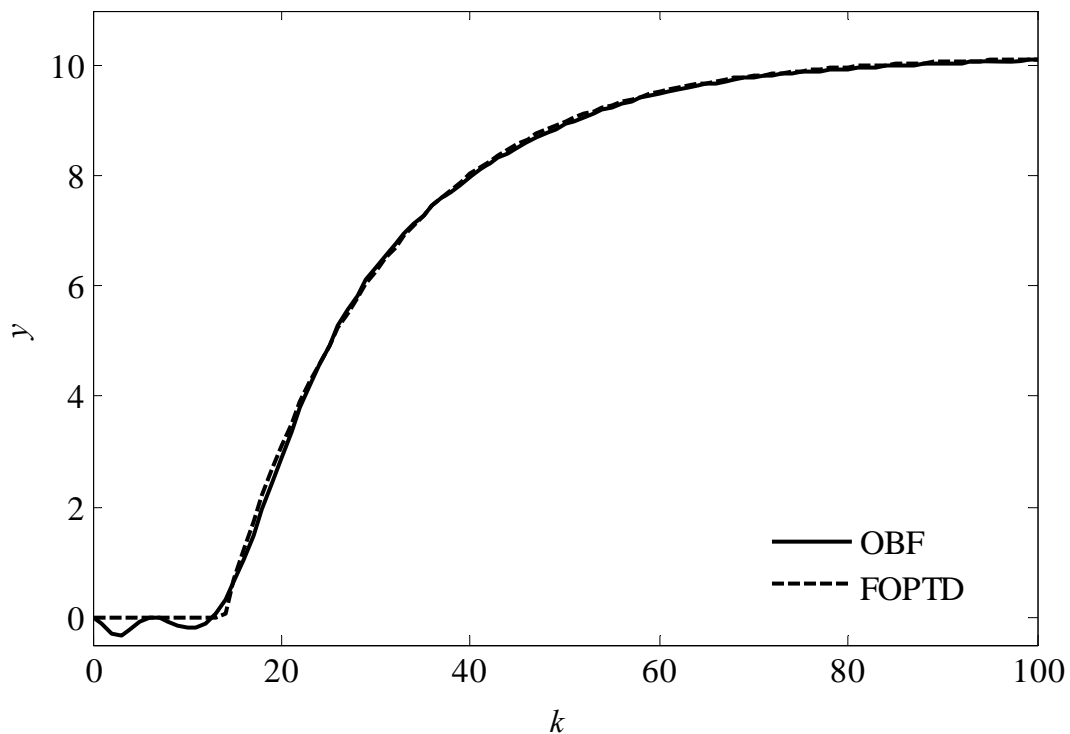
Figure 3.5 Step responses of the OBF and estimated FOPTD model of system (3.36)

3.11   Development of SOPTD model from OBF models

Second order plus time delay (SOPTD) model can be similarly developed from the noise-free OBF model. As it is already pointed out, the time delay in OBF models is approximated by non-minimum phase zeros. Because of this approximate nature of the time delay, current methods of developing a SOPTD model from step response of OBF models are not effective. The two commonly used methods for development of SOPTD model from the step response of linearly approximated systems are the Smith method [9, 99] and the Rangaiah and Krishnaswamy methods [35, 36].

The Smith method is a graphical method of determining the SOPTD parameters from the step response of a system. The time at which the normalized step response reaches 20% (t_{20}) and 60% (t_{60}), with apparent time delay removed, are first determined from the step response data. The value of the damping coefficient, ζ, and τ/t_{60} are then determined from a graph using the ratio t_{20}/t_{60}. From τ/t_{60} and t_{60}, the natural period, τ, is calculated. The method can be used to identify both underdamped and overdamped systems.

Rangaiah and Krishnaswamy [100, 101] proposed various methods for determining the parameters of SOPTD models. For underdamped systems they presented two different methods. The methods are based on finding three points that minimize the integral absolute error (IAE) between the actual response and the step response of a SOPTD model by which the process is to be approximated. Seborg *et al.* [7] indicates that the methods works quite well for the range $0.707 \leq \zeta \leq 3.0$.

The Smith technique has major difficulties in its application. Removing the apparent time delay in finding t_{60} and t_{20} is not a simple task and it is even more difficult for OBF step responses. Graphical method for estimating the apparent time delay is usually inaccurate and the parameter estimation is seriously affected. The Rangaiah and Krishnaswamy method gives good results only in a limited range and, in addition, it doesn't treat both the underdamped and overdamped cases together.

In this section, a novel method for determining the parameters of the SOPTD model is presented. The method is uniquely effective in developing SOPTD models from OBF models. It can be used to identify both underdamped and overdamped second order systems with or without apparent time delay and to approximate a higher order system with a SOPTD model. It eliminates the need of estimating the apparent time delay separately and enables to determine all the parameters including the apparent time delay with high accuracy.

3.11.1 Estimation of SOPTD Model Parameters

In the following part the development of this novel method is discussed. The discussion is based on overdamped response, however, it can be easily shown, the results hold true for underdamped response also without any change.

The transfer function of a second order system with time delay is given by

$$G(s) = \frac{Y(s)}{U(s)} = \frac{Ke^{-\tau_d s}}{\tau^2 s^2 + 2\zeta\tau s + 1} \tag{3.38}$$

where

$K = Gain$

$\tau_d = $ time delay

$\zeta =$ damping coefficient

$\tau =$ natural period of oscillation

3.11.1.1 The Damping Factor

The expression for the normalized step response of an over-damped second order process is given by

$$\bar{y}(t) = 1 - e^{-\frac{\zeta}{\tau}t}\left[\cosh\left(\frac{\sqrt{\zeta^2-1}}{\tau}t\right) + \frac{\zeta}{\sqrt{\zeta^2-1}}\sinh\left(\frac{\sqrt{\zeta^2-1}}{\tau}t\right)\right] \tag{3.39}$$

where $\bar{y}(t) = \dfrac{y(t)}{KM}$ is the normalized response.

Differentiating (3.39) with respect to time and rearranging

$$\frac{d\bar{y}}{dt} = \frac{e^{-\frac{\zeta}{\tau}t}}{\tau\sqrt{\varsigma^2-1}}\sinh(\omega t) \tag{3.40}$$

or using a for slope of the tangent

$$a = \frac{e^{-\frac{\zeta}{\tau}t}}{\tau\sqrt{\varsigma^2-1}}\sinh(\omega t) \tag{3.41}$$

The time to reach the inflection point t_i is found by differentiating (3.41) with respect to time and equating it to zero and solving the resulting equation for t_i. This is based on the fact that the slope of the tangent attains its maximum value at the inflection point. Differentiating (3.41) with respect to time and equating it to zero and rearranging

$$\frac{t_i}{\tau} = \frac{\sinh^{-1}\left(\sqrt{\varsigma^2-1}\right)}{\sqrt{\varsigma^2-1}} \tag{3.42}$$

or

$$\tau = \frac{t_i}{\alpha_1} \tag{3.43}$$

where

$$\alpha_1 = \frac{\sinh^{-1}\left(\sqrt{\varsigma^2 - 1}\right)}{\sqrt{\varsigma^2 - 1}}$$

(3.44)

Evaluating $\bar{y}$ at t_i using (3.39)

$$\bar{y}_i = 1 - e^{-\frac{\varsigma}{\tau}t_i}\left[\cosh\left(\frac{\sqrt{\varsigma^2 - 1}}{\tau}t_i\right) + \frac{\varsigma}{\sqrt{\varsigma^2 - 1}}\sinh\left(\frac{\sqrt{\varsigma^2 - 1}}{\tau}t_i\right)\right]$$

(3.45)

Using (3.43) in (3.45)

$$\bar{y}_i = 1 - e^{-\varsigma\alpha_1}\left[\cosh\left(\alpha_1\sqrt{\varsigma^2 - 1}\right) + \frac{\varsigma}{\sqrt{\varsigma^2 - 1}}\sinh\left(\alpha_1\sqrt{\varsigma^2 - 1}\right)\right]$$

(3.46)

Simplifying and rearranging (3.46) results in

$$\bar{y}_i = 1 - 2\varsigma e^{-\varsigma\alpha_1}$$

(3.47)

Equation (3.47) shows that the normalized response at the inflection point, $\bar{y}_i$, depends only on the damping coefficient. Figure 3.6 shows this relation, $\varsigma = f(\bar{y}_i)$, in a graphical form.
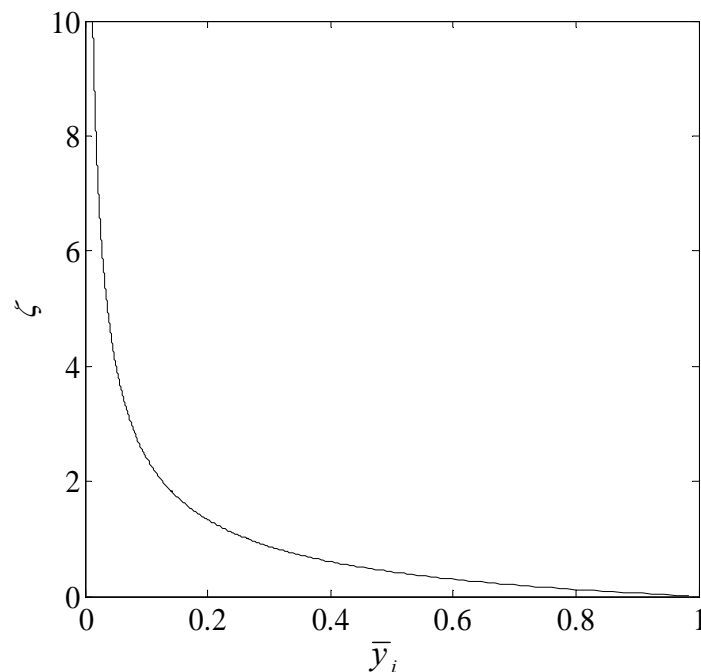
Figure 3.6 Damping coefficient, ς, as a function of the normalized step response at the inflection point, $\bar{y}_i$, for second order processes

If the normalized response at the inflection point is obtained, the damping coefficient can be estimated using (3.47). However, since (3.47) is implicit in ζ, the solution should be obtained either using the graph, Figure 3.6, or a root finding method like false position, bisection or Newton Raphson method. It should be noted that the graph covers both the overdamped and underdamped cases.

It is proposed that the false position method is applied if numerical software packages like MATLAB are used. This is because the method is fast and if any interval containing the root is known finding the root is guaranteed. The following, novel, explicit empirical formula gives a very good first estimate for the damping coefficient as a function of $\bar{y}_i$ and hence the initial interval for the false position method.

$$\zeta_0 = \sqrt{\frac{1.805}{\bar{y}_i} + 1.805} - 1.9 \tag{3.48}$$

The actual damping coefficient ζ is

$$\zeta = \zeta_0 (1 \pm 0.07) \tag{3.49}$$

Therefore the false position method can be easily used with the initial interval given by (3.48). It is observed that only three to four iterations are required to get ζ with acceptable accuracy. If the step response of the system is underdamped an improved result can be obtained by measuring the overshoot. In this case, the following relation can be used,

$$\zeta = \frac{w}{\sqrt{w^2 + \pi^2}} \tag{3.50}$$

where $w = \ln(overshoot)$.

3.11.1.2 The Natural Frequency

An equation relating the natural frequency of a SOPTD model to any time differences and their corresponding values of the normalized step response is derived in this section.

The normalized response for SOPTD model is

$$\bar{y}(t) = 1 - e^{-\frac{\zeta}{\tau}(t-\tau_d)} \left[\cosh\left(\frac{\sqrt{\zeta^2 - 1}}{\tau}(t-\tau_d)\right) + \frac{\zeta}{\sqrt{\zeta^2 - 1}} \sinh\left(\frac{\sqrt{\zeta^2 - 1}}{\tau}(t-\tau_d)\right) \right] \tag{3.51}$$

Note that (3.51) is different from (3.39) because of the time delay term in (3.51).

From (3.51), it is observed that

$$e^{-\frac{t-\tau_d}{\tau}} = f(\bar{y}, \zeta)$$

(3.52)

Since the LHS of (3.52) contains t, τ_d and τ, the remaining variables that determine (3.51) are $\bar{y}$ and ζ, which constitute the RHS of (3.52).

Consider two distinct points, m and n, on the normalized step response curve. The t_m and t_n are the times at which the normalized step response reaches $m\%$ and $n\%$ of the ultimate response, respectively. Applying (3.52) at the points m and n yields

$$e^{-\frac{t_m-\tau_d}{\tau}} = f(\bar{y}_m, \zeta)$$

(3.53)

$$e^{-\frac{t_n-\tau_d}{\tau}} = f(\bar{y}_n, \zeta)$$

(3.54)

Dividing (3.53) by (3.54) and taking the logarithm on both sides

$$\frac{t_n - t_m}{\tau} = \ln\left(\frac{f(\bar{y}_m, \zeta)}{f(\bar{y}_n, \zeta)}\right)$$

(3.55)

If m and n are fixed, the RHS of (3.55) will be a function of ζ only. Rearranging (3.55)

$$\tau = m_1(t_n - t_m)$$

(3.56)

where

$$m_1 = g(\zeta)$$

(3.57)

and $g(\zeta) = \ln\left(\frac{f(\bar{y}_m, \zeta)}{f(\bar{y}_n, \zeta)}\right)$.

Graphical representation of (3.57) is easily generated from the standard response of a second order process by varying ζ while keeping all other parameters constant. Figure 3.7 shows (3.57) in graphical form.
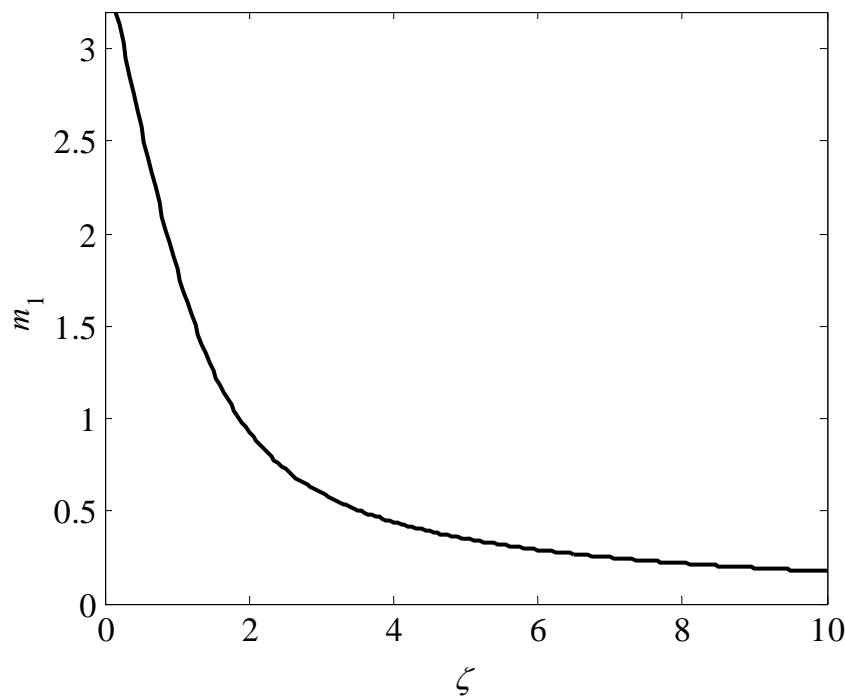
Figure 3.7 Coefficient, m_1, as a function of the damping coefficient

for t_m and t_n equal to t_{20} and t_{40}, respectively

Equation (3.56) and Figure 3.7 are sufficient to determine the natural frequency of the SOPTD transfer function. Since the apparent time delay is cancelled from any difference of response times the result of (3.56) does not depend on the apparent time delay.

3.11.1.3   Estimation of time delay

Figure 3.8 depicts a typical step response of an overdamped second order plus time delay process. The most commonly used method for determining the time delay is the maximum slope method. In this method, a tangent is drawn at the inflection point and the intersection point to the time axis is taken as the approximate value of the time delay. In the proposed method, the time delay by this maximum slope method is divided into two parts: the apparent time delay (τ_d) and the contributed time delay (τ_{dc}) as shown in Figure 3.8. The contributed time delay is that part of the time delay added to the true time delay (apparent time delay) when the tangent method is used due to the sigmoidal nature of the response curves of second and higher order systems. The total time delay (τ_{dt}) determined by the maximum-slope method is the sum of τ_d and the τ_{dc}. Hence, the apparent time delay can be calculated by subtracting the contributed time delay from the time delay determined by the maximum slope method.
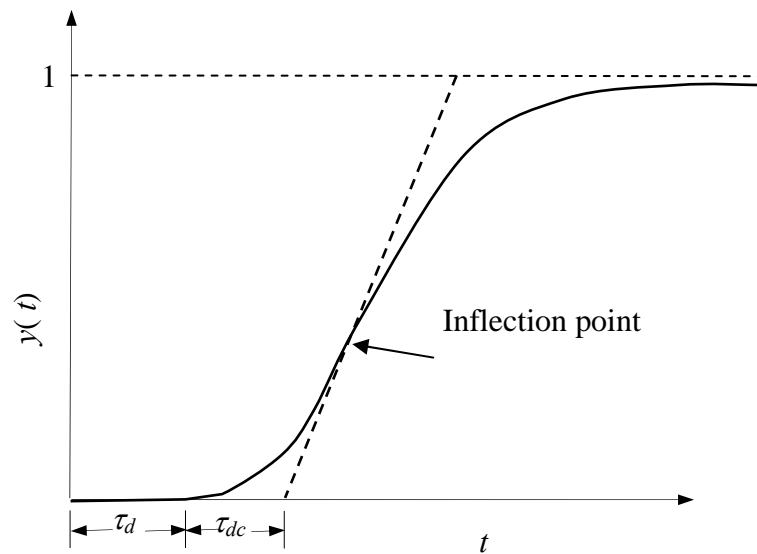
Figure 3.8 Typical step response of an overdamped SOPTD system
with apparent time delay and contributed time delay separated

$$\tau_d = \tau_{dt} - \tau_{dc}$$

(3.58)

Since the contributed time delay does not depend on the pure time delay, it can be calculated from the parameters of the second order transfer function without the apparent time delay. Consider the step response of a second order process without time delay shown in Figure 3.9.
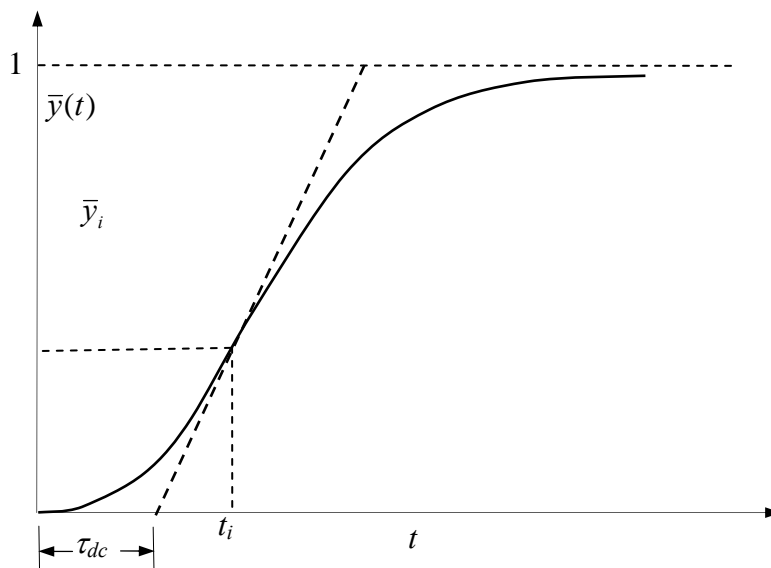
Figure 3.9 Step response of an overdamped second order system
without time delay

In this case, the time delay by the maximum-slope method equals to the contributed time delay since the apparent time delay is zero.

Let $\bar{y}_i$ and t_i be the normalized response at the inflection point and the time to reach the inflection point, respectively, as shown in Figure 3.9. From the equation of the tangent we get,

$$\tau_{dc} = t_i - \frac{\bar{y}_i}{a_i} \tag{3.59}$$

where a_i is the slope of the tangent at the inflection point.

Evaluating the slope given by (3.41) at t_i

$$a_i = \frac{e^{-\frac{\varsigma}{\tau}t_i}}{\tau\sqrt{\varsigma^2-1}}\sinh(\omega t_i) \tag{3.60}$$

Using (3.43) in (3.60)

$$a_i = \frac{e^{-\varsigma\alpha_1}}{\tau\sqrt{\varsigma^2-1}}\sinh\alpha_1\left(\sqrt{\varsigma^2-1}\right) \tag{3.61}$$

or

$$\tau = \frac{\alpha_2}{a_i} \tag{3.62}$$

where

$$\alpha_2 = \frac{1}{\sqrt{\varsigma^2-1}}e^{-\varsigma\alpha_1}\sinh\left(\alpha_1\sqrt{\varsigma^2-1}\right) \tag{3.63}$$

Note that α_2 also depends on ζ only.

Using (3.62) and (3.43) in (3.59)

$$\tau_{dc} = \tau\left(\alpha_1 - \frac{\bar{y}_i}{\alpha_2}\right) \tag{3.64}$$

To avoid error propagation due to using calculated value of τ, we can directly calculate τ_{dc}. Using (3.56) in (3.64) and rearranging

$$\tau_{dc} = m_2(t_n - t_m) \tag{3.65}$$

where

$$m_2 = m_1\left(\alpha_1 - \frac{\bar{y}_i}{\alpha_2}\right) \tag{3.66}$$

In (3.66) m_1 and m_2 depend only on the damping coefficient and since the damping coefficient is a function of $\bar{y}_i$ only, the value in the bracket can be obtained if $\bar{y}_i$ is known. The value of m_2 can be calculated directly or using a graph. Figure 3.10 shows the graphical representation of $m_2 = f(\zeta)$.
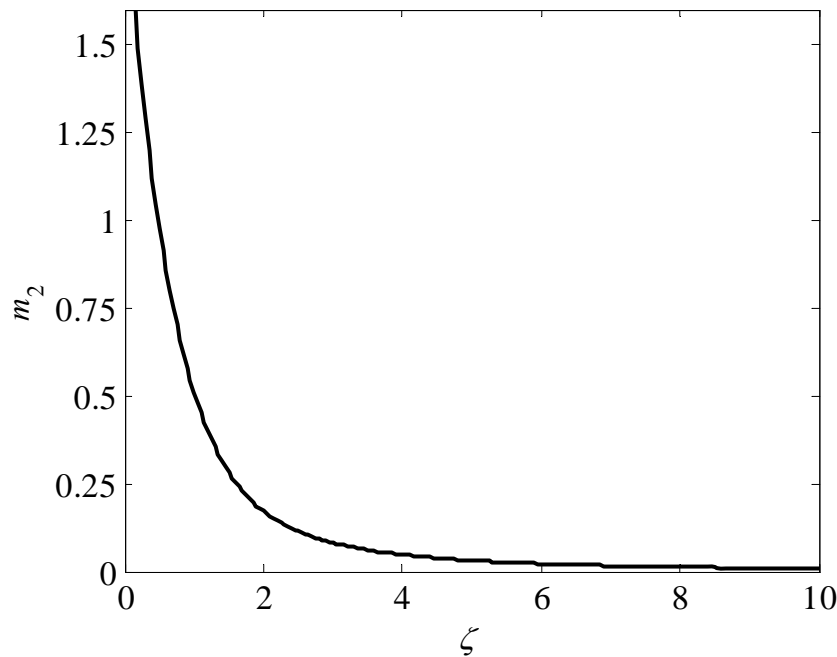
Figure 3.10 Coefficient, m_2, as a function of the damping coefficient
for t_m and t_n equal to t_{20} and t_{40}, respectively

3.11.1.4 Estimation of dominant poles

For systems that are second or higher order dynamics with two dominant poles, the poles estimated by the proposed method are close to the two dominant poles of the system. This is because, if the system has two dominant poles the contribution of the other poles die out quickly and the dynamics of the system is mainly dominated by the two dominant poles.

In summary, once the gain is determined from the ultimate response, the remaining parameters can be easily determined from the normalized step response. The damping coefficient is a function of the value of the normalized response at the inflection point only. It is directly read from Figure 3.6 or determined by root finding method using

(3.47). The natural period and the contributed time delay are calculated from the values of t_{20} and t_{40} using (3.56) and (3.65), respectively. The values of m_1 and m_2 are obtained from Figures 3.7 and 3.10 using the damping coefficient. Step by step description is given in the Algorithm 1. Good estimates of two of the dominant poles of the system are obtained from the two poles of the SOPTD model.

Algorithm 3.1

1. Determine the gain from the ultimate response
2. Determine t_i and $\bar{y}_i$ at the inflection point in the normalized response curve
3. Estimate the total time delay, τ_{dt}, by the tangent method
4. Determine t_n and t_m (e.g. t_{20} and t_{40}) of the normalized response
5. Estimate ζ using Figure 3.6 or solving (3.47)
6. Estimate τ using (3.56)
7. Determine the contributed time delay τ_{dc} using (3.65)
8. Estimate the apparent time delay using (3.58)

3.11.2 Simulation Case Studies

In the previous section, an algorithm is developed to obtain a SOPTD model from the step response of an OBF model. The purpose of the simulation case studies in this section is to demonstrate that an SOPTD model with good accuracy can be developed from a noisy data of a higher order system using the proposed methods and an arbitrarily chosen pair of poles. In addition, it is also shown that the two poles of the estimated SOPTD model are good estimates of the two dominant poles of the system and the estimated time delay is closer to the time delay of the system than the time delay estimate by the tangent method proposed by Patwardhan and Shah [8]. The first and the second case studies consider a well damped and a weakly damped higher-order systems that have two dominant poles, respectively.

3.11.2.1 Identification of a well damped higher order system

The system is represented by the well damped fourth order transfer function and unmeasured disturbance

$$Y(s) = \frac{10e^{-12s}}{(16s+1)(6s+1)(s+1)(0.5s+1)} U(s) + \frac{1}{2s+1} E(s) \qquad (3.67)$$

It can be observed from the transfer function (3.67) that the system has two dominant time constants, 16 and 6. The corresponding dominant poles of the system are -1/16 and -1/6. Since OBF is a discrete time model, the corresponding discrete time dominant poles for a sampling interval of 1 time unit is calculated using (3.9) and their values are 0.9394, 0.8465. The unmeasured disturbance has a transfer function given by the second term of the RHS of (3.67) with white noise $E(s)$ of mean 0.0319 and standard deviation 1.2925 and the SNR is 7.8960. The input output data used for identification is shown in Figure 3.11.
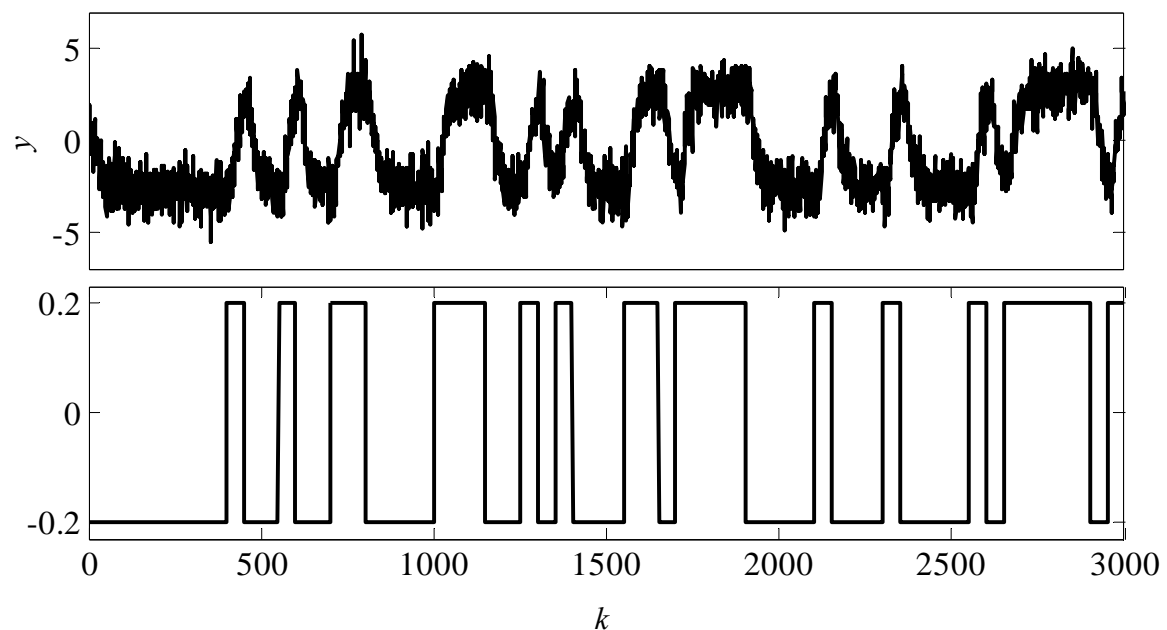
Figure 3.11 Input u(k) and output $y(k)$ used for identification of system(3.67)

An OBF model is developed with 12 parameters and alternating poles of 0.7165 and 0.9672 corresponding to time constants of 3 and 30, which are crude estimates of the dominant time constants. Estimates of the parameters of the OBF model and the time delay are

$l =$ -0.1343   1.1591   0.6331   0.3694   -0.5841   -0.1390   0.3581   -0.0673   0.1021
     0.0021   0.0091   -0.0357]

τ_d=15 (discrete)

The step responses of the system and the OBF model are shown in Figure 3.12.
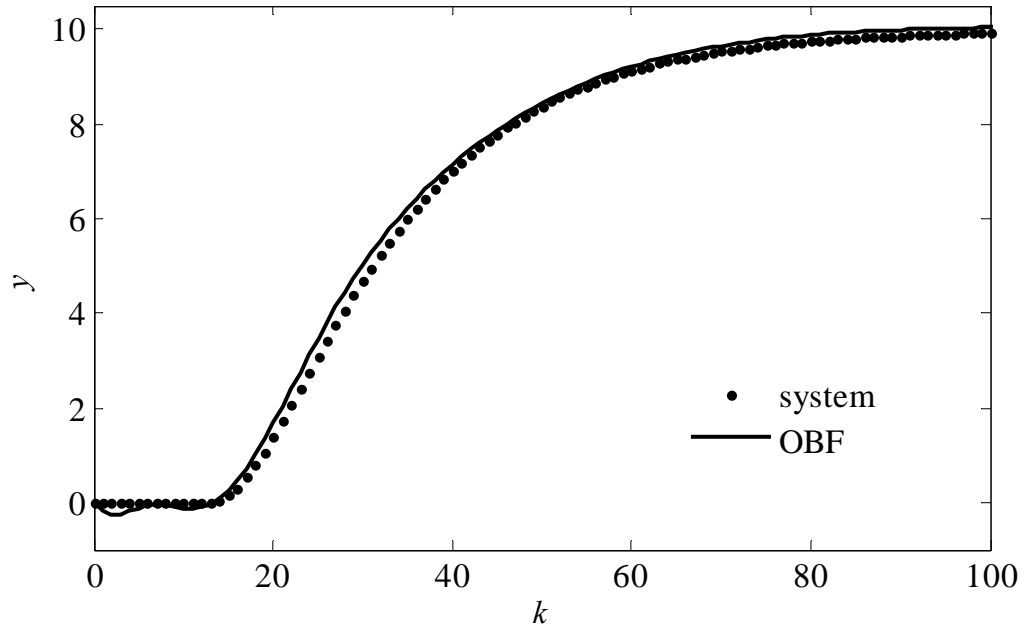
Figure 3.12 Step responses of the system, OBF model and SOPTD model

for system (3.67)

The estimated SOPTD model from the noise free OBF model by the proposed method is

$$\hat{G}(s) = \frac{10.05e^{-13.3s}}{(15.8104s + 1)(5.8730s + 1)} \tag{3.68}$$

The discrete poles of the estimated SOPTD model are 0.9365 and 0.8540. The two discrete poles of the estimated SOPTD model compared, obviously, are close to the dominant poles of the system 0.9376 and 0.8473. The best estimate of the time delay by the tangent method is 16.0386 and the time delay estimated by the proposed method is 13.3. Clearly, the time delay estimate by the proposed method is closer to the true time delay than that estimated by the tangent method. The step response of the OBF model and the estimated SOPTD model are shown in Figure 3.13. It is observed from Figure 3.13 that the SOPTD model approximates the OBF model with good accuracy.
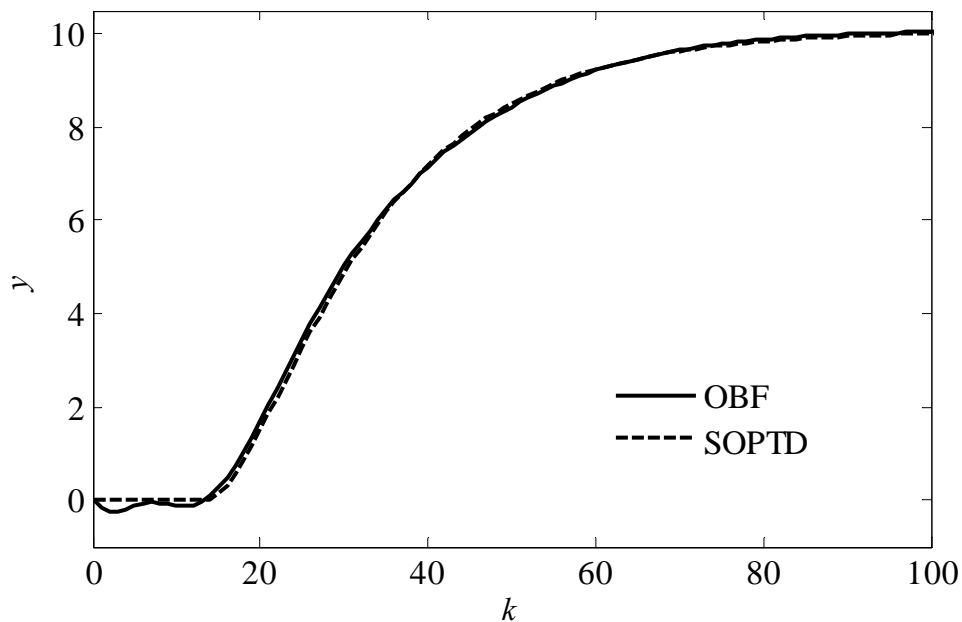
Figure 3.13 Step response of the OBF and SOPTD models for system (3.67)

3.4.2.2 Identification of a weakly damped higher order system

This case study is the extension of the previous case study for a weakly damped system. The transfer function of the system is given by

$$Y(s) = \frac{10e^{-12s}}{(25s^2 + 5s + 1)(s + 1)(0.5s + 1)} U(s) + \frac{1}{2s + 1} E(s) \tag{3.69}$$

The system has a pair of conjugate poles $-0.1000 \pm 0.1732i$ and two real poles -1 and -2. The corresponding discrete poles of the system for a sampling interval of 1 time unit are $0.8913 \pm 0.1559i$, 0.1353 and 0.3679.

A PRBS signal with band [0 0.02] is introduced into the system to generate the identification data. The system output is corrupted with unmeasured disturbance whose input is a white noise signal of mean and standard deviations of 0.0368 and 1.4914, respectively. The signal to noise ratio is 8.3532. The input-output data used for identification is shown in Figure 3.14.
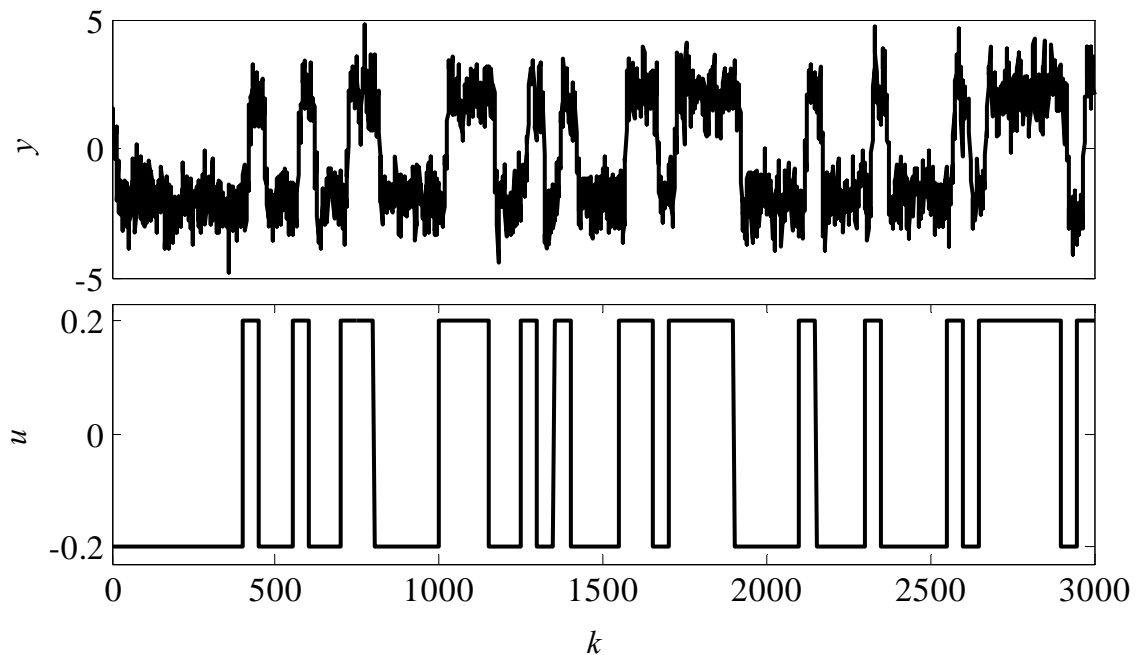
Figure 3.14 Input u(k) and output y(k) used for identification of system(3.69)

An OBF model with twelve parameters and alternating discrete poles of 0.7165 and 0.9672, corresponding to time constants of 3 and 30 with sampling interval of 1 time unit is developed. The poles are purposefully chosen far away from the dominant poles for demonstrating the effectiveness of the system. Estimates of the parameters of the OBF model and the time delay are

l = [1.4029 1.1528 -0.3492 -1.2825 0.2691 1.4680 -0.6332 -0.8240 0.8638 -0.6611
-0.4047   0.6879]

τ_d = 13 (discrete)

SOPTD model is developed from the step response of the estimated OBF model. The step response of the system and the OBF model are compared in Figure 3.15. The estimated SOPTD model from the noise free OBF model by the proposed method is

$$\hat{G}(s) = \frac{10.19e^{-13.2s}}{(26.17s^2 + 5.318s + 1)}$$
(3.70)

The discrete poles of the estimated SOPTD model are $0.8925 \pm 0.1514i$. Compared to the four discrete poles of the system 0.1353, 0.3679, $0.8756 \pm 0.1367i$, the two discrete complex conjugate poles of the estimated SOPTD model are, obviously, close to the dominant complex conjugate poles of the system. The best estimate of the time delay by

the tangent method is 15.2590; the time delay estimated by the proposed method is 13.2, therefore, closer to the true time delay, $\tau_d = 12$, than the estimate by the tangent method. The step response of the OBF model and SOPTD model are shown in Figure 3.16.
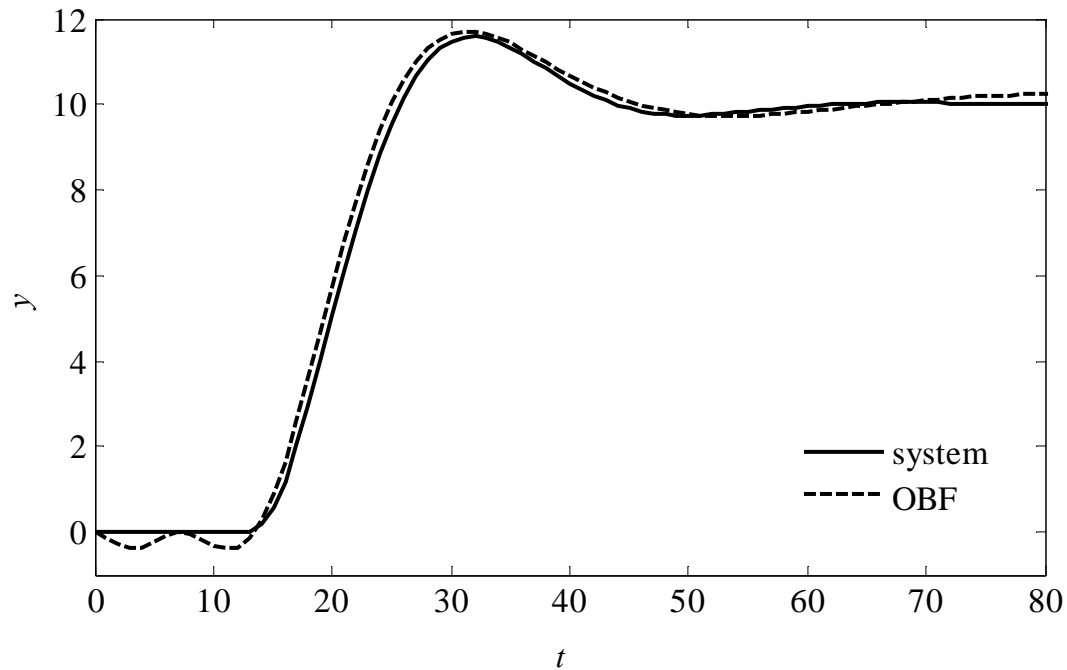
Figure 3.15 Step responses of the system and OBF model for system (3.69)
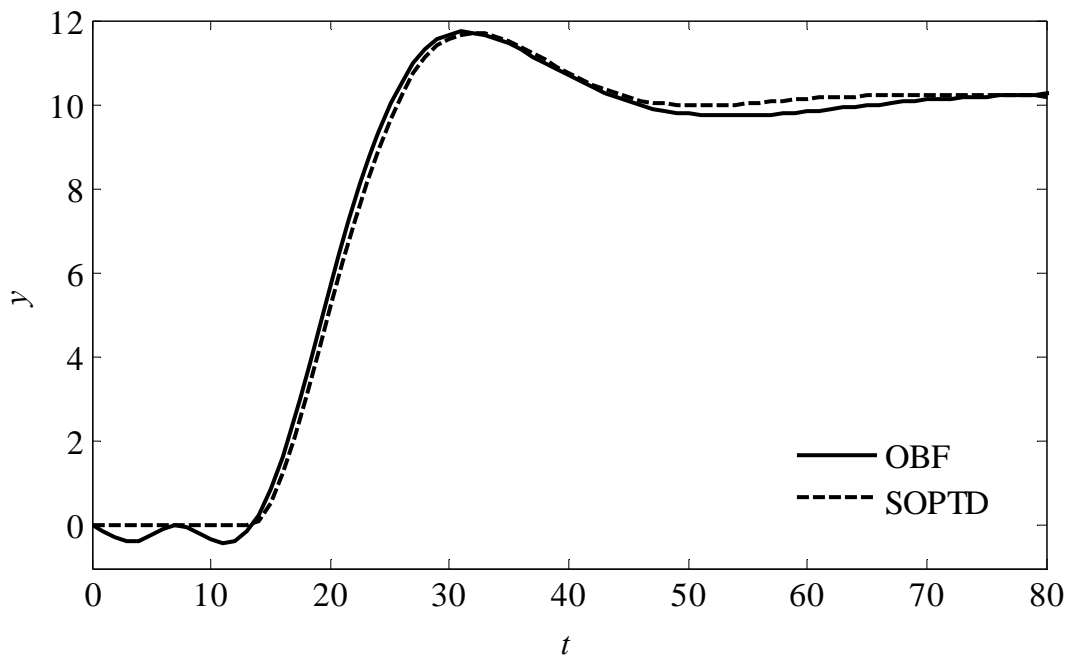
Figure 3.16 Step response of the OBF model and the estimated SOPTD model for system (3.69)

The result of the simulation studies demonstrate that SOPTD model can be effectively developed from the step response of an OBF model that is developed from a noisy data and an arbitrary pairs of poles. It is also shown that the two poles of the SOPTD model are good estimates of the dominant poles of the system and the time delay is closer to the time delay of the system than that estimated by the tangent method proposed by Patwardhan and Shah [8].

3.12 Parsimonious OBF modeling

It is already pointed out in various sections that one of the main advantages of OBF models is the fact that they are parsimonious in parameters. Nevertheless, it is shown that to get parsimonious OBF model, the poles used in the filters must be close to the dominant poles of the system [8, 48, 92]. When the dominant poles of the system are not available and using arbitrarily chosen poles may lead to models that require larger number of parameters to capture the dynamics with reasonable accuracy, i.e., the models will be non-parsimonious. However, there are many situations where it is difficult to get good estimates of the dominant poles of the system directly. One such situation is when there is significant unmeasured disturbance in the system. In the previous sections, two novel schemes were formulated for developing FOPTD and SOPTD models from the step response of a noise free OBF model which, itself, is developed from a noisy identification data and arbitrarily chosen poles. It was also shown that the poles of the FOPTD and SOPTD models are good estimates of the dominant poles of the system. These poles can be used to develop parsimonious OBF model. The iteration continues until the percentage prediction error improvement is small enough.

The proposed iterative scheme is shown in flow chart in Figure 3.17. First, an OBF mode is developed from the identification data using a crude estimate or arbitrarily chosen poles. Then, one or two of the dominant poles of the system are estimated using the methods proposed in the previous sections. The estimated dominant poles are used to develop more accurate OBF model. A better estimate of the dominant poles is obtained from the new OBF model. The process is repeated until a convergence criterion is satisfied. One possible convergence criteria is the improvement in the percentage prediction error. For a fixed number of parameters, the percentage prediction error improves as the estimate of dominant pole is improved.
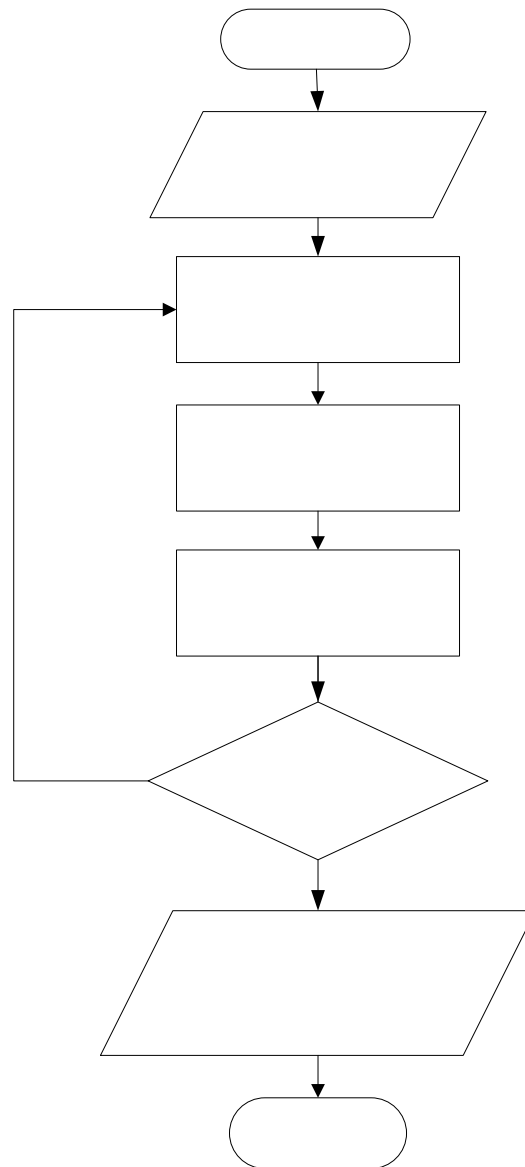
Figure 3.17 Flowchart for developing a parsimonious OBF,

FOPTD or SOPTD model iteratively

3.13   Case Studies

In this section, three full scale system identification case studies for a well damped and a weakly damped higher order systems using the proposed schemes are presented. In the first case study, a well damped fifth order system that has one dominant pole is modeled by parsimonious OBF model using the proposed iterative method based on FOPTD model with an arbitrarily chosen pole. In the second and third case studies a well damped and a weakly damped systems, respectively, are modeled by a parsimonious OBF model using the proposed iterative scheme based on SOPTD model with arbitrarily chosen pair of

poles. The accuracy of the developed OBF models are tested using percentage prediction errors (PPE) and residual analysis. Since, noise model development issues are not yet considered, only white noise is added to the systems so as to make the residual analysis possible. The percentage prediction error is defined as

$$(\text{PPE})_i = \frac{\sum\limits_{i=1}^{n}(y_i(k) - \hat{y}_i(k))^2}{\sum\limits_{i=1}^{n}\left((y_i(k) - \bar{y}_i(k))^2\right)} \times 100 \tag{1.6}$$

where $\bar{y}_i$ represents the mean value of measurements $\{y_i(k)\}$ and $\hat{y}_i(k)$ predicted value of $y_i(k)$.

3.13.1 Identification of well damped system with one dominant pole

In this case study, the system is represented by (3.71)

$$Y(s) = \frac{13.5e^{-12s}}{(18s+1)(1.4s+1)(1.2s+1)(0.6s+1)(0.3s+1)}U(s) + E(s) \tag{3.71}$$

where $E(s)$ is a white noise signal.

The discrete poles of the system, for a sampling interval of 1 time unit are 0.9460 0.4895, 0.4346, 0.1889 and 0.03570. The system is well damped and has one dominant pole 0.9460. Figure 3.18 presents the plot of the input output data used for identification.

Figure 3.18 Input-output data used in identification of system (3.71)

To conduct the identification, a 'PRBS' input signal is introduced to the system with band [0 0.01]. Four thousand data points with sampling time interval of 1 time unit are generated using SIMULNIK and 3000 of these data points are used for identification and the remaining 1000 data points are used for validation. White noise, $e(t)$, with mean and standard deviation of 0.8948 and 0.0221, respectively, is added to the output of the system. The signal to noise ratio is 7.9064.

To choose the number of parameters, first OBF models with 6, 8, 10 and 12 Laguerre filters are developed with an initial pole of 0.3679 corresponding to a time constant of 1 time unit. The pole is chosen purposely far away from the true pole for demonstrating the effectiveness of the proposed iterative scheme. The percentage prediction errors for the four OBF models in three iterations are given in Table 3.1.

Table 3.1 Percentage prediction errors for system (3.71)

iterations	OBF-6	OBF-8	OBF-10	OBF-12
1	30.9343	22.8916	18.1122	14.9787
2	12.7496	10.1990	9.7751	9.5985
3	9.7741	9.7665	9.7468	9.5983

It is observed from Table 3.1 that, although, the percentage prediction error improvements from 6 parameters to 12 parameters OBF models are high at the first and second iterations, at the third iteration the difference is less than 0.2%. Therefore, considering the prediction error improvement to be insignificant compared to the number of parameters difference, OBF model with 6 parameters is chosen to be a parsimonious OBF model with acceptable accuracy

The estimated time constant is 20.75 after three iterations. The dominant pole of the system is estimated to be 0.9643. The final OBF model is developed with 6 Laguerre filters and one pole equal to 0.9643. The estimated OBF parameters and the time delay are

l = [0.3278 1.4428 1.4512 -0.0700 -3.1896e-004 0.1574]

τ_d = 13 sampling intervals

Model Validation

Figure 3.19 depicts the OBF model output and the noisy actual output of the system for the validation data points 3001-4000. The noise free output of the system and the OBF output of the validation data are depicted in Figure 3.20.
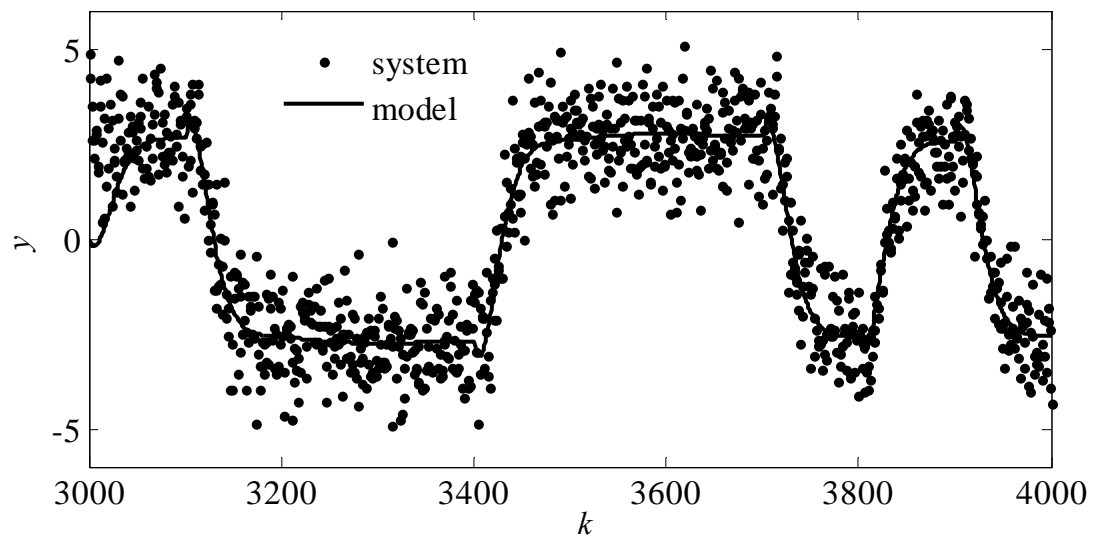
Figure 3.19 Noisy system (3.71) output and the OBF output

for the validation data points
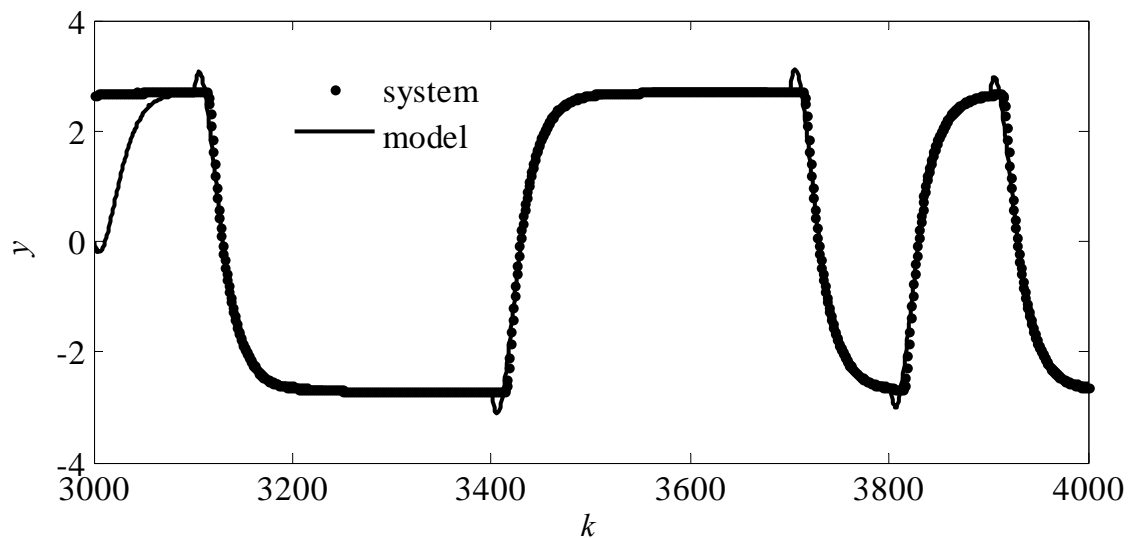
Figure 3.20 Noise free output of system (3.71) and

the OBF predictions of the output

The step responses of the OBF model and the SOPTD estimated model are shown in Figure 3.21.
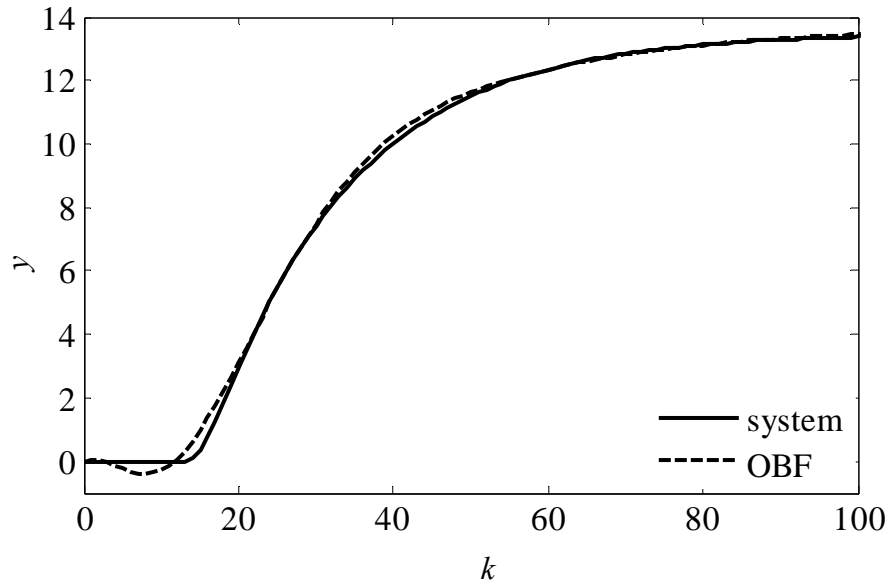
Figure 3.21 Comparison of step responses of the system without noise, the SOPTD model and the OBF model of system (3.71)

3.13.1.1 Residual Analysis

The qq-plot of the residual and the white noise introduced into the system is shown in Figure 3.22.
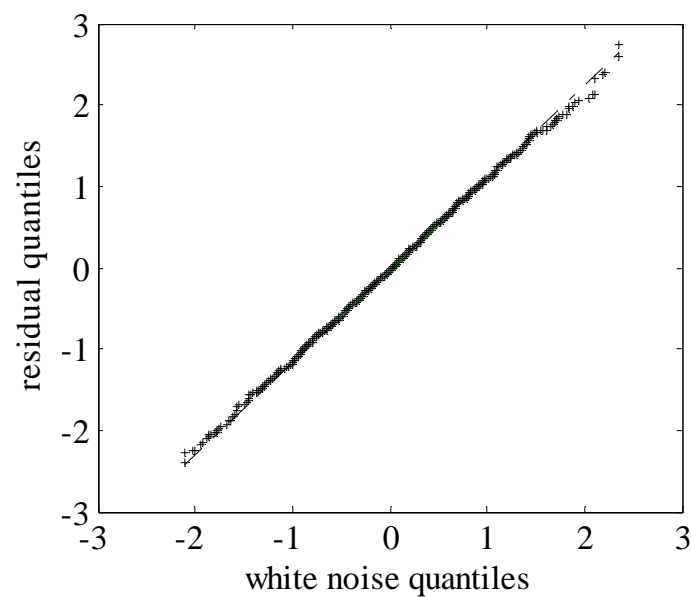
Figure 3.22 qq-plot of the residual and the white noise introduced into system (3.71)

In plotting Figure 3.22, the first 30 residuals are removed because of the initial condition requirement of prediction equations.Figure 3.23 shows the distribution of the residuals compared to the distribution of the white noise added into the system.
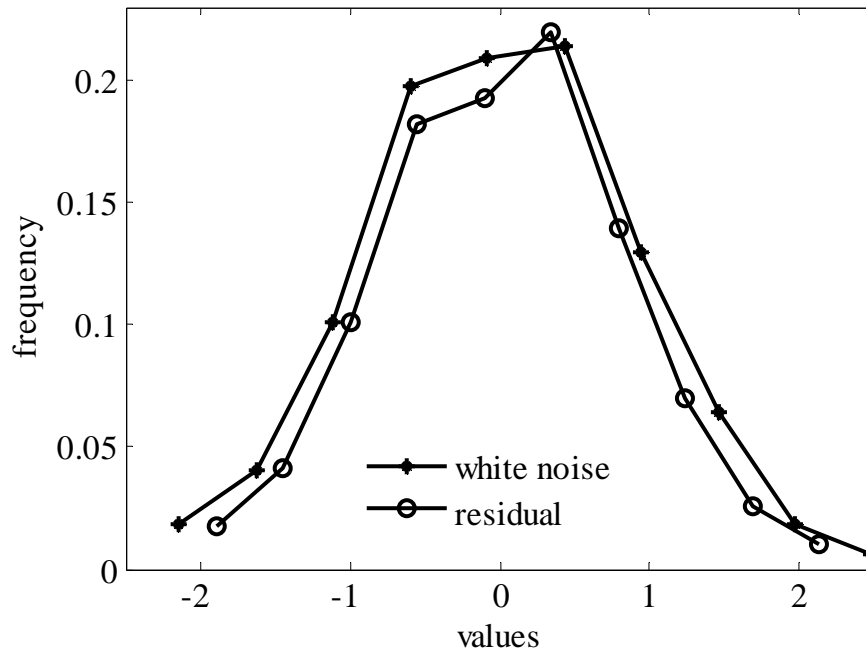
Figure 3.23 Distribution of the residual of the OBF model and the original white noise introduced into the system

Correlation among the residuals is given by

$\hat{R} = $ [-0.0070 0.0093 -0.0148 -0.0044 0.0005 0.0279 -0.0465 -0.0056 0.0401 -0.0132]

This simulation study shows that a parsimonious OBF model can be effectively developed from a noisy identification data and arbitrarily chosen poles using the proposed iterative method based on FOPTD model, for well damped higher order systems that have one dominant pole. The residual analysis results also show that the parsimonious OBF model is accurate enough because the residual of the model is almost the same white noise added to the system. It means, essentially all the dynamics of the deterministic part is captured by the parsimonious OBF model.

3.13.2 Identification of well damped system–two dominant poles

In this case study, the system is represented by (3.72)

$$Y(s) = \frac{11.5e^{-12s}}{(21.5s+1)(12s+1)(0.6s+1)(0.3s+1)}U(s) + E(s) \tag{3.72}$$

where E(s) is a white noise signal.

The discrete poles of the system, for a sampling interval of 1 time unit are 0.9546, 0.9200, 0.1889 and 0.0357. The system is well damped and its two dominant discrete poles are 0.9546 and 0.9200. White noise, $e(t)$, with mean and standard deviation of 0.0147 and 0.5966, respectively, is added to the output of the system. The signal to noise ratio is 8.5225. To conduct the identification, a 'PRBS' input signal is introduced into the system with band [0 0.02]. Four thousand data points, with sampling interval of 1 time unit, are generated using SIMULNIK and 3000 of these data points are used for identification and the remaining 1000 data points for validation. The input-output data used for identification are shown in Figure 3.24.
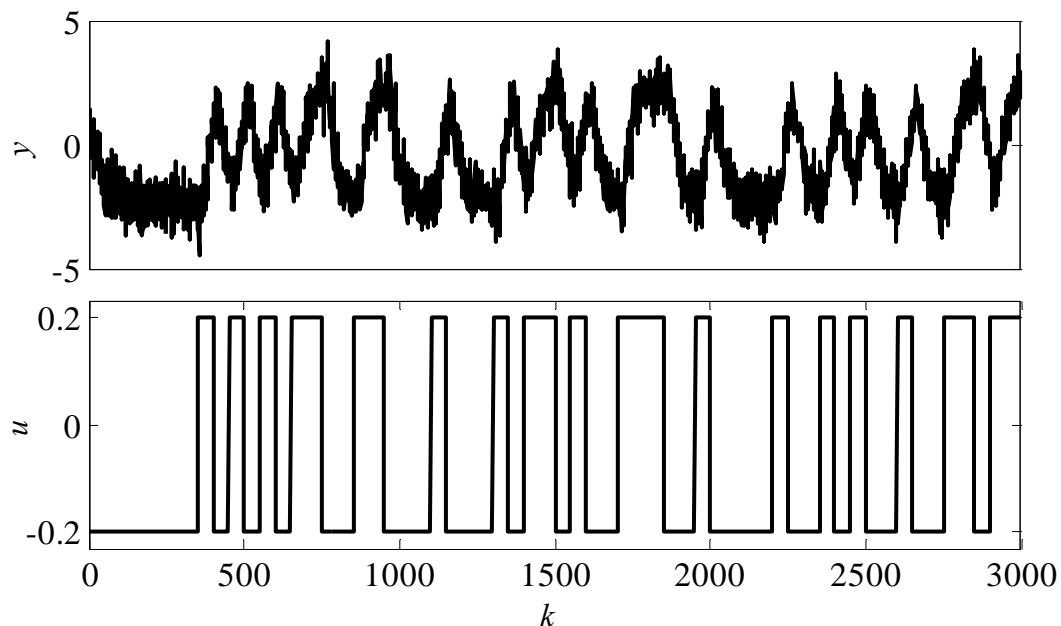
Figure 3.24 Input-output data used in identification for system (3.72)

To choose the number of parameters, OBF models with 6, 8, 10 and 12 GOBF filters are developed with an initial alternating poles 0.3679 and 0.6065 corresponding to time constants of 1 and 2 time units. The poles are purposely chosen far away from the true

pole for demonstrating the effectiveness of the iterative scheme. The percentage prediction errors for the four OBF models after sufficient number of iterations for convergence are given in Table 3.2. It is observed from Table 3.2 that, although, the percentage prediction error improvements from 6 to 12 parameters are high at the first iteration the percentage prediction errors are almost the same after convergence. Therefore GOBF model with six parameters (GOBF-6) is selected to be the parsimonious GOBF model without much compromise on the accuracy.

Table 3.2 Percentage prediction errors of system (3.72)

iterations	GOBF-6	GOBF-8	GOBF-10	GOBF-12
1	54.4639	41.8491	31.4682	23.8351
2	18.6767	22.8638	11.8885	11.9926
3	12.5275	12.0272	11.8553	11.8696
4	11.9232	11.8638	-	11.8657
5	11.8738	-	-	-
6	11.8686	-	-	-

The dominant discrete poles of the system after convergence are estimated to be 0.9433 and 0.9115. The final model is developed with 6 GOBF filters with alternating poles of 0.9433 and 0.9115. The estimated GOBF parameters and the time delay are

l = [0.6730 1.0197 0.5912 -0.4760 0.1321 -0.0759]

τ_d = 14 sampling intervals

Model Validation

Figure 3.25 depicts the GOBF model output and the noisy actual output of the system for the validation data points 3001-4000. The noise free output of the system and the GOBF output of the validation data are depicted in Figure 3.26.
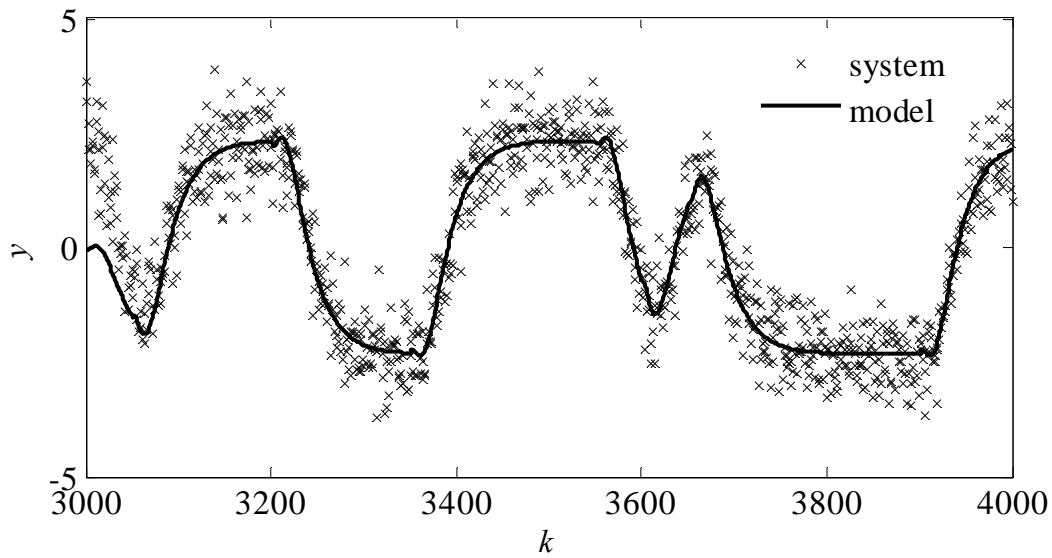
Figure 3.25 GOBF model output and the noisy actual output of the system for the
validation data points of system (3.72)
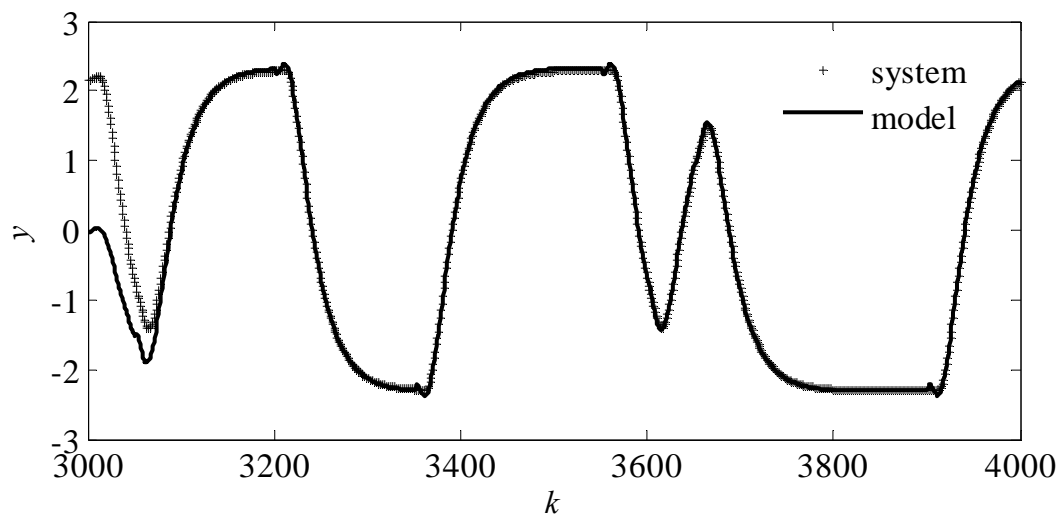
Figure 3.26 Noise free output of the system and the GOBF simulation output
for the validation data of system (3.72)

The step responses of the system (without the noise) and the GOBF model are shown in
Figure 3.27. It is observed from Figure 3.27 that the step response of the parsimonious
GOBF model is very close to the step response of the system.
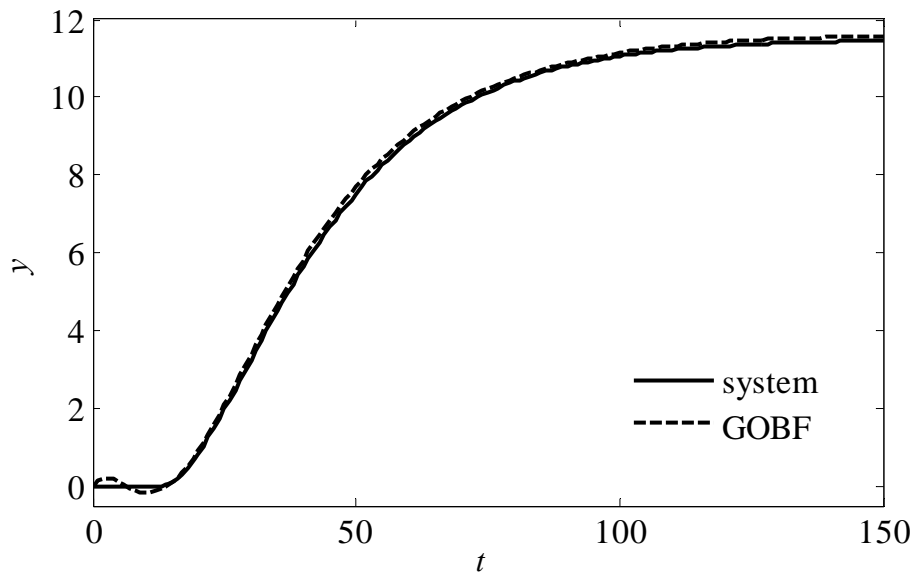
Figure 3.27 Comparison of step responses of system (3.72) without noise

and the corresponding GOBF model

3.13.2.1   Residual Analysis

The qq-plot of the residual and the white noise introduced into the system is shown in Figure 3.28. In plotting Figure 3.28, the first 30 residuals are removed because of the initial condition requirement of prediction equations. Figure 3.29 shows the distribution of the residuals compared to the distribution of the white noise added into the system.
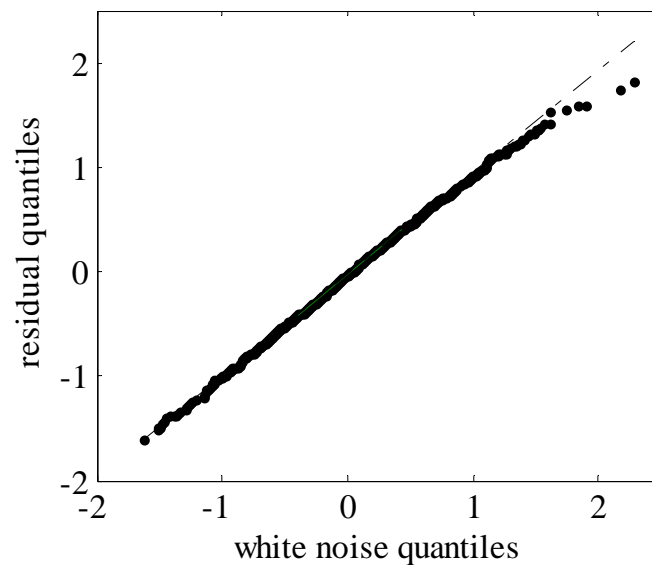
Figure 3.28 qq-plot of the residual and the white noise introduced
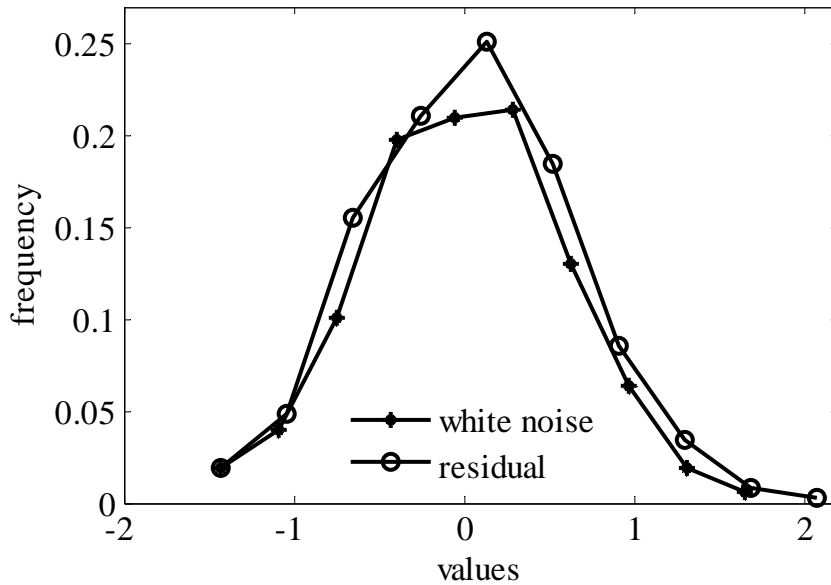
into system (3.72)

Figure 3.29 Distribution of the residual of the OBF model and the original white noise introduced into system (3.72)

Correlation among the residuals is given by

$$\hat{R} = [0.0028 \ 0.0140 \ -0.0019 \ 0.0055 \ 0.0095 \ 0.0284 \ -0.0200 \ 0.0075 \ 0.0379 \ 0.0028]$$

This simulation study shows that a parsimonious OBF model can be effectively developed from a noisy identification data and arbitrarily chosen poles using the proposed iterative method for well damped higher order systems. The residual analysis results also show that the parsimonious OBF model is accurate enough because the residual of the model is almost the same white noise added to the system. It means, essentially all the dynamics of the deterministic part is captured by the parsimonious OBF model.

3.13.3 Identification of weakly damped system

In this simulation study, an underdamped fifth order system with time delay and additive white noise is considered. The transfer function of the system is given by (3.73) with poles, $-0.0667 \pm 0.1528i$, -0.8333, -1.2500 and -1.6667. The corresponding discrete poles for a sampling interval of 1 time unit are $0.9246 \pm 0.1423i$, 0.4346, 0.2865 and 0.1889.

$$Y(s) = \frac{13.5e^{-12s}}{(36s^2 + 4.8s + 1)(1.2s + 1)(0.8s + 1)(0.6s + 1)} U(s) + E(s) \qquad (3.73)$$

The mean and standard deviation of the white noise added to the output of the system has mean and standard deviation of 0.0245 and 0.9943, respectively, and the signal to noise ratio is 8.5755. The input-output data used for model development are shown in Figure 3.30.
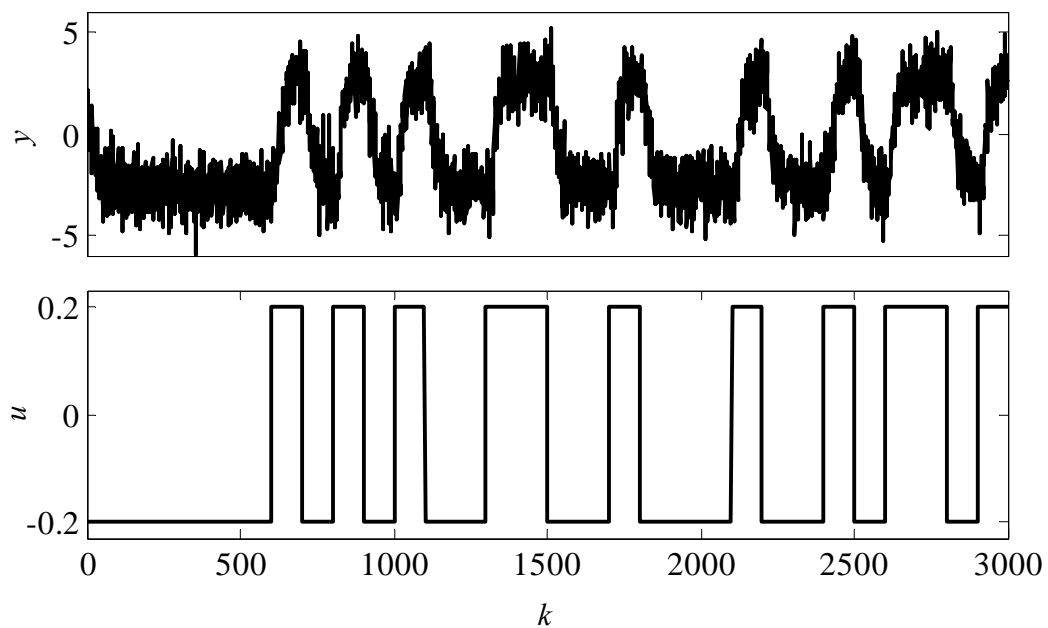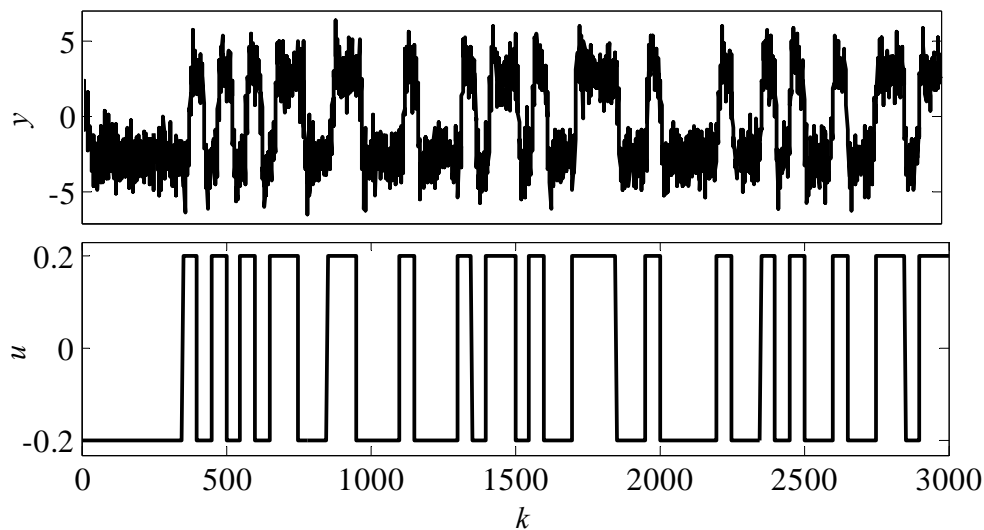

Figure 3.30 Input-output data used in identification of system (3.73)

To conduct the identification, a 'PRBS' input signal is introduced to the system with band [0 0.02]. Four thousand data points are generated using SIMULNIK and 3000 of these data points are used for identification and the remaining 1000 data points are used for validation.

To choose the number of parameters GOBF models with 6, 8, 10 and 12 parameters are developed with an initial discrete alternating poles of 0.3679 and 0.6065 corresponding to a time constant of 1 and 2 time units with sampling interval of 1 time unit. The initial pair of poles is chosen purposely far away from the true poles to show the effectiveness of the iterative scheme. Note that the dominant poles of the system are complex conjugates while the initial poles chosen are real. The percentage prediction errors for the four OBF models in three iterations are given in Table 3.3. It is observed from Table 3.3 that, although, the percentage prediction error has larger variation at the first iteration with increase in number of parameters, after convergence OBF-6 (OBF with 6 parameters) the difference is very small. The improvement in PPE from 6 to 12 parameters is less than 0.5% and it can be considered insignificant. Therefore OBF-6 is chosen as the best

structure since it provides the most parsimonious model without significant compromise on the accuracy.

Table 3.3 Percentage prediction errors for system (3.73)

iterations	OBF-6	OBF-8	OBF-10	OBF-12
1	19.2845	13.9814	13.5539	12.7687
2	14.9182	12.7760	12.3463-	12.2426
3	13.1845	12.5346	-	-
4	12.6423	12.4953	-	-
5	-	12.4885	-	-
6	-	12.4884	-	-

The dominant discrete poles of the OBF-6 model, after convergence, are estimated to be $0.8877 \pm 0.1357i$ at the fourth iteration. The final OBF model is developed with 6 Kautz filters and a pair of complex conjugate poles $0.8877 \pm 0.1357i$. The estimated OBF parameters and time delay are

l = [0.0245 -0.7936 4.1265 0.6691 -0.2770 -0.1524]

τ_d = 14 sampling intervals

The best time delay estimate by the tangent method is 16.8201.

Model Validation

Figure 3.31 depicts the OBF model output and the noisy actual output of the system for the validation data points 3001-4000. The noise free output of the system and the GOBF output of the validation data are depicted in Figure 3.32.
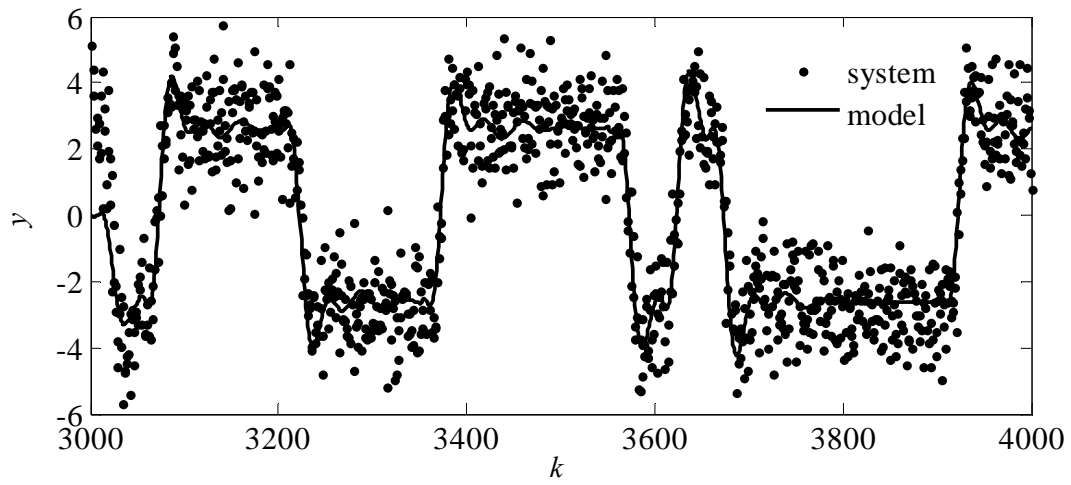
Figure 3.31 GOBF model output and the noisy actual output of the system for the
validation data points of system (3.73)
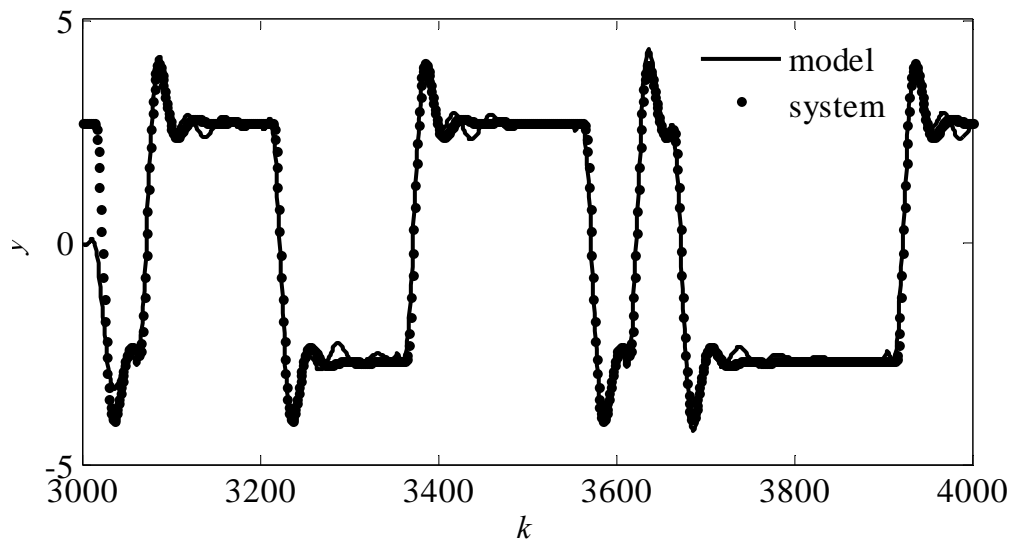
Figure 3.32 Noise free output of the system (3.73) and the GOBF predictions
of the output

The step responses of the system (without the noise) and the parsimonious GOBF model
are shown in Figure 3.33.
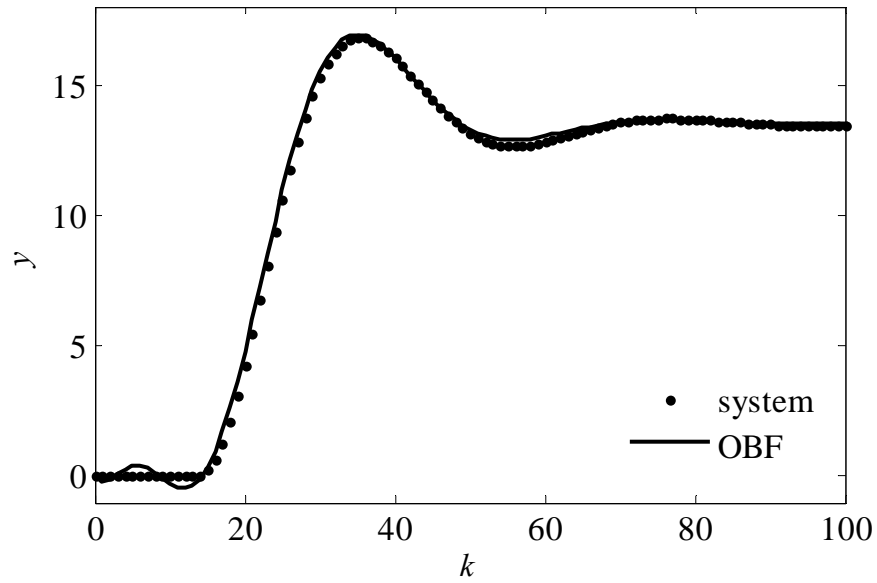
Figure 3.33 Comparison of step responses of system (3.73) without noise

and the OBF model

3.13.3.1   Residual Analysis

The qq-plot of the residual and the white noise introduced into the system is shown in Figure 3.34. In plotting Figure 3.34, the first 30 residuals are removed because of the initial condition requirement of prediction equations.
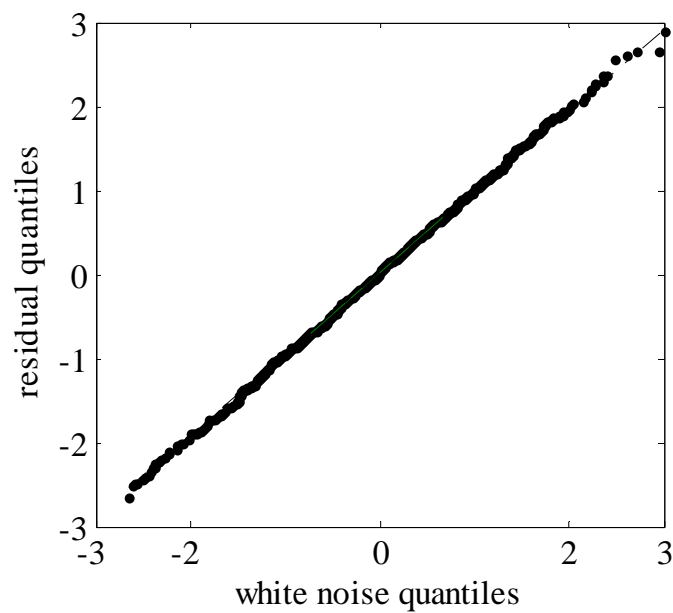
Figure 3.34 qq-plot of the residual and the white noise introduced into system (3.73)

Figure 3.35 shows the distribution of the residuals compared to the distribution of the white noise added into the system.
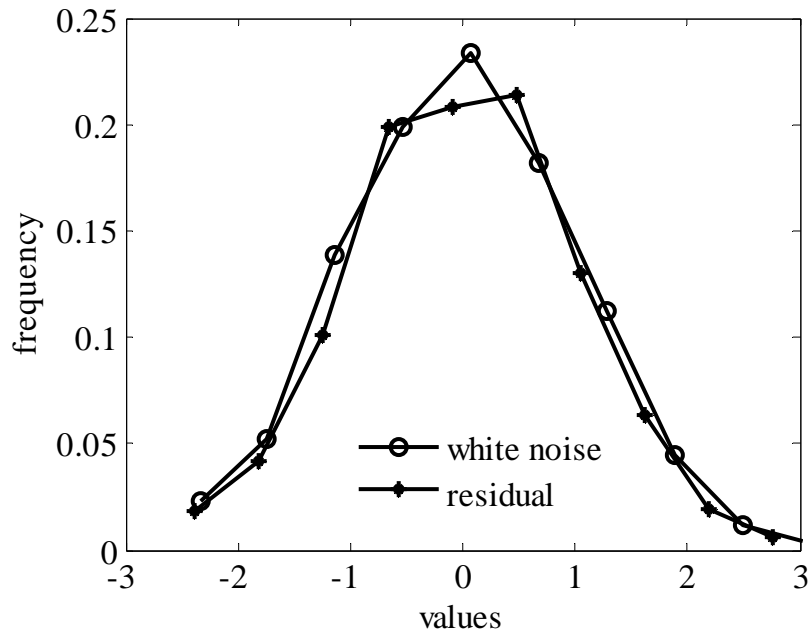
Figure 3.35 Distribution of the residual of the OBF model and the original white noise introduced into system (3.73)

Correlation among the residuals is given by

$$\hat{R} = [\text{-0.0110}\ \ 0.0199\ \text{-0.0168}\ \ 0.0039\ \ 0.0102\ \ 0.0545\ \text{-0.0616}\ \ 0.0029\ \ 0.0734\ \text{-0.0106}]$$

This simulation study, like the previous two simulation studies, shows that a parsimonious OBF model can be effectively developed from a noisy identification data and arbitrarily chosen poles using the proposed iterative method for weakly damped higher order systems also. The residual analysis results also show that the parsimonious OBF model is accurate enough because the residual of the model is almost the same white noise added to the system. It means, essentially all the dynamics of the deterministic part is captured by the parsimonious OBF model.

3.14   Summary

In this chapter, two important problems related to OBF model development were solved. One of the problems is, how to develop parsimonious OBF model if good estimate of the dominant pole of the system is not available. The other problem is how to get a better time delay estimate when the system has second or higher order dynamics.

The first problem is addressed by developing an iterative scheme in which the dominant poles of the system is estimated from the noise-free OBF model, which itself is developed from the noisy identification data with arbitrarily chosen poles. Parsimonious OBF models of well damped, higher order systems can be developed using the proposed method based on pole estimation with FOPTD models or SOPTD models. Parsimonious OBF models of weakly damped, higher order systems can be developed using the proposed method based on pole estimation with SOPTD models. When FOPTD model based iterative method is used Laguerre filters are the most appropriate since only one pole is estimated. When SOPTD based iterative method is used, both GOBF and Kautz filters (for weakly damped systems) can be used. The second problem is addressed by reducing the contributed time delay from the time delay estimate by the tangent method. For this purpose the SOPTD model is used. Therefore, when the SOPTD based iterative method is used two dominant poles and a better time delay estimate is obtained.

Three different approaches are compared for determining the FOPTD parameters the interpolation method is found effective. A novel method for estimating the parameters of the SOPTD model is developed. While the method is effective for estimating the SOPTD model from the step response of any system it is uniquely effective for estimating the SOPTD parameters from step response of OBF models.

Each major section is supported by relevant simulation study. The final simulation study shows all major identification issues including residual analysis. The simulation study also confirms that the proposed method is reliable and effective in developing parsimonious OBF models from a crude estimate or arbitrarily chosen poles.

CHAPTER 4

OBF BASED PREDICITON MODELS

4.5   Introduction

Conventional OBF models are simulation models and they do not include explicit noise models [2, 8, 20]. In their conventional form, OBF model structures, therefore, cannot be effectively used in the presence of unmeasured disturbances, unless a noise model is separately estimated and included. Patwardhan *et al*. [8] showed that the regulatory performance of MPC system improves significantly by including a noise model to the OBF simulation model. In their work, the residual of the OBF model is whitened with Auto Regressive (AR) noise model. The AR noise model is parameterized in terms of OBF parameters and a minimal order state space model was realized. In their subsequent paper [9], they used this state space model in MPC and fault tolerant control systems. However, AR models are not parsimonious and they need a large number of parameters to capture the dynamics of the unmeasured disturbance with acceptable accuracy. In addition, development of the noise model could be integrated with the development of the OBF model so that a unified OBF plus noise model is developed as a single model. Combining the noise model to an OBF model and treating it as a single model would also improve the prediction capability of the model.

Another related issue is that, although, there is a wide-ranging literature on closed loop identification, only limited material related to closed loop identification using OBF plus noise models is available. Gáspér *et al*. [30] presented a paper on closed-loop identification related to OBF models. However the paper lacks clarity and depth on its presentation. First, in the simulation model, which was used to generate the identification data, only the plant and the controller transfer functions were given. It appears that, no noise or unmeasured disturbance is introduced into the simulation system. This makes the identification simulation case-study less relevant to closed-loop identification; since it was the correlation of the noise sequence to the input sequence that makes closed-loop identification unique and difficult. When a system identification test is carried out in open loop, in general, the noise sequence is not correlated to the input sequence and OBF model identification is carried in a straight forward manner. However, when the system identification test is carried out in closed loop, the input sequence is correlated to the

noise sequence and conventional OBF model development procedures fail to provide consistent model.

Nevertheless, there are several reasons to conduct identification tests in closed-loop. Some of the compelling reasons for conducting identification test on closed loop are [1, 2, 30-32]:

- Feedback controller is required to stabilize the process
- Safety and cost consideration may not allow the process to run open-loop
- The excited frequencies in closed-loop operation are better suited than the frequency band in open-loop operation
- The linearization of the controller is desired
- The model is to be used for the design of improved controller

Therefore, closed loop identification using OBF plus noise model is an important issue to be addressed to make full use of the benefits of OBF models.

In this chapter, unified schemes for developing OBF based prediction models from open-loop and closed-loop identification data that provide explicit noise model are proposed. In the first section, two novel unified schemes in which Box-Jenkins (BJ) type models are developed by combining orthonormal basis filter model and conventional time series models are presented. In the second section, novel schemes for developing OBF-based prediction model from closed loop data are presented. In each section, the structure of the proposed models, the procedures for estimation of model parameters and the formula for multi-step ahead predictions are presented. The proposed schemes are demonstrated using simulation and real plant case studies.

4.6   Open-loop Identification using OBF–AR and OBF-ARMA Models

In this section, two novel unified schemes for developing BJ type models from open-loop identification data by combining orthonormal basis filter model and conventional time series models are presented. The models have an OBF deterministic part and an AR or ARMA noise part. The proposed models inherit all the advantages of an OBF model together with an explicit noise model. This enables the design of control systems for disturbance rejection that results in better regulatory performance. Furthermore, combining a noise model to an OBF model and treating it as a single model results in a prediction model with a higher prediction capability than an OBF simulation model. The

proposed methods are easily extended to develop models for MIMO systems using multiple MISO models. The advantages of the proposed models over BJ models are:

- Model parameters can be easily and accurately determined without involving non-linear optimization

- Time delays can be easily estimated, and unlike in BJ models, a prior knowledge of time delays is not required

- The identification and prediction schemes can be easily extended to MIMO systems.

The basis of OBF-AR/ARMA models is the fact that when the noise sequences are uncorrelated with the input sequence an OBF model can be easily developed for the deterministic part regardless of the type of noise. Van den Hof *et al.* [46] showed that if the noise sequences are uncorrelated with the input sequences, a parsimonious GOBF model can be developed even if the noise is colored. They demonstrated in their simulation study that the residuals of the GOBF model closely match the noise introduced into the system. In this section, the OBF models are independently developed assuming the noise sequences are uncorrelated with the input sequences which is generally the case for open-loop identification.

4.6.1 Model Structures

The BJ model structure (4.1) is known to be more flexible and comprehensive structure of the conventional linear models[1, 2, 16].

$$y(k) = \frac{B(q)}{F(q)}u(k) + \frac{C(q)}{D(q)}e(k)$$

(4.1)

In the BJ model, $B(q)/F(q)$ describes the deterministic part of the model whereas $C(q)/D(q)$ describes the stochastic part of the model. The proposed BJ-type model structure is obtained by replacing the deterministic part of the model with OBF model structure. In the following part, the structure of the proposed models and their corresponding block diagrams are presented.

4.6.1.1 OBF-AR model structure

The OBF-AR model structure assumes an OBF and AR structures for the input and noise transfer functions, respectively. Figure 4.1 illustrates the structure of OBF-AR models.
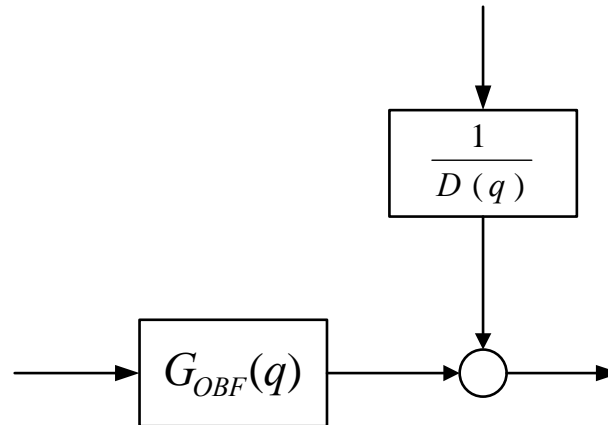
Figure 4.1 OBF-AR structure

The corresponding transfer function model for the OBF-AR model is given by

$$y(k) = G_{OBF}(q)u(k) + \frac{1}{D(q)}e(k) \tag{4.2}$$

4.6.1.2 OBF-ARMA model structure

The OBF-ARMA structure has more flexible noise model than the OBF-AR structure. The OBF-ARMA structure is depicted in Figure 4.2.
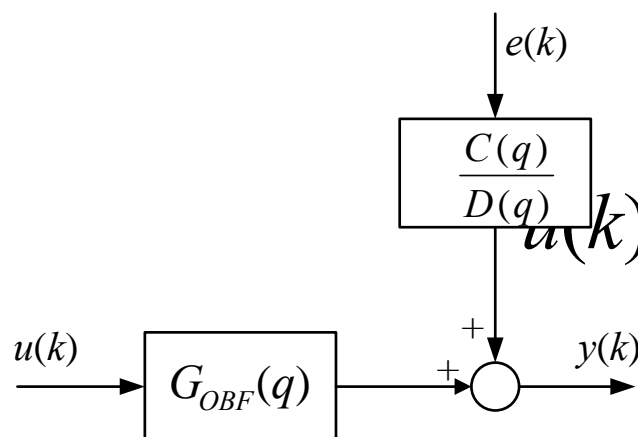
Figure 4.2 OBF – ARMA structure

Equation (4.3) represents the corresponding transfer function for the OBF-ARMA structure.

$$y(k) = G_{OBF}(q)u(k) + \frac{C(q)}{D(q)}e(k)$$

(4.3)

It can be noted from (4.3) that the OBF-ARMA structure does not assume common denominator dynamics and hence it should not be confused with an OBF model with an ARMAX structure. However, since the orthonormal filters have both numerator and denominator polynomials it is similar to BJ structure.

4.6.2 Estimation of Model Parameters

The model parameters of both OBF-AR and OBF-ARMA structures are estimated based on the prediction error method as explained in the following sections.

The prediction error *e(k)* is defined as

$$e(k) = y(k) - \hat{y}(k \mid k-1)$$

(4.4)

4.6.2.1 Estimation of Model Parameters for OBF-AR model structure

Introducing the prediction error (4.4) in (4.2) and rearranging leads to

$$\hat{y}(k \mid k-1) = D(q)G_{OBF}(q)u(k) + \big(1 - D(q)\big)y(k)$$

(4.5)

Assuming that the noise sequence is uncorrelated to the input sequence, the parameters of the OBF model can be estimated separately. These parameters can then be used to calculate the OBF simulation model output using (4.6).

$$y_{obf}(k) = G_{OBF}(q)u(k)$$

(4.6)

Inserting (4.6) in (4.5)

$$\hat{y}(k \mid k-1) = D(q)y_{obf}(k) + \big(1 - D(q)\big)y(k)$$

(4.7)

Equation (4.7) is linear in parameters since $y_{obf}(k)$ is already known. With *D(q)* monic, (4.7) can be expanded and rearranged to yield

$$\hat{y}(k \mid k-1) = y_{obf}(k) - d_1 r(k-1) - d_2 r(k-2) - \ldots - d_m r(k-n_D)$$

(4.8)

where

n_D *is* the order of the polynomial $D(q)$

$$r(i) = y(i) - y_{obf}(i)$$

Note that $r(i)$ represents the residual of the output $y(k)$ of the system from the OBF model output $y_{obf}(k)$. The model parameters in (4.8) can be calculated by the linear least square formula (3.20) with the regressor matrix given by (4.9).

$$X = \begin{bmatrix} y_{obf}(n) & -r(n-1) & -r(n-2) - & \dots & -r(1) \\ y_{obf}(n+1) & -r(n) & -r(n-1) - & \dots & -r(2) \\ . & . & . & . \\ . & . & . & . \\ . & . & . & . \\ y_{obf}(N) & -r(N-1) & -r(N-2) - & \dots & -r(N-n) \end{bmatrix} \tag{4.9}$$

where $n = n_D$.

The step-by-step procedure for estimating the OBF-AR model parameters, explained above, is outlined in Algorithm 1.

Algorithm 4.1

1. Develop parsimonious OBF model

2. Determine the output sequence of the OBF model $y_{obf}(k)$ for the corresponding input sequence $u(k)$

3. Determine the residuals of the simulation model $r(k) = y(k) - y_{obf}(k)$

4. Develop the regression matrix X given by (4.9)

5. Determine the parameters of the noise model using (3.19) enforcing monic condition, i.e., $d_0 = 1$.

It may be noted that if estimates of the dominant poles of the deterministic part are not available, an iterative technique proposed in Chapter 3 can be followed in order to develop a parsimonious OBF model.

4.6.2.2 Estimation of Model Parameters for OBF-ARMA model structure

The OBF-ARMA equation is given by (4.3)

$$y(k) = G_{OBF}(q)u(k) + \frac{C(q)}{D(q)}e(k)$$

(4.3)

Substituting the prediction error in (4.3) and rearranging yields

$$C(q)\hat{y}(k \mid k-1) = D(q)G_{OBF}(q)u(k) - D(q)y(k) + C(q)y(k)$$

(4.10)

As in the case of OBF-AR model, if the noise sequence is uncorrelated with the input sequence, the OBF model parameters can be calculated separately and be used to calculate the simulation model output $y_{obf}(k)$ using (4.6).

Introducing (4.6) in (4.10) results in

$$C(q)\hat{y}(k \mid k-1) = D(q)y_{obf}(k) - D(q)y(k) + C(q)y(k)$$

(4.11)

Expanding and rearranging (4.11) results in

$$\hat{y}(k \mid k-1) = y_{obf}(k) - d_1 r(k-1) - d_2 r(k-2) - ... - d_m r(k-m) +$$
$$c_1 e(k-1) + c_2 e(k-2) + ... + c_n e(k-n)$$

(4.12)

where $e(k)$ is the prediction error sequence as defined by (4.4).

Equation (4.12) in the form shown above is similar to linear regression. However, since the prediction error sequence, $e(k-i)$, itself is a function of the model parameters, it is nonlinear in parameters. To emphasize the significance of these two facts such structures are commonly known as pseudo-linear[1, 2]. The model parameters can be estimated by either a nonlinear optimization method or an extended least square method [2]. In this work, the extended least square method is used to estimate the parameters. A simple two-step method is also proposed.

The extended least square method is an iterative method where the prediction error sequence is estimated and updated at each iteration using the prediction error of OBF-ARMA model. A good initial estimate of the prediction error sequence is obtained from the OBF-AR model. The parameters for the noise model are estimated using the linear least square method with (4.13) and (4.14) as parameters vector and regressor matrix, respectively. From the derivation, it should be remembered that all the poles and zeros of the noise models should be inside the unit circle and both the numerator and denominator polynomials should be monic. If an OBF-AR model with a high-order noise model can be developed, the residuals of the OBF-AR model will generally be close to white noise. In such cases, the noise model parameters of the OBF-ARMA model can be

estimated using linear least square method in one iteration. Such a simplified method is called a two-step method in this study. The step-by-step procedure for estimating OBF-ARMA model parameters is outlined in Algorithm 4.2.

$$\theta = [d_1 \ d_2 \ ... d_m \ c_1 \ c_2 \ ... \ c_n]^T$$

(4.13)

where $n = n_C$, the order of the polynomial $C(q)$

   $m = n_D$, the order of the polynomial $D(q)$

   $mx = max \ (m, \ n)+1$

$$X = \begin{bmatrix} y_{obf}(mx) & -r(mx-1) & -r(mx-2) -... -r(mx-n) & e(mx-1) \ e(mx-2) \ ...e(mx-m) \\ y_{obf}(mx+1) & -r(mx) & -r(mx-1) -...-r(mx-n+1) & e(mx) \ e(mx-1)...e(mx-m+1) \\ . & . & . & . \quad . \quad . \quad . \\ . & . & . & . \quad . \quad . \quad . \\ . & . & . & . \quad . \quad . \quad . \\ y_{obf}(N) & -r(N-1) & -r(N-2) -... \quad -r(N+1) & e(N-1) \ e(N-2)... \quad e(N-m+1) \end{bmatrix}$$

(4.14)

$$y = [y(mx) \quad y(mx+1) \ ... \ y(N)]^T$$

(4.15)

Algorithm 4.2

1. Develop a parsimonious OBF model

2. Determine the OBF simulation model output $y_{obf}(k)$ for the corresponding input sequence $u(k)$

3. Determine the residual of the simulation model $r(k) = y(k) - y_{obf}(k)$

4. Develop OBF-AR prediction model

5. Determine the residual of the OBF-AR model, $\hat{e}(k)$

6. Use $y_{obf}(k), r(k)$ and $e(k) \approx \hat{e}(k)$ to develop (4.14)

7. Use (3.20) to estimate the parameters of the OBF-ARMA model

8. Re-estimate the prediction error $e(k) = y(k) - \hat{y}(k)$ from the OBF-ARMA model developed in step 7

9. Repeat steps 6 to 8 until convergence is achieved

Convergence criteria

There are several possibilities for the convergence criteria. One possibility is the maximum deviation in the parameters of the noise models in two consecutive iterations can be taken as convergence criteria. When the model is intended for prediction the improvement in percentage prediction errors can be used as convergence criteria.

4.6.3 Multi-step ahead Prediction

Multi-step ahead predictions are required in several applications such as model predictive control. In this section multi-step ahead prediction equation and related procedures for both OBF-AR and OBF-ARMA are derived.

4.6.3.1 Multi-step ahead Prediction using OBF-AR model

Using (4.6) in (4.2) the OBF-AR equation becomes

$$y(k) = y_{obf}(k) + \frac{1}{D(q)} e(k) \tag{4.16}$$

i-step ahead prediction is obtained by replacing k with $k + i$

$$y(k+i) = y_{obf}(k+i) + \frac{1}{D(q)} e(k+i) \tag{4.17}$$

To calculate the i-step ahead prediction, the error term should be divided into current and future parts as shown in (4.18) [16].

$$y(k+i) = y_{obf}(k+i) + \frac{F_i(q)}{D(q)} e(k) + E_i(q)e(k+i) \tag{4.18}$$

The last term in (4.18) contains only the future error sequence which is not known. However, since $e(k)$ is assumed to be a white noise with mean zero, (4.18) can be simplified to

$$\hat{y}(k+i \mid k) = y_{obf}(k+i) + \frac{F_i(q)}{D(q)} e(k) \tag{4.19}$$

F_i and E_i are determined by solving the Diophantine equation (4.20) which is obtained by comparing (4.17) and (4.18)

$$\frac{1}{D(q)} = E_i(q) + \frac{q^{-i}F_i(q)}{D(q)} \tag{4.20}$$

Equation (4.19) could be taken as the final form of the i-step ahead prediction equation. However, in application, since $e(k)$ is not measured the equation cannot be directly used. The next steps are added to solve this problem.

Rearranging (4.16)

$$\frac{1}{D(q)} e(k) = y(k) - y_{obf}(k) \tag{4.21}$$

Using (4.21) in (4.19) to eliminate $e(k)$

$$\hat{y}(k+i \mid k) = y_{obf}(k+i) + F_i(q)(y(k) - y_{obf}(k)) \tag{4.22}$$

Rearranging (4.22)

$$\hat{y}(k+i \mid k) = y_{obf}(k+i)(1 - F_i(q)q^{-i}) + F_i(q)y(k) \tag{4.23}$$

Rearranging the Diophantine equation (4.20)

$$\left(1 - q^{-i}F_i(q)\right) = D(q)E_i(q) \tag{4.24}$$

Using (4.24) in (4.23)

$$\hat{y}(k+i \mid k) = E_i(q)D(q) \, y_{obf}(k+i) + F_i(q)y(k) \tag{4.25}$$

Equation (4.25) is the usable form of the multi-step ahead prediction equation for the OBF-AR model. Given an OBF-AR model, the solution of the Diophantine equation to get E_i and F_i and the prediction equation (4.25) forms the procedure for i-step ahead prediction of the OBF-AR model.

4.6.3.2 Multi-step ahead Prediction using OBF-ARMA Model

Using (4.6) in (4.3) the OBF-AR equation becomes

$$y(k) = y_{obf}(k) + \frac{C(q)}{D(q)} e(k) \tag{4.26}$$

i-step ahead prediction is obtained by replacing k with $k + i$

$$y(k+i) = y_{obf}(k+i) + \frac{C(q)}{D(q)} e(k+i) \tag{4.27}$$

To calculate the i-step ahead prediction, the error term should be divided into current and future parts.

$$y(k+i) = y_{obf}(k+i) + \frac{F_i(q)}{D(q)} e(k) + E_i(q)e(k+i) \tag{4.28}$$

Since $e(k)$ is assumed to be a white noise with mean zero, the mean of $E_i(q)\, e(k+i)$ is equal to zero, and therefore (4.28) can be simplified to

$$\hat{y}(k+i\,|\,k) = y_{obf}(k+i) + \frac{F_i(q)}{D(q)} e(k) \tag{4.29}$$

F_i and E_i are determined by solving the Diophantine equation (4.30) which is obtained by comparing (4.27) and (4.28)

$$\frac{C(q)}{D(q)} = E_i(q) + \frac{q^{-i} F_i(q)}{D(q)} \tag{4.30}$$

Rearranging (4.26)

$$\frac{1}{D(q)} e(k) = \frac{1}{C(q)} \big(y(k) - y_{obf}(k)\big) \tag{4.31}$$

Using (4.31) in (4.29) to eliminate $e(q)$

$$\hat{y}(k+i\,|\,k) = y_{obf}(k+i) + \frac{F_i(q)}{C(q)} \big(y(k) - y_{obf}(k)\big) \tag{4.32}$$

Rearranging (4.32)

$$\hat{y}(k+i\,|\,k) = y_{obf}(k+i)\left(1 - \frac{F_i(q)q^{-i}}{C(q)}\right) + \frac{F_i(q)}{C(q)} y(k) \tag{4.32}$$

Rearranging the Diophantine equation (4.30)

$$\left(1 - \frac{q^{-i} F_i(q)}{C(q)}\right) = \frac{D(q)E_i(q)}{C(q)} \tag{4.33}$$

Using (4.33) in (4.32) results in the final usable form of the i-step ahead prediction for OBF-ARMA model.

$$\hat{y}(k+i \mid k) = \frac{E_i(q)D(q)}{C(q)} y_{obf}(k+i) + \frac{F_i(q)}{C(q)} y(k)$$

(4.34)

Since $y_{obf}(k+i)$ is the output sequence of the simulation OBF model, if the OBF model parameters are determined its value depends only on the input sequence $u(k+i)$. Therefore, the i-step ahead prediction according to (4.34) depends on the input sequence up to instant $k+i$ and the output sequence up to instant k.

4.6.4 Multiple-Input Multiple-Output (MIMO) Systems

The procedures for estimating the model parameters and i-step ahead prediction can be easily extended to MIMO systems by using multiple-MISO models[2]. First, a MISO OBF model is developed for each output using the input sequences and the corresponding orthonormal basis filters. Then, AR model is developed using $y_{obf}(k)$ and the residual of the OBF simulation model. The OBF-ARMA model is developed in a similar manner, with an OBF model relating each output with all the relevant inputs and one ARMA noise model for each output using Algorithm 4.2.

4.6.5 Case Studies

In this section, the proposed methods are illustrated using three case studies. The objective in the first two simulation case studies is to establish the fact that the proposed methods are effective in developing prediction models that have acceptable accuracy for linear time invariant systems for both well damped and weakly damped systems. In addition, the prediction capability of the GOBF-AR and GOBF-ARMA models are compared. The plant model is validated using a separate validation data for each simulation case study and by comparing the percentage prediction errors. The accuracy of the noise models are compared by using the noise spectrum, and the percentage prediction error of the spectrum of the noise model.

In the first and second case studies a well damped system and a weakly damped system with unmeasured disturbances, respectively, are considered. In the third case study, the proposed method is used for developing OBF-ARMA model for a pilot-scale binary distillation column. The distillation column is part of a reaction-separation system which uses acetone-iso propyl alcohol as feed material. The case study is a multiple-input multiple output (MIMO) real plant case study.

4.2.5.1 Well damped System with Box Jenkins Structure

In this simulation case study, OBF-AR and OBF-ARMA models are developed for a well damped system that has a Box-Jenkins structure. The OBF-AR and OBF-ARMA models are developed with various orders and compared within themselves and with each other. The system is represented by (4.35). Note that both the numerator and denominator polynomials of the noise model are monic and their roots are located inside the unit circle. Figure 4.3 shows the input–output sequences used for model development.

$$y(k) = q^{-6} \frac{1 - 1.3q^{-1} + 0.42q^{-2}}{1 - 2.55q^{-1} + 2.165q^{-2} - 0.612q^{-3}} u(k) + \frac{1 + 0.6q^{-1}}{1 - 1.15q^{-1} + 0.58q^{-2}} e(k) \quad (4.35)$$
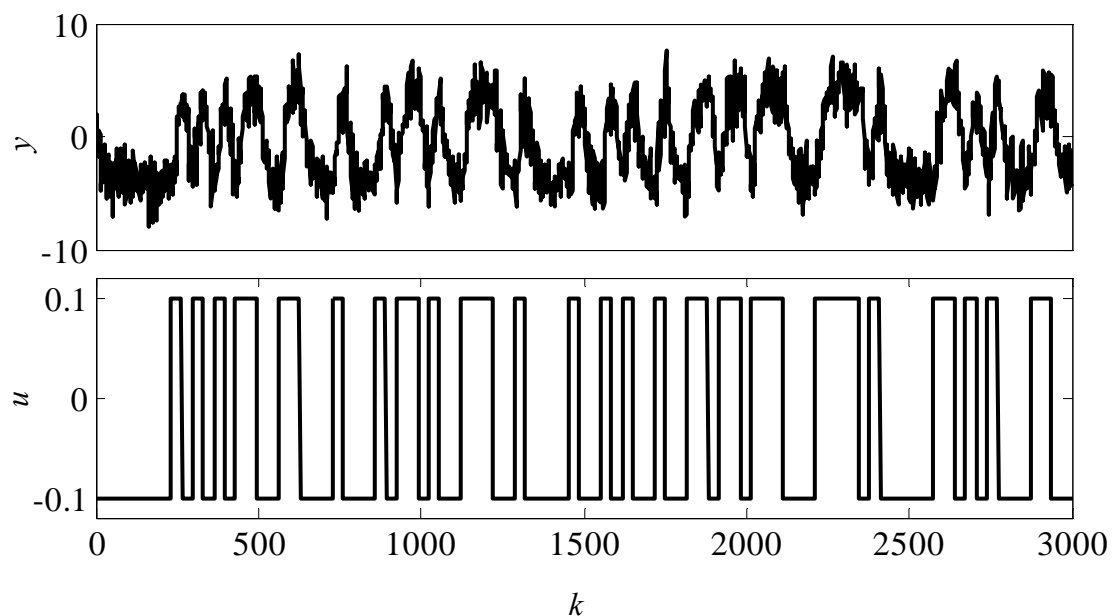
Figure 4.3 Output $y(k)$ and input sequences $u(k)$ used for
identification of system (4.35)

The mean and standard deviations of the white noise, $e(k)$, added to the system are 0.0123 and 0.4971, respectively, and the signal to noise ratio (SNR) is 6.6323 . The input signal is a pseudo random binary signal (PRBS) of 4000 data points generated using the *'idinput'* function in MATLAB with band [0 0.03] and levels [-0.1 0.1]. Three thousand of the data points are used for model development and the remaining 1000 for validation. The corresponding output sequence of the system is generated using SIMULINK with a sampling interval of 1 time unit.

OBF-AR model development

Following the principle applied in Chapter 3, the number of OBF model parameters is chosen to be six and estimated dominant poles 0.9114 and 0.8465. Therefore, a GOBF model with six parameters and alternating poles of 0.9114 and 0.8465 is developed. The estimated GOBF model parameters and the time delay (τ_d) respectively, are:

l= [3.7273 5.6910 1.0981 -0.9955 0.3692 -0.2252]

τ_d = 5 time units

The estimated noise models with n_D = 2, 5 and 7 for GOBF-AR model are given by (4.36), (4.37) and (4.38), respectively. The corresponding standard deviations of the residuals are 0.5573, 0.5055 and 0.5040.

$$\frac{1}{D(q)} = \frac{1}{1-1.3631q^{-1}+0.7485q^{-2}} \tag{4.36}$$

$$\frac{1}{D(q)} = \frac{1}{1-1.7524q^{-1}+1.6256q^{-2}-0.9184q^{-3}+0.4217q^{-4}-0.1148q^{-5}} \tag{4.37}$$

$$\frac{1}{D(q)} = \frac{1}{1-1.7646q^{-1}+1.6685q^{-2}-1.0119q^{-3}+0.5880q^{-4}-0.3154q^{-5}+0.1435q^{-6}-0.0356q^{-7}} \tag{4.38}$$

Noise model selection

Figure 4.4 presents the spectrum of the three noise models (4.36)-(4.38). The percentage predication errors of the spectrums of the three noise models with respect to the original transfer function of the noise in the system are given in Table 4.1.

Table 4.1 PPE of the three AR noise models of system (4.35)

n_D	PPE
3	54.3378
5	1.5137
7	0.9104
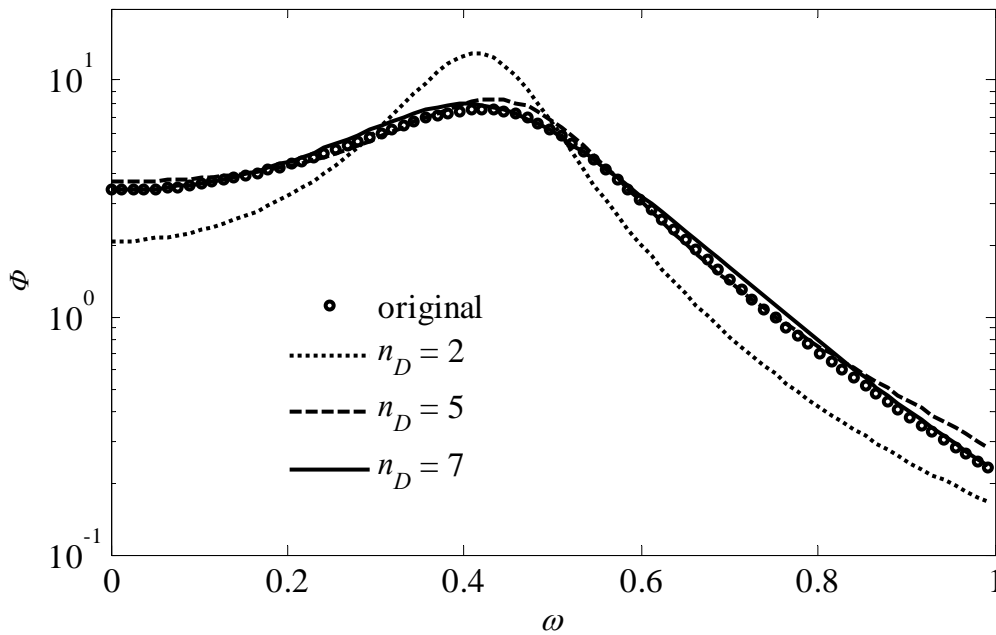
Figure 4.4 Spectrums of the AR noise models for $n_D = 2$, 5 and 7 compared to the noise transfer function of system (4.35)

It is obvious from both Figure 4.4 and Table 4.1 that the noise model with $n_D = 7$ is the closest to the original noise transfer function of the system. Therefore this noise model together with the GOBF model described earlier form the OBF-AR model representing the system.

Model Validation

In the following part, the validation of the OBF-AR model is conducted. The one-step-ahead prediction of the OBF-AR, the prediction of the OBF (simulation model) and the system output for the validation data are shown in Figure 4.5. For the sake of clarity only the first 200 data points are shown in the figure. The PPE of the one step-ahead prediction of the OBF and OBF-AR models with respect to the original output are 21.9474 and 2.7826, respectively. It is observed from Figure 4.4 and the PPE values that the OBF-AR model gives a much better prediction than the OBF model alone.
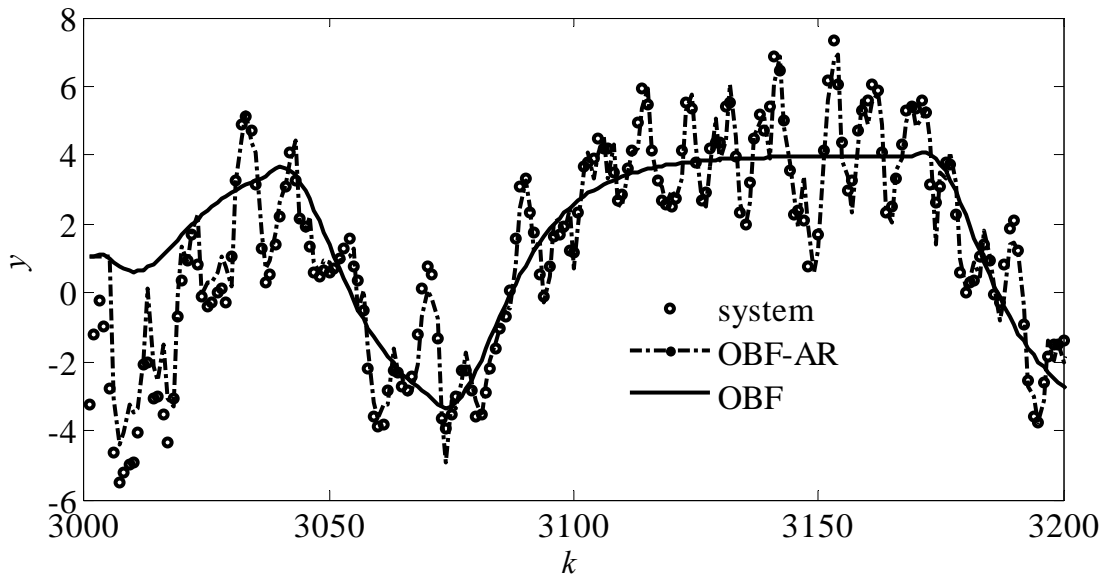
Figure 4.5 Validation of GOBF and GOBF-AR model with $n_D = 7$ for system (4.35)

The spectrum of the final estimated noise model compared to the system's noise transfer function is shown in Figure 4.6. The PPE of the spectrum of the estimated noise model compared to the noise transfer function in the system is 0.9104.
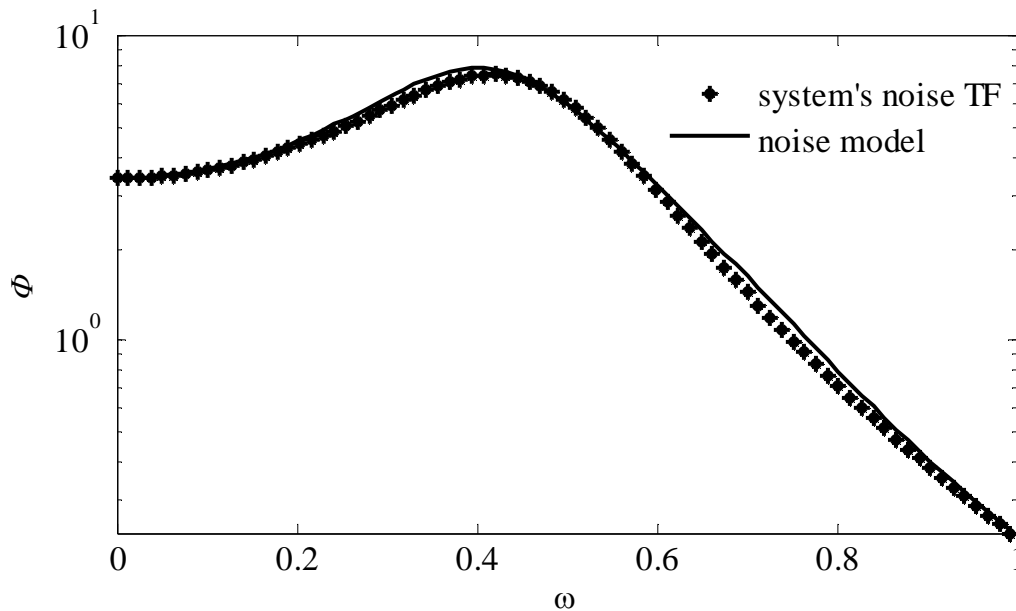
Figure 4.6 Spectrum of the system's noise transfer function compared to the estimated noise model for system (4.35)

Residual Analysis

A model is assumed to have captured the dynamics of the system if it predicts all information except the white noise. In the following part the white noise added to the system and the residuals are compared. Figure 4.5 depicts the qq-plot of the white noise added to the system and the residuals of the OBF-AR model.

Figure 4.7 qq-plot for the white noise added to the system and the residuals of the OBF-AR model for system (4.35)

Figure 4.8 presents the distribution of the residuals of the OBF-AR model compared to the white noise added to the system. It is observed from the figure that the distribution of the residuals closely matches the distribution of the white noise added to the system.

Figure 4.8 Distribution of the residual compared to the white noise for system (4.35)

The correlation among the residuals is given by

$\hat{R} =$ [-0.0112 0.0034 -0.0058 -0.0067 0.0024 0.0040 -0.0136 -0.0006 0.0166 -0.0064]

This simulation case study demonstrates that an OBF-AR model can be effectively developed using the proposed algorithm. It is observed from Figure 4.5 that the plant model mismatch caused by the unmeasured disturbance is taken care of by the AR noise model. It is also observed that to capture the dynamics with acceptable accuracy the AR model order should be large enough.

OBF-ARMA model development using two-step method

In this section an OBF-ARMA model is developed using the proposed two step method for the system described by (4.35). Since the system is the same as that used for OBF-AR model and since the OBF model does not depend on the type of the noise model the same OBF model is used. Thus, a GOBF model with six parameters and alternating poles of 0.9114 and 0.8465 is developed. The estimated GOBF model parameters and the time delay (τ_d) respectively, are:

$l =$ [3.7273 5.6910 1.0981 -0.9955 0.3692 -0.2252]

$\tau_d = 5$ time units

The noise model

The residuals of the OBF-AR model with the given OBF model and an AR model with $n_D = 7$ is used to estimate the parameters of the ARMA model with orders $n_D = n_C = 2$, 4, 6 and the corresponding models are given by (4.39) (4.40) and (4.41), respectively.

$$\frac{C(q)}{D(q)} = \frac{1+0.6187q^{-1}-0.0047q^{-2}}{1-1.1479q^{-1}+0.5801q^{-2}} \tag{4.39}$$

$$\frac{C(q)}{D(q)} = \frac{1-0.1560q^{-1}-0.1926q^{-2}+0.1530q^{-3}-0.0133q^{-4}}{1-1.9237q^{-1}+1.7617q^{-2}-0.8010q^{-3}+0.1805q^{-4}} \tag{4.40}$$

$$\frac{C(q)}{D(q)} = \frac{1-0.6808q^{-1}+0.3534q^{-2}-0.4005q^{-3}-0.2106q^{-4}+0.2790q^{-5}-0.0298q^{-6}}{1-1.24484q^{-1}+3.2363q^{-2}-3.2032q^{-3}+2.4248q^{-4}-1.2024q^{-5}+0.2847q^{-6}}$$

$$\tag{4.41}$$

Selection of noise model order

Figure 4.9 presents the spectrum of the three noise models (4.39)-(4.41). It is observed from the figure that the spectrums of the noise models for $n_D = n_C = 2$ and $n_D = n_C = 4$ are close to the system's noise transfer function.
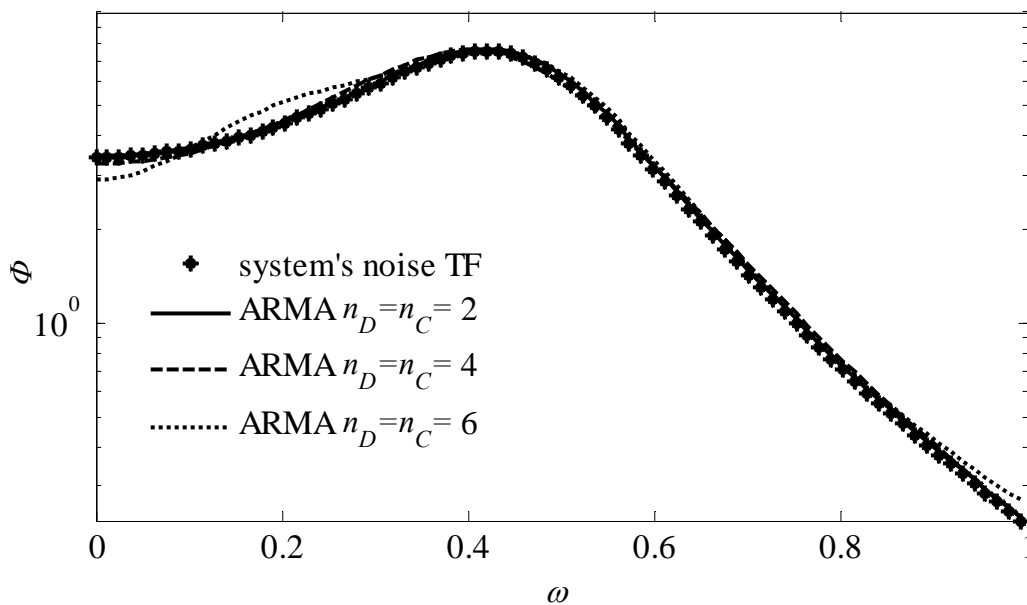
Figure 4.9 Spectrums of the ARMA noise models for $n_D = n_C = 2$, 4 and 6 compared the noise transfer function of system (4.35)

The percentage predication errors of the spectrums of the three noise models with respect to the original system's noise transfer function are given in Table 4.2.

Table 4.2 PPE of the three ARMA noise models for system (4.35)

$n_D=n_C$	PPE
2	0.0739
4	0.4261
6	1.7496

Although it is difficult to choose which noise model is the closest to the system's noise transfer function from Figure 4.9, it is observed from Table 4.2 that the noise model with $n_D = n_C = 2$ is the closest, it is also the most parsimonious. Therefore this model together with the GOBF model described previously is chosen as the OBF-ARMA model of the system.

Model validation

The validation of the OBF-ARMA model developed using the two-step method is presented in this part. Figure 4.10 shows the comparison between the one-step-ahead predictions of the OBF-ARMA model compared to the systems output for the validation data (3001-3200).
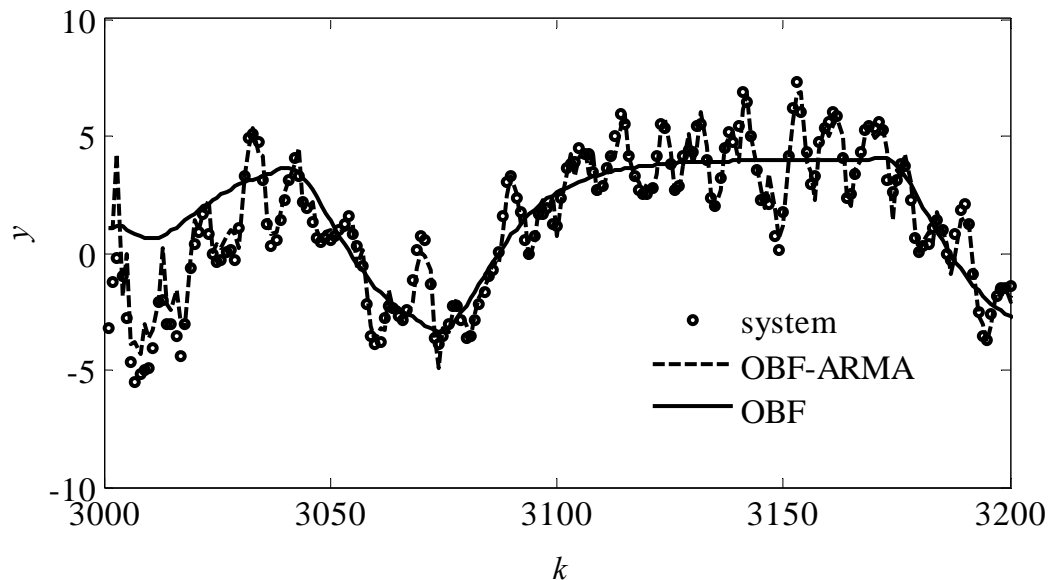
Figure 4.10 One-step-ahead prediction of the OBF-ARMA model compared to the system's output for the validation data for system (4.35)

The percentage prediction error of the OBF-ARMA model with respect to the system's output is 2.7148. The accuracy of the model is acceptable if this prediction error can be accounted for by the white noise that cannot be predicted. Figure 4.11 depicts the comparison between the spectrums of the selected ARMA noise model and the system's noise transfer function.
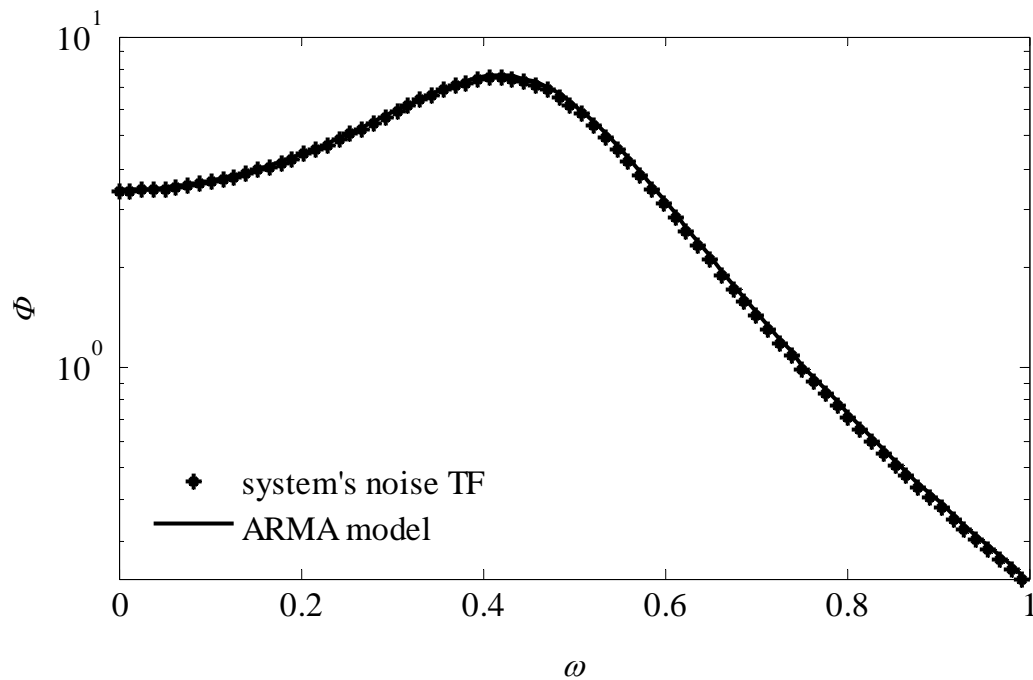
Figure 4.11 Spectrum of the noise model compared to the spectrum of the system's noise transfer function for system (4.35)

Residual Analysis

The qq-plot of the residuals compared to the white noise is shown in Figure 4.12. It is observed that most points lie on a straight line with a slope equal to one and passing through the origin. This shows that the residual has the same distribution as the white noise added to the system. Figure 4.13 depicts the distribution of the residual compared to the white noise.
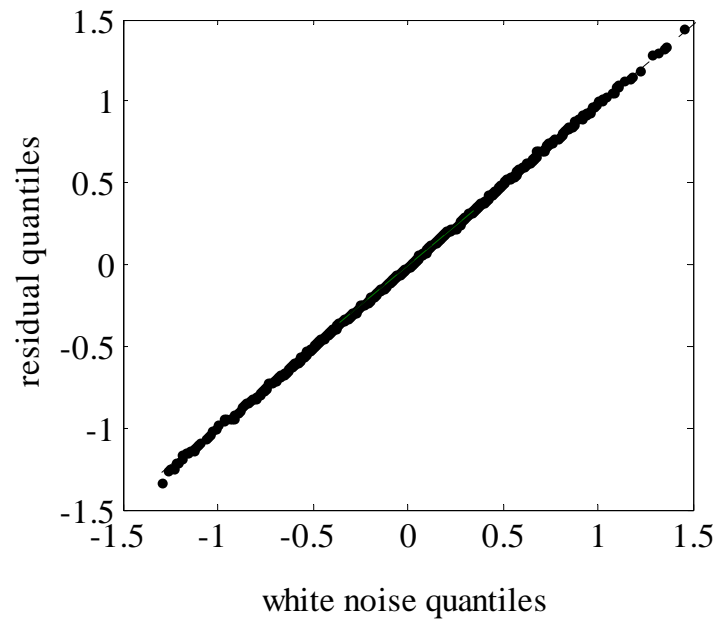
Figure 4.12 qq-plot of the white noise introduced into system (4.35)

and the residuals of the OBF-ARMA model
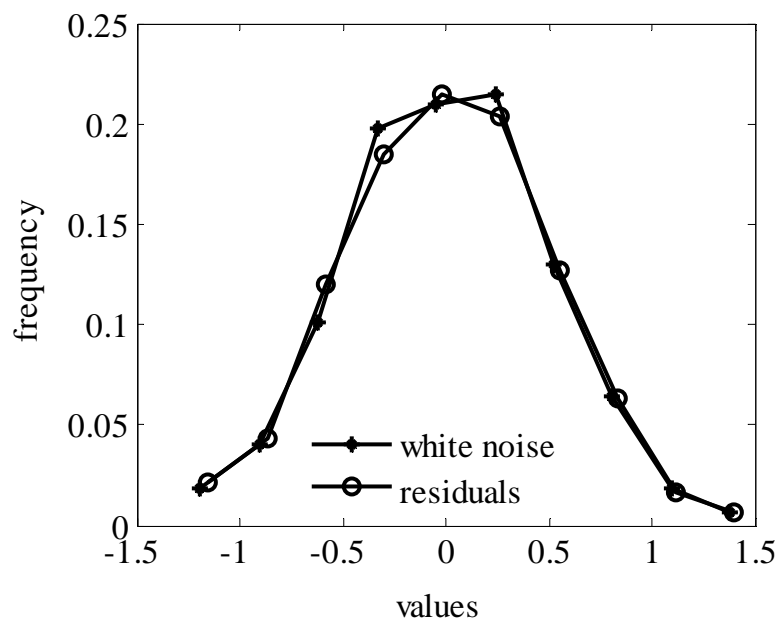
Figure 4.13 Distribution of the residual compared to the

white noise introduced to system (4.35)

The correlation among the residuals is given by

$\hat{R}$ = [-0.0128 0.0051 -0.0079 -0.0028 -0.0033 0.0104 -0.0166 -0.0004 0.0169 -0.0052]

It is observed from the residual analysis that most points in the qq-plot lie on a straight line and the slope of the qq-plot is equal to 1, indicating the residual and the white noise are from the same distribution. This is confirmed by Figure 4.13 which shows that the distribution of the residual and the white noise. The fact that the values of the correlation among the residual for the first ten sequences are close to zero shows that there is no correlation among the residuals which shows that the residual can be considered white noise.

OBF-ARMA model using the iterative method

In this section the same system (4.35) is identified using the OBF-ARMA model by the iterative (extended least square) method. The OBF model is not changed by the structure of the noise model. Therefore, the OBF model is defined by the six GOBF filters and alternating poles of 0.9114 and 0.8465 with parameters

l= [3.7273 5.6910 1.0981 -0.9955 0.3692 -0.2252]

τ_d = 5 time units

Noise model selection

The percentage prediction errors of OBF-ARMA model with various orders of noise model that converge after different number of iterations are shown in Table 4.3.

Table 4.3 PPE of OBF-ARMA models with different orders of noise model that converge after different iterations for system (4.35)

iterations	PPE		
	$n_D = n_C = 2$	$n_D = n_C = 4$	$n_D = n_C = 6$
1	2.2948	2.3188	2.3321
2	2.2872	-	2.3311
3	2.2867	-	-
4	2.2860	-	-

Te noise model with $n_D = n_C = 2$ which is obtained at the fourth iteration is the one that has the minimum PPE, the noise model is given by (4.42). Therefore, GOBF model together with this ARMA noise model comprise the OBF-ARMA prediction model.

$$\frac{C(q)}{D(q)} = \frac{1 + 0.6248q^{-1} + 0.0022q^{-2}}{1 - 1.1436q^{-1} + 0.5777q^{-2}} \qquad (4.42)$$

Model Validation

The one-step-ahead prediction of the OBF-ARMA model and the out put of the system for the validation data points 3001-3200 are depicted in Figure 4.14.
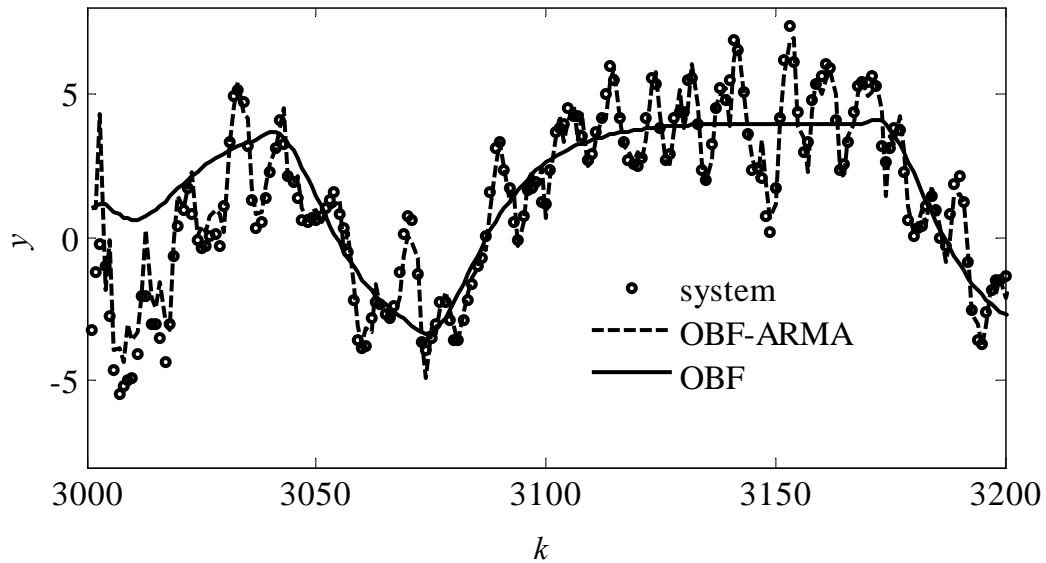
Figure 4.14 One step ahead prediction of the OBF-ARMA model compared to the output of system (4.35)

The PPE of the one step-ahead prediction of the OBF-ARMA model for the validation data points 3001-4000 is 2.8374.

The spectrum of the final estimated noise model compared to the original transfer function of the noise It is observed from Figure 4.14 that including the ARMA noise model has significantly improved the prediction capacity of the model. It is also observed from Figure 4.15 that the noise model is also close to the system's noise transfer function. The PPE of the spectrum of the noise model with respect to the spectrum of the system's noise transfer function is 0.0647%. in the system is shown in Figure 4.15.
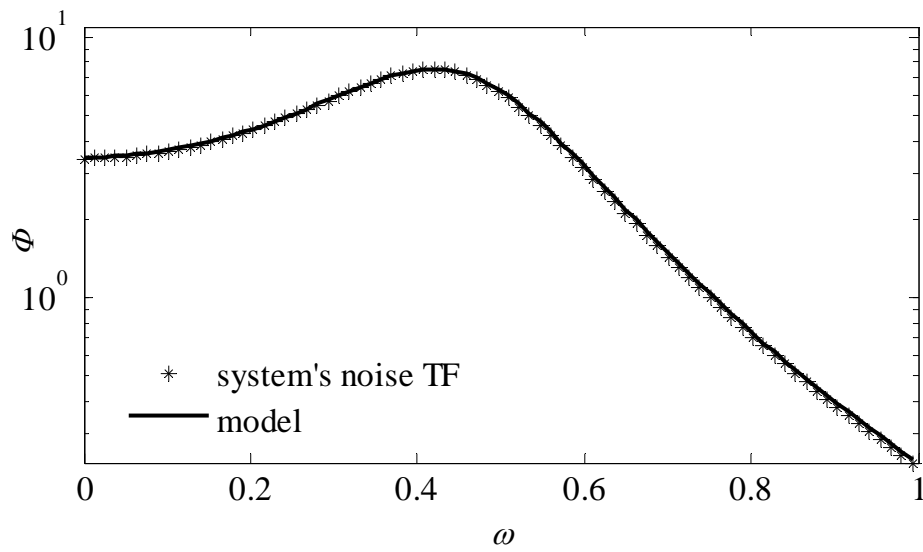
Figure 4.15 Spectrum of the ARMA noise model by the iterative method compared to the noise transfer function of system (4.35)

Residual Analysis

If the residual is close to white noise it means the remaining prediction error 0.9104 % cannot be predicted and the accuracy of the model is acceptable. Figure 4.16 depicts the qq-plot of the white noise added to the system and the residuals of the OBF-ARMA model.
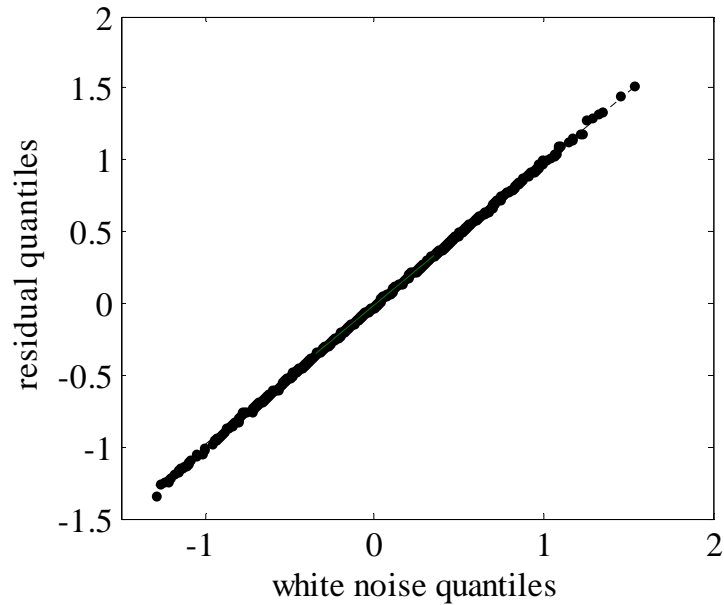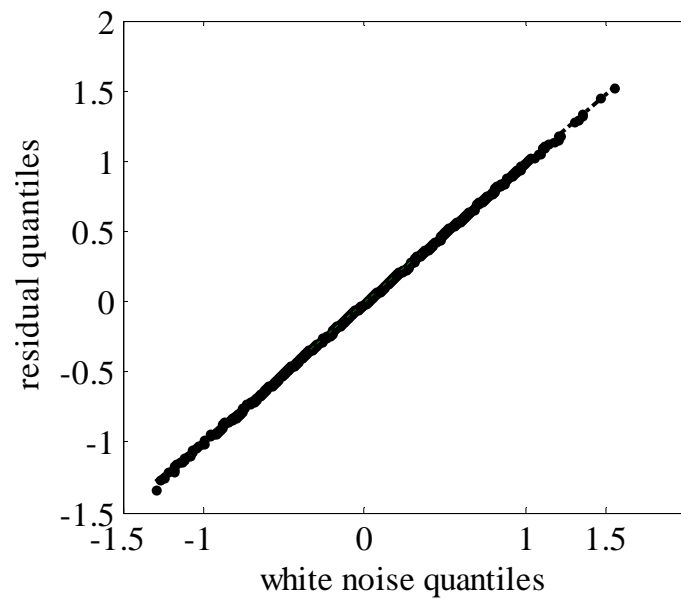

Figure 4.16 qq-plot for the white noise added to the system and the residuals of the OBF-AR model of system (4.35)

Figure 4.17 presents the distribution of the residuals of the OBF-ARMA model, developed using the iterative method, compared to the white noise added to the system. It is observed from the figure that the distribution of the residuals closely matches the distribution of the white noise added to the system.
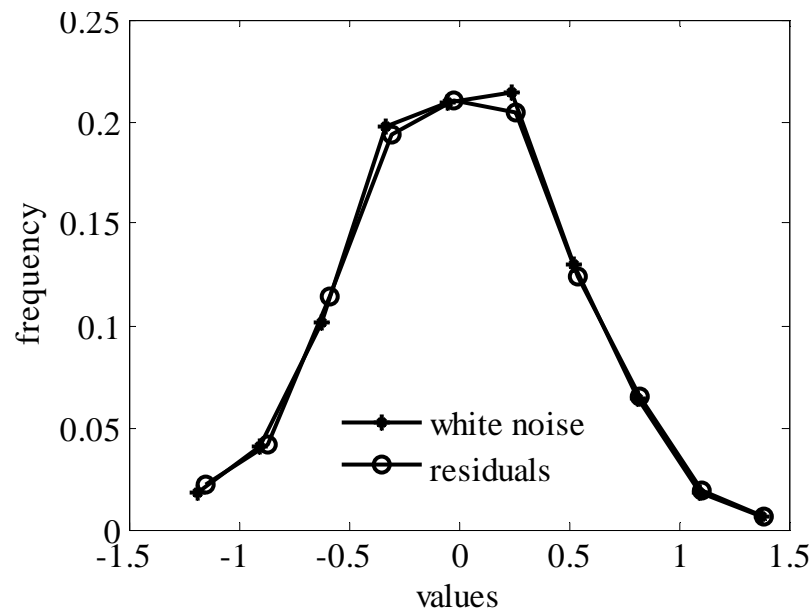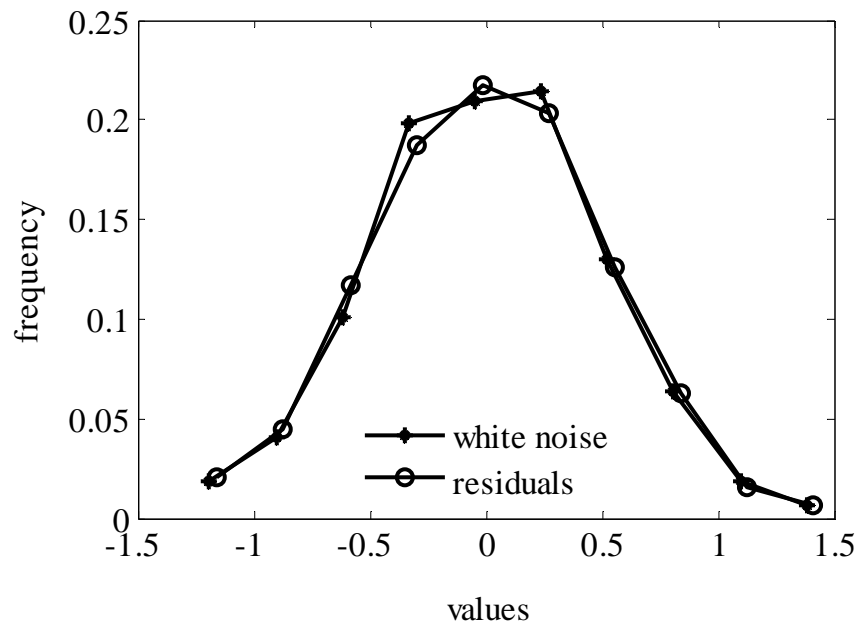

Figure 4.17 Distribution of the residual compared to
the white noise introduced to system (4.35)

The correlation among the residuals is given by

$$\hat{R} = [-0.0130\ 0.0055\ -0.0106\ -0.0018\ -0.0031\ 0.0092\ -0.0190\ -0.0024\ 0.0156\ -0.0048]$$

The result of the validation and residual analysis shows that the iterative (extended least square method) also gives models with acceptable accuracy. It also gives the means by which to compare and choose the number of iterations that gives best predictions. The residual analysis shows that the residual has the same distribution as the white noise with mean close to zero.

Multi-step-ahead Predictions

Table 4.4 gives the percentage prediction errors for 1 to 5 steps ahead using the OBF, OBF-AR and OBF-ARMA modes of system (4.35). The OBF model used is the common one in the case study while the AR and ARMA noise models are those given by (4.36)

and (4.42). It is noted from the table that the OBF-AR and the OBF-ARMA models significantly improve the short term prediction capability of the OBF model.

Table 4.4 The PPEs for 1 to 5 step- ahead- predictions of OBF-AR and OBF-ARMA models compared to OBF model for system (4.35)

i	OBF	OBF-AR	OBF-ARMA
1	21.9474	2.5190	2.5208
2	21.7492	11.1503	11.0782
3	21.6920	18.7316	18.5377
4	21.6725	21.6287	21.3985
5	21.6238	21.6258	21.4287

4.2.5.2 Weakly Damped System with Box-Jenkins Structure

In this simulation case study, OBF-AR and OBF-ARMA models are developed for a weakly damped system that has a Box-Jenkins structure using the proposed methods. The system is represented by (4.43). The roots of the system's input transfer function are 0.8, 0.4 and $0.9000 \pm 0.2000i$. Because of the complex conjugate poles, the system is weakly damped.

$$y(k) = q^{-10} \frac{1 - 2.5q^{-1} + 0.3q^{-2}}{1 - 3.0q^{-1} + 3.33q^{-2} - 1.596q^{-3} + 0.272q^{-4}} u(k) + \frac{1 + 0.8q^{-1}}{1 - 1.2q^{-1} + 0.5364q^{-2}} e(k) \qquad (4.43)$$

Both the numerator and denominator polynomials of the noise model are monic and their roots are located inside the unit circle. The white noise sequence, $e(k)$, added to the system has mean 0.0041 and standard deviation of 0.4974. The signal to noise ratio is 6.9654. The input used for excitation is a pseudo random binary signal of band [0 0.03] and level [-0.02 0.02]. Figure 4.3 shows the input and output sequences used for identification.
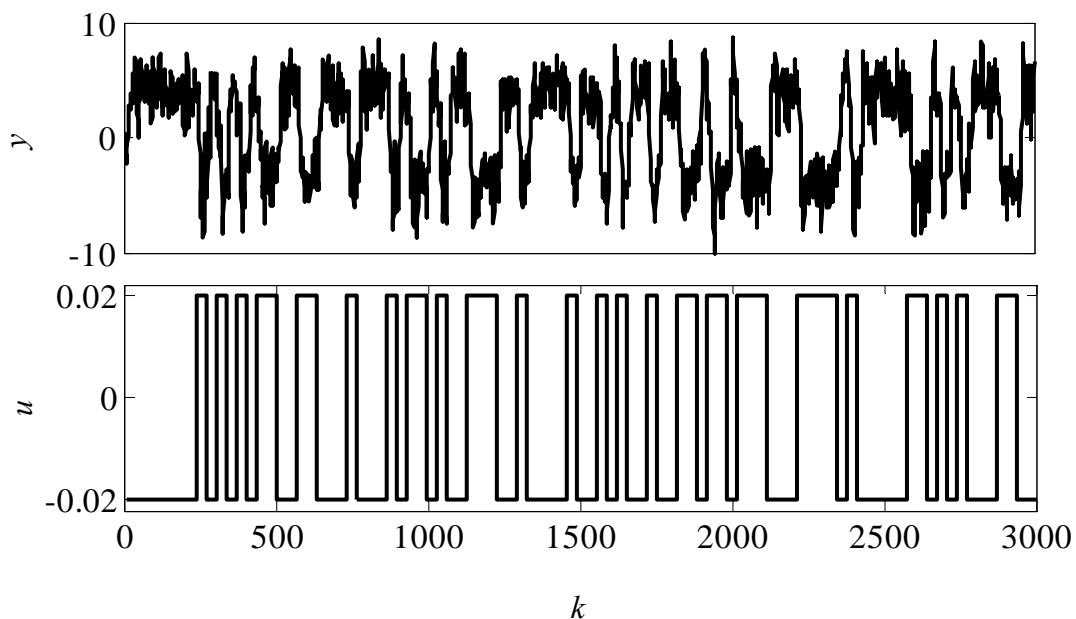
Figure 4.18 Output $y(k)$ and input sequences $u(k)$ used for

identification of system (4.43)

Four thousand data points generated using SIMULNK, with a sampling interval of 1 time unit and 3000 of them are used for identification and the remaining for validation.

OBF-AR model development

Following the principle used in Chapter 3, the number of OBF model parameters is chosen to be eight and estimated dominant poles $0.9262 \pm 0.1341i$. Therefore, an OBF model with eight Kautz filters and complex conjugate poles of $0.9262 \pm 0.1341i$ is developed. The estimated OBF model parameters and the time delay (τ_d) respectively, are:

$l = [\text{-16.2951 28.1518 -18.0434 -43.9996 -25.4772 -8.5612 -1.8118 11.2131}];$

$\tau_d = 12$ sampling intervals

The estimated noise models with $n_D = 2$, 5 and 7 for GOBF-AR model are given by (4.44), (4.45) and (4.46), respectively. The corresponding standard deviations of the residuals are 0.5977, 0.5127 and 0.5065.

$$\frac{1}{D(q)} = \frac{1}{1-1.4379q^{-1}+0.7384q^{-2}} \tag{4.44}$$

$$\frac{1}{D(q)} = \frac{1}{1 - 1.9151q^{-1} + 1.8774q^{-2} - 1.2147q^{-3} + 0.6189q^{-4} - 0.1885q^{-5}} \quad (4.45)$$

$$\frac{1}{D(q)} = \frac{1}{1 - 1.9588q^{-1} + 2.0203q^{-2} - 1.4920119q^{-3} + 1.0475q^{-4} - 0.6815q^{-5} + 0.3520q^{-6} - 0.1033q^{-7}}$$
$$(4.46)$$

Noise model selection

Figure 4.19 presents the spectrums of the three noise models (4.44)-(4.46).
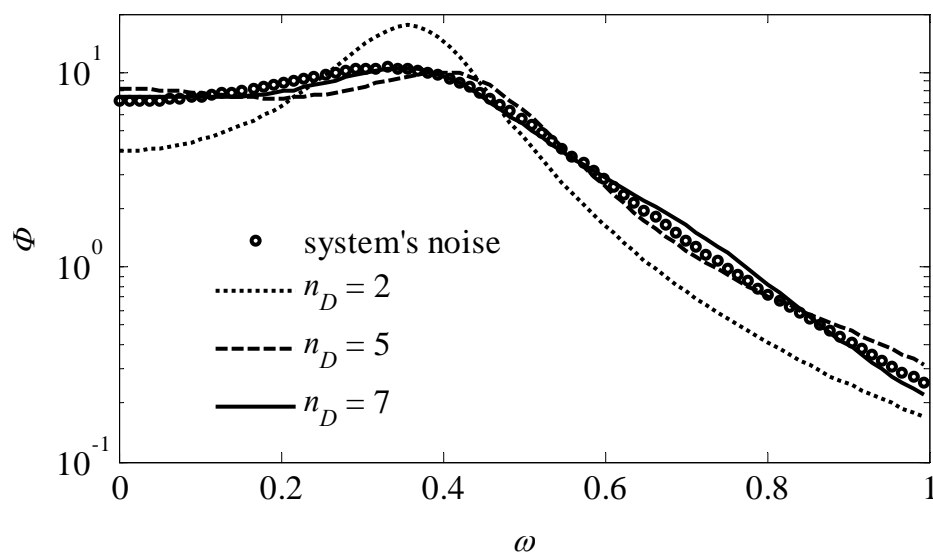
Figure 4.19 Spectrums of the noise models for $n_D = 2$, 5 and 7 compared to the noise

transfer function of system (4.43)

The PPE of the spectrums of the three noise models with respect to the original transfer function of the noise in the system are given in Table 4.5.

Table 4.5 PPE of the three noise models for system (4.43)

n_D	PPE
3	43.6865
5	5.5449
7	1.0426

From Figure 4.9 and Table 4.5, it is determined that the noise model with nD = 7 is the closest to the original noise transfer function of the system. Therefore this noise model together with the OBF model described earlier forms the OBF-AR model of the system.

Model Validation

The one-step-ahead prediction of the OBF-AR, the prediction of the OBF (simulation model) and the system output for the validation data are shown in Figure 4.20. For the sake of clarity only the first 200 data points are shown in the figure.
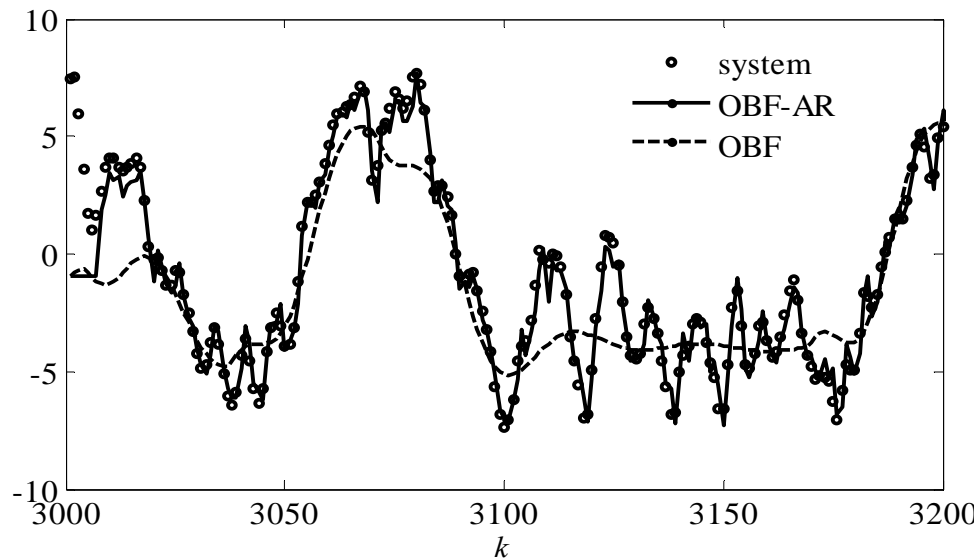
Figure 4.20 Validation of OBF and OBF-AR model of system (4.43)

The PPE of the one step-ahead prediction of the OBF and OBF-AR models with respect to the original output are 22.5394 and 2.9289, respectively. It is observed from Figure 4.4 and the prediction is highly improved by including the noise model.

The spectrum of the final estimated noise model compared to the original transfer function of the noise in the system is shown in Figure 4.6. The PPE of the spectrum of the estimated noise model compared to the noise transfer function in the system is 1.0426.

Figure 4.21 Spectrum of the system's noise transfer function compared to the estimated AR noise model of system (4.43)

Residual Analysis

Figure 4.22 depicts the qq-plot of the white noise added to the system and the residuals of the OBF-AR model.

Figure 4.22 qq-plot for the white noise to system (4.43) and the residuals of the OBF-AR model.

Figure 4.23 presents the distribution of the residuals of the OBF-AR model compared to the white noise added to the system. It is observed from the figure that the distribution of the residuals closely matches the distribution of the white noise added to the system.

Figure 4.23 Distribution of the residual compared to

the white noise for system (4.43)

The correlation among the residuals is given by

$\hat{R}$ = [0.0090 0.0018 0.0163 -0.0076 0.0181 -0.0226 0.0110 0.0061 -0.0076 0.0031]

From the study in this section it is observed that weakly damped systems are also identified with acceptable accuracy using the proposed OBF-AR structure. It is also noted that just as in the case of the well damped system, the order of the AR model should be large enough to capture the dynamics accurately. The validation analysis shows that the PPE of the one-step-ahead prediction of the OBF-AR model is 2.9289. The residual analysis shows that the residual of the OBF-AR model can be considered white noise and its distribution is the same as the distribution of the white noise introduced into the system.

OBF-ARMA model development using two-step method

OBF model

OBF model with eight Kautz filters and complex conjugate poles of $0.9262 \pm 0.1341i$ and model parameters

l = [-16.2951 28.1518 -18.0434 -43.9996 -25.4772 -8.5612 -1.8118 11.2131];

τ_d = 12 sampling intervals

define the OBF model.

The residuals of the OBF-AR model with the given OBF model and an AR model with $n_D = 7$ is used to estimate the parameters of the ARMA models with orders $n_D = n_C = 2, 4,$ 6 and the models (4.47) - (4.49) are obtained. The standard deviation of the residuals of the OBF-ARMA model with the three noise models for $n_D = n_C = 2, 4, 6$ are 0.5011, 0.4956, 0.4950, respectively.

$$\frac{C(q)}{D(q)} = \frac{1 + 0.7815q^{-1} - 0.0042q^{-2}}{1 - 1.1874q^{-1} + 0.5307q^{-2}} \tag{4.47}$$

$$\frac{C(q)}{D(q)} = \frac{1 - 0.5190q^{-1} - 0.2286q^{-2} + 0.5879q^{-3} - 0.0229q^{-4}}{1 - 2.5061q^{-1} + 2.8962q^{-2} - 1.6682q^{-3} + 0.4347q^{-4}} \tag{4.48}$$

$$\frac{C(q)}{D(q)} = \frac{1 - 0.3102q^{-1} - 0.0364q^{-2} - 0.3519q^{-3} - 0.2288q^{-4} - 0.0142q^{-5} - 0.0585q^{-6}}{1 - 2.3014q^{-1} + 2.6930q^{-2} - 1.8823q^{-3} + 0.7953q^{-4} - 0.1883q^{-5} + 0.0201q^{-6}}$$

$$\tag{4.49}$$

Selection of noise model order

Figure 4.24 depicts the spectrums of the three noise models given by (4.47)-(4.49). It is observed from the figure that the spectrums of all the noise models are close to the system's noise transfer function.
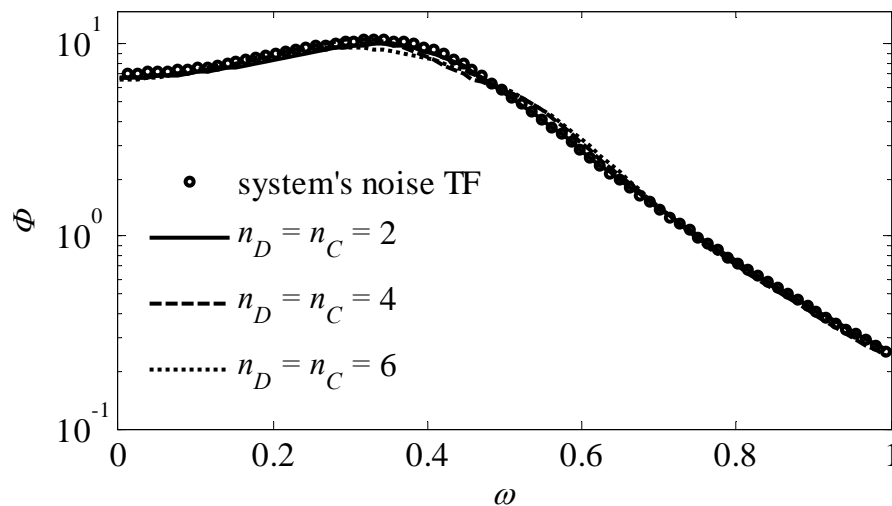
Figure 4.24 Spectrums of the ARMA noise models for $n_D = n_C = 2, 4$ and 6 compared to the system's noise transfer function of system (4.43)

The percentage predication errors of the spectrums of the three noise models with respect to the original system's noise transfer function are given in Table 4.6.

Table 4.6 PPE of the three ARMA noise models for system (4.43)

$n_D = n_C$	PPE
2	0.6866
4	0.8788
6	1.6681

Although it is difficult to choose which noise model is the closest to the system's noise transfer function from Figure 4.24, it is observed from Table 4.6 that the noise model with $n_D = n_C = 2$ is the closest, it is also the most parsimonious. Therefore this noise model together with the OBF model already stated form the OBF-ARMA model of the system.

Model validation

Figure 4.25 shows the comparison between the one-step-ahead predictions of the OBF-ARMA model and the systems output for the validation data points (3001-3200). The percentage prediction error of the OBF-ARMA model with respect to the system's output for the validation data points is 3.2539.
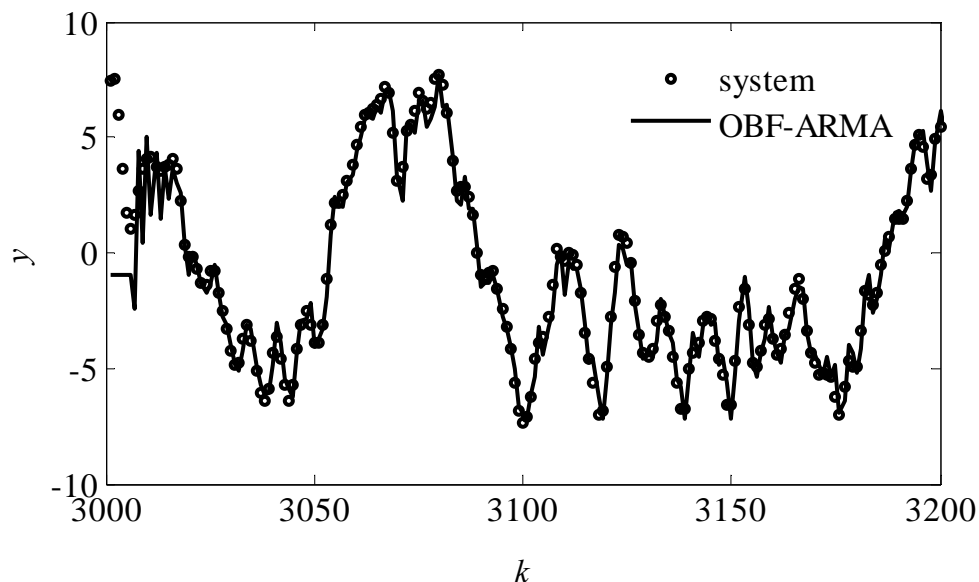
Figure 4.25 One-step-ahead prediction of the OBF-ARMA model compared to the output of system (4.43) for the validation data

Figure 4.11 presents the comparison between the spectrums of the selected ARMA noise model and the system's noise transfer function.
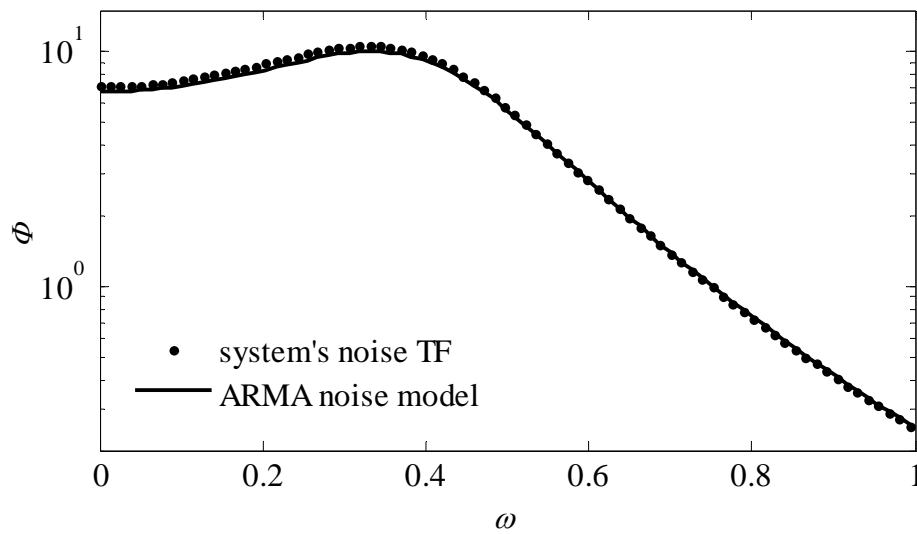
Figure 4.26 Spectrum of the noise model compared to the spectrum noise transfer function of system (4.43)

Residual Analysis

The qq-plot of the residuals with respect to the white noise added to the system are shown in Figure 4.27. The distribution of the residual compared to the white noise is shown in Figure 4.28.
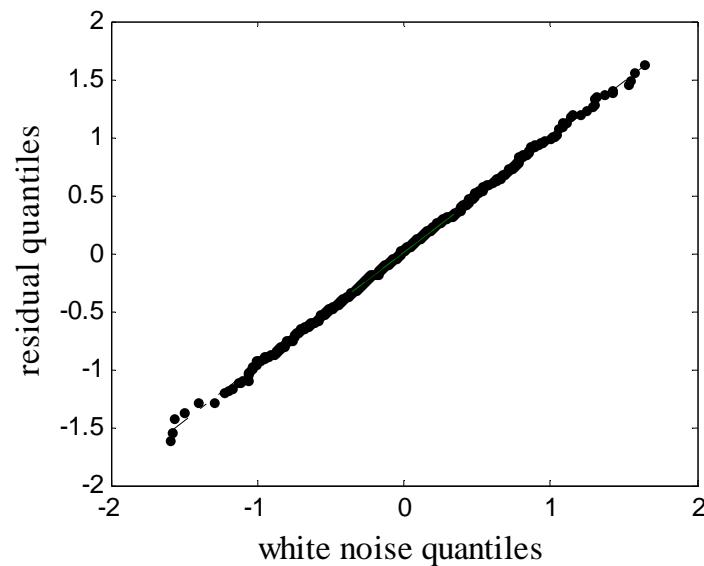
Figure 4.27 qq-plot of the white noise introduced into system (4.43) and the residuals of the OBF-ARMA model
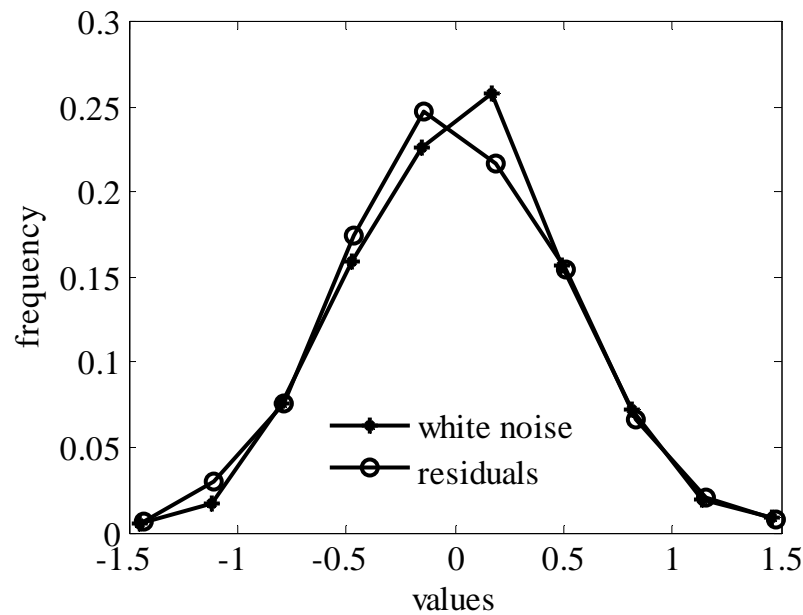
Figure 4.28 Distribution of the residual compared to the white
noise introduced to system (4.43)

The correlation among the residuals is given by

$\hat{R}$ = [0.0090 0.0018 0.0163 -0.0076 0.0181 -0.0226 0.0110 0.0061 -0.0076 0.0031]

It is observed from the results in this section that the two-step method of developing the OBF-ARMA model results in a model with acceptable accuracy for weakly damped systems also. The residual analysis shows that the distribution and size of residuals of the OBF-ARMA model, developed using the two-step method, are close to that of the white noise added to the system.

OBF-ARMA model development using the iterative method

In this section the same weakly damped system (4.43) is identified using the OBF model by the iterative (extended least square) method. The OBF model is not changed by the structure of the noise model. Therefore, the OBF model is defined by the eight Kautz filters with complex conjugate poles of $0.9262 \pm 0.1341i$ and model parameters and time delay given by:

l = [-16.2951   28.1518 -18.0434 -43.9996 -25.4772 -8.5612 -1.8118 11.2131];

τ_d = 12 sampling intervals

Noise model selection

The residuals of the OBF-ARMA model with $n_D = 7$ is used for the first iteration, to estimate the parameters of the ARMA model with orders $n = m = 2$, 4, 6 and the minimum percentage prediction errors of the OBF-ARMA model are found iteratively to be 1.4596, 1.4536 and 1.4562, respectively. The noise models corresponding to these PPE values are given by (4.50)-(4.52) and their respective standard deviations are 0.4958, 0.4961 and 0.4969.

$$\frac{C(q)}{D(q)} = \frac{1 + 0.8303q^{-1} + 0.0412q^{-2}}{1 - 1.1619q^{-1} + 0.5142q^{-2}} \tag{4.50}$$

$$\frac{C(q)}{D(q)} = \frac{1 + 0.1992q^{-1} - 0.7946q^{-2} - 0.2837q^{-3} - 0.0462q^{-4}}{1 - 1.7928q^{-1} + 0.9383q^{-2} + 0.0261q^{-3} - 0.1565q^{-4}} \tag{4.51}$$

$$\frac{C(q)}{D(q)} = \frac{1 + 0.0587q^{-1} + 0.2197q^{-2} - 0.2693q^{-3} - 0.5622q^{-4} + 0.1120q^{-5} - 0.0657q^{-6}}{1 - 1.9337q^{-1} + 2.2296q^{-2} - 2.2722q^{-3} + 1.6916q^{-4} - 0.7396q^{-5} + 0.1235q^{-6}}$$

$$\tag{4.52}$$

The percentage prediction errors of the spectrums of the three noise models (4.50)-(4.52) are found to be 0.8628, 1.1043 and 1.4638, respectively. Therefore, the noise model that has the minimum PPE and the most parsimonious (4.50) is chosen to represent the system's noise transfer function. This noise model and the OBF model mentioned earlier constitute the OBF-ARMA model of the system.

Model Validation

The one-step-ahead prediction of the OBF-ARMA and the output of the system for the validation data points 3001-3200 are depicted in Figure 4.29. The PPE of the one step-ahead prediction of the OBF-ARMA model for the validation data is 3.1247.
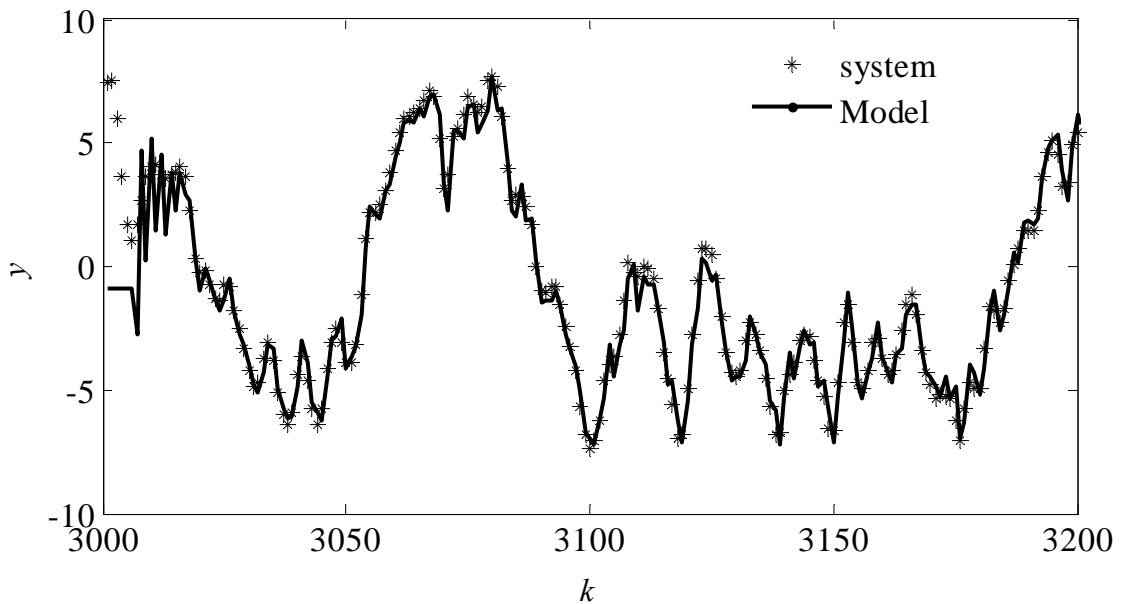
Figure 4.29 One step ahead prediction of the OBF-ARMA model compared to the output of system (4.43)

The spectrum of the final estimated noise model compared to the noise transfer function in the system is shown in Figure 4.30. The PPE of the spectrum of the estimated noise model compared to the noise transfer function in the system is 0.8628.
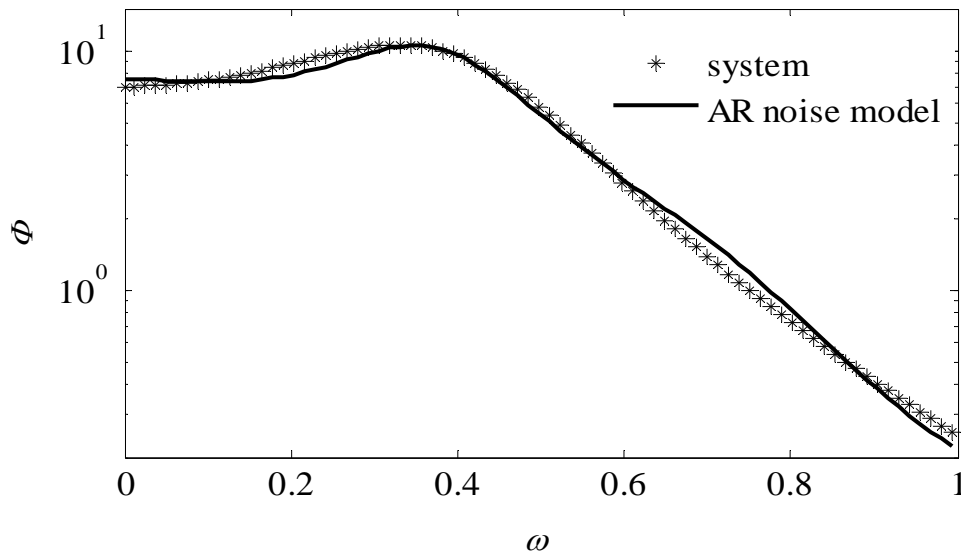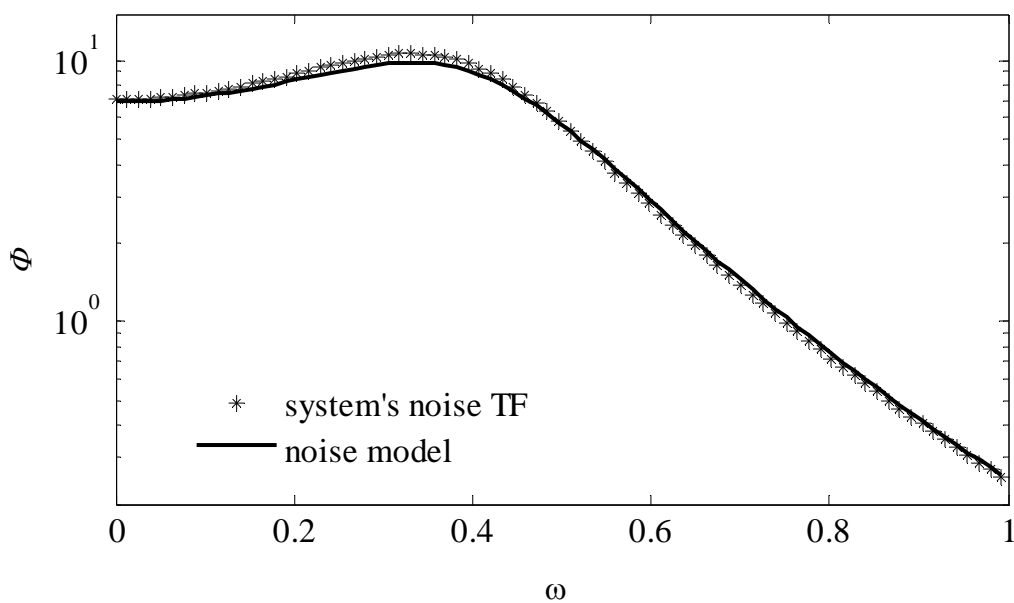

Figure 4.30 Spectrum of the ARMA noise model by the iterative method compared to the noise transfer function of system (4.43)

Residual Analysis

Figure 4.31 depicts the qq-plot of the white noise added to the system and the residuals of the OBF-ARMA model developed using the iterative extended least square method. Figure 4.32 presents the distribution of the residuals of the OBF-ARMA model, developed using the iterative method, compared to the white noise added to the system.
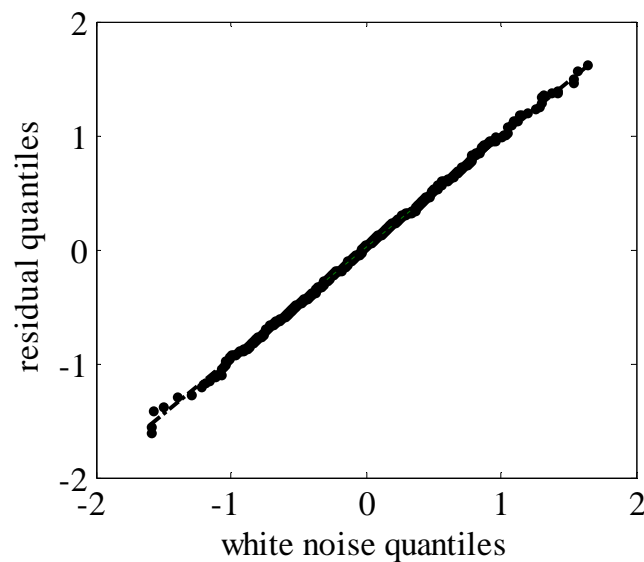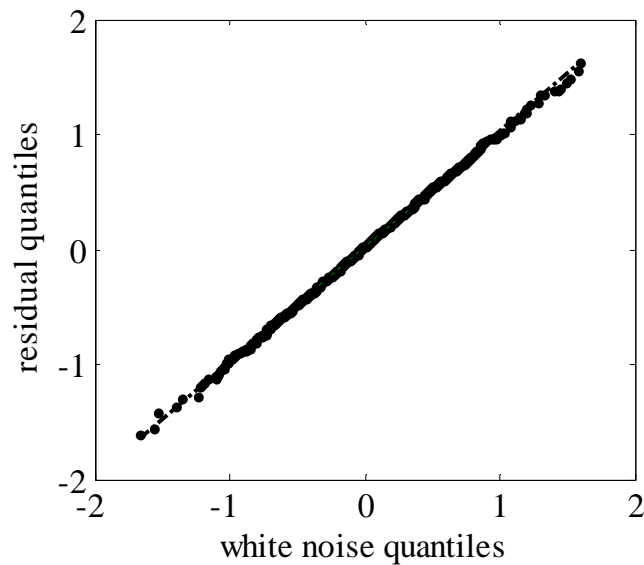

Figure 4.31 qq-plot for the white noise added to system (4.43) and the residuals of the OBF-AR model
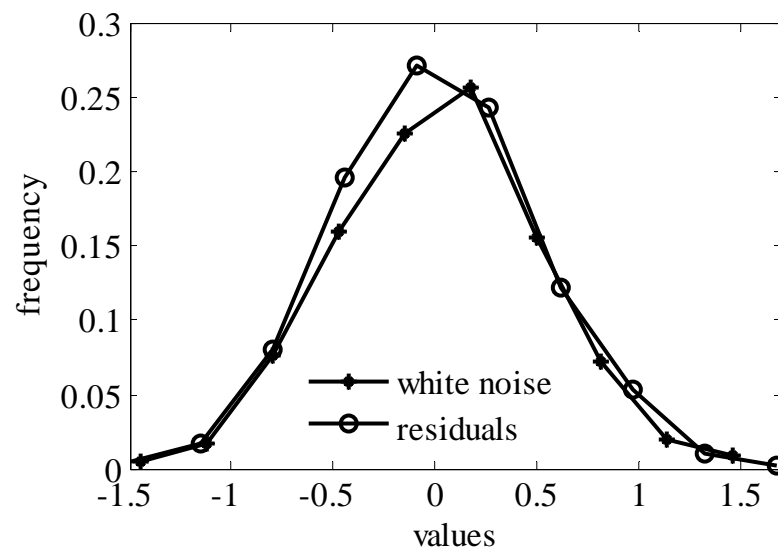
Figure 4.32 Distribution of the residual compared to the white noise introduced into system (4.43)

It is observed from the figure that the distribution of the residuals closely matches the distribution of the white noise added to the system.
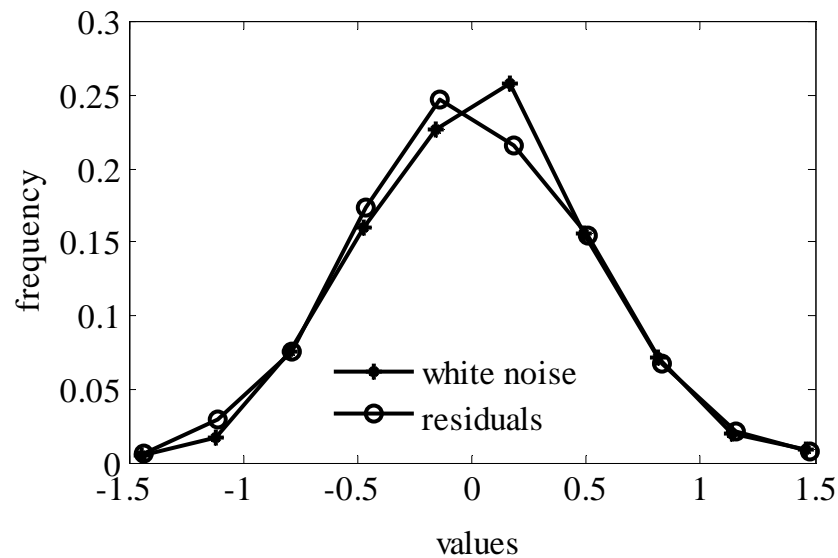
The correlation among the residuals is given by

$\hat{R}$ = [0.0050 0.0096 0.0074 0.0018 0.0037 -0.0022 0.0019 0.0039 -0.0045 0.0062]

The result of the validation and residual analysis shows that the iterative (extended least square method) also gives models with acceptable accuracy. It also gives the means by which to compare and choose the number and best values of the parameters of the ARMA noise model.

Multi-step-ahead predictions

Table 4.7 gives the percentage prediction errors for 1 to 5 steps ahead using the OBF, OBF-AR and OBF-ARMA modes of system (4.43). The OBF model used is the common one in the case study while the AR and ARMA noise models are those given by (4.46) and (4.50), respectively. In this case study also, the short tem predictions (1 and 2) are improved significantly.

Table 4.7 The PPE for 1 to 5 step- ahead- predictions of OBF-AR and OBF-ARMA models compared to OBF model for system (4.43)

i	OBF	OBF-AR	OBF-ARMA
1	17.6009	1.6837	1.6815
2	17.2751	9.1221	9.1705
3	17.0646	17.3056	17.4871
4	16.9795	22.0325	22.3616
5	16.9501	23.4470	23.8396

4.2.5.3 Identification of a Pilot –Scale Binary Distillation Column

Model development for a pilot scale binary distillation column is considered in this real plant case study. The distillation column is a part of a reaction-separation system where the output from the reactor is the feed for the distillation column. Isopropyl Alcohol (IPA) is dehydrogenated in the catalytic packed bed tubular reactor. The products from the reactor, acetone and hydrogen, together with unreacted IPA are cooled in a plate heat exchanger and sent to a vapor-liquid separator where hydrogen is separated from condensed acetone and IPA. This acetone-IPA mixture is stored in an intermediate

storage vessel and fed to the distillation column for separation. The bottom product of the column consisting mainly of IPA is recycled back to the reactor. In the present study, the distillation column alone is operated with an acetone-IPA mixture as the feed and the product streams are recombined.

A snapshot of the 5.5m high distillation column is shown in Figure 4.33. The major dimensions of the column and the nominal operating conditions are given in Table 4.8. The column is provided with RTD sensors and sampling ports at every tray, flow meters in the feed line, product streams and reflux line, differential pressure sensors in the stripping and enriching sections and a pressure sensor at the top of the column. Appropriately sized control valves are provided in all flow lines.

Figure 4.33 Snapshot of the distillation column

Table 4.8. Major dimensions and nominal operating conditions of the distillation column

Description	Value
Height	5.5 m
Diameter	0.15 m
Number of trays	15
Type of tray	Bubble cap
Tray spacing	35 cm
Tray numbering	Bottom to top
Feed Tray	Tray 7
Feed rate	0.5 l/min
Reflux flow rate	0.7 l/min
Steam flow rate	20 kg/hr
Distillate flow rate	0.3 l/min
Bottom product flow rate	0.2 l/min
Feed composition, mole fraction	0.1824 (acetone)
Bottom Temperature	80.5 $^{\circ}$C
Top temperature	72.7 $^{\circ}$C
Column pressure	1.013 bar

A Honeywell Experion PKS DCS is installed for data acquisition and control. Experiments are conducted for a constant feed rate and fixed feed composition for variations in reflux flow rate and steam flow rate. The column pressure is maintained constant by manipulating the cooling water flow rate to the condenser. The liquid levels in the reflux drum and column bottom are controlled by manipulating the top and bottom product flow rates, respectively. The reflux and steam flow rates are varied by changing

the setpoints of the respective controllers according to a PRBS sequence. The temperatures at tray 1 (bottom) and tray 14 (top) are used as output signals. The input signals to the reflux flow rate (F_R) and steam flow rate (F_{st}) controllers and the output signals of temperatures from tray 1 (T_1) and tray 14 (T_{14}) are used for the system identification in this case study.

For the system identification tests, the input sequences are designed as a low frequency pseudo random binary signal (PRBS) generated using the '*idinput*' function in MATLAB with band [0 0.04] and levels [18 22] kg/hr and [0.4 0.8] lt/min for steam and reflux flow rates, respectively. The input levels are selected such that maximum excitation is achieved while enabling the smooth running of the column.

Four thousand data points are collected with a sampling interval of 5s. The first three thousand data points are used for model identification and the rest 1000 data points are used for validation. Since, it is already shown that OBF-ARMA is more flexible, parsimonious and accurate, in this case study, the distillation column is developed using GOBF-ARMA model. The input and output sequences used for identification are presented in Figure 4.34.
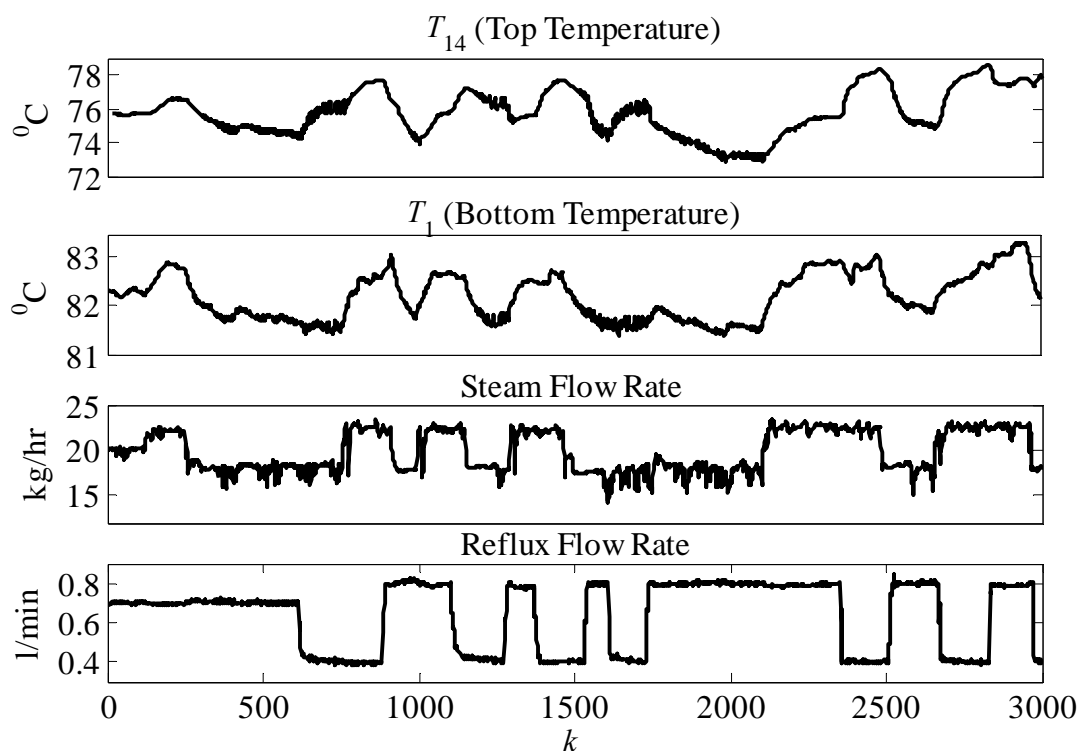
Figure 4.34 Input-output sequences used for identification of the distillation column

GOBF-ARMA Model

The present case study is a 2 x 2 system and therefore four OBF models and two noise models are required to be developed. The transfer function of the distillation column is given in the following form

$$\begin{bmatrix} T_{14} \\ T_1 \end{bmatrix} = \begin{bmatrix} G_{11} & G_{12} \\ G_{21} & G_{22} \end{bmatrix} \begin{bmatrix} F_{st} \\ F_R \end{bmatrix} + \begin{bmatrix} H_1 \\ H_2 \end{bmatrix} \begin{bmatrix} e_1 \\ e_2 \end{bmatrix}$$

(4.53)

where

G = OBF models

H = Stochastic part of the model (ARMA)

$e_1,\ e_2$ = innovation sequences

Selection of OBF model

Preliminary studies using the procedure developed in Chapter 3 show that the four transfer function relating the two outputs to the two inputs are described better by one dominant pole and six Laguerre filters. The estimated dominant poles for the four transfer functions are given by

$$p = \begin{bmatrix} 0.9515 & 0.4112 \\ 0.8805 & 0.9702 \end{bmatrix}$$

(4.54)

Therefore, four OBF models, each with six Laguerre filters and one dominant pole given by (4.54), were developed. The estimated OBF model parameters are

L_{11} = [0.0298   0.0037   0.0035   0.0018   -0.0005   0.0050]

L_{12} = [0.0214   0.1017   0.0497   -0.0949   0.1252   -0.0112]

L_{21} = [0.0137   0.0326   0.0028   0.0348   -0.0128   0.0375]

L_{22} = [-0.8330   0.2001   -0.2893   0.0377   -0.1374   0.0870]

The time delay estimates in number of sampling intervals are

$$\tau_d = \begin{bmatrix} 0 & 5 \\ 5 & 0 \end{bmatrix}$$

Selection of noise model

Noise models with various orders are compared, the minimum percentage prediction error of the OBF-ARMA model with the selected OBF model and various orders of noise models using the proposed iterative extended least square method are given in Table 4.9. The order of the first AR noise model is 6.

Table 4.9 Minimum prediction errors for distillation column

Model order $n_D=n_c$	Minimum PPE
2	0.2269
3	0.1904
4	0.1910
5	0.1907

Since the percentage prediction error difference between orders 2 and 3 is less than 0.05% and since order 2 is more parsimonious (2 numerator, 2 denominator) the noise order is chosen as $n_D = n_C = 2$.

The two ARMA noise models are given by (4.55) and (4.56), respectively.

$$H_1 = \frac{1 - 0.8415q^{-1} - 0.1225q^{-2}}{1 - 1.9077q^{-1} + 0.9082q^{-2}} \tag{4.55}$$

$$H_2 = \frac{1 - 0.2176q^{-1} - 0.64265q^{-2}}{1 - 1.7575q^{-1} + 0.7607q^{-2}} \tag{4.56}$$

The standard deviations of the innovation sequences e_1 and e_2 are 0.0288 and 0.0655, respectively.

Model Validation

The outputs of the OBF model (simulation model) of the distillation column top and bottom temperature compared to the system outputs for the validation data points are shown in Figure 4.35 (a) and (b). The percentage prediction error of the OBF model for the top and bottom temperatures, respectively are 11.5293 and 18.7596.
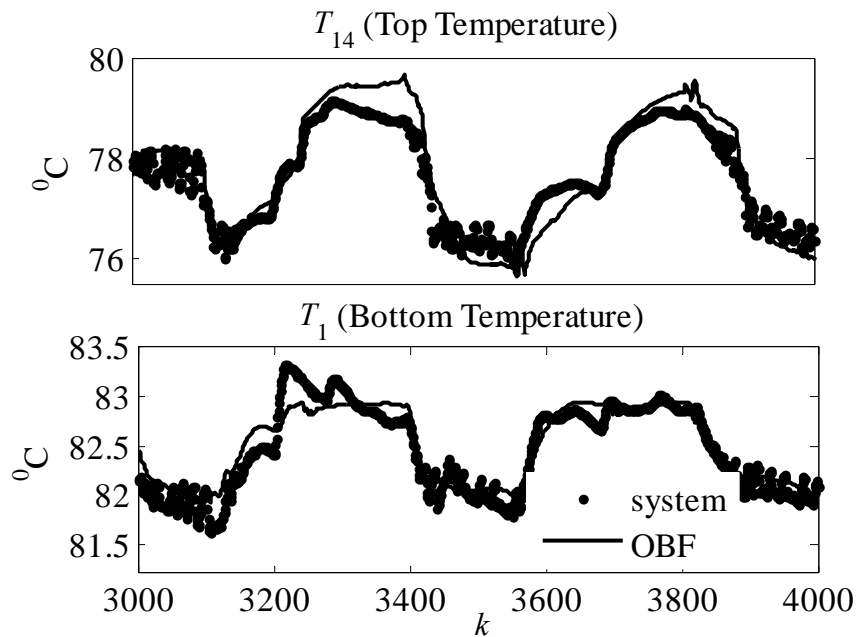
Figures 4.35 Prediction by the OBF-simulation model compared to the systems output for top (a) and bottom (b) Temperatures

The one-step-ahead prediction by the OBF-ARMA model compared to the system's outputs is shown in Figure 4.36 (a) and (b). The PPE values of the OBF-ARMA model for the validation data points for the top and bottom temperatures are 0.4345 and 0.6562 respectively.
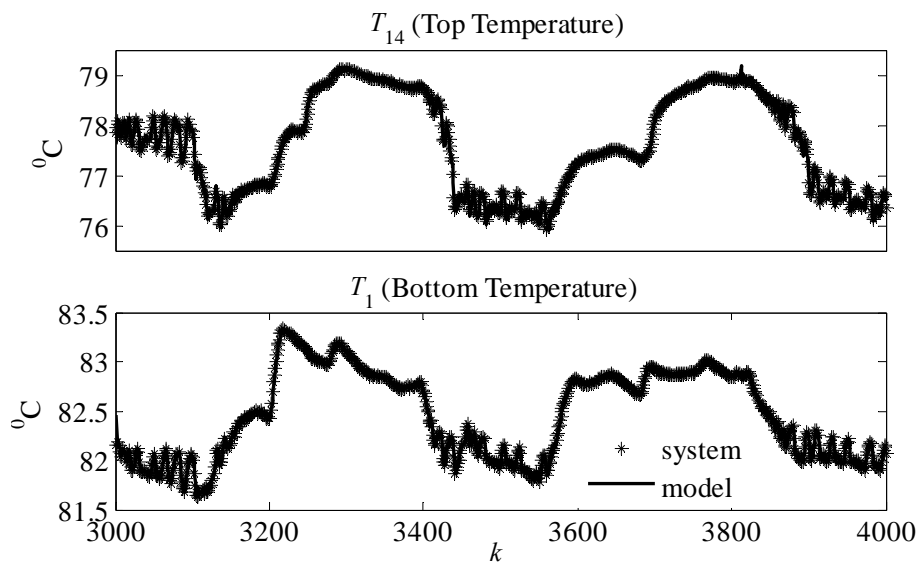
Figures 4.36 One-step-ahead prediction by the OBF-ARMA model compared to the systems output for top (a) and bottom (b) Temperatures

It is observed from the values of the PPE and Figure 4.36 that the noise model has significantly improved the prediction capability of the model.

Residual Analysis

The distribution of the residuals of the OBF-ARMA model for the validation data, for the top and bottom temperatures are shown in Figure 4.37 (a) and (b), respectively. The correlation among the residuals is given by

$$\hat{R}_1 = 10^{-3} \times [0.5481 \quad 0.2218 \quad 0.0660 \quad -0.0458 \quad -0.0928 \quad -0.1238 \quad -0.1077 \quad -0.0762 \quad -0.0539 \\ 0.0405]$$

$$\hat{R}_2 = 10^{-3} \times [0.9227 \quad 0.9406 \quad -0.4896 \quad -0.4175 \quad -0.7111 \quad -0.5041 \quad -0.1605 \quad -0.1698 \quad -0.0329 \\ -0.0043]$$

This case study of a real plant clearly shows the effectiveness of the proposed OBF-ARMA model. Besides providing explicit noise models for each output channel, including the noise model has greatly improved prediction capacity of the models. The distributions of the residuals are close to a normal distribution with mean zero. The values of the correlation among the residuals are close to zero, which means that the sequences of the residuals are not correlated. The residual analysis, therefore, confirms also that the model has acceptable accuracy.
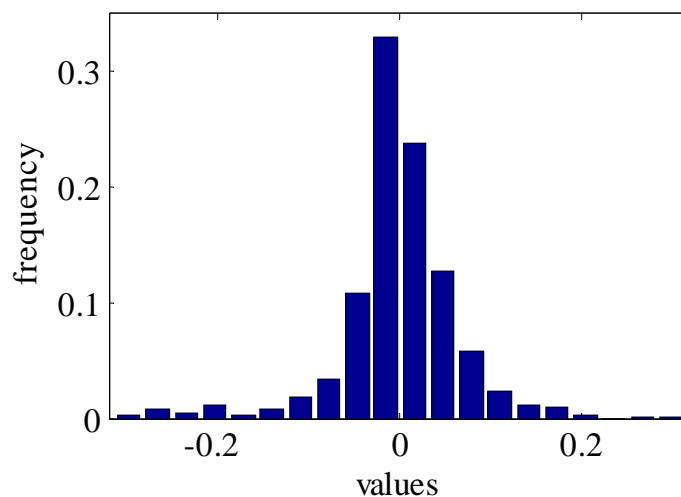
(a)
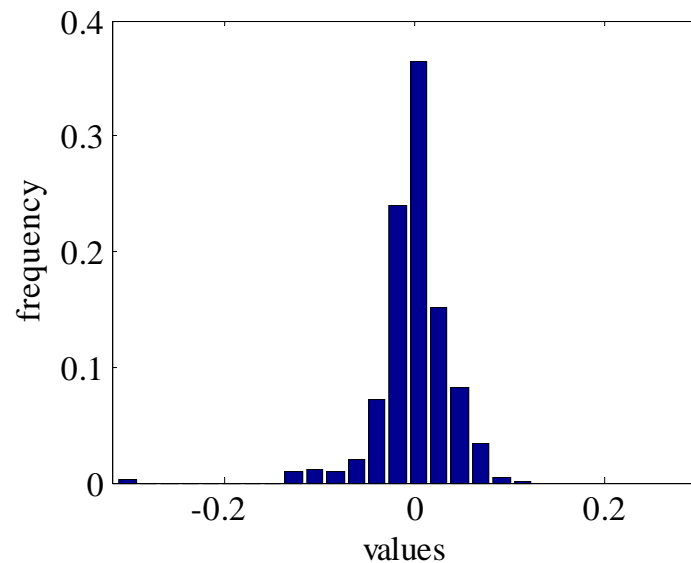
(b)

Figure 4.37 Distribution of the residuals of the OBF-ARMA model of the distillation column for the validation data points: (a) Top temperature and (b) Bottom temperature

In this section, a unified scheme for developing BJ type time series models from open-loop test data by combining orthonormal basis filter model and conventional time series models is presented. The models have an OBF deterministic model and an AR or ARMA noise model. It is illustrated that the proposed model structures inherit all the advantages of an OBF model together with an explicit noise model. Furthermore, it is shown that combining the noise model to an OBF model and treating it as a single model results in a prediction model with a higher prediction capability than the conventional OBF model, in the presence of unmeasured disturbances. Algorithms for estimating the model parameters are developed. In addition, schemes for multi-step ahead prediction for both OBF-AR and OBF-ARMA models are developed. It is illustrated by both simulation and real plant case study that the proposed methods are effective for system identifications of both SISO and MIMO systems.

4.7   OBF based prediction Models from Closed-Loop Data

When a system identification test is carried out in open loop, in general, the input sequence is not correlated to the noise sequence and OBF model identification is carried out in a straight forward manner. However, when the system identification test is carried

out in closed loop the input sequence is correlated to the noise sequence and conventional OBF model development procedures fail to provide consistent model parameters.

In this section, the problem of model development from closed-loop data is considered. The problem has two distinct aspects, namely, model development from closed loop data when the system is open-loop stable and when the system is open-loop unstable. In all cases, both the system and noise model are considered important. Three different methods based on direct and indirect approaches are used to deal with the problems. The first is based on the indirect approach while the second and third are based on the direct approach.

While the general approaches dealing with closed loop system identification are not new, the special nature of OBF structure makes a direct implementation of conventional OBF model development impossible, and therefore considerable adjustments are required. First, from the structure of OBF models it can be easily seen that it have non-minimum phase zero. This will make it impossible to use in denominator, since that will make the resulting models unstable. This is particularly related to the two-step, indirect identification approach. Second, as it is pointed out in the theory of OBF model, in Chapter 3, the conventional OBF structure is designed for stable processes. Therefore, as a direct implication they cannot be used to model open-loop unstable processes.

In the first section, the two-step indirect identification approach is presented. In this thesis, this method is named the "decorrelation method" to identify it from the two-step method proposed in Chapter 3. In the second and third sections, the direct closed loop identification methods using OBF models with ARX and ARMAX structures, respectively, are discussed. In the last section, two simulation and one real plant case studies related to the proposed methods are presented.

4.7.1   Indirect Closed-loop Identification Using the Decorrelation Method

In this section, a two step method which is based on decorrelating the noise sequence from the input sequence is adopted for OBF model development. While the general approach is not new, it needs some serious considerations and changes to use it for OBF model development. In this respect the scheme is novel.

4.7.1.1 Identification Scheme

Consider the closed-loop block diagram shown in Figure 4.38.
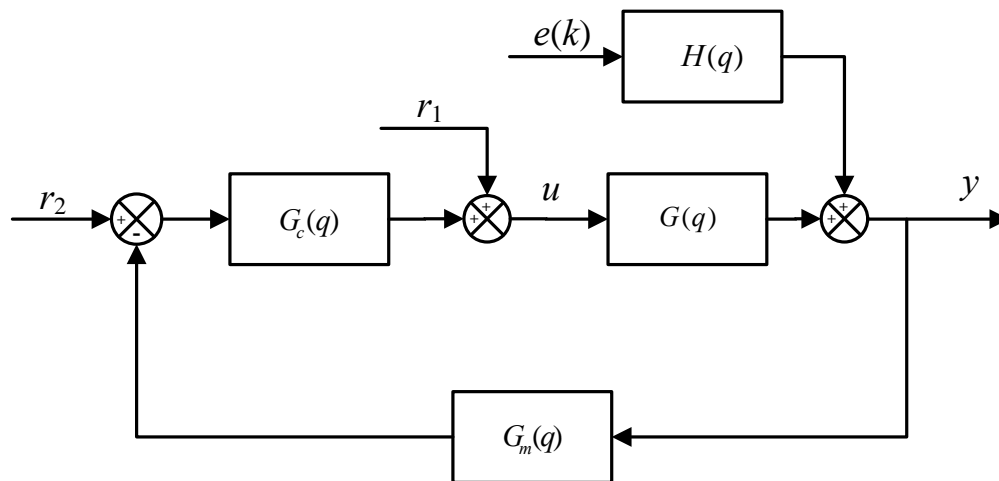
Figure 4.38 Block diagram of the system used in closed-loop identification

In the figure

r_1 = is the external excitation signal

r_2 = set point

$G(q)$ = process model to be identified

$H(q)$ = disturbance model to be identified

$G_c(q)$ = controller transfer function

$G_m(q)$ = sensor and transmitter transfer function

$e(k)$ = innovation sequence

The decorrelation method is based on using a simulated input u^r, which is not correlated with the noise, in place of the plant input u which is correlated with the noise. Then, the standard prediction error method can be utilized with the prediction errors.

$$e^r(k) = \frac{1}{H^r(q)}\big(y(k) - G(q)u^r(k)\big)$$

$$(4.57)$$

where $H^r(q)$ describes the influence of the disturbance in the closed loop system, i.e.,

$$H^r(q) = \frac{H(q)}{1 + G_c(q)G(q)G_m(q)}$$

$$(4.58)$$

To perform the identification, first the transfer function from r_1 to u is identified.

$$S(q) = \frac{u(k)}{r_1(k)} \tag{4.59}$$

From closed-loop relations

$$S(q) = \frac{1}{1 + G_c(q)G(q)G_m(q)} \tag{4.60}$$

The simulated input u^r is obtained by filtering r_1(k) using $S(q)$

$$u^r(k) = S(q)r_1 \tag{4.61}$$

The prediction error (4.56) based identification method is used to obtain $\hat{G}(q)$ and $\hat{H}^r(q)$. The actual noise model is estimated using (4.62), which is derived from (4.58) and (4.60)

$$\hat{H}(q) = \frac{H^r(q)}{S(q)} \tag{4.62}$$

In order to develop the GOBF-ARMA model, at the first stage, any appropriate structure can be chosen for $S(q)$. However, the selected structure should satisfy the following conditions

(1) It should not have non-minimum phase zeros, otherwise the noise model obtained from (4.62) will be unstable

(2) The numerator of $S(q)$ should be monic so that the denominator of the noise model will be monic and prediction becomes possible.

In light of the above conditions, OBF structure cannot be used in the first stage to identify $S(q)$, because it contains non-minimum phase zero and therefore it does not satisfy condition (1). BJ and Output Error (OE) can be used with special modifications; however, the requirement of nonlinear optimization makes them not good choices. Modified forms of ARX structures could be used; however preliminary simulation studies indicate that the inconsistency problem seriously affects the accuracy of the final models. It is found that a modified form of the ARMAX structure results in models that have acceptable accuracy. The proposed modified ARMAX structure for the first stage, modeling of $S(q)$, is discussed below.

In the development of the standard linear structures, the model is generally assumed to be strictly proper[2]. This is because the input does not affect the output instantaneously. The resulting standard ARMAX model is

$$y(k) + a_1 y(k-1) + \ ... \ + a_n y(k-n) = b_1 u(k-1) + \ ... \ + b_m u(k-m)$$
$$+ e(k) + c_1 e(k-1) + ... + c_p e(k-p) \quad (4.63)$$

However, (4.63) does not satisfy the second condition, since the coefficient of $u(k)$ is different from 1, $i.e.$, $b_0 = 0 \neq 1$, not monic. To satisfy this requirement that the numerator should be monic, (4.63) is modified to the following form.

$$y(k) + a_1 y(k-1) + ... + a_n y(k-n) = u(k) + b_1 u(k-1) + ... + b_m u(k-m) +$$
$$e(k) + c_1 e(k) + ... + c_p e(k-p) \quad (4.64)$$

Since ARMAX is not the final model of the system, but an intermediate stage for estimating the simulated input and the noise model, the modification will not affect the quality of the final model negatively.

4.7.1.2 Estimating the Modified ARMAX Model parameters

From (4.64) the one step-ahead prediction becomes

$$\hat{y}(k \mid k-1) = -a_1 y(k-1) - ... - a_n y(k-n) +$$
$$u(k) + b_1 u(k-1) + ... b_m u(k-m) +$$
$$c_1 e(k-1) + ... + c_p e(k-p) \quad (4.65)$$

The regressor matrix for finding the parameters of (4.64) is for $m = n = p$

$$X = \begin{bmatrix} -y(m-1) & -y(m-2) \ ... -y(1) & u(m) & u(m-1)...u(1) & e(m-1) & e(m-2) & ... & e(1) \\ y(m) & -y(m-1) \ ... -y(2) & u(m+1) & u(m) \ ... & u(2) & e(m) & e(m-1) & ... e(2) \\ . & . & . & . & . & . & . & . \\ . & . & . & . & . & . & . & . \\ . & . & . & . & . & . & . & . \\ y(N-1) & -y(N-2) ...-y(N-m) & u(N) & u(N-1) \ ... u(N-m) & e(N-1) & e(N-2)... & e(N-m) \end{bmatrix} \quad (4.66)$$

where $e(i)$ is the prediction error.

The prediction error can be estimated from a corresponding ARX model with high order. The regressor matrix for the corresponding ARX model is

$$X = \begin{bmatrix} -y(m-1) & -y(m-2) \ ... & -y(1) & u(m) & u(m-1) \ ... \ u(1) \\ y(m) & -y(m-1) \ ... & -y(2) & u(m+1) & u(m) \ ... \ u(2) \\ . & . & . & . & . & . \\ . & . & . & . & . & . \\ . & . & . & . & . & . \\ y(N-1) & -y(N-2) \ ... - y(N-m) & u(N) & u(N-1) ... \ u(N-m) \end{bmatrix} \quad (4.67)$$

Using (4.67) in the least square formula (3.20) the parameters of the high-order ARX model are estimated. The model parameters are used to estimate the one- step-ahead prediction. The prediction error is then calculated using the one step-ahead prediction and the actual output using

$$e(k) = y(k) - \hat{y}(k \mid k-1) \tag{4.68}$$

The prediction error estimate is used in forming the regressor matrix (4.66). The parameters of the modified ARMAX model are, then, estimated using (4.66) in (3.20). The prediction error, and consequently the ARMAX parameters can be improved by estimating the parameters of the ARMAX and using it in (4.66) iteratively.

4.7.1.3 The simulated input

Once the modified ARMAX mode is developed, its deterministic part is taken as an estimate of $S(q)$. Therefore the simulated input is obtained by

$$u^r(k) = \frac{B(q)}{A(q)} r_1(k) \tag{4.69}$$

4.7.1.4 The Final Model

Using the simulated input from (4.69) as an input and the plant output, $y(k)$, an OBF-ARMA model is developed using the Algorithm 4.2. While the OBF model is the deterministic part of the estimate of the plant model, $G(q)$, the ARMA noise model obtained at this stage is not the true noise model. It is the effect of the noise on the closed loop response denoted by $\hat{H}^r(q)$ in (4.62). The true noise model is estimated using the noise model from the OBF-ARMA model, $C(q)/D(q)$, in (4.62). Note that $S(q) = B(q) / A(q)$ from the modified ARMAX model.

$$\hat{H}(q) = \frac{C(q)/D(q)}{B(q)/A(q)} \tag{4.70}$$

Therefore the, OBF model together with the noise model given by (4.70) defines the proposed OBF-ARMA model.

4.7.2 Direct Closed-loop Identification

The motivation for the structures proposed in this section is the problem of closed-loop identification of open-loop unstable processes. Closed-loop identification of open-loop unstable processes requires that any unstable poles of the plant model $G(q)$ should be shared by the noise model $H(q)$, otherwise the predictor will not be stable. It is indicated by both Ljung [1] and Nelles [2] that if this requirement is satisfied closed-loop identification of open-loop unstable processes can be handled without problem. Based on this fact, the decorrelation method cannot be used for open-loop unstable processes, because the OBF component in the OBF-ARMA structure is inherently stable, i.e. no unstable poles, and it does not necessarily share any pole with the noise model. In this section, two different linear structures that satisfy these requirements and which are based on OBF structure are proposed. While the proposed models are, specially, effective for developing prediction model for open-loop unstable process that are stabilized by feedback controller, they can be used for open-loop stable process also. These two linear model structures are OBF-ARX and OBF- ARMAX structures.

4.7.3 Closed–loop Identification Using OBF-ARX model

Consider an OBF model with ARX structure given by (4.71)

$$y(k) = \frac{G_{OBF}(q)}{A(q)}u(k) + \frac{1}{A(q)}e(k) \tag{4.71}$$

Rearranging (4.71)

$$\hat{y}(k \mid k-1) = G_{OBF}(q) - (1 - A(q))y(k) \tag{4.72}$$

With $A(q)$ monic (4.72) can be expanded to

$$\hat{y}(k \mid k-1) = G_{OBF}(q) - a_1 y(k-1) - a_2 y(k-2) - a_m y(k-m) \tag{4.73}$$

Note that, (4.73) can be further expanded to

$$\hat{y}(k \mid k-1) = l_1 u_{f1}(k) + l_2 u_{f2}(k) + ... + l_m u_{fm}(k) -$$
$$a_1 y(k-1) - a_2 y(k-2) - ... - a_n y(k-n) \tag{4.74}$$

Therefore, the regressor matrix for the OBF-ARX structure is given by

$$X = \begin{bmatrix} u_{f1}(mx) \; u_{f2}(mx-1)..u_{fm}(mx-m) & -y(mx-1) \; -y(nx-2)...-y(mx-n) \\ . & . & . & . & . & . \\ . & . & . & . & . & . \\ . & . & . & . & . & . \\ u_{f1}(N) \; u_{f2}(N-1)...u_{fm}(N-m) & -y(N-1) \; -y(N-2)...-y(N-n) \end{bmatrix} \tag{4.75}$$

where m = order of the OBF model

n = order of $A(q)$

mx = max $(n, m) + 1$

u_{fi} = input u filtered by the corresponding OBF filter f_i

The parameters are estimated using (4.75) in the least square equation (3.20). Note that in using (3.20) the size of y must be from mx to N.

4.7.4 Closed–loop Identification Using OBF-ARMAX model

Consider the OBF model with ARMAX structure

$$y(k) = \frac{G_{OBF}(q)}{A(q)} u(k) + \frac{C(q)}{A(q)} e(k) \tag{4.76}$$

Rearranging (4.76)

$$\hat{y}(k \mid k-1) = G_{OBF}(q) - (1 - A(q))y(k) + (C(q)-1)e(k) \tag{4.77}$$

With $A(q)$ and $C(q)$ monic, expanding (4.77)

$$\hat{y}(k \mid k-1) = l_1 u_{f1}(k) + l_2 u_{f2}(k) + ... + l_m u_{fm}(k) +$$
$$- a_1 y(k-1) - a_2 y(k-2) - ... - a_n y(k-n) +$$
$$c_1 e(k-1) + c_2 e(k-2) + ... + c_n e(k-n) \tag{4.78}$$

From (4.78) the regressor matrix is formulated for orders m, n, p

$$X = \begin{bmatrix} u_{f1}(mx) & u_{f2}(mx-1)...u_{fm}(mx-m) & -y(mx-1) & -y(nx-2)...-y(mx-n) \\ \cdot & \cdot & \cdot & \cdot & \cdot & \cdot \\ \cdot & \cdot & \cdot & \cdot & \cdot & \cdot \\ \cdot & \cdot & \cdot & \cdot & \cdot & \cdot \\ u_{f1}(N) & u_{f2}(N-1)...\, u_{fm}(N-m) & -y(N-1) & -y(N-2)...-y(N-n) \end{bmatrix}$$

$$\begin{matrix} -e(mx-1) & -e(mx-2)...-e(mx-p) \\ \cdot & \cdot & \cdot \\ \cdot & \cdot & \cdot \\ \cdot & \cdot & \cdot \\ -e(N-1) & -e(N-2)...-e(N-p) \end{matrix} \qquad (4.79)$$

where m = order of the OBF model

n = order of the $A(q)$

p = order of $C(q)$

mx = max $(n, m, p) + 1$

u_{fi} = input u filtered by the corresponding OBF filter f_i

$e(i)$ = the prediction error

To develop an OBF-ARMAX model, first an OBF-ARX model with high $A(q)$ order is developed. The prediction error is estimated from this OBF-ARX model and used to form the regressor matrix (4.79). The parameters of the OBF-ARMAX model are, then, estimated using (4.79) in (3.20). The prediction error, and consequently the OBF-ARMAX parameters can be improved by estimating the parameters of the OBF-ARMAX model iteratively.

4.7.5   Multi-step ahead Prediction using OBF-ARX /ARMAX models

In this section the schemes for multi-step ahead prediction of the OBF-ARX and OBF-ARMAX structures are formulated.

4.7.5.1 Multi-step ahead Prediction using OBF-ARX Model

Consider the OBF-ARX model

$$y(k) = \frac{y_{obf}(k)}{A(q)} + \frac{1}{A(q)}e(k) \qquad (4.80)$$

i-step ahead prediction is obtained by replacing k with $k + i$

$$y(k+i) = \frac{y_{obf}(k+i)}{A(q)} + \frac{1}{A(q)}e(k+i) \tag{4.81}$$

To calculate the *i*-step ahead prediction, the noise term can be divided into current and future parts.

$$y(k+i) = \frac{y_{obf}(k+i)}{A(q)} + \frac{F_i(q)}{A(q)}e(k) + E_i(q)e(k+i) \tag{4.82}$$

Since $e(k)$ is assumed to be a white noise with mean zero, the mean of $E_i(q)$ $e(k+i)$ is equal to zero, and therefore (4.82) can be simplified to

$$\hat{y}(k+i \mid k) = \frac{y_{obf}(k+i)}{A(q)} + \frac{F_i(q)}{A(q)}e(k) \tag{4.83}$$

Rearranging (4.82)

$$y(k+i) = \frac{y_{obf}(k+i)}{A(q)} + e(k+i)\left(\frac{q^{-i}F_i(q)}{A(q)} + E_i(q) \right) \tag{4.84}$$

Comparing (4.81) and (4.84), F_i and E_i can be calculated by solving the Diophantine equation.

$$\frac{1}{A(q)} = E_i(q) + \frac{q^{-i}F_i(q)}{A(q)} \tag{4.85}$$

Rearranging (4.80)

$$\frac{1}{A(q)}e(k) = y(k) - \frac{y_{obf}(k)}{A(q)} \tag{4.86}$$

Using (4.86) in (4.83) to eliminate $e(k)$

$$\hat{y}(k+i \mid k) = \frac{y_{obf}(k+i)}{A(q)} + F_i(q)\left(y(k) - \frac{y_{obf}(k)}{A(q)} \right)$$

$$= y_{obf}(k+i)\left(\frac{1}{A(q)} - \frac{q^{-i}F_i(q)}{A(q)} \right) + F_i(q)y(k) \tag{4.87}$$

Rearranging the Diophantine equation (4.85)

$$E_i(q) = \frac{1}{A(q)} - \frac{q^{-i}F_i(q)}{A(q)} \tag{4.88}$$

Finally using (4.88) in (4.87), the usable form of the *i*-step ahead prediction formula, (4.89), is obtained.

$$\hat{y}(k+i \mid k) = E_i(q)\, y_{obf}(k+i) + F_i(q)y(k)$$

$$(4.89)$$

Note that in (4.89), there is no any denominator polynomial and hence no unstable pole. Therefore, the predictor is stable regardless of the presence of unstable poles in the OBF-ARX model. It should also be noted that, since $y_{obf}(k+i)$ is the output sequence of the simulation OBF model, once the OBF model parameters are determined its value depends only on the input sequence $u(k+i)$. Therefore, the *i*-step ahead prediction according to (4.89) depends on the input sequence up to instant $k+i$ and the output sequence up to instant k.

4.7.5.2 Multi-step ahead Prediction using OBF-ARMAX Model

Consider the OBF-ARMAX model (4.90)

$$y(k) = \frac{y_{obf}(k)}{A(q)} + \frac{C(q)}{A(q)}e(k)$$

$$(4.90)$$

The *i*-step ahead prediction is obtained by replacing k with $k + i$

$$y(k+i) = \frac{y_{obf}(k+i)}{A(q)} + \frac{C(q)}{A(q)}e(k+i)$$

$$(4.91)$$

To calculate the *i*-step ahead prediction, the error term should be divided into current and future parts.

$$y(k+i) = \frac{y_{obf}(k+i)}{A(q)} + \frac{F_i(q)}{A(q)}e(k) + E_i(q)e(k+i)$$

$$(4.92)$$

Since $e(k)$ is assumed to be a white noise with mean zero, the mean of $E_i(q)\, e(k+i)$ is equal to zero, and therefore (4.92) can be simplified to

$$\hat{y}(k+i \mid k) = \frac{y_{obf}(k+i)}{A(q)} + \frac{F_i(q)}{A(q)}e(k)$$

$$(4.93)$$

Rearranging (4.93)

$$y(k+i) = \frac{y_{obf}(k+i)}{A(q)} + e(k+i)\left(\frac{q^{-i}F_i(q)}{A(q)} + E_i(q) \right)$$

$$(4.94)$$

Comparing (4.94) to (4.91), F_i and E_i can be calculated by solving the Diophantine equation.

$$\frac{C(q)}{A(q)} = E_i(q) + \frac{q^{-i}F_i(q)}{A(q)} \qquad (4.95)$$

Rearranging (4.90)

$$\frac{1}{A(q)}e(k) = \frac{1}{C(q)}\left(y(k) - \frac{y_{obf}(k)}{A(q)}\right) \qquad (4.96)$$

Using (4.96) in (4.93) to eliminate $e(k)$

$$\hat{y}(k+i \mid k) = \frac{y_{obf}(k+i)}{A(q)} + \frac{F_i(q)}{C(q)}\left(y(k) - \frac{y_{obf}(k)}{A(q)}\right)$$

$$= y_{obf}(k+i)\left(\frac{1}{A(q)} - \frac{F_i(q)}{C(q)}\frac{1}{A(q)}\right) + \frac{F_i(q)}{C(q)}y(k) \qquad (4.97)$$

Rearranging the Diophantine equation, (4.95)

$$\frac{E_i(q)}{C(q)} = \frac{1}{A(q)} - \frac{q^{-i}F_i(q)}{C(q)A(q)} \qquad (4.98)$$

Finally using (4.98) in (4.97), the usable form of the i-step ahead prediction formula, (4.99), is obtained.

$$\hat{y}(k+i \mid k) = \frac{E_i(q)}{C(q)}y_{obf}(k+i) + \frac{F_i(q)}{C(q)}y(k) \qquad (4.99)$$

When OBF-ARMAX model is used for modeling open-loop unstable processes that are stabilized by a feedback controller, the common denominator $A(q)$ that contains the unstable pole does not appear in the predictor equation, (4.99). Therefore, the predictor is stable regardless of the presence of unstable poles in the OBF-ARMAX model, as long as the noise model is invertible. Invertiblity is required because $C(q)$ appears in the denominator. It should also be noted that, since $y_{obf}(k+i)$ is the output sequence of the simulation OBF model, once the OBF model parameters are determined its value depends only on the input sequence $u(k+i)$. Therefore, the i-step ahead prediction according to (4.99) depends on the input sequence up to instant $k+i$ and the output sequence only up to instant k.

4.7.6   Case Studies

In this section, three case studies that demonstrate the application of the proposed closed-loop identification techniques are presented. The first and second case studies are simulation case studies while the third one is a real plant case study. The first case study demonstrates how OBF-ARMA, OBF-ARX and OBF-ARMAX models can be developed from closed-loop data of a feedback controlled open-loop stable system. In the second case study closed loop identification of an open-loop unstable system that is stabilized by a feedback controller is presented. In all case studies, the accuracies of the models are examined by residual analysis.

4.7.6.1 Close-loop identification of open-loop stable process

In this closed-loop identification simulation case study, an open-loop stable system is identified from closed-loop test data using GOBF-ARMA, GOBF–ARX, GOBF-ARMAX models. The GOBF-ARMA model is developed using the de-correlation (two-step) method, which is an indirect closed loop identification method. The second and third models are developed using direct closed loop identification approaches. The deterministic and stochastic components of the system are given by (4.100a) and (4.100b), respectively.

$$G(s) = \frac{0.25e^{-5s}}{(12s+1)(5s+1)} \tag{4.100a}$$

$$H(z) = \frac{1-0.6z^{-1}}{1-1.342z^{-1}+0.421z^{-2}} \tag{4.100b}$$

A feedback proportional controller, with K_c=1.0 is used to control the system. The controller gain is chosen so that the closed loop response is stable and gives not more than 25% overshoot. The block diagram of the feedback controlled system is shown in Figure 4.39. A white noise sequence with mean -0.0070 and standard deviation 0.0993 is introduced into the system. The signal to noise ratio (SNR) is 6.7350. An external excitation signal, r_1, is used for the purpose of identification.
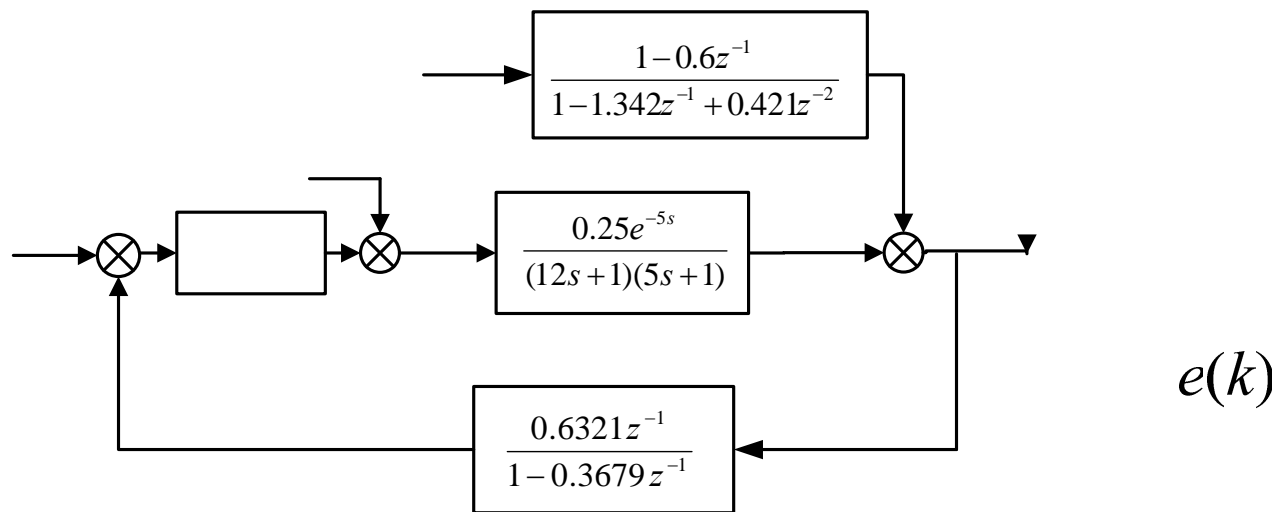
Figure 4.39 Block diagram of the closed loop system

The excitation signal, r_1, is a '*PRBS*' signal generated using the MATLAB function '*idinput*' with band [0 0.02] and level [2 -2]. Four thousand data points are generated and 3000 of these data points are used for identification while the remaining 1000 data points are used for validation. The changes in the external excitation signal, r_1, system input, $u(k)$, and system output, $y(k)$, are shown in Figure 4.40.
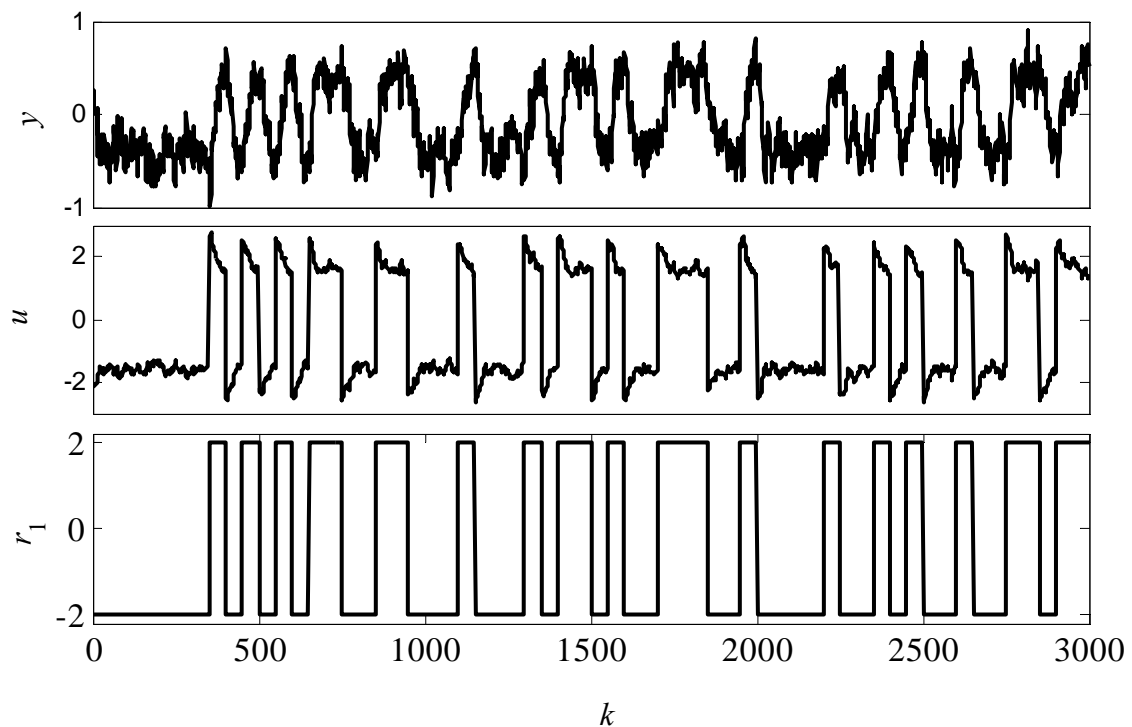
Figure 4.40 Data used for system identification of system (4.100)

OBF-ARMA model using the decorrelation method

To determine the simulated input, the transfer function $S(q)$, from r_1 to u is first estimated using the proposed modified ARMAX model

$$S(q) = \frac{1 - 1.35q^{-1} + 0.3774q^{-2}}{1 - 1.3514q^{-1} + 0.3843q^{-2}} \tag{4.101}$$

The simulated input u^r is then estimated by filtering r_1 with $S(q)$. The next step is developing the OBF-ARMA model using u^r as the input and y as output. To estimate the dominant pole, assuming they are not known, a preliminary test is conducted using the SOPTD and FOPTD iterative methods developed in Chapter 3 starting with poles 0.3679 and 0.6065. It was found that the system can be expressed with acceptable accuracy using OBF models with four Laguerre filters and one dominant pole 0.9326. The OBF parameters are found to be:

$l = [0.0275\ 0.0304\ -0.0160\ 0.0054]$

$\tau_d = 5$ sampling intervals.

The ARMA noise model, which reflects the effect of the noise in the closed-loop response, is given by

$$H^r = \frac{1 + 0.2524q^{-1} - 0.0316q^{-2}}{1 - 0.4968q^{-1} - 0.2232q^{-2}} \tag{4.102}$$

Using (4.101) and (4.102) in (4.62) we get estimate of the noise model,

$$\hat{H} = \frac{1 - 1.0856q^{-1} - 0.0126q^{-2} + 0.153q^{-3} - 0.0144q^{-4}}{1 - 1.8475q^{-1} + 0.8171q^{-2} + 0.1255q^{-3} - 0.0876q^{-4}} \tag{4.103}$$

Model Validation

The simulation output of the OBF model compared to the system's output for the validation data points is shown in Figure 4.41. The percentage prediction error of the OBF output compared to the systems output is 16.4473. The spectrum of the estimated noise model compared to the system's noise model has a percentage prediction error of 0.7629 and is shown in Figure 4.42.

Figure 4.41 Output of the OBF model compared to the output of system (4.100) for the validation data points

Figure 4.42 Spectrum of the noise model compared to the system's noise transfer function of system (4.100)

The one-step-ahead prediction of the OBF-ARMA model developed using the decorrelation method compared to the system's output, for the first 500 validation data points, is shown in Figure 4.43.
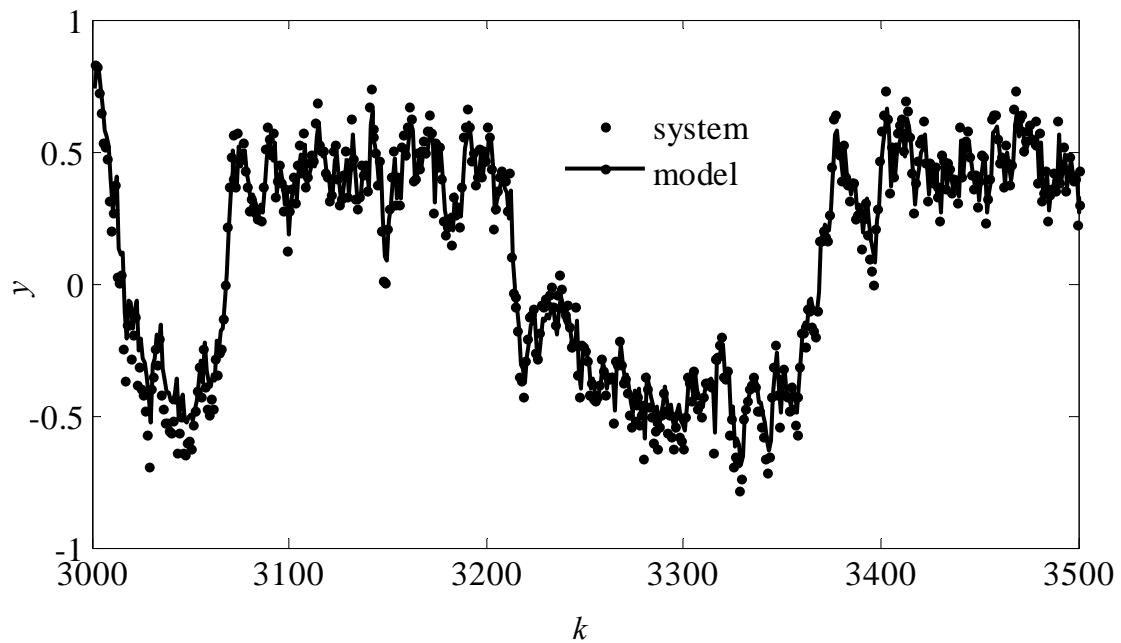
Figure 4.43 One-step ahead prediction of the OBF-ARMA model identified using the closed-loop data compared to the output of (4.100) for the validation data points

The PPE for the whole validation data points (3001-4000) is 1.3615. The accuracy of the OBF-ARMA model is acceptable if the remaining prediction error can be accounted for by the white noise. This is checked by comparing the residual of the OBF-ARMA model to the white noise of the system using residual analysis.

Residual Analysis

The qq-plot of the residual of the OBF-ARMA model and the white noise added to the system for the validation data points is shown in Figure 4.44. The distribution of the residuals of the OBF-ARMA model compared to the white noise added to the system is shown in Figure 4.45. The correlation among the residuals

$$\hat{R} = [0.0002\ 0.0007\ 0.0003\ 0.0006\ 0.0003\ 0.0011\ \text{-}0.0000\ 0.0005\ 0.0012\ 0.0005]$$
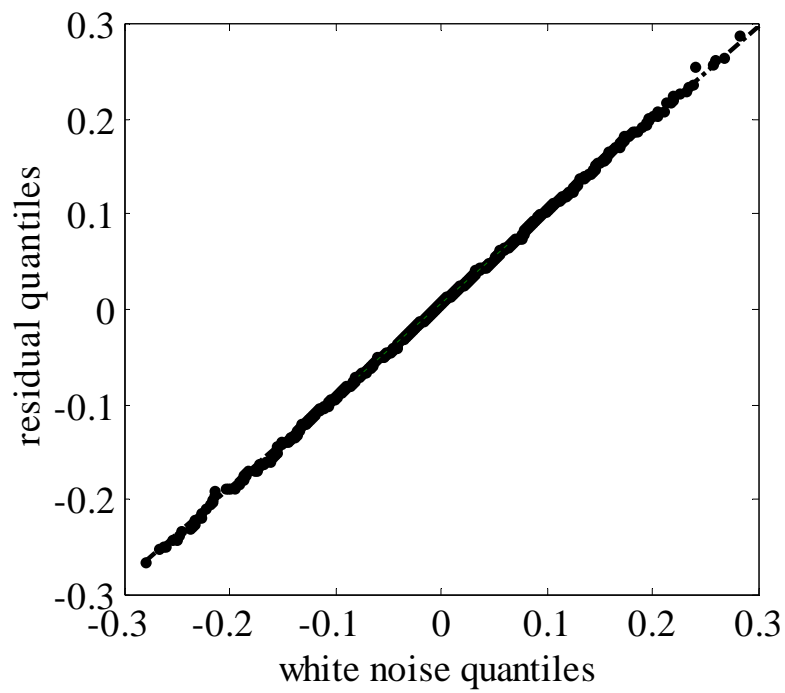
Figure 4.44 qq-plot of the residual with respect to the white noise

added into system (4.100)
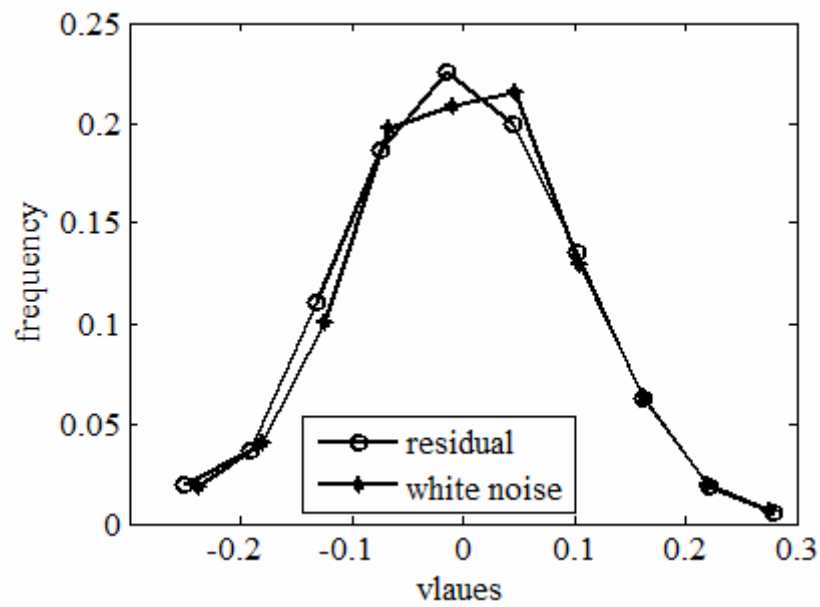
Figure 4.45 Distribution of the residual of the OBF-ARMA model compared to the white

noise added into system (4.100)

OBF-ARX model using the direct identification method

Pole and number of parameters selection

The dominant pole method to develop parsimonious models is not applicable in the OBF-ARX structure since the two structures are different. However, the best pole and number of OBF parameters can be estimated by comparing the PPE of various poles and number of OBF parameters. The results of such a comparison are presented in Table 4.10.

Table 4.10 PPE for various poles and number of OBF parameters for $n_A = 4$ for system (4.100)

	Number of OBF parameters			
pole	4	5	6	7
0.6	6.1217	6.1371	6.1375	6.1263
0.7	6.1388	6.1319	6.0690	6.0384
0.8	6.1060	5.9931	6.0039	6.0033
0.9	6.0200	6.0190	6.0174	5.9929
0.91	6.0180	6.0175	6.0129	6.0083
0.92	6.0166	6.0172	6.0123	6.0102
0.93	6.0192	6.0187	6.0179	5.9978

From Table 4.10 it is observed that the effect of the poles and the number of parameters on the percentage prediction error is very small. The difference between the minimum PPE with 7 and 4 numbers of parameters is less than 0.03%. A further study on the order of the noise polynomial, shows that the accuracy is almost the same for $n_A = 3$. Therefore the most parsimonious model, with four OBF parameters and pole 0.92, with noise order 3 is chosen.

OBF-ARX model

The OBF parameters for 4 Laguerre filters and pole of 0.92 is

$$l = [0.0071 \quad 0.0061 \quad -0.0022 \quad 0.0006];$$

The denominator polynomial $A(q)$

$$A(q) = 1 - 0.7600q^{-1} + 0.0072q^{-2} - 0.0303q^{-3}$$

Therefore the noise model is

$$\hat{H}(q) = \frac{1}{1 - 0.76q^{-1} - 0.0072q^{-2} - 0.0303q^{-3}} \tag{4.104}$$

Model Validation

The output of the deterministic component the OBF-ARX model (simulation model) compared to the system's output for the validation data points is shown in Figure 4.46. The PPE of the simulation model compared to the systems output is 15.4916.
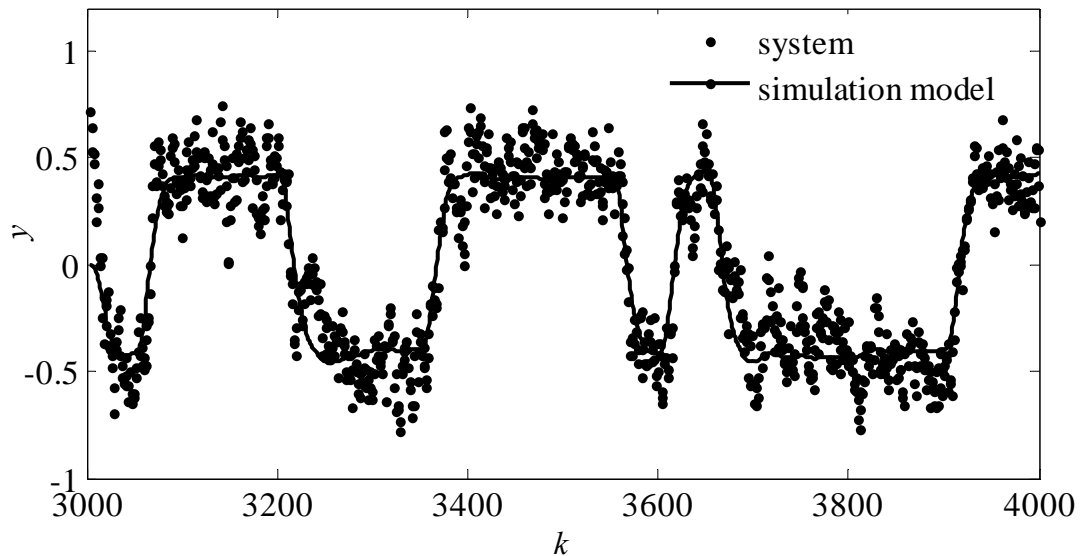
Figure 4.46 Output of the simulation model compared to the output of system (4.100) for the validation data points

The spectrum of the noise model (4.104) compared to the spectrum of the system's noise transfer function (4.100b) is shown in Figure 4.47. The standard deviation of the residuals of the OBF-ARX model is 0.0993. The PPE of the spectrum of the noise model compared to the system's noise transfer function is 2.2431.
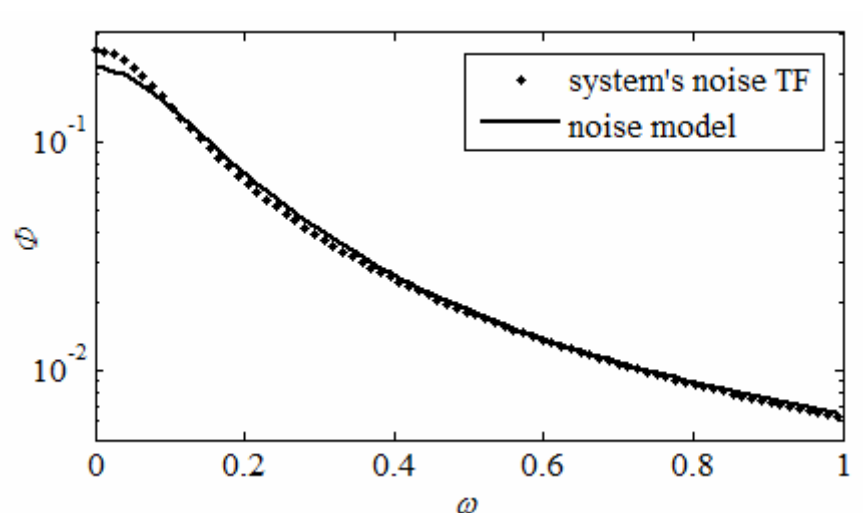
Figure 4.47 Spectrum of the noise model compared to the s noise transfer function of system (4.100)

The one step-ahead-prediction using the OBF-ARX model compared to the system's output for the validation data points is shown in Figure 4.48 and the PPE is 6.0047.
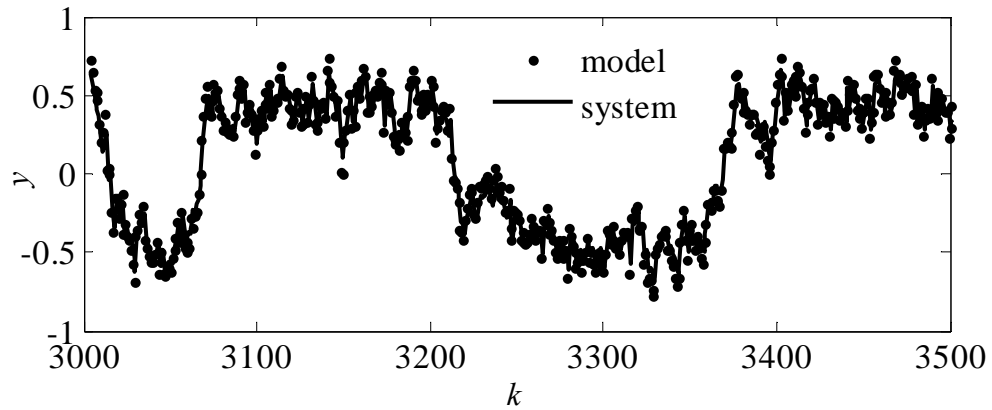
Figure 4.48 One-step-ahead prediction of the OBF-ARX model compared to the output of system (4.100) for the validation data points

Residual Analysis

The qq-plot and of the residuals with respect to the white noise added to the system is shown in Figure 4.49. It is observed from the figure that almost all the points on the qq-plot lie on a straight line with slope equal to one. This shows that the residuals have nearly the same distribution as the white noise.
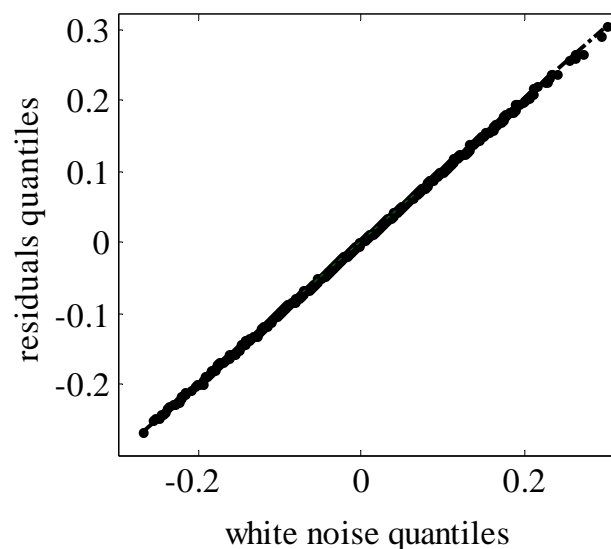
Figure 4.49 qq-plot of the residual compared to the white noise added into system (4.100)

Figure 4.50 shows the distribution of the residuals compared to the white noise. It is noted from the figure that, just it is observed in the qq-plot, the two distributions are nearly the same.
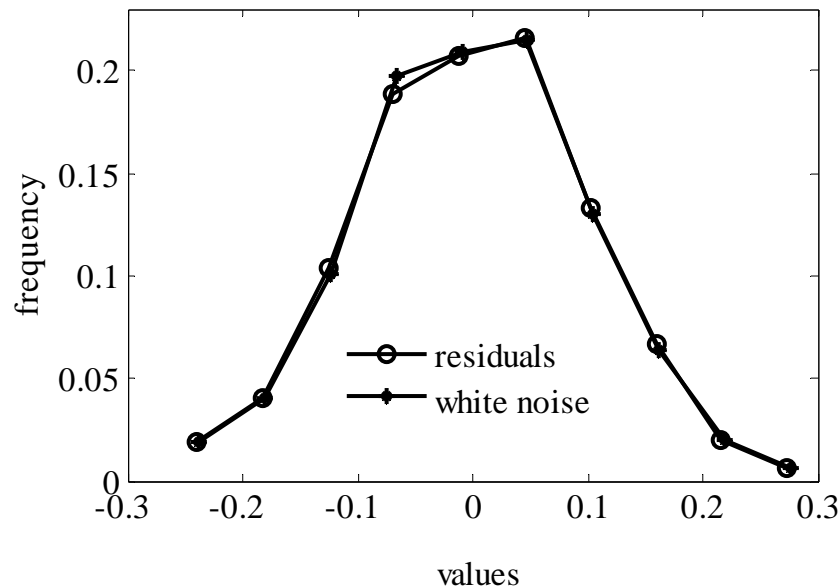
Figure 4.50 Distribution of the residuals compared to the white noise

added into system (4.100)

The correlation among the residuals for $\tau = 10$ is

$$\hat{R} = 10^{-3}[\text{-0.5670 0.0210 -0.3419 -0.0552 -0.3030 0.4642 -0.6579 -0.1072 0.5404 -0.1271}]$$

The correlation among the residuals which is close to zero also shows that the residuals are white and there is no significant correlation among the residuals.

OBF-ARMAX model using the direct identification method

Pole and number of parameters selection

The dominant pole method to develop parsimonious models is not applicable in the OBF-ARX structure since the two structures are different. However, the best pole and number of OBF parameters can be estimated by comparing the PPE of various poles and number of OBF parameters. The results of such a comparison are presented in Table 4.11. From Table 4.11 it is observed that the minimum PPE for OBF-4 (the most parsimonious among the tested) is 6.7929 while the smallest PPE in all the tabulated values is 6.7440 for OBF-7. The difference between the two percentage prediction errors is less than 0.05% which is insignificant.

Table 4.11 PPE for various poles and number of OBF parameters for $n_D = n_C = 2$ of system (4.100)

pole	OBF-4	OBF-5	OBF-6	OBF-7	OBF-8
0.7	8.2334	8.6993	6.9257	6.8113	6.7927
0.8	6.9117	6.7680	6.7455	6.7440	6.8056
0.9	6.7929	6.8001	6.7599	6.8777	6.8925
0.91	6.7978	6.8122	6.7551	6.7898	6.8858
0.92	6.8123	6.8303	6.7702	6.7527	6.7920

Therefore the most parsimonious model, OBF-4 with pole 0.9 is chosen for the OBF-ARMAX model. It is also observed that increasing the order of the noise model does not improve the prediction capacity. Therefore the most parsimonious model, with four OBF parameters and pole 0.9, with noise order $n_D = n_C = 2$ is selected.

OBF-ARMAX model

The OBF parameters for 4 Laguerre filters and pole of 0.90 is

l = [0.0068 0.0079 -0.0010 2.5302e-004];

The denominator polynomial $A(q)$

$$A(q) = 1 - 0.6401q^{-1} - 0.1268q^{-2}$$

Therefore the noise model is

$$\hat{H}(q) = \frac{1 + 0.1196q^{-1} - 0.0446q^{-2}}{1 - 0.6401q^{-1} - 0.1268q^{-2}} \tag{4.105}$$

Model Validation

The output of the deterministic component the OBF-ARMAX model (simulation model) compared to the system's output for the validation data points is shown in Figure 4.51. The PPE of the simulation model compared to the systems output is 16.7642. The spectrum of the noise model (4.105) compared to the spectrum of the system's noise transfer function (4.100b) is shown in Figure 4.47. The standard deviation of the residuals of the OBF-ARMAX model is 0.0992. The PPE of the spectrum of the noise model compared to the system's noise transfer function is 2.3659.
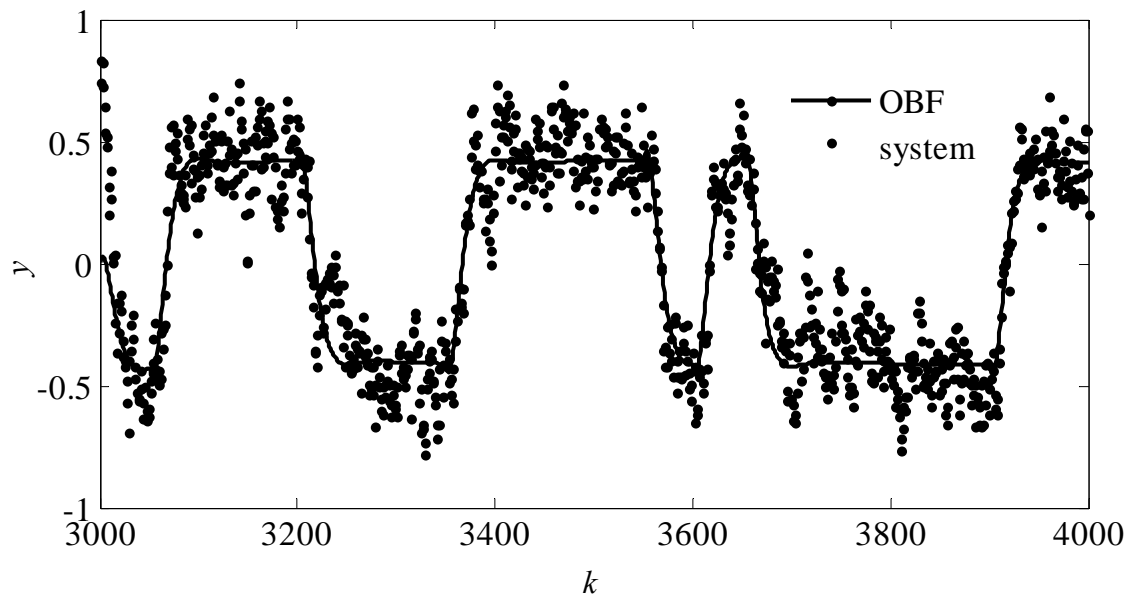
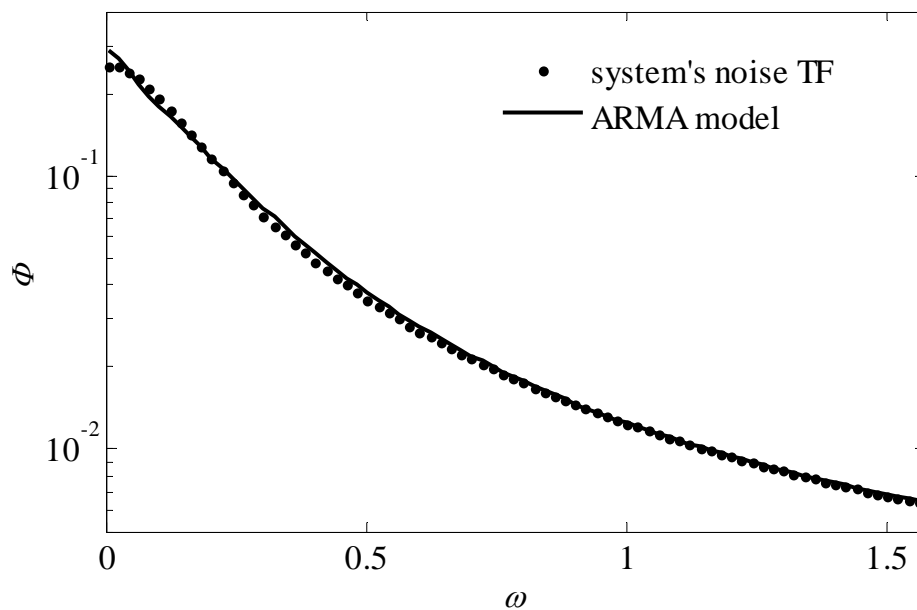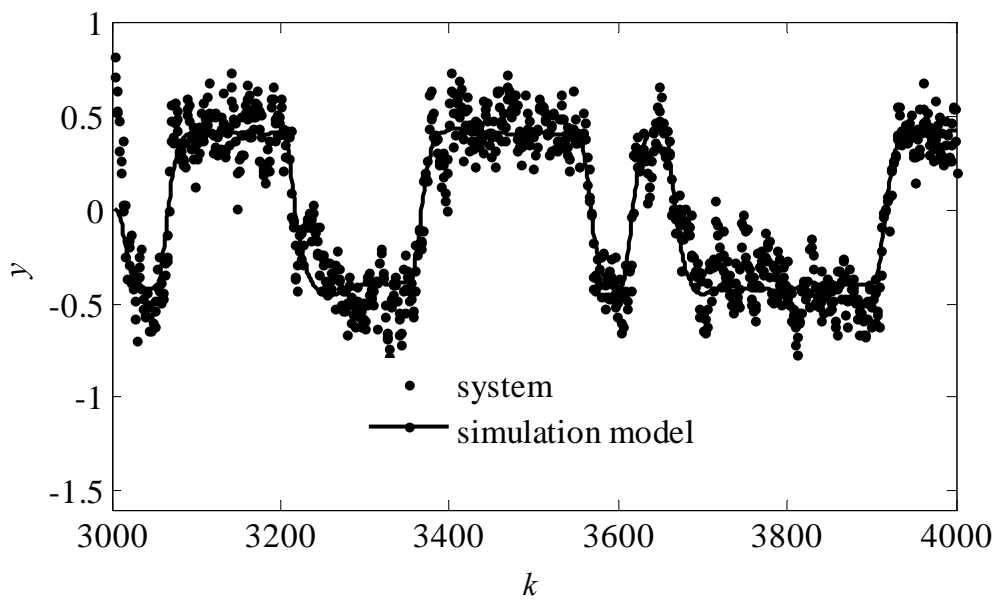Figure 4.51 Output of the simulation model compared to the output of system (4.100) for the validation data points
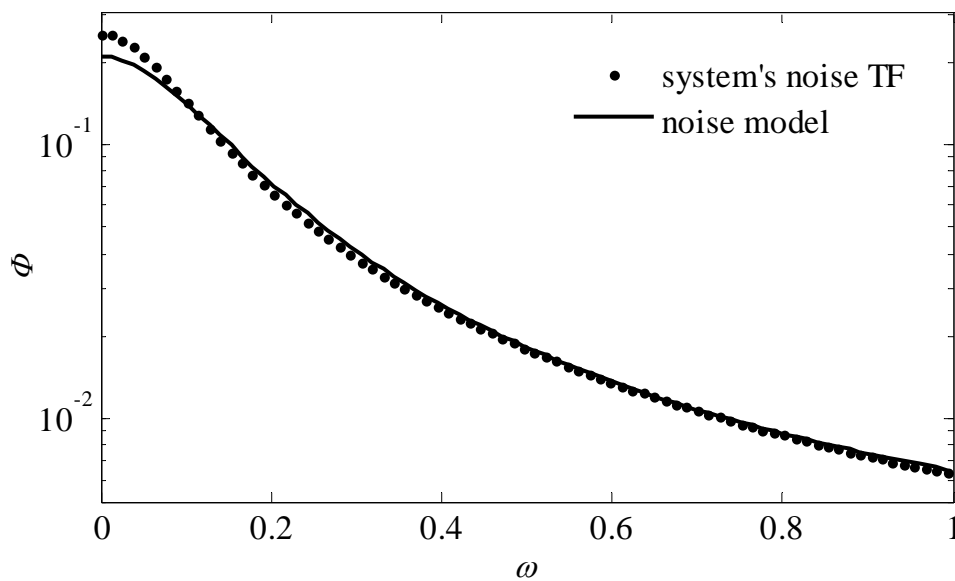
Figure 4.52 Spectrum of the noise model compared to the noise transfer function of system (4.100)

The one step-ahead-prediction using the OBF-ARMAX model compared to the system's output for the validation data points (3001-3500) is shown in Figure 4.52 and the PPE is 6.7929.
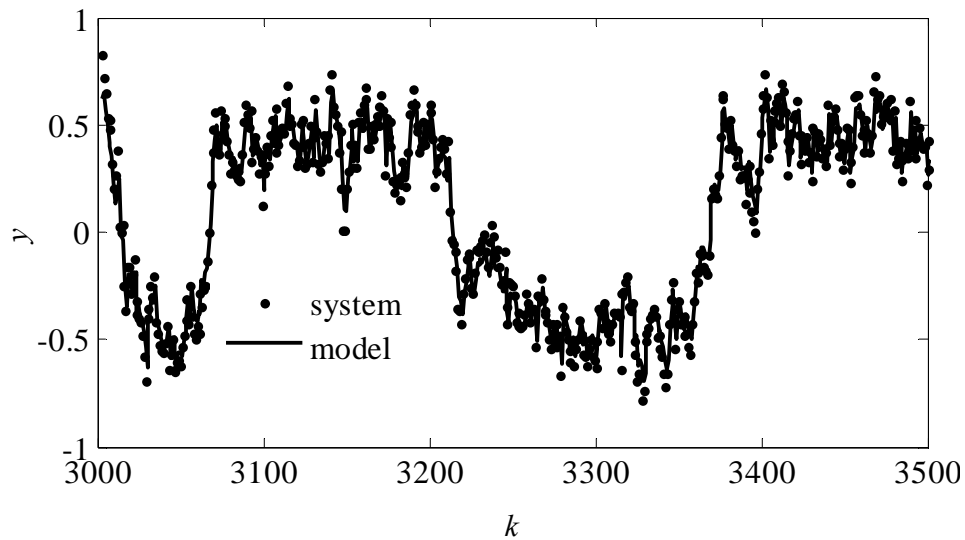
Figure 4.53 One-step-ahead prediction of the OBF-ARMAX model compared to the system output for the validation data points for the system (4.100)

Residual Analysis

The qq-plot and of the residuals with respect to the white noise added to the system is shown in Figure 4.54. It is observed from the figure that almost all the points on the qq-plot lie on a straight line with slope equal to one. This shows that the residuals have nearly the same distribution as the white noise. Figure 4.55 shows the distribution of the residuals compared to the white noise. It is noted from the figure that the two distributions are nearly the same.
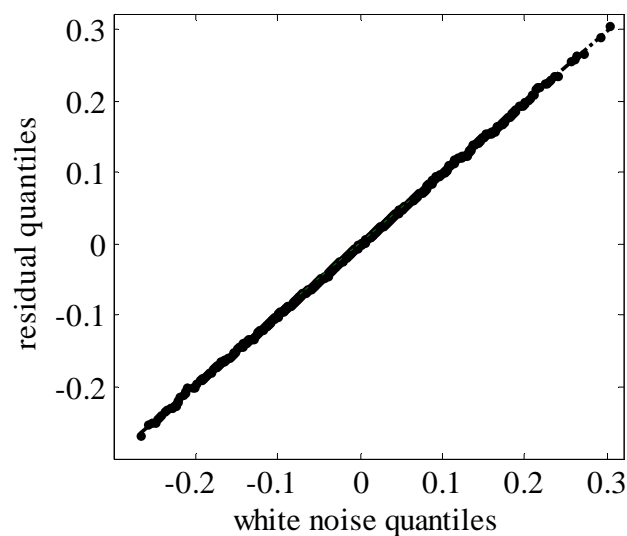
Figure 4.54 qq-plot of the residual compared to the white noise for the system (4.100)
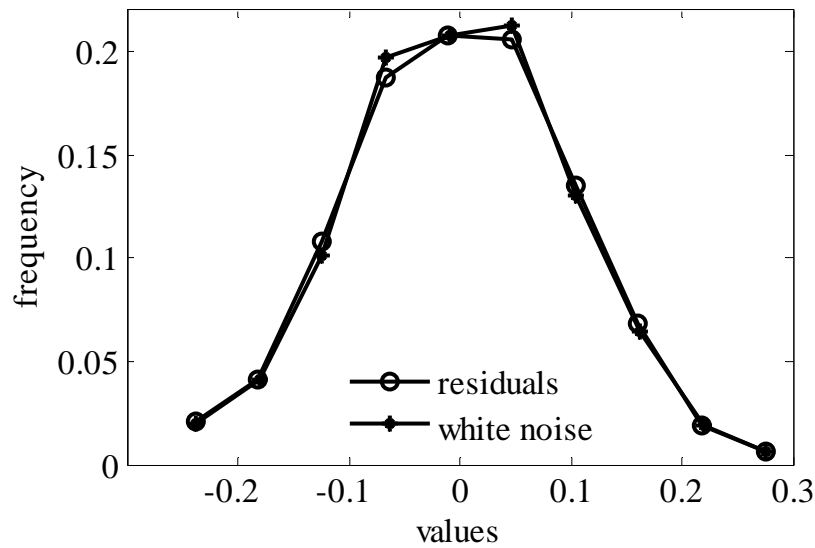
Figure 4.55 Distribution of the residuals compared to the white noise

for the system (4.100)

The correlation among the residuals for $\tau = 10$

$$\hat{R} = 10^{-3}[0.2161\ 0.2646\ -0.2554\ 0.0676\ -0.1891\ 0.5927\ -0.6389\ -0.1289\ 0.6668\ 0.1040]$$

The correlation among the residuals which is close to zero also shows that the residuals are white and there is no significant correlation among the residuals.

This case study demonstrates that closed-loop identification of open-loop stable processes can be effectively carried out using the proposed methods, namely the decorrelation method, the direct methods using OBF-ARX and OBF-ARMAX models. The accuracy of the models in each modeling approach is checked by residual analysis and it is shown that the accuracy is acceptable in all cases.

Multi-step-ahead predictions

The PPEs of the 1 to 5 step ahead predictions of the OBF-ARX and OBF-ARMAX models are shown in Table 4.12. The noise models for the OBF-ARX and OBF-ARMAX models are given by (4.104) and (4.105) respectively. It should be noted that the simulation model in OBF-ARX and OBF-ARMAX models is no more the OBF model but OBF/A(q) as it can be observed from (4.80) and (4.90). Therefore, it is the simulation model that is compared with the prediction model in the multi-step ahead predictions shown in Table 4.12. It is observed in this case study also that the short tem predictions of the model are improved significantly by using prediction models.

Table 4.12 The PPE for 1 to 5 step- ahead- predictions of OBF-AR and OBF-ARMA models compared to OBF model for system (4.100)

	OBF-AR		OBF-ARMA	
i	Simulation	Prediction	Simulation	Prediction
1	13.9972	5.7058	14.0022	5.7075
2	13.6573	8.5580	13.6632	8.5571
3	13.3222	10.1461	13.3295	10.1473
4	13.0615	11.0073	13.0704	11.0043
5	12.8490	11.5397	12.8595	11.5363

4.7.6.2 Close-loop identification of open-loop unstable process

In this case study, an OBF model with ARX and ARMAX structures are used to identify an open-loop unstable process which is stabilized by a feedback control system. The plant and noise transfer functions of the system are given by (4.106a) and (4.106b)

$$G(s) = \frac{0.12e^{-1.2s}}{(15s-1)(7s+1)} \tag{4.106a}$$

$$H(z) = \frac{1-0.6z^{-1}}{1-1.342z^{-1}+0.421z^{-2}} \tag{4.106b}$$

The plant transfer function has one RHS pole, 1/15, therefore is open-loop unstable. The system is stabilized using a proportional feedback controller with $K_c = 11$. A white noise sequence with mean 0.0049 and standard deviation 0.1989 is added to the system and the SNR is 9.9702. An external excitation signal, r_1, is introduced into the system to conduct the identification. The excitation signal is, a PRBS signal generated using the MATLAB function '*idinput*' with band [0 0.02] and level of [-1 1]. The block diagram of the feedback control system to be identified is shown in Figure 4.56.
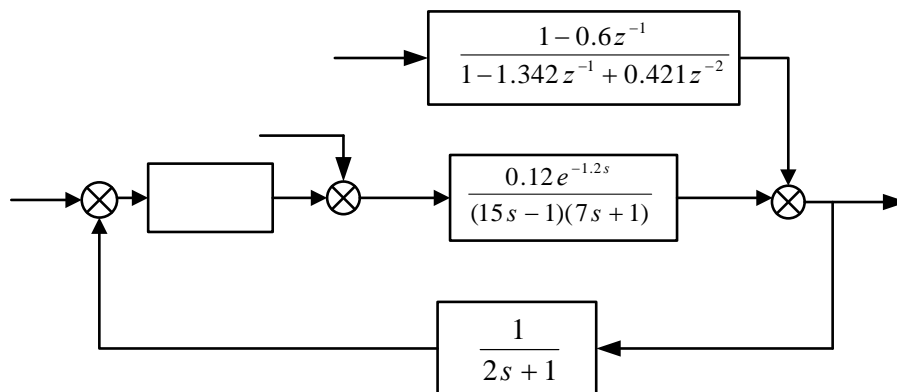
Figure 4.56 System stabilized by feedback controller

The excitation signal, the plant input and the plant output used for identification are shown in Figure 4.57. Four thousand data points, with a sampling interval of one time unit, are generated using SIMULINK and 3000 of them were used for identification and the remaining 1000 are used for validation.
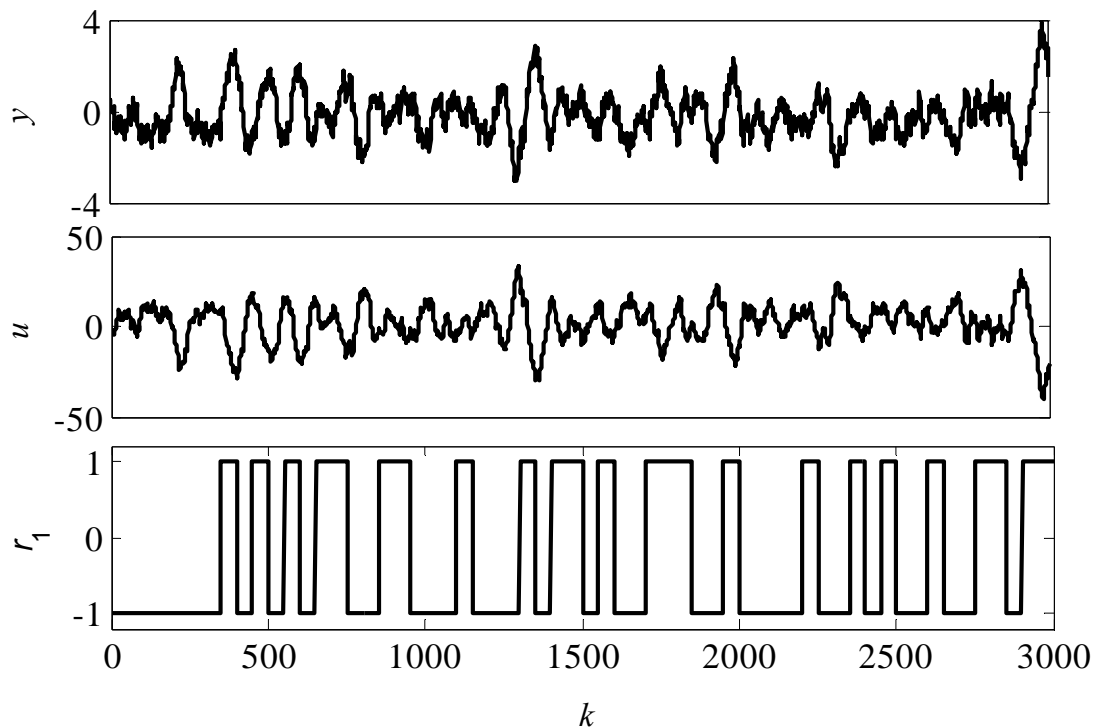
Figure 4.57 Data sequences used for identification

Closed-loop identification using OBF-ARX model

Pole and number of parameters selection

The dominant pole method to develop parsimonious models is not applicable here because the plant is open-loop unstable and the OBF poles should be stable by definition. Only the poles of the polynomial $A(q)$ which is common for both the plant and noise model can contain the unstable pole. The pole and number of OBF-parameters can be selected by comparing the PPE as it is done in the previous case study. Such a comparison is carried out using the values of PPE for various poles and order $A(q)$ equal to 4 is shown in Table 4.13. Further study shows that increasing the order of the polynomial $A(q)$ doe not reduce the PPE. From Table 4.13 it is observed that the effect of the poles and the number of parameters on the percentage prediction error is very small, it is however clear that OBF model with 5 Laguerre filters and a pole between 0.3 and 0.4 gives the lowest PPE. It was further checked that the pole equal to 0.4 is good enough.

Table 4.13 PPE for various poles and number of OBF parameters for $n_A = 4$ for system (4.106)

pole	Number of OBF parameters			
	4	5	6	7
0.2	5.6688	5.6461	5.6285	5.6285
0.3	5.6628	5.6239	5.6384	5.6384
0.4	5.6567	<u>5.6143</u>	5.6502	5.6358
0.5	5.6421	5.6254	5.6556	5.6298
0.6	5.6412	5.6345	5.6518	5.6420

OBF-ARX model

The OBF model has five Laguerre filters with pole 0.4 and the parameters are estimated to be

$$l = [0.0168 \quad -0.0191 \quad 0.0137 \quad -0.0107 \quad 0.0081];$$

The denominator polynomial $A(q)$ is estimated

$$A(q) = 1 - 0.9103q^{-1} - 0.1268q^{-2} - 0.0298q^{-3} - 0.04q^{-4}$$

Therefore the noise model is

$$\hat{H}(q) = \frac{1}{1 - 0.9103q^{-1} - 0.1268q^{-2} - 0.0298q^{-3} - 0.04q^{-4}} \tag{4.107}$$

Note that the poles of the noise model are shared by the plant model as defined by (4.71). The four poles of the noise model are 1.0840, -0.3284, $0.0774 \pm 0.3261i$. The pole 1.0840 is outside the unit circle and is shared by both the plant model and the noise model, in accordance with the theory.

Model Validation

The one-step-ahead prediction by the OBF-ARX model compared to the output of the stabilized system for the validation data points is shown in Figure 4.58 and the corresponding PPE is 5.6143. The simulation model and the noise spectrum are irrelevant for such cases, because both are unstable. However, the accuracy of the model can be checked by residual analysis.
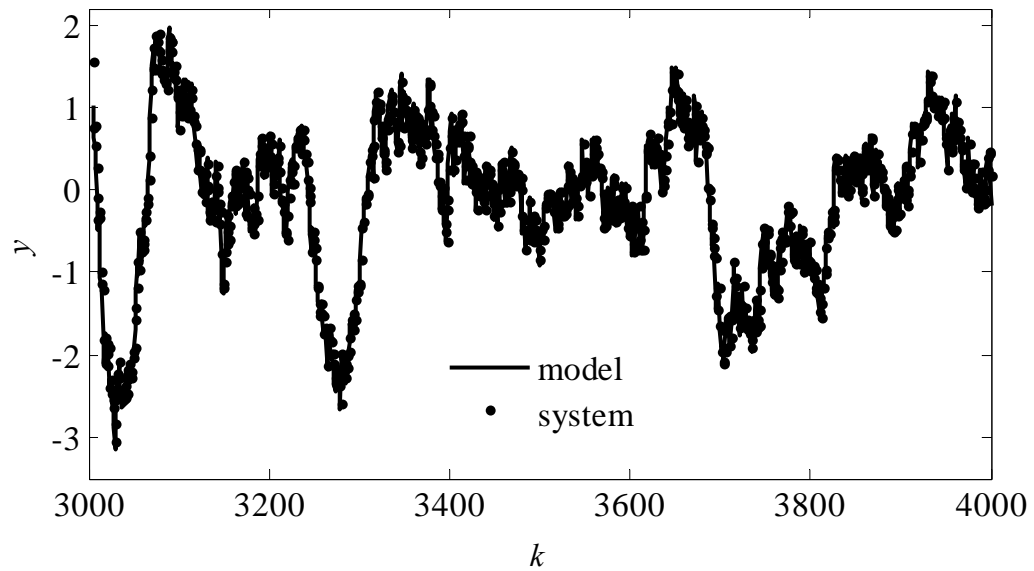
Figure 4.58 One-step ahead prediction by the OBF-ARX model compared to the output of system (4.106)

Residual Analysis

Figure 4.59 shows the qq-plot of the OBF-ARX model with respect to the white noise added to the closed-loop system. The distribution of the residual compared to the white noise is shown in Figure 4.60. It is observed that the figure that the residuals have similar distribution to the white noise.
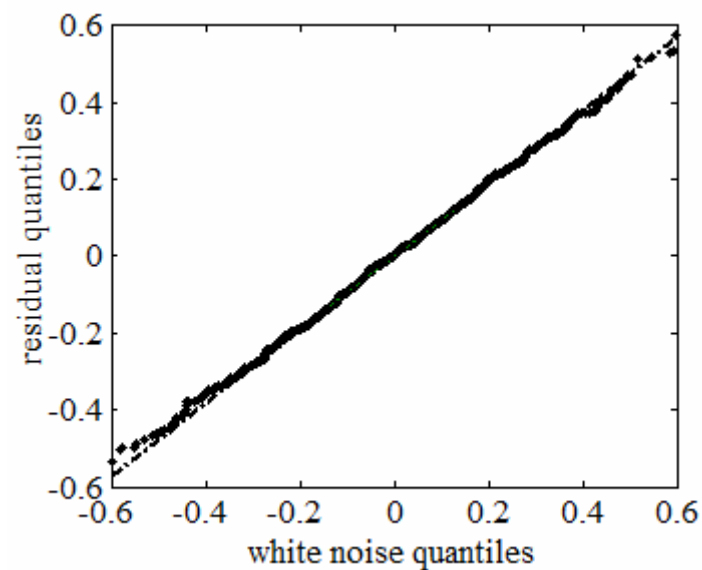
Figure 4.59 qq-plot of the residual of the OBF-ARX model compared to the white noise added into system (4.106)
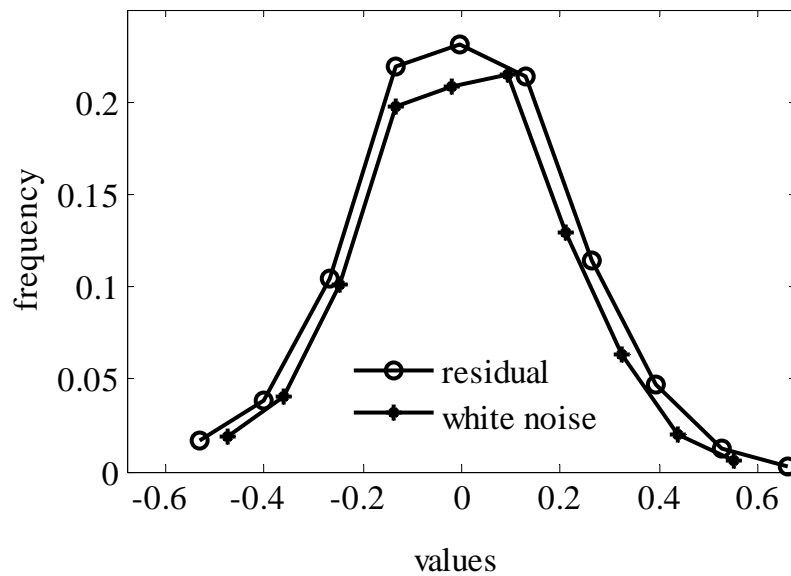
Figure 4.60 Distribution of the residuals compared to the white noise

added into system (4.106)

The correlation among the residuals is estimated to be

$$\hat{R} = [\text{-}0.0021\ 0.0007\ \text{-}0.0005\ \text{-}0.0006\ \text{-}0.0007\ 0.0027\ \text{-}0.0034\ \text{-}0.0008\ 0.0022\ \text{-}0.0012]$$

It is observed from both the-one-step ahead prediction and the residual analysis that the OBF-ARX prediction model captures the dynamics of the open-loop unstable system with acceptable accuracy.

Closed-loop identification using OBF-ARMAX model

Pole and number of parameters selection

The same procedure as the previous case is used to determine the number of OBF-parameters and the OBF-pole. OBF model with four numbers of parameters and pole equal to 0.7 is chosen to develop the OBF-ARMAX model.

Table 4.14 PPE for various poles and number of OBF parameters for $n_D = n_C = 2$ for system (4.106)

pole	Number of OBF parameters			
	4	5	6	7
0.3	6.2929	6.3150	6.2252	6.2007
0.4	6.2835	6.2590	6.1969	6.1892
0.5	6.2624	6.1718	6.2410	6.2448
0.6	6.2154	6.3477	6.3457	6.4538
0.7	<u>6.1931</u>	6.4100	6.3964	6.4847
0.8	6.2722	6.2559	6.2801	6.3174
0.9	6.4841	6.3211	6.3245	6.3227

OBF-ARMAX model

The OBF model has four Laguerre filters with pole 0.4 and parameters

l = [0.0028 -0.0014 2.9540e-004 9.5944e-004];

The denominator polynomial $A(q)$

$$A(q) = 1 - 1.3696q^{-1} - 0.3289q^{-2}$$

The noise model is

$$\hat{H}(q) = \frac{1 - 0.4728q^{-1} - 0.0683q^{-2}}{1 - 1.4963q^{-1} - 0.4503q^{-2}} \tag{4.108}$$

The discrete poles of the noise model that are also shared by the plant model are 1.0590 and 0.3106. It is observed that one of the poles, 1.0590, is outside the unit circle hence it is the unstable pole shared by the plant model and the noise model as the theory requires. Note that the poles of the noise model are shared by the plant model as defined by (4.76).

Model Validation

The one-step-ahead prediction by the OBF-ARMAX model compared to the output of the stabilized system for the validation data points is shown in Figure 4.61 and the corresponding PPE is 6.1931.
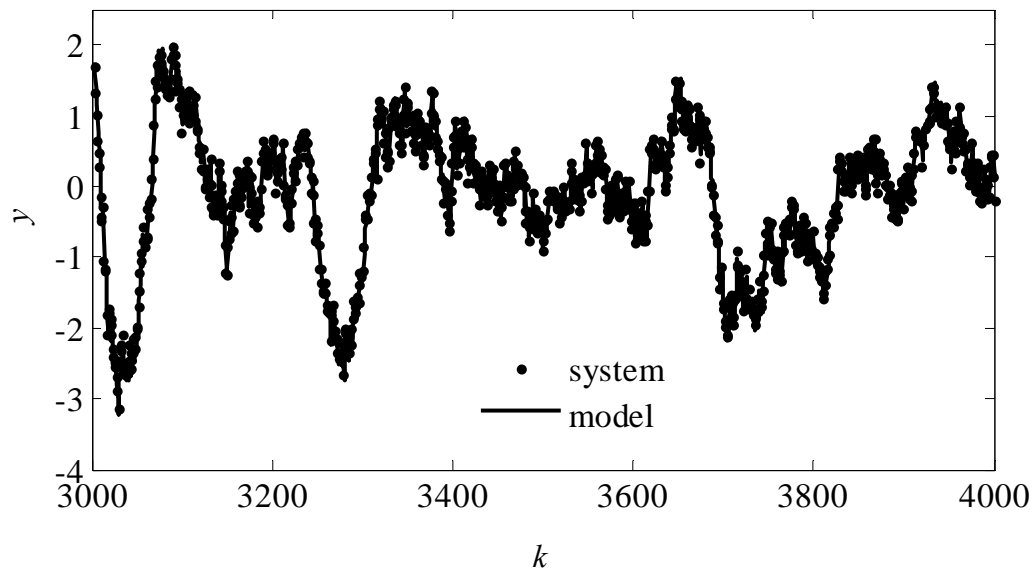
Figure 4.61 One-step-ahead prediction of the OBF-ARMAX model compared to the output of the system for the validation data points

The simulation model and the noise spectrum are irrelevant for such cases, because both are unstable. The accuracy of the model can be checked by residual analysis, as in the case of the OBF-ARX.

Residual Analysis

The mean and standard deviation of the residuals of the OBF-ARMAX model are -0.0026 and 0.2160. The qq-plot of the residual of the OBF-ARMAX model with respect to the white noise added to the system for the validation data points are shown in Figure 4.62. It is noted from the figure that, the residual is a normally distributed signal with mean around zero, similar to the white noise. However, it can also be observed that there is small deviation at the intercept. This is due to a small increase in the standard deviation of the residual as compared to the white noise as can be seen in Figure 4.63 also. The distribution of the residuals of the OBF-ARMAX model compared to the white noise added to the system is shown in Figure 4.63.
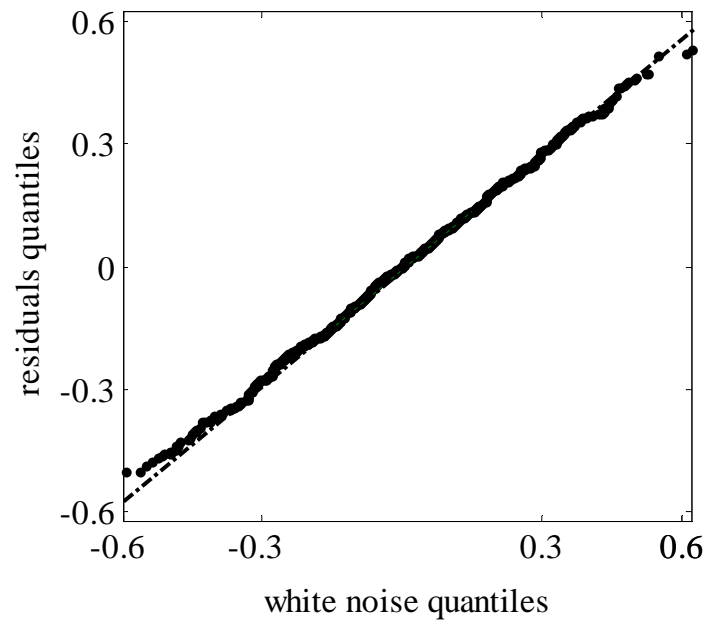
Figure 4.62 The qq-plot of the residual of the OBF-ARMAX model with respect to the white noise added into system (4.106)
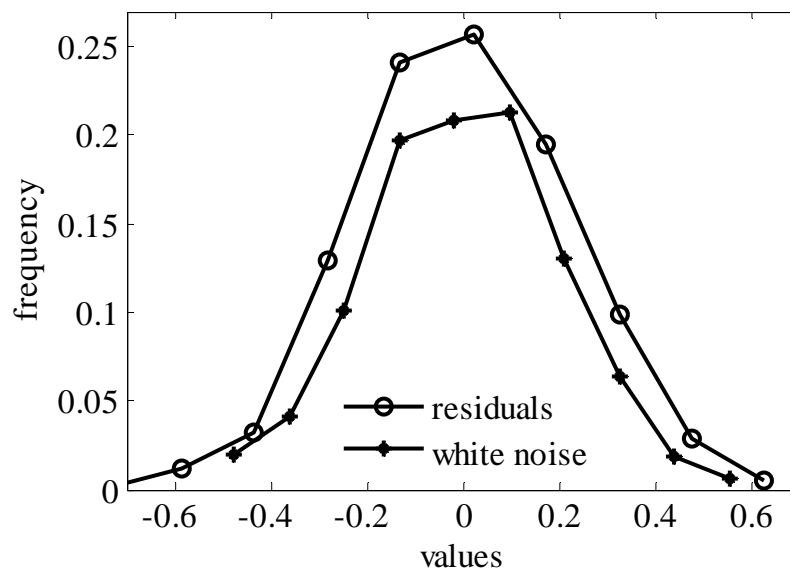
Figure 4.63 Distribution of the residual of the OBF-ARMAX model compared to the white noise added into system (4.106)

The correlation among the residuals is given by

$\hat{R} = [0.0079\ 0.0063\ 0.0042\ 0.0037\ 0.0024\ 0.0057\ \text{-}0.0007\ 0.0009\ 0.0047\ 0.0025]$

Multi-step-ahead predictions

In this case study, the system is open-loop unstable and the simulation model is therefore unstable. However, it is already noted that OBF-ARX and OBF-ARMAX models provide stable predictors. Table 4.15 shows the 1 to 5 step-ahead predictions using OBF-ARX and OBF-AMAX models for system (104). No comparison is made with the simulation model because the system is unstable and any simulation model will result in unbounded prediction.

Table 4.15 The PPE for 1 to 5 step- ahead- predictions of OBF-AR and OBF-ARMA models compared to OBF model for system (4.106)

i	OBF-AR	OBF-ARMA
1	5.4142	5.3191
2	9.4583	9.2860
3	14.0973	12.8947
4	19.1860	16.4497
5	25.1145	20.3734

4.3.6.3 Real plant case study

In this case study, closed loop identification of a real plant is presented. The system to be identified is a reflux drum of a pilot-scale distillation column where the liquid level is controlled by a PI controller with controller gain, $K_c=10$, and integral time, $\tau_I=5$min. The set point is kept at 200mm. An excitation signal is added just after the controller, as shown in the schematic and block diagrams, Figures 4.64 and 4.65 respectively.
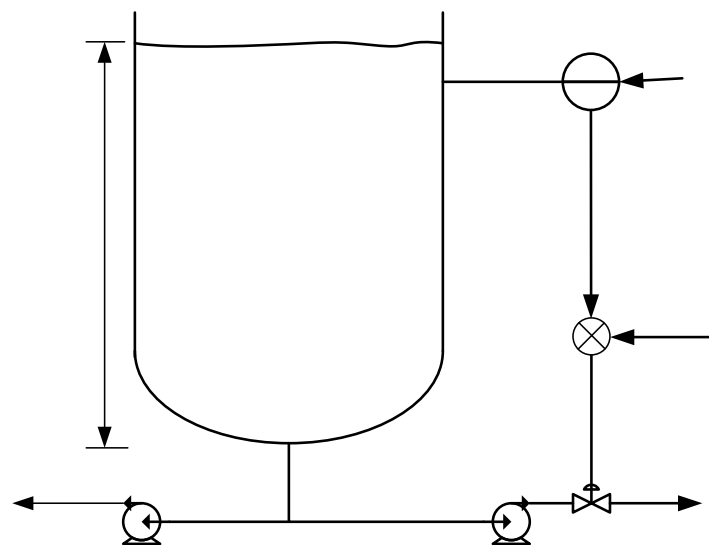
Figure 4.64 Reflux drum level control system
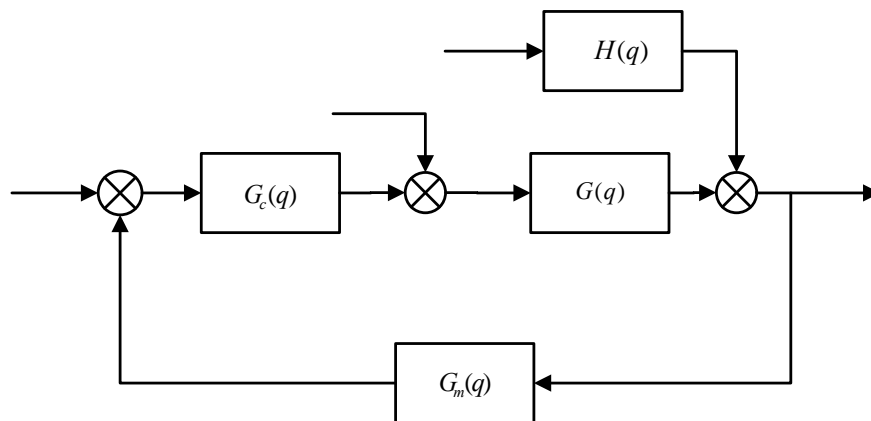
Figure 4.65 Block diagram of the reflux drum level control system

In the figure

r_1= is the external excitation signal

r_2=set point

$G(q)$= The process model to be identified

$H(q)$ = disturbance model to be identified

$G_c(q)$= controller transfer function (known)

$G_m(q)$= Sensor and transmitter transfer function (known)

$e(k)$= innovation sequence, to be estimated from the residual

The external excitation signal introduced for the purpose of identification, the plant input $u(k)$ and plant output $y(k)$ are shown in Figure 4.66.
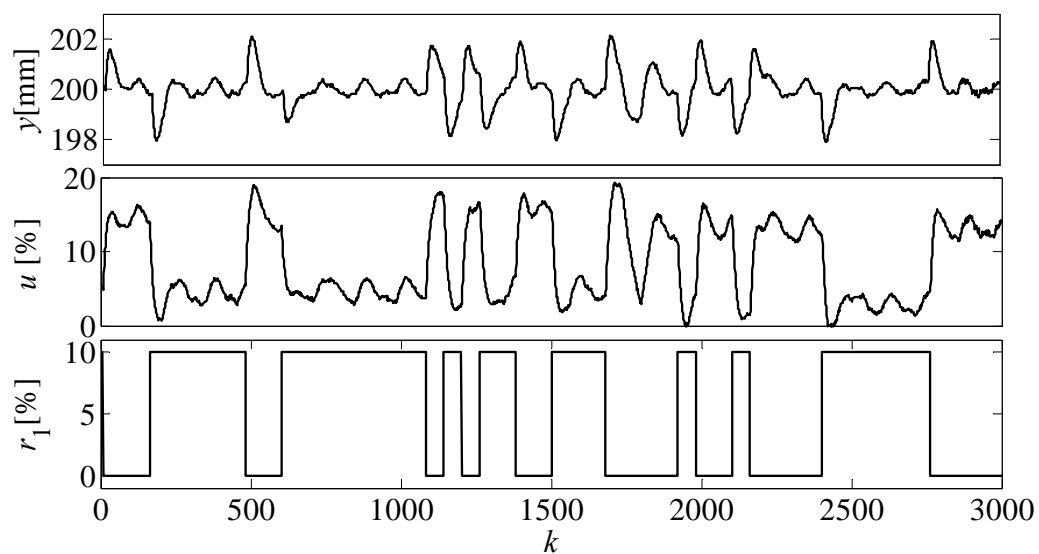
Figure 4.66 Closed loop data used for identification of the reflux drum liquid level control system

GOBF-ARX model

A preliminary study shows that the OBF-ARX gives more accurate models than the other two. Therefore, the OBF-ARX model is reported in this section.

Selection of OBF- pole and number of parameters

The number of OBF- parameters and the OBF pole are selected so that the model attains minimum PPE.

Table 4.16 PPE for various poles and number of OBF parameters for $n_A = 4$ for the reflux drum liquid level control system

pole	Number of OBF parameters			
	4	5	6	7
0.1	0.6410	-	0.6405	-
0.2	<u>0.6355</u>	0.6446	0.6403	0.6403
0.3	0.6430	0.6379	0.6444	0.6391
0.4	-	0.6421	-	0.6421

Based on the above analysis, it is found that the OBF pole and the number of OBF parameters that give the minimum PPE and are 0.2 and 4, respectively.

OBF-ARX model

The OBF-ARX model is defined by four Laguerre filters with pole equal to 0.2. The OBF parameters are estimated

$$l = [0.0442 \quad -0.0368 \quad 0.0042 \quad -0.0125]$$

The estimate of the denominator polynomial $A(q)$ is

$$A(q) = 1 - 0.9852q^{-1} - 0.185q^{-2} + 0.0666q^{-3} + 0.1274q^{-4}$$

The noise model is

$$\hat{H}(q) = \frac{1}{1 - 0.9852q^{-1} - 0.1850q^{-2} + 0.06660.0298q^{-3} + 0.1274q^{-4}} \quad (4.109)$$

The four poles of the noise model are 0.9629, 0.6513 -0.3145 ± 0.3228i, obviously, there is no pole outside the unit circle and the system is open loop stable.

Model Validation

The one-step-ahead prediction by the OBF-ARX model compared to the output of the system, *i.e.,* the liquid level in the reflux drum is shown in Figure 4.67 and the corresponding PPE is 0.6355.
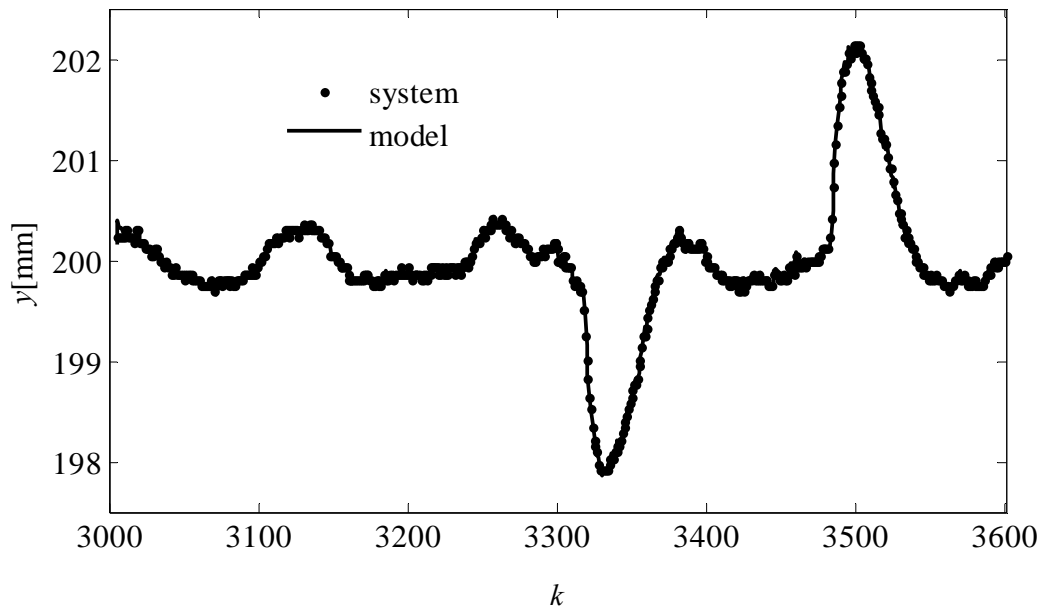
Figure 4.67 One-step ahead prediction of the OBF-ARX model compared to the output of the closed loop system for the validation data points

Residual Analysis

The mean and standard deviations of the residuals of the OBF-ARX model are -0.0026 and 0.2160, respectively. The distribution of the residuals is shown in Figure 4.68. It is observed that the residuals are close to normal distribution with mean zero.
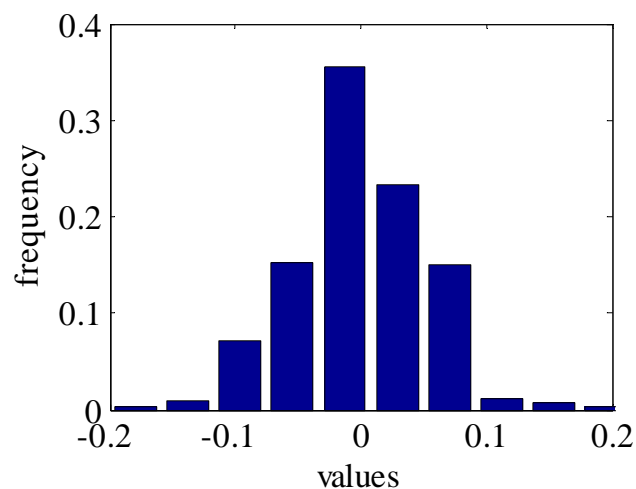
Figure 4.68 Distribution of the residuals for the reflux drum level control system

The correlation among the residuals for the first ten instants are given by

$$\hat{R} = 10^{-3} [\text{ -0.1239 -0.5639 -0.2348 0.4281 0.1199 -0.0474 -0.2713 0.2021 0.0988 -0.1089}]$$

It is noted that the values of the correlation among the residuals is close to zero indicating that there is no significant correlation among the residuals. The distribution of the residuals together with the values of the correlation among the residuals indicates that the residuals can be assumed white noise. Therefore, the accuracy of the OBF-ARX model is acceptable.

In this section, closed loop identification using OBF based prediction models is presented. Novel schemes that are based on both direct and indirect identification are proposed. The indirect identification method is based on using a simulated input rather than the plant input that is correlated with the noise. The direct identification method is based on OBF-ARX and OBF-ARMAX model structures. Open-loop stable processes can be identified from closed loop data using any of the proposed methods. The appropriate method for a given problem can be chosen by comparing the percentage prediction errors of the validation data points. Open-loop unstable processes that are stabilized by feedback controllers can be identified using OBF-ARX and OBF-ARMAX models. However, the decorrelation method cannot be used in such cases.

4.8   Summary

Conventional OBF models are simulation models and they do not provide explicit noise models. However, in several control system design and implementations the noise model plays very critical role. In addition, the prediction capacity of OBF model can be improved significantly by including noise model as integral part of the OBF-models. In this chapter, this major problem is addressed for control relevant system identification both from open-loop and closed loop test data.

Open-loop identifications using OBF plus noise models are successfully carried out using OBF-AR and OBF-ARMA models. These model structures inherit all the advantages of the OBF model structures and the model parameters can be easily estimated without involving nonlinear optimization. Both SISO and MIMO systems can be easily handled. The OBF-ARMA model is more parsimonious than the OBF-AR model.

Closed loop identification schemes that are based on OBF plus noise model are also proposed. The schemes address the two major problems of closed loop identification, namely closed loop identification of open loop stable processes and open loop unstable process that are stabilized by feedback controllers. Methods based on the two commonly known approaches were proposed for handling open-loop stable processes. The direct identification approach uses the OBF-ARX or OBF-ARMAX models while the indirect approach uses the OBF-ARMA model based on the decorrelation method. Open-loop unstable processes that are stabilized by feedback controller are easily and directly handled by OBF-ARX or OBF-ARMAX models.

The schemes for estimating the parameters and the i-step-ahead prediction, for all the proposed structures, are formulated. Each major section is demonstrated by relevant simulation studies and a real plant case study. The real plant case study considers a MIMO system identification of a pilot scale distillation column which involves, experiment design, test for identification, modeling and validation. All identification case studies include residual analysis for testing the accuracy of the models. From the simulation and real plant case studies it is observed that when the identification test is properly conducted, the methods can provide both plant and noise models that have acceptable accuracy.

CHAPTER 5

RESULTS AND DISCUSSIONS

5.5 Introduction

OBF models have several characteristics that make them very promising for control relevant system identification compared to most classical linear models. They are parsimonious in their parameters, the parameters can be easily calculated using linear least square method, their models are consistent in parameters and time delays can be easily estimated and incorporated into the model. However, there are several problems that were not yet addressed which this research attempted to address. Some of the most outstanding problems addressed in this research are:

- How to develop parsimonious OBF models when the dominant poles of the system are not known?

- How to make a better estimate of time delay for second or higher order systems?

- How to include an explicit noise model in the framework of OBF model structures, estimate the parameters and compute multi-step-ahead predictions?

- How to address closed-loop identification problems in this new OBF plus noise model frame work?

The first and second problems were addressed in Chapter 3 while the third and fourth problems were addressed in Chapter 4. In this chapter, the results of the works that address these issues are presented and discussed.

5.6 Development of Parsimonious OBF model using Iterative Method

It is already noted, in the literature review, that OBF models can capture the dynamics of linear systems with a fewer number of parameters if appropriate filter type and pole(s) are used to build the model [8, 48, 92]. If, for example, Laguerre filters are used for modeling weakly damped systems, the OBF model needs larger number of parameters to obtain models with acceptable accuracy. On the other hand, even if the appropriate filter type is used, still a more parsimonious model can be developed if the pole used in the OBF model is close to the dominant pole of the system [8, 48, 92]. Therefore, it is necessary to find a way to know whether the system is well or weakly damped and to estimate the dominant pole(s) of the system from the identification data.

In section 3.2.2, estimation of GOBF poles was discussed. It was noted that Van den Hof *et al*. [92] proposed (3.13) for estimating the poles that gives the most parsimonious model. However, this formula cannot be directly used in real system identification problems, because the poles of the system in actual problems are not known. However, the implication of that formula is very important, namely, the poles estimated using (3.13) closely match the dominant pole(s) of the system.

Sometimes, the dominant pole is estimated from simple step tests. However, this may lead to a very inaccurate result for systems involving significant unmeasured disturbances. In addition, when an appropriate identification test is to be carried out for modeling the system, there is no need to use a less accurate step test for estimating the dominant pole. In this research, this problem is addressed by developing an iterative scheme in which one or two of the dominant poles of the system are estimated and used to develop a parsimonious OBF model that has acceptable accuracy. The results are presented and discussed in the following sections.

5.6.1 Estimation of time delay and dominant time constants

The method proposed in section 3.3 for estimating one dominant pole and time delay of a system was based on developing a first order plus time delay model from the noise-free OBF model. In this approach, first an OBF model was developed using arbitrarily chosen poles and generalized orthonormal basis filters. Then, a FOPTD model is developed from the step response of the noise-free OBF model. This is the key step which makes the proposed method efficient. Instead of making a step test on the plant and estimate the pole, a step test can be conducted on the noise free OBF model. This has two major advantages. First, since the OBF model can effectively separate the deterministic component from the stochastic, the presence of unmeasured disturbances will not affect the estimation. Second, the step test can be conducted as many times as necessary without incurring any significant cost on the identification process. This becomes especially useful in determining the optimum number of OBF parameters as illustrated in the case studies.

Three different methods of estimating the FOPTD parameters were discussed. These methods are: the moment method, the tangent method and the interpolation method. From extensive simulation studies it is observed that the interpolation method results in more accurate result than the other two. This may be due to the unique nature of the step

response of OBF models. As it was shown in Figure 3.1, the step response of OBF models has inverse type response. This is the case even if the system to be identified does not have a non-minimum phase zero. The reason is the fact that the orthonormal basis filters themselves, have non-minimum phase zero in their structure. This can be easily observed from the Laguerre, Kautz and GOBF filters in (3.8), (3.10) and (3.11), respectively. When the moment method is used, the oscillation due to these non minimum phase zeros results in wrong estimation of the moment, which is latter reflected in the estimation of the parameters of the FOPTD model. On the other hand, the tangent method results in less accurate estimation than the interpolation method because the tangent method relies on the value at one point only, *i.e.*, inflection point, while the interpolation method uses average values. It should be noted that in the interpolation method, unlike the moment method, the oscillatory part of the step response is not involved in the estimation and it does not affect the accuracy of the estimation.

According to the proposed interpolation method, the time delay was obtained by drawing a tangent at the inflection point of the normalized step response of the OBF model and taking the intersection of the tangent to the time axis as estimate of the time delay, as shown in Figure 5.1. This is the same time delay estimation method suggested by Patwardhan and Shah [8]. The time constant is estimated by finding the time, in terms of the time constant, τ, to reach certain level of the normalized step response and estimating the mean time constant using (3.35)

$$\tau = \frac{\sum_{i=1}^{n}(t_{\alpha i} - \tau_d)}{\sum_{i=1}^{n}\alpha_i} \qquad (3.35)$$

where $t_{\alpha i}$ is the time that the normalized step response takes to reach a level in α time constants plus the time delay. For example, the normalized response reaches a level of 0.632 in one time constant plus the time delay. For this case $\alpha = 1$, $t_{\alpha i}$ is obtained by finding the time, the normalized response takes to reach 0.632 and the time delay, τ_d, is estimated by the tangent method.
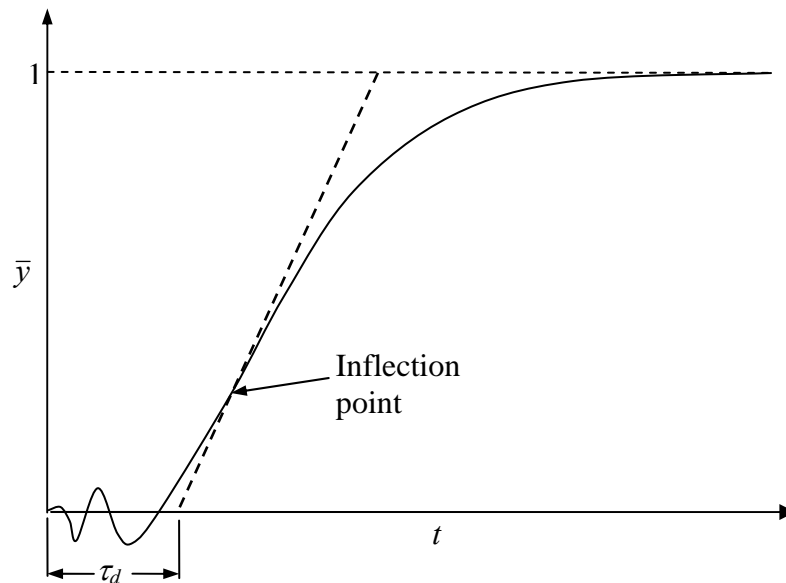
Figure 5.1 Time delay estimation by the tangent method

The simulation study in section 3.3.3 clearly demonstrated the effectiveness of estimating the dominant pole of the system in the presence of significant unmeasured disturbances. It is clear from the value of the signal to noise ratio, SNR=7.7356, that there is a significant disturbance in the system. This can be observed, clearly, from Figure 3.3 also. The dominant time constant of the system was 16, while the estimated value by the proposed method is 16.8. The accuracy of the estimation should not be surprising when it is observed how close the step response of the OBF model was to the step response of the system without disturbance, as shown in Figure 3.4. The FOPTD method, however, is useful for system identification problems involving well damped systems that can be modeled by Laguerre filters only. For weakly damped systems, the Kautz filters are the most appropriate choice and they need estimates of a conjugate complex pair of poles. If GOBF is the intended type of filter to be used, the FOPTD based method is not the appropriate choice to estimate the dominant poles.

The second order plus time delay (SOPTD) based method enables obtaining the estimation of two dominant poles and the time delay with a better accuracy than the tangent method. A novel method, for estimating the SOPTD parameters from the step response of OBF models, was developed which is more effective and more accurate than the methods suggested by Smith [37] and Rangaiah and Krishnaswamy [35, 36], especially for obtaining the parameters from the step response of OBF models.

The damping coefficient, natural frequency and the time delay can be easily determined from the step response of the OBF model using Algorithm 3.1. The relevant equations are given by (3.44), (3.47), (3.56), (3.58) and (3.65). The coefficient m_1 and m_2 are determined using Figures 3.7 and 3.10, respectively.

$$\alpha_1 = \frac{\sinh^{-1}\left(\sqrt{\varsigma^2 - 1}\right)}{\sqrt{\varsigma^2 - 1}} \qquad (3.44)$$

$$\bar{y}_i = 1 - 2\zeta e^{-\zeta \alpha_1} \qquad (3.47)$$

$$\tau = m_1 (t_n - t_m) \qquad (3.56)$$

$$\tau_d = \tau_{dt} - \tau_{dc} \qquad (3.58)$$

$$\tau_{dc} = m_2 (t_n - t_m) \qquad (3.65)$$

Once, the response at the inflection point is obtained a very good estimate of the damping coefficient, ζ, is found from the empirical relation

$$\zeta_0 = \sqrt{\frac{1.805}{\bar{y}_i} + 1.805} - 1.9 \qquad (3.48)$$

where
$$\zeta = \zeta_0 (1 \pm 0.07) \qquad (3.49)$$

This will enable using the false position root finding method to get more accurate estimates using (3.44) and (3.47). One of the major advantages of this method compared to the Smith [37] method is , to use the Smith method, the apparent time delay should be separately estimated and subtracted from the response time. Therefore, the accuracy of the estimated parameters highly depends on the accuracy of the estimate of the apparent time delay. The newly proposed method does not depend on the apparent time delay since the time delay is eliminated when $(t_n\text{-}t_m)$ is used as in (3.56) and (3.58). In addition, the proposed method enables accurate estimation of the apparent time delay itself. The main advantage of the proposed method to the Rangaiah [35, 36] methods is that the oscillatory part of the step response which is caused by the non-minimum phase zero is not involved in the estimation process in the proposed method. The Rangaiah [35, 36] method will involve this part of the response and if the oscillation is large it will lead to erroneous results. In addition, it is reported [7], that the accuracy of the Rangaiah method is good enough only in limited range of the damping coefficient.

From the damping coefficient and natural frequency the estimates of the two dominant poles of the system can be estimated directly. The poles are real if the system is well damped and complex conjugate if the system is weakly damped. Therefore, the SOPTD based method can also be used to identify the appropriate type of filter to be used, by checking the damping coefficient.

The time delay estimation method which was proposed by Patwardhan and Shah [8] is accurate enough for systems with first order plus time delay dynamics. However, for second and higher order systems it is less accurate. The time delay estimation method proposed in this research gives more accurate estimates than that proposed by Patwardhan and Shah. Nevertheless, one may wonder if the error introduced by the tail of the sigmoidal curve, τ_{dc}, on the time delay estimated by the tangent method is really significant. The answer is, it depends on the values of the damping coefficient and the natural frequency. From (3.56) and (3.65) it can be seen that this contributed time delay is directly proportional to the natural frequency. From Figure 3.10 and (3.65) it was observed that the smaller the value of the damping coefficient the larger is the value of the contributed time delay. Table 5.1 shows the values of the contributed time delay for various values ζ for $\tau = 1$ for a second order process.

Table 5.1 The contributed time delay for various ζ and $\tau = 1$

ζ	2	1.5	1	0.5	0.1
τ_{dc}	0.1845	0.2236	0.2817	0.3787	0.5187

Since the contributed time delay is directly proportional to the natural frequency, if the natural frequency is 10 for a given second order system, the contributed time delay will be ten times that shown in Table 5.1.

The effectiveness of the SOPTD based method was demonstrated by relevant simulation studies for both well damped and weakly damped cases. The simulation studies are designed with the intention to reflect the application of the proposed method. Hence, both systems (3.68) and (3.69) include colored noise that might represent significant unmeasured disturbances in the system, since that is expected in normal identification applications.

In case study 1, section 3.4.3, the system is well damped and has two dominant poles. In the estimation, an OBF model with 12 GOBF parameters and two alternating poles of 0.7165 and 0.9672 corresponding to time constants of 3 and 30 were used. Note that these time constants are far away from the true dominant time constants 6 and 16. In addition, the system is a fourth order system to be estimated by SOPTD model. From Figure 3.12, it was observed that even though the OBF poles are far away from the true dominant poles of the system the step response of the OBF model is close to the step response of the system. This is possible because relatively large number of parameters, 12, was used. It was observed from the final SOPTD estimate given by (3.68) that the estimate of the dominant time constants is very close to the true time constant.

Case study 2 in Section 3.4.4, in addition to showing that the proposed method is effective for weakly damped systems, attempts to answer a very important question. The questions can be described as follows. It is normally very difficult to identify whether a system is weakly damped or well damped from the identification data. In such cases, how is it possible to select the appropriate filter type to develop the first OBF model? This case study attempts to answer this question. The system is weakly damped and the true dominant poles of the system are complex conjugates with poles $-0.1000 \pm 0.1732i$ corresponding to the discrete poles $0.8913 \pm 0.1559i$ with sampling interval of 1 time unit. However, the OBF model is developed from the two real poles $-1/3$ and $-1/30$ with 12 GOBF parameters. The closeness of the OBF model to the system can be observed from the step response of the model and the system shown in Figure 3.15. The SOPTD estimate of the system is given by (3.70) and the corresponding estimates of the poles are $0.8925 \pm 0.1514i$. These estimated poles of the SOPTD model are very close to the dominant poles of the system. This case study, therefore, made it clear that even though the system is weakly damped if the number of parameters is large enough a very good estimate can be obtained regardless of the filter type used and the initial poles used for the OBF model. The only problem this OBF model is that it is not parsimonious, which is one of the major promises of OBF models.

It was confirmed from the logical development of the methods and the case studies that it is possible to get a good estimate of one or two of the dominant poles of a system and the time delays using the proposed methods.

5.6.2   Development of parsimonious OBF models

The next question is, how is this information used to develop parsimonious OBF models? There are two logical approaches to answer this question

(i) Develop OBF models, first with relatively larger number of parameters and estimate the dominant pole of the system. Then develop a parsimonious OBF model using these estimated dominant poles. The minimum number of parameters with acceptable accuracy can be chosen by comparing the PPEs.

(ii) Fix the number of OBF parameters to the desired parsimonious value and develop OBF model from arbitrarily chosen poles. Improve the accuracy of the OBF model by estimating the dominant pole and using it to develop improved OBF model iteratively.

The first approach does not need any more explanation since it was illustrated that the dominant poles can be successfully estimated using the proposed method. If the dominant poles are used in OBF model development, it is already an established fact that the resulting OBF models converge quickly [8, 20, 48, 92] showing that the OBF models can describe the system with a fewer number of parameters with acceptable accuracy.

The second approach was illustrated by the flow diagram shown in Figure 3.17 and three relevant case studies. In all the three case studies, the unmeasured disturbance was intentionally made white noise because, at this level, the issue of noise models is not yet addressed and it will be impossible to test the accuracy of the model if the noise is colored. However, noise models were treated in Chapter 4 and relevant simulation case studies with colored noise were provided.

In Case study 3 in Section 3.6.1, the identification of a well damped system that had one dominant pole with an additive white noise using the iterative method was demonstrated. The convergence criteria used was the minimum PPE. This convergence criterion is very practical because it will enable choosing the model structure that will result in the more accurate prediction, which is the intended use of models in many control relevant implementations. It was observed in Table 3.1 that the PPE was very large at the first iteration with around 30% for 6 OBF parameters and around 15% for 12 OBF parameters. The reason is that at the first iteration the OBF pole used was far away from the dominant pole of the system and the model needs large number of parameters to capture the system

dynamics accurately. However, at the second iteration the accuracy with each number of parameters has improved. At the third iteration, the minimum PPE was attained. The difference between the values of the PPE at this iteration is very small. It is, obviously, advantageous to choose the most parsimonious model that has six OBF parameters.

Model validation was carried out by using the developed parsimonious OBF model for simulation with a separate validation data that was not used in identification. Figure 3.25 shows the prediction by the developed parsimonious OBF model compared to the noisy output data of the system. It was noted from the figure that the prediction is very good. However, the next figure, Figure 3.27 gives more insight into the accuracy of the OBF model. It was noted in this figure that except at the first few instants the prediction is very good.

The large deviation in the first few instants is due to the initial conditions of the simulation. OBF models are infinite impulse response type of models. As it was observed from (3.2), for simulation with infinite responses, all previous values back to minus infinity are theoretically required. However, the validation data is taken from 3001 to 4000.

$$y(t) = \sum_{k=0}^{\infty} g_k u(t - k)$$

(3.2)

The response is assumed zero for all instants before 3001. This causes deterioration in the simulation performance of the model. However, for stable models, the initial conditions die out exponentially with time and the simulation becomes reasonably accurate for $k > 3\tau/T_S$, where τ is the dominant time constant and T_S is the sampling time [2]. In this particular case study, the dominant time constant is 18 and the sampling interval is 1, therefore the simulation becomes reasonably accurate for $k > 54$.

Figure 3.21 shows the step response of the parsimonious OBF model compared to the noise-free step response of the system. It was observed that the OBF model approximates the system reasonably accurately. It was also noted that the OBF model approximates the time delay by non-minimum phase zeros that appears as inverse response in the step response.

The residual analysis is a good way of testing the accuracy of models. A model is considered the best if it can predict all the output except the white noise, because white

noise is random and it cannot be predicted [1, 2]. Therefore, in residual analysis the objective is to check whether the residual is close to white noise. If the residual is close to white noise the accuracy of the model is acceptable. In case of simulation studies, the white noise added to the system is known. Therefore it can be further checked whether the white noise is close to the white noise added to the system. The qq-plot of the residuals with respect to the white noise added to the system, the distribution of the residuals and the correlation among the residuals are good indicators for the whiteness of the residuals. If the residual is white noise, all the points in the qq-plot will lie on a straight line. If the residuals have the same distribution as the white noise that is added to the system the qq-plot will be a straight line with slope equal to 1 and passes through the origin. The distribution of the residuals become close to normal distribution with mean zero if they are close to white noise. If the residual is white the correlation among the residuals will be close to zero, indicating that the there is no correlation among the residuals. In this particular case study, all the whiteness tests indicate that the noise is close to the white noise added to the system. Therefore, the accuracy of the parsimonious models is acceptable.

Case study 4 demonstrates the use of the SOPTD-based iterative method for developing parsimonious OBF models for a well damped system given by (3.72). The system has two dominant real poles. The output was corrupted with additive white noise with SNR of 8.5225. In the OBF model development, the iteration was started with poles far from the dominant poles of the system. It was observed from Table 3.2 that at the first iteration the PPE is very high and it gets smaller as the number of OBF parameters increases. It is also observed that convergence is attained after different number of iterations for the models with different number of OBF parameters. However, after all models come to convergence the difference between the PPE for different number of parameters is insignificant and obviously, the best choice will be the one with the smallest number of parameters, OBF-6. The residual analysis also confirms that the accuracy of this model is acceptable.

Case study 5 in Section 3.6.3, considers identification of weakly damped system using the proposed SOPTD-based method. In this case study also, the initial pole is real and far from the dominant poles of the system which are complex conjugates. However, the iteration scheme converges to a parsimonious OBF model that has acceptable accuracy in

four iterations. Both model validation and residual analysis show that the parsimonious OBF model has acceptable accuracy. It is also noted that in all the three case studies the time delay estimation is better than that estimated by the tangent method. In summary, the results in this section confirm that parsimonious OBF models that have acceptable accuracy can be developed starting from an arbitrarily selected poles using the proposed iterative method.

5.7 OBF based prediction models

Conventional OBF models are simulation models and they do not include explicit noise model in their structure. However, in many control system designs and implementations the noise model plays a very important role. In this research, BJ type structures obtained by combining OBF model and conventional time series models, and modified OBF structures are proposed. Models with these structures inherit all the benefits of OBF models and they include explicit noise model. Algorithms for estimating the model parameters and the multi-step ahead prediction are developed and relevant simulation and real plant case studies are presented in Chapter 4.

Both open-loop and closed-loop identifications were considered and the appropriate identification scheme based on OBF plus noise model were proposed. Open-loop identifications were carried out using OBF-AR or OBF-ARMA models while closed-loop identifications were carried out using direct identification with OBF-ARX or OBF-ARMAX model or with indirect identification method using OBF-ARMA model. Results and discussions on these issues are presented in the following sections.

5.7.1 Open-loop Identification Using OBF-AR and OBF-ARMA models

OBF-AR models have an OBF deterministic component and AR noise model. The model is given by

$$y(k) = G_{OBF}(q)u(k) + \frac{1}{D(q)}e(k)$$

(4.2)

The models parameters are easily estimated using linear least square method using Algorithm 4.1. However, the order of the noise model should be large enough to capture the dynamics of the system accurately.

OBF-ARMA models are more flexible, have the BJ-type structure and result in parsimonious OBF and noise models. The model parameters can be estimated using the

extended least square method or two-step method as described in Algorithm 4.2. It was already shown in the case studies that the two-step method, when properly applied, leads to models that are nearly as accurate as the extended least square method. The GOBF-ARMA models are given by (4.3)

$$y(k) = G_{OBF}(q)u(k) + \frac{C(q)}{D(q)}e(k)$$

(4.3)

In section 4.2.5, three different case studies were presented that address the various issues related to OBF plus noise model in open-loop identification. The first two case studies were intended to show the effectiveness of the proposed identification scheme for both weakly-damped and well-damped systems in the presence of unmeasured disturbances. Unlike the previous case studies, in these case studies the disturbance is not white noise, the accuracies of the plant, the noise and the overall models were evaluated. The third case study is a comprehensive identification case study of a real plant with multiple-input multiple-output (MIMO) system. The case study includes all phases of identification from design of experiment to validation of the plant model.

In Case study 4.1, a well damped system with unmeasured disturbance is identified. The SNR is 6.6323, which shows that there is significant unmeasured disturbance in the system. The iterative method, developed in Chapter 3 which was also discussed in the previous section in this chapter, was used to determine the poles and the minimum number of OBF parameters that result in parsimonious OBF model with acceptable accuracy. In the first part of the OBF-AR model development, the method for selecting the order of the AR noise model was presented.

In all simulation studies, in section 4.2.5, the accuracy of the noise models was presented by comparing the noise spectrum of the system and the model. Ljung [1] discusses, in detail, the estimation of the noise spectrum. The comparison of the spectrum of the noise models and the noise transfer function of the system in Figure 4.4 shows that the order of the noise model should be large enough to capture the dynamics of the noise transfer function. However, it should also be noted that using too large order of noise model causes the variance error to increase and the overall quality of the model to degrade [2]. In the given case study $n_D = 7$ gives the minimum PPE which is less than 1%. Whether this 1% prediction error is large or small is determined from the residual analysis.

In validation of the models in all identification case studies, the simulation output was included. This is because the long term (steps-ahead) prediction capability of the overall model of the system highly depends on the accuracy of the simulation models. The next logical question is, when is the accuracy of the simulation model acceptable? If the noise model and the overall prediction models are checked to be accurate enough then the simulation model is accurate because it is just the difference of the two. In the case study considered here, both the noise model and the overall prediction of the validation data is reasonably accurate. In addition, all the results of the residual analysis show that the distribution of the residual is close to the distribution of the white noise added to the system. The qq-plot, Figure 4.7, is linear with slope equal to 1 and passing through the origin, the plot of the distribution of the residuals, Figure 4.8, is close to the white noise and the correlation among the residuals is close to zero. Therefore, the accuracy of the model is acceptable and the method is shown to be effective.

The case study shows also that the OBF-ARMA model has some better qualities than the OBF-AR model. First, the noise model is more parsimonious than the AR model. The order of the numerator and denominator polynomial that give the minimum PPE is two. Which means only four parameters should be estimated compared to 7 parameters in the OBF-AR case. In addition, comparing Figures 4.6, 4.11 and 4.15, it is observed that the accuracy of the noise model of the OBF-ARMA model developed using both methods is better than that of the OBF-AR model. Finally, it is also observed that for the case studies under consideration the accuracy of the OBF-ARMA model using the two-step method is very close to that obtained by the iteration method. However, the iterative method gives the possibility of selecting the prediction model with the minimum possible PPE. Therefore when the computational burden is the most important issue the two-step method can be used, otherwise the iteration method is the most effective.

Case study 4.2 is similar to case study 4.1, except the fact that in case study 4.2 the system is weakly damped. The analysis in this case study also leads to the same conclusion as before. From the validation and residual analysis it is observed that the proposed identification schemes with OBF-AR and OBF-ARMA models are reliable for identification of weakly damped systems also.

Case study 4.3 considers identification of a pilot scale distillation column used for separating Isopropyl Alcohol (IPA) and acetone. The distillation column is a part of a

reaction-separation system where the output from the reactor is the feed for the distillation column. It is already established that while both OBF-AR and OBF-ARMA models are effective in capturing the dynamics of linear systems, OBF-ARMA models are more accurate and more parsimonious. Because of this in case study 4.3, the distillation column was identified using OBF-ARMA model.

Using the iterative method the dominant poles (4.54) of the four transfer functions were identified.

$$p = \begin{bmatrix} 0.9515 & 0.4112 \\ 0.8805 & 0.9702 \end{bmatrix} \tag{4.54}$$

Then four OBF models, each with six Laguerre filters and one dominant pole given by (4.54), were developed. The estimated OBF model parameters are

$L_{11} = [0.0298 \quad 0.0037 \quad 0.0035 \quad 0.0018 \quad -0.0005 \quad 0.0050]$

$L_{12} = [0.0214 \quad 0.1017 \quad 0.0497 \quad -0.0949 \quad 0.1252 \quad -0.0112]$

$L_{21} = [0.0137 \quad 0.0326 \quad 0.0028 \quad 0.0348 \quad -0.0128 \quad 0.0375]$

$L_{22} = [-0.8330 \quad 0.2001 \quad -0.2893 \quad 0.0377 \quad -0.1374 \quad 0.0870]$

The time delay estimates in number of sampling intervals are

$$\tau_d = \begin{bmatrix} 0 & 5 \\ 5 & 0 \end{bmatrix}$$

The orders of noise model that give the most parsimonious model with reasonable accuracy were chosen. Accordingly, the order of the noise models chosen are $n_D = n_C = 2$. The two ARMA noise models are given by (4.55) and (4.56), respectively.

$$H_1 = \frac{1 - 0.8415q^{-1} - 0.1225q^{-2}}{1 - 1.9077q^{-1} + 0.9082q^{-2}} \tag{4.55}$$

$$H_2 = \frac{1 - 0.2176q^{-1} - 0.64265q^{-2}}{1 - 1.7575q^{-1} + 0.7607q^{-2}} \tag{4.56}$$

The validation and residual analysis show that the model has acceptable accuracy. It is observed from Figure 4.35 that the simulation model also had good accuracy. The percentage prediction errors of the OBF model for the top and bottom temperatures, respectively, are 11.5293 and 18.7596. This ensures that the multi-step-ahead predictions will also have acceptable accuracy. Most of the remaining predictions are taken care of by

the noise model. This is observed from Figure 4.36 (a) and (b) where the one-step-ahead prediction is compared to the system outputs using the validation data points. The PPE values of the OBF-ARMA model for the validation data points for the top and bottom temperatures are 0.4345 and 0.6562, respectively. The distributions of the residuals of the one-step-ahead prediction of the OBF-ARMA are shown in Figures 4.37 (a) and (b). From both figures it is observed that the distributions of the residual are normal like distribution with mean close to zero. This together with the very small correlations among the residuals confirms that the residuals are close to white noise. Therefore, the 2×2 OBF-ARMA model of the distillation column had acceptable accuracy. The correlation among the residuals for the first 10 instants for the bottom and to temperatures are given by

$$\hat{R}_1 = 10^{-3} \times [0.5481\ 0.2218\ 0.0660\ \text{-}0.0458\ \text{-}0.0928\ \text{-}0.1238\ \text{-}0.1077\ \text{-}0.0762\ \text{-}0.0539 \quad 0.0405]$$

$$\hat{R}_2 = 10^{-3} \times [0.9227 \quad 0.9406 \quad \text{-}0.4896 \quad \text{-}0.4175 \quad \text{-}0.7111 \quad \text{-}0.5041 \quad \text{-}0.1605 \quad \text{-}0.1698 \quad \text{-}0.0329$$
$$\text{-}0.0043]$$

5.7.2 Closed loop Identification

When system identification test is carried out in closed loop, the input sequence is correlated to the noise sequence and conventional OBF model development procedures fail to provide consistent model parameters. In this research three different methods that address the issue of closed loop identification were proposed. The methods are designed so that they address the two distinct aspects of the problem, namely, model development from closed loop data when the system is open-loop stable and when the system is open-loop unstable. In all cases, both the system and noise model are considered important.

Closed-loop identification of open-loop stable processes can be handled by any of the three proposed methods. Case study 4.4 clearly demonstrates that all the three approaches can be effectively used to develop OBF based prediction models from closed loop data of open-loop stable systems. The validation and the residual analysis also confirm this fact. However, the selection of the best structure for a given problem can be made based on comparison of the PPE. When, the difference between the PPE is small the OBF-ARMA model is preferable because the simulation model is simple and stable. This is observed from the structure of the three model types given by (4.3) (4.71) and (4.76).

$$y(k) = G_{OBF}(q)u(k) + \frac{C(q)}{D(q)}e(k)$$
(4.3)

$$y(k) = \frac{G_{OBF}(q)}{A(q)} + \frac{1}{A(q)}e(k)$$
(4.71)

$$y(k) = \frac{G_{OBF}(q)}{A(q)} + \frac{C(q)}{A(q)}e(k)$$
(4.76)

Note that the simulation model of the GOBF-ARMA model (4.3) is just the OBF model, and OBF model by design is stable. However, the simulation model of (4.71) and (4.76) is $G_{OBF}(q) / A(q)$ and it's stability is not ensured because of the denominator $A(q)$.

For conducting closed-loop identification of open-loop unstable systems the structures OBF-ARX and OBF-ARMAX were proposed. The scheme for estimating the parameters of the models and the multi-step ahead prediction are developed in sections 4.3.3-4.3.5. Case study 4.5 demonstrates closed-loop identification of open-loop unstable processes that are stabilized by feedback controller. In such identification problems, the objective is to develop a predictor that is stable. It should be noted that the simulation and noise models, separately, are unstable. As it is shown in section 4.3.5 the unstable poles do not appear in the predictor, therefore the predictor is stable. In this case study, the model validation and the residual analysis confirm the effectiveness of the proposed closed-loop identification schemes.

The last case study in Chapter 4, Case study 4.6, presents closed-loop identification of a level control system of the reflux drum of the distillation column discussed in Case study 4.3. As it is observed from the identification data shown in Figure 4.66 the noise level is of the output is low. A preliminary study with all the model types show that the OBF –ARX model give slightly better prediction than GOBF-ARX. GOBF-ARMA model develops good prediction model when the correlation of the input and the noise is ignored and the GOBF-ARMA model is directly developed. This is probably due to the low level of the noise in the system. Therefore, in the case study the OBF-ARX model is developed using the closed-loop identification data. The PPE for the one-step-ahead compared to the output using the validation data is 0.6355 and as it is also observed in Figure 4.67 it is very small. The distribution of the residuals, shown in Figure 4.68, and the low level of the correlation among the residuals indicate that the residuals are close to white noise. Therefore the model has acceptable accuracy.

5.8   Summary

In this chapter the results of the present research were presented and discussed. The results give solution to the research problems. An iterative scheme was developed that enables developing parsimonious OBF models that have acceptable accuracy starting from an arbitrarily selected poles. A method for estimating the time delay more accurately than the tangent method was developed. A unified scheme that will provide OBF plus noise models both from open-loop and closed loop data was developed. The methods for estimating the model parameters and the multi-step ahead predictions were formulated. The proposed methods were demonstrated with extensive simulation studies and real plant case studies and the result shows that they are effective.

CHAPTER 6

CONCLUSIONS AND RECOMMENDATIONS

6.7 Introduction

One of the most important factors in selecting model structures is the computational burden in estimating the model parameters. Auto Regressive with Exogenous Input (ARX) and Finite Impulse Response (FIR) models have been popular because of the computational simplicity with which the model parameters are estimated. In both cases, linear least square method can be used. Output error (OE) and Box Jenkins (BJ) structure are very rarely used for complex problems, like MIMO, because of the heavy computation burden related to their parameter estimation. Parameter estimations in both OE and BJ involve nonlinear optimization. In addition, BJ models parameter estimations involve additional burden due to the large number of parameters, related to the four polynomials in its structure. Due to these problems, BJ models are rarely used in MIMO system identification problems, even though they are believed to be the most flexible of the linear structures.

Another important factor which is related to the quality of the models is consistency of the parameters. Structures suffering from inconsistency in their parameters will result in biased estimates of the parameters and the bias will not be eliminated even if the number of data points is increased to infinity. ARX and ARMAX models suffer from inconsistency in most open-loop identification problems. This is because of the common denominator dynamics of the deterministic and stochastic components, represented by $A(q)$, that the structure requires and which many practical open-loop problems do not satisfy.

The number of parameters required to capture the dynamics of a system with acceptable accuracy is still another important issue in linear system identifications. This will affect both the identification and implementation phases of the model. It is known that, no matter what the linear structure is, when the number of parameters increases the variance error in parameters estimation increase[2]. Nelles [2] noted that for infinite data points, the variance error is directly proportional to the number of parameters to be estimated. This shows that models which need large number of parameters to capture the dynamics of a system will face the problem of increased variance error in the estimation of their parameters. On the other hand, during implementation like in MPC, an optimization

problem is solved using the models to obtain the control output at each move. When the complexity of the model increases, obviously, the computational burden on the optimization at each control moves increases. Therefore, it is very advantageous both at identification and implementation stage to get models that are parsimonious in their parameters. Finite Impulse Response (FIR) models suffer heavily from this problem. They generally require large number of parameters to describe linear systems with acceptable accuracy.

Estimation of time delay is another critical issue in linear model development. All classical linear model structures, except FIR, need the time delay of the system to be separately estimated and included in the model development process. The accuracy of the time delay estimation affects both the model parameter estimation and implementation in control systems.

OBF models have several characteristics that make them very promising for control relevant system identification compared to most classical linear models. Their parameters can be easily calculated using linear least square method. They are consistent in their parameters for most practical open-loop identification problems. Parsimonious OBF models can be developed when the dominant pole(s) of the system is (are) known. Time delays can be easily estimated and incorporated into the model. However, there are several problems that were not yet addressed which this research attempted to address. Some of the most outstanding problems are addressed in this research. They are:

(i)   How to develop parsimonious OBF models when the dominant poles of the system are not known

(ii)   How to obtain a better estimate of time delay for second or higher order systems

(iii)   How to include an explicit noise model in the framework of OBF model structures and determine the parameters and multi-step ahead predictions

(iv)   How to address closed-loop identification problems in this new OBF plus noise model frame work

6.8 Development of Parsimonious OBF model

The first problem was addressed by developing a method in which the dominant pole(s) of the system are estimated and used to develop a parsimonious OBF model. The two approaches proposed in this research are:

(i)   Develop OBF models with relatively larger number of parameters and estimate the dominant pole of the system. Then, develop a parsimonious OBF model using these estimated dominant poles. The minimum number of parameters with acceptable accuracy can be chosen by comparing the PPEs.

(ii)   Fix the number of OBF parameters to the desired parsimonious value and develop OBF model from arbitrarily chosen poles. Improve the accuracy of the OBF model by estimating the dominant pole and using it to develop improved OBF model iteratively.

It was shown in Chapter 3, by appropriate mathematical derivations and extensive simulation studies that one or two of the dominant pole(s) of a linear system can be estimated with reasonable accuracy using the proposed FOPTD based or SOPTD based methods, respectively. Three different methods: the tangent, the moment and interpolation methods, of estimating the FOPTD parameters were compared and the interpolation method were found to be the simplest and most accurate method. A novel method for estimating the SOPTD parameters was developed. The validity of the method was shown both by rigorous mathematical derivation and by relevant simulation studies. The proposed novel method can be used to estimate the SOPTD parameter from any noise free step response of a system. However, it is uniquely effective in estimations of the stated parameters from the step response of OBF models.

6.9 Better Estimate of Time Delay

The SOPTD method addresses the second problem also. It was shown in Chapter 3 and discussed in Chapter 5 that the proposed SOPTD based method gives a better estimate of the time delay than the tangent method which was used by Patwardhan and Shah [8]. It described in Chapter 5 that the deviation of the estimate of the time delay by the tangent method from the true value depends on the damping coefficient and natural period of oscillation of the estimated SOPTD model of the system. The smaller the damping coefficient the larger is the deviation and it is directly proportional to the natural period of oscillation. Therefore, based on the magnitude of the damping coefficient and the natural period the deviation has the potential to be significantly high. The proposed SOPTD based method removes this deviation by appropriately determining and subtracting it from the time delay estimate by the tangent method.

6.10   Open-loop identification Using OBF based prediction models

Conventional OBF models are simulation models and they do not include explicit noise model in their structure. However, in many control system designs and implementations the noise model plays a very important role. In this research, BJ type models obtained by combining OBF model and conventional time series models are proposed. Models with these structures inherit all the benefits of OBF models and they provide explicit noise model.

The OBF-AR model structure has an OBF deterministic and AR stochastic components. The model parameters are easily determined using the least square method. The step-by-step procedure is given by Algorithm 4.1. The OBF-ARMA model structure has an OBF deterministic component and an ARMA stochastic component. The parameters in OBF-ARMA model are estimated using the iterative extended least square method or the two step method as given by Algorithm 4.2. The multi-step-ahead prediction schemes for both model types were developed in Chapter 4.

The effectiveness of the proposed structures and methods was demonstrated in Chapter 4 using simulation and real plant case studies. The accuracies of the models both in the simulation and real plant case studies were validated by using the developed model to predict a separate validation data that is not used in identification and by residual analysis. All case studies confirmed the effectiveness of the proposed methods for open-loop identifications. In addition, the accuracy of the noise models were validated by comparing the spectrum of the estimated noise models to the noise transfer function of the system. The comparisons showed that the spectrums of estimated noise models closely matched the spectrums of the noise transfer functions of the system.

6.11   Closed-loop identification Using OBF based prediction models

The input and noise sequences in closed-loop identification are correlated and conventional OBF model development procedures fail to provide consistent model parameters in such cases. In this research, three different methods that address the issue of closed loop identification using OBF plus noise models are proposed. Two of the methods are based on the direct identification approach with OBF-ARX and OBF-ARMAX models. The third method is an indirect identification method using OBF-ARMA model with simulated input of the plant, which is not correlated to noise, in stead of the actual

input of the plant, which is correlated to the noise. The parameters of the OBF-ARX models are estimated using the least square method and the parameters of the OBF-ARMAX models are estimated using the extended least square method as explained in Chapter 4. In addition, the multi-step-ahead prediction schemes were presented in Chapter 4.

The proposed methods are designed so that they address the two distinct aspects of closed-loop identification problems, namely, model development from closed loop data when the system is open-loop stable and when the system is open-loop unstable.

It was shown, by appropriate mathematical derivation and simulation studies in Chapter 4, that closed-loop identification of open-loop stable processes can be handled by any of the three proposed methods. However, the selection of the best structure for a given problem can be made by comparing the PPEs. When, the difference between the PPEs is small the OBF-ARMA model is preferable, because the simulation model is simple and stable. Closed-loop identifications of open-loop unstable processes can be handled using OBF-ARX and OBF-ARMAX models.

All the proposed closed-identification structures and methods were demonstrated using simulation case studies and one real plant case study. Model validation was conducted in each case study using separate validation data and residual analysis. The case studies confirmed that all the three proposed methods are effective when they are appropriately used for identification problems they are designed for.

6.12 Recommendations

In this research, most of the outstanding problems related to linear OBF model development are addressed. Further research can be conducted in OBF based non-linear system identification and implementation of the results of the current research. The various nonlinear identification frame works can be used with orthonormal basis filters and the research can be extended in this direction also. Development of dynamic local linear neuron-fuzzy models with linear OBF models is one of the potentially attractive research areas in this respect. Implementation is another area where further research can be carried out with potential benefit in the chemical and petrochemical industry. Research related to the implementations of OBF models in Model Predictive Control (MPC) systems and fault tolerant control are recommended for further research.

REFERENCES

[1]   L. Ljung, *System Identification: Theory for the User*. New Jersey: Prentice Hall PTR, 1999.

[2]   O. Nelles, *Nonlinear System Identification*. Berlin Heidel Berg: Springer-Verlag, 2001.

[3]   C. R. Cutler and B. C. Ramaker, "Dynamic Matrix Control – A Computer Control Algorithm," in *Automatica Control Conference*, San Fransisco, 1980.

[4]   J. Richalet, A. Rault, J. L. Testud, and J. Papon, "Model Predictive Heuristic Control:Application to Industrial Processes," *Automatica,* vol. 14, pp. 413-428, 1978.

[5]   E. F. Camacho and C. Bordon, *Model Predictive Control*: Springer Verlag Limited, London, 2004.

[6]   J. B. Rawlings, "Tutorial Overview of Model Predictive Control," *IEEE control Systems Magazine,* 2000.

[7]   L. Ljung, "Identification for Control: Simple Process Models," in *41st IEEE Conference on Decision and Control*, Las Vegas, Nevada, USA, 2002, pp. 4652-4657.

[8]   S. C. Patwardhan and S. L. Shah, "From data to diagnosis and control using generalized orthonormal basis filters, Part I: Development of state observers," *Journal of Process Control,* vol. 15, pp. 819-835, 2005.

[9]   D. E. Seborg, T. F. Edgar, and D.A. Mellichamp, *Process Dynamics and Control*, 2nd ed.: John Wiley & Sons. 2004.

[10]   S. C. Patwardhan, S. Manuja, S. Narasimhan , S. L. Shah, "From data to diagnosis and control using generalized orthonormal basis filters, Part II: Model predictive and Fault Tolerant Control," *Journal of Process Control,* vol. 16, pp. 157-175, 2006.

[11]   J.D. Gibbons and S. Chakrabort (2003), *Nonparametric Statistical Inference,* 4th ed.: CRC Press.2003.

[12]   E. H. K. Fung, Y. K. Wong, H. F. Ho, and M. P. Mignolet, "Modelling and prediction of machining errors using ARMAX and NARMAX structures," *Applied Mathematical Modelling* 611–627 2003.

[13]   S. M. Moore, J. C. S. Lai, and K. Shankar, "ARMAX modal parameter identification in the presence of unmeasured excitation—II: Numerical and experimental verification," *Mechanical Systems and Signal Processing* pp. 1616–1641, 2007.

[14]   C. Özsoy, A. Kural, and C. Baykarza, "Modeling of the Raw Mixing Process in Cement Industry," *IEEE XPLORE,* 2001.

[15]   J. C.-M. Yiu and S. Wang, "Multiple ARMAX modeling scheme for forecasting air conditioning system performance, "*Energy Conversion and Management* pp. 2276–2285, 2007.

[16]   L. Ljung, "State of the Art in Linear System Identification: Time and Frequency Domain Methods," in *the 2004 American Control Conference*, Boston, Massachusetts 2004.

[17]   E. Ikonen and K. Najim, *Advanced Process Identification and Control*. New York: Marcel Dekker Inc, 2002.

[18]   J. Mikleš and M. Fikar, *Process Modelling, Identification, and Control*. Berlin Heidelberg: Springer-Verlag 2007.

[19]   R. S. S. Peña, J. Q. Casín, and V. P. Cayuela, *Identification and Control, the Gap between Theory and Practice*. New York: Springer-Verlag, 2007

[20]   P. S. C. Heuberger, P. M. J. Van den Hof, and B. Wahlberg, *Modeling and Identification with Rational Orthogonal Basis Functions*: Springer-Verlag London Limited, 2005.

[21]   L. Wang and W. R. Cluett, *From Plant Data to Process Control*. London: Taylor & Francis, 2000.

[22]   Y. Zhu, *Multivariable System Identification for Process Control*: Elsevier Science & Technology Books, 2001.

[23]   H. Garnier and L. Wang, *Identification of Continuous-time Models from Sampled Data*. London: Springer-Verlag, 2008.

[24]   A. Gangopadhyay and P. Meckl, "Modeling, Validation and System Identification of a Natural Gas Engine," in *of the American Control Conference*, Albuquerque, New Mexico, 1997.

[25]   M. Gilson and P. V. d. Hof, "Instrumental variable methods for closed-loop system identification ," *Automatica* pp. 241 – 249, 2005.

[26]   L. Guo and L. Ljung, "The Role of Model Validation for Assessing the Size of the Unmodelled Dynamics," in *the 33rd Conference on Decision and Control*, Lake Buena V i , FL, 1994.

[27]   F. Hossein-Babaei and S. M. Hosseini-Golgoo, "Analyzing the Responses of a Thermally Modulated Gas Sensor Using a Linear System Identification Technique for Gas Diagnosis," *IEEE Sensors Journal,* vol. 8, 2008.

[28]   S. M. Moore, J. C. S. Lai, and K. Shankar, "ARMAX modal parameter identification in the presence of unmeasured excitation—I: Theoretical background," *Mechanical Systems and Signal Processing* pp. 1601–1615, 2007.

[29]   R. Pintelon and J. Schoukens, "Box–Jenkins identification revisited—Part I: Theory," *Automatica,* vol. 42, pp. 63 – 75, 2005.

[30]   R. Pintelon, Y. Rolain, and J. Schoukens, "Box–Jenkins identification revisited—Part II: Applications," *Automatica,* vol. 42, pp. 77–84, 2005.

[31]   R. Pintelon, J. Schoukensa, and P. Guillaumeb, "Box–Jenkins identification revisited—Part III Multivariable systems," *Automatica,* vol. 43 pp. 868 – 875, 2007.

[32]   R. Wallin, A. J. Isaksson, and L. Ljung, "An iterative method for identification of ARX models from incomplete data," in *the 39th IEEE Conference on Decision and Control*, Sydney, Australia December, 2000.

[33]   Z.-X. Zhu and A. Jutan, "Model identification of a distillation column," *Journal of Process Control,* vol. v, pp. 105-107, 1995.

[34]   T. Söderström, H. Fan, and B. Carlsson, "Least Squares Parameter Estimation of Continuous Time ARX Models from Discrete-Time Data," *IEEE Transactions on automatic control,* vol. 42, 1997.

[35]   K. Lo and W. H. Kwon, "A New Identification Approach for FIR Models," *IEEE Transactions on Circuits and Systems—II: Analog and Digital Signal Processing,* vol. 49, 2002.

[36]   S. Takenaka, "On the orthogonal functions and a new formula of interpolation," *Japanese Journal of Mathematics,* pp. 129–145, 1925.

[37]   J. L. Walsh, "Interpolation and Approximation by Rational Functions in the Complex Domain," *American Mathematical Society Colloquium Publications,* vol. XX, 1975.

[38]   N. Wiener, *Extrapolation, Interpolation and Smoothing of Stationary Time Series*: M.I.T.-Press, Cambridge, MA 1949.

[39]   W. H. Kautz, "Transient synthesis in the time domain," *IRE Transactions on Circuit Theory,* pp. 29-39, 1954.

[40]   W. H. Kautz., "Network synthesis for specified transient response," Massachusetts Institute of Technology, Research Laboratory of Electronics 1952.

[41]   R. E. King and P. N. Paraskevopoulos, "Parametric identification of discrete time SISO systems," *International Journal of Control,* pp. 1023–1029, 1979.

[42] H. Akçay and B. M. Ninness., "Rational basis functions for robust identification from frequency and time-domain measurements," *Automatica,* vol. 34, pp. 1101–1117, 1998.

[43] R. Cluett and L. Wang, "Frequency smoothing using Laguerre model," *IEEE Proceedings-D,* vol. 139, pp. 88–96, 1992.

[44] P. S. C. Heuberger, P. M. J. Van den Hof, and O. H. Bosgra, "A Generalized Orthonormal Basis for Linear Dynamical Systems," *IEEE Transactions On Automatic Control,* vol. 40, pp. 451-465, 1995.

[45] B. M. Ninness and F. Gustafsson, "A unifying construction of orthonormal bases for system identification," *IEEE Transactions on Automatic Control,* vol. 42, pp. 515– 521, 1997.

[46] P. M. J. Van den Hof, P. S. C. Heuberger, and J. Bokor, "System Identification with Generalized Orthonormal Basis Functions," *Automatica,* vol. 31, pp. 1821-1834, 1995.

[47] B. Wahlberg, "System identification using Kautz models," *IEEE Transactions on Automatic Control,* vol. 39, pp. 1276–1282, 1994.

[48] B. Walberg, "System Identification using Laguerre filters," *IEEE Trans. Autom. Control,* vol. 36, pp. 551-562, 1991.

[49] A. C. d. Brinker, "Laguerre-domain adaptive filters," *IEEE Transactions on Signal Processing,* vol. 42, pp. 953–956, 1994.

[50] G. W. Davidson and D. D. Falconer, "Reduced complexity echo cancellation using orthonormal functions," *IEEE Transactions on Circuits and Systems,* vol. 38, pp. 20-28, 1991.

[51] B. M. Ninness and J. C. G´omez., "Frequency domain analysis of tracking and noise performance of adaptive algorithms " *IEEE Transactions on Signal Processing,* vol. 46, pp. 1314–1332, 1998.

[52] H. Perez and S. Tsujii, "A system identification algorithm using orthogonal functions," *IEEE Transactions on Signal Processing,* vol. 38, pp. 752–755, 1991.

[53] G. A. Williamson, "Tracking random walk systems with vector space adaptive filters," *IEEE Transactions on Circuits and Systems,* vol. 42, pp. 543–547, 1995.

[54] P. Dewilde and H. Dym, "Schur recursions, error formulas, and convergence of rational estimators for stationary stochastic sequences," *IEEE Transactions on Information Theory,* pp. 446-461, 1981.

[55] P. Dewilde and H. Dym, "Lossless inverse scattering, digital filters and estimation theory," *IEEE Transactions on Information Theory,* vol. IT-30, pp. 664–662, 1984.

[56]   H. Akçay, "Synthesis of complete rational orthonormal bases with prescribed asymptotic order," *Automatica,* pp. 559–564, 2001.

[57]   H. Akçay, "Orthonormal basis functions for modelling continuous-time systems," *Signal Processing,* pp. 261–274, 1999.

[58]   H. Akçay, "Discrete-time system modelling in Lp with orthonormal basis functions,"*Systems & Control Letters,* pp. 365–376, 2000.

[59]   H. Akçay, "Paley inequalities for discrete-time rational orthonormal bases," *Signal Processing,* pp. 2449–2455, 2000.

[60]   H. Akçay, "On the uniform approximation of discrete-time systems by generalized Fourier series," *IEEE Transactions on Signal Processing,* pp. 1461–1467, 2001.

[61]   H. Akçay., "On the existence of a disk algebra basis," *Signal Processing,* pp. 903–907, 2000.

[62]   B. R. Fischer and A. Medvedev, "L2 time delay estimation by means of Laguerre functions," in *American Control Conf.*, San Diego, CA, June 1999, pp. 455–259.

[63]   A. Lecchini and M. Gevers, "Explicit expression of the parameter bias in identification of Laguerre models from step responses," *Systems & Control Letters,* pp. 149–165, 2004.

[64]   Z. Szabó and J. Bokor, "Lp norm convergence of rational orthonormal basis function expansions," in *the 38th IEEE Conf. on Decision and Control*, Phoenix, AZ, USA., 1999, pp. 3218–3223.

[65]   R. J. G. B. Campello, G. Favier, and W. C. d. Amaral, "Optimal expansions of discrete-time Volterra models using Laguerre functions," *Automatica,* pp. 815–822, 2004.

[66]   M. Casini, A. Garulli, and A. Vicino, "On worst-case approximation of feasible system sets via orthonormal basis functions," *IEEE Transactions on Automatic Control,* vol. 48, pp. 96–101, 2003.

[67]   A. M. Sabatini, "A hybrid genetic algorithm for estimating the optimal time scale of linear systems approximations using Laguerre models," *IEEE Transactions on Automatic Control,* vol. 45, pp. 1007–1011, 2000.

[68]   B. E. Sarrouhk, A. C. d. Brinker, and S. J. L. v. Eijndhoven, "Optimal parameters in modulated Laguerre series expansions," in *Fifth International Symp. on Signal Processing and Its Applications*, Brisbane, Australia, August 1999, pp. 187–190.

[69]   B. E. Sarroukh, S. J. L. V. Eijndhoven, and A. C. D. Brinker, "An iterative solution for the optimal poles in a Kautz series," in *IEEE International Conf. on Acoustics, Speech, and Signal Processing (ICASSP'01)*, Salt Lake City, Utah, USA, May 2001, pp. 3949–3952.

[70]   N. Tanguy, R. Morvan, P. Vilbé, and L. C. Calvez, "Improved method for optimum choice of free parameter in orthogonal approximations," *IEEE Transactions on Signal Processing,* vol. 47, pp. 2576–2578, 1999.

[71]   N. Tanguy, R. Morvan, P. Vilbé, and L. C. Calvez, "Pertinent choice of parameters for discrete Kautz approximation," *IEEE Transactions on Automatic Control,* vol. 47, pp. 783–787, 2002.

[72]   N. Tanguy, R. Morvan, P. Vilbé, and L. C. Calvez., "Online optimization of the time scale in adaptive Laguerre-based filters," *IEEE Transactions on Signal Processing,* vol. 48, pp. 1184–1187, 2000.

[73]   S. S. Abeysekera and X. Yao, "Design of Narrow-band Laguerre Filters Using a Min-Max Criterion," in *IEEE International Conf. on Acoustics, Speech, and Signal Processing Proceedings (ICASSP'00)*, Istanbul, Turkey, June 2000, pp. 137–140.

[74]   T. J. d. Hoog, P. S. C. Heuberger, and P. M. J. Van den Hof, "A general transform theory of rational orthonormal basis function expansions," in *39th IEEE Conf. on Decision and Control*, Sydney, Australia, December 2000, pp. 4649–4654.

[75]   T. J. d. Hoog, P. S. C. Heuberger, and P. M. J. Van den Hof., "On partial realization and interpolation of models from orthogonal basis function expansions," in *38th IEEE Conf. on Decision and Control*, Phoenix, USA, December 1999, pp. 3212–3218.

[76]   T. J. d. Hoog, Z. Szabó, P. S. C. Heuberger, P. M. J. Van den Hof, and J. Bokor, "Minimal partial realization from generalized orthonormal basis function expansions," *Automatica,* vol. 38, pp. 655–669, 2002.

[77]   B. Ninness and H. Hjalmarsson, "Model Structure and Numerical Properties of Normal Equations," *IEEE Transactions on circuits and systems—I: Fundamental theory and applications,* vol. 48, pp. 425-437, 2001.

[78]   T. Oliveira-e-Silva, "On the asymptotic eigenvalue distribution of block-Toeplitz matrices related to the generalized orthonormal basis functions model," *Automatica,* vol. 35, pp. 1653–1661, 1999.

[79]   T. V. Schroeter, "Frequency warping with arbitrary all pass maps," *IEEE Signal Processing Letters,* vol. 6, pp. 116–118, 1999.

[80]   Z. Szabó, P. S. C. Heuberger, J. Bokor, and P. M. J. Van den Hof, "Extended Ho-Kalman algorithm for systems represented in generalized orthonormal bases," *Automatica,* vol. 36, pp. 1809–1818, 2000.

[81]   P. Van-gucht and A. Bultheel, "State space representation for arbitrary orthogonal rational functions," *Systems & Control Letters,* pp. 91–98, 2003.

[82]   Q. G. Zhou and E. J. Davison, "A simplified algorithm for balanced realization of Laguerre network models," in *39th IEEE Conf. on Decision and Control*, Piscataway, NJ,USA, December 2000, pp. 4336–4640.

[83]   Q. G. Zhou and E. J. Davison, "Balanced realization of Laguerre network models," in *2000 American Control Conf.*, Chicago, IL,USA, June 2000, pp. 2874–2878.

[84]   R. Merched, "Extended RLS lattice adaptive filters," *IEEE Transactions on Signal Processing,* vol. 51, pp. 2294–2309, 2003.

[85]   R. Merched and A. H. Sayed, "Order-recursive RLS Laguerre adaptive filtering," *IEEE Transactions on Signal Processing,* vol. 48, pp. 3000–3010, 2000.

[86]   R. Merched and A. H. Sayed, "Extended fast fixed-order RLS adaptive filters," *IEEE Transactions on Signal Processing,* vol. 49, pp. 3015–3031, 2001.

[87]   R. Merched and A. H. Sayed, "RLS-Laguerre lattice adaptive filtering: Error feedback, normalized, and array-based algorithms," *IEEE Transactions on Signal Processing,* vol. 49, pp. 2565–2576, 2001.

[88]   B. M. Ninness and F. Gustafsson, "A unifying construction of orthonormal basis for system identification," *IEEE Transactions on Automatic Control,* vol. 42, pp. 515-521, 1997.

[89]   C. Bruni, "Analysis of Approximation of Linear and Time-Invariant Systems Pulse Response by Means of Laguerre Finite Term Expansion," *IEEE Transactions on Automatic Control,* vol. 9, pp. 580–581, 1964.

[90]   C. T. Chou, M. Verhaegen, and R. Johansson, "Continuous-Time Identification of SISO Systems Using Laguerre Functions," *IEEE Transactions on signal processing,* vol. 47, pp. 349-362, 1999.

[91]   L. Knockaert and D. D. Zutter, "Laguerre-SVD Reduced-Order Modeling," *IEEE Transactions on microwave theory and techniques,* vol. 48, 2000.

[92]   P. M. J. Van den Hof, B. Walhberg, P. S. C. Heurberger, B. Ninness, J. Bokor, and T. Oliver e Silva, "Modeling and identification with rational orthonormal basis functions," in *IFAC SYSID* Santa Barbara, California, 2000.

[93]   K. R. Muske and T. A. Badgwell, "Disturbance modeling for offset-free linear model predictive control," *Journal of Process Control,* pp. 617-632, 2002.

[94]   P. Gáspár, Z. Szabó, and J. Bokor, "Closed-loop identification using generalized orthonormal basis functions," in t*he 38th Conference on Decision & Control* Phoenix, Arizona USA December 1999.

[95]   I. Ananth and M. Chidambaram, "Closed-loop identification of transfer function model for unstable systems," *Journal of the Franklin Institute* pp. 1055-1061, 1999.

[96]   P. M. J. Van den Hof, "Closed-loop identification issues in system identification," *Annual Reviews in Control,* pp. 173-186, 1998.

[97]   P. S. C. Heuberger, P. M. J. V. d. Hof, and O. H. Bosgra, "A generalized orthonormal basis for linear dynamical systems," *IEEE Transactions on Automatic Control,* vol. 40, pp. 451–465, 1995.

[98]   B. A. Ogunnaike and W. H. Ray, *Process dynamics, modeling and control*. New York: Oxford University Press, 1994.

[99]   C. L. Smith, *Digital Computer Process Control,* In text, Scranton, PA, 1972.

[100] G. P. Rangaiah and P. R. Krishnaswamy, "Estimating Second-Order Dead Time Parameters from Underdamped Process Transients.," *Chemical Engineering Science,* vol. 51, pp. 1149-1155, 1996.

[101] G. P. Rangaiah and P. R. Krishnaswamy, "Estimating Second-Order Plus Dead Time Model Parameters," *Ind. Eng. Chem. Res.,* vol. 33, 1994.